COMPARATIVE MORPHOLOGY AND EVOLUTIONARY RELATIONSHIPS OF THE SPARIDAE (TELEOSTEI: PERCOIDEI)

by

JULIA JANE DAY

A thesis submitted for the degree of Doctor of Philosophy,
University of London

January 2000

Department of Biology
University College London
Gower Street
London, WC1E 6BT

Department of Palaeontology
The Natural History Museum
Cromwell Road
London, SW7 5BD

ProQuest LLC.
789 East Eisenhower Parkway
P.O. Box 1346
Ann Arbor, MI 48106 – 1346

ABSTRACT

The comparative morphology of the family Sparidae is described comprehensively for the first time and is used to formulate character data for phylogenetic analysis. The data is found to be particularly character rich in areas such as the braincase, jaws and gill arches. Phylogenetic analysis, using PAUP* was performed in order to resolve the evolutionary relationships for 29 sparid genera and representatives sparoid families: Centracanthidae; Lethrinidae; Nemipteridae. Parsimony analysis of this data yielded three equally parsimonious trees. The Sparidae constitute a monophyletic group, with the inclusion of Centracanthidae, which is embedded within cladistically derived sparids. A grouping of derived sparids are found to be reasonably well supported when judged by Bremer support and bootstrapping, while relationships amongest those taxa more basal are found to be weakly supported. Further analysis of the data is assessed from 1) character quality through application of Le Quesne probabilities; 2) data partitioning; 3) influence of outgroups; 4) effects of ordering and 5) recoding, using non-additive binary coding. These analyses also support a hypothesis of relationships amongest derived sparids that is both well supported and resolved. However, the relationships of basal sparids are sensitive to these analyses, suggesting that not much confidence may be placed in the revealed theories of their interrelationships. The conflict between alternative trees reflects the high levels of homoplasy, which is not uncommon for percoid data sets. The geographic distribution is explained using three methods of cladistic biogeography, based on irreversible and reversible methods of ancestral area analysis and dispersal-vicariance analysis. The Indo-Pacific is identified as the most likely ancestral area for the Sparidae. Reconstruction of the evolution of feeding strategies among sparids suggests that there is a progressive transition from generalist to specialized feeders with four assemblages recognized. The diversification of feeding strategies within the Sparidae may have had important consequences for the evolution of the group which is discussed. Fossil sparid material from the Early to Middle Eocene is redescribed and included in the Recent matrix for further phylogenetic analyses. Comparison of the fossil material warrants the erection of a new genus and species, *Ellaserrata monksi* and a new genus *Abromasta microdon* is erected for *Pagellus microdon*. A minimum age of origin for the group can be postulated at 55Ma.

PREFACE

I declare that this dissertation is the result of my own work and includes nothing that is the outcome of work done in collaboration. No part of this work has been submitted for a degree, diploma or any other qualification at any other University.

.....

Julia J. Day

ACKNOWLEDGEMENTS

I am indebted to my supervisors, Michael Coates and Peter Forey for providing me with the opportunity to work within the field of systematic biology and for their continued support and encouragement. I would particularly like to express my thanks to Peter, for devoting time and energy into critically reviewing my work. I gratefully acknowledge the receipt of a BBSRC grant 96700156 which was the primary source of funding for this project, in addition to the Margaret-Brown Scholarship from University College London. I also thank the Systematics Association and the American Museum of Natural History for providing additional support for travel.

This project as been carried out in the Department of Palaeontology, at The Natural History Museum, London, and for this I thank Robin Cocks and his successor Stephen Donovan for making me welcome here. I extend my sincere gratitude to all those at the NHM and UCL who provided help and encouragement over the past years, in particular; Claudia Amphlett, Helen Chatterjee, Siân Evans, Charlotte Jeffrey, Paul Jeffrey, David Lees, Claire Mellish, Neale Monks, Brian Rosen, Phil Rye, Marcello Ruta, Steve Salisbury, Jackie Skipper, Andrew Smith, John Stuart, Jon Todd, Paul Taylor, Mike Weedon, Sally Young. I would particularly like to thank Mark Wilkinson, Marcello Ruta and David Gower for discussion and their invaluable help into the theory and practice of cladistics and Neale Monks for Mac support. I would also like to thank the members of the fish research group of the Department of Zoology, NHM, in particular, Tony Gill, Ollie Crimmen and Sean Davidson for help with finding and preparing specimens. Thanks also to the NHM's library services and photographic units, especially Phil Crabb and Nick Hayes.

I am grateful to David Bellwood who brought the subject matter of this thesis to my attention and to David Johnson for his encouragement with pursuing this project. I also benefited from David's capacious knowledge in interpreting the anatomy of gill arches, not to mention the provision of some indispensable dissection equipment.

My work on the collections at the following institutions was made possible by Barbara Brown at The American Museum of Natural History; David Catania at the Californian Academy of Sciences; George Burgess at the Florida Museum of Natural History, Gainesville; Roberto Zorzin and Chiara Sorbini at the Museo Civico di Storia Naturale, Verona, Italy and Daniel Goujet at the Muséum National d'histoire Naturelle, Paris, whom I thank for their help. I am also deeply grateful to the JLB Smith Institute of Ichthyology, South Africa, for the donation of specimens to the Natural History Museum, and in particular to Andrew Bentley who organised this for me.

Thank you to all my friends, in particular Charlo, Claudia, Helen and Sarah for their much needed support. My special thanks to Mark for things more than I can say, but above all for being a wonderful friend. And to my parents, for their unending support and encouragement. I owe you all, thank you so much.

CONTENTS

LIST OF FIGURES

CHAPTER 1

CHAPTER 2

LIST OF PLATES

LIST OF TABLES

CHAPTER 1

INTRODUCTION

"Fishes considered collectively...offer to the philosopher an endless source of meditation and surprise."

J.-A. Brillat-Savarin
The Philosopher in the Kitchen (1825)
after G.D. Johnson and C. Patterson (1993)

General introduction

Percoid fishes represent the largest and most diverse assemblage of the perciform suborders, yet nowhere is the lack of understanding of their interrelationships more evident (Johnson 1984). In order to establish these relationships and to determine or challenge the monophyly of Percoidei, discovery of the characters of monophyletic families provides the first approach and should lead to a more complete understanding of evolutionary relationships (Johnson 1980). A particularly problematic area are the relationships within the superfamily Sparoidei, which have not been defined using cladistic methodology. In order to begin to understand higher order relationships, investigation at the family-level is presented here for the Sparidae.

While the main aim of this thesis is to provide a phylogenetic hypothesis for the Sparidae, they provide a particularly interesting study group due to the diverse morphological variation exhibited throughout the family, distribution, diet and fossil record. Their morphological diversity is reflected in the diverse range of feeding strategies, which includes species that are strongly herbivorous, piscivorous, while others possess durophagous dentitions for feeding on hard-bodied invertebrates. Furthermore, they have a broad geographical distribution and are the only sparoids to inhabit the Western Atlantic region (Helfman *et al.* 1997). The occurrence of a fossil record that extends to the early Eocene provides an opportunity not only to examine the morphology of the earliest known members of this family, but their inclusion within the Recent data matrix provides a historical scenario for the origin and diversification of the group as well as enriching theories of character evolution.

Overview of the current problems in percoid systematics

While teleostean monophyly has been established from morphological data (de Pinna 1996), higher level interrelationships of the most derived group of teleosts the Percomorpha (comprising 10000 species) are yet to be answered. Rosen (1973: fig. 129) recognized the Percomorpha; the equivalent of Greenwood *et al.'s* (1966) Acanthopterygii, as the most derived clade of euteleostean fishes, however, he failed to establish any defining characters. Since the publication of Rosen's (1973) work, progress has been made in elucidating these interrelationships, yet conflicting classifications are given for the monophyly of the group due to the exclusion or inclusion of some orders (Stiassny 1990; Stiassny and Moore 1992; Roberts 1993; Johnson and Patterson 1993). Figure 1.0 summarizes the later authors' hypothesis of the interrelationships of acanthomorph fishes.

The Perciformes is the largest vertebrate order, which includes 20 suborders and at least 6900 species (Lauder and Liem 1983). Yet the Percoidei, the largest and most diverse sub-order of perciform fishes, remain one of the least defined groups in systematic ichthyology. Johnson (1984) defined 80 percoid families and 12 *incertae sedis* genera in his study, a figure that is only slightly modified from Greenwood *et al.* (1966), while Nelson (1994) includes 71 families within Percoidei, representing about 2860 species. Both Perciformes and Percoidei are most certainly polyphyletic (Lauder and Liem 1983; Johnson 1993), however, as yet there have been no serious attempts to define or challenge their monophyly.

As with Perciformes, there is no overall or partial phylogeny of the suborder Percoidei (Johnson 1993). The initial and perhaps most significant attempt to classify the group to date was by Regan (1913), and consisted of a short description of each family. Regan (1913:112) defined the percoids based on symplesiomorphy referring to the group '...by the absence of the special peculiarities which characterize the other suborders of the Percomorphi [Perciformes].' It thus appears that the Percoidei is an assemblage that represents a repository for generalized perciform fishes the affinity of which is not particularly obvious. Johnson (1980:4) summarized the current status of this assemblage and how best we may tackle this problem.

> 'Percoid evolution has been characterized by considerable adaptive plasticity, and it is only through comprehensive group studies that we can come to recognize the evolutionary malleability of various character complexes and thereby better identify the most phylogenetically significant. It is my opinion that valid phylogeny in the percoids will result from the family and family complex approach, wherein numerous aspects of the anatomy of all recognized genera can be evaluated, integrated and compared.'

Lack of progress may be attributed to the size and diversity of the group along with the paucity of salient morphological specializations identifiable as synapomorphies. Systematic work on percoids is, however, progressing, with definition of monophyletic families (e.g. Serranidae,

Johnson 1983, Baldwin and Johnson 1993; Grammatidae, Gill and Mooi 1993; Congrogadidae, Godkin and Winterbottom 1985; Cheilodactylidae, Randall 1983; Epigoninae, Johnson 1984; Pempheridídae, Tominaga 1965, 1968; Girellidae, Johnson and Fritzsche 1989; Terapontidae, Vari 1978. In addition, Johnson (1980) recognized three monophyletic superfamilies including eight families: Lutjanoidea (Lutjanidae, Caesionidae), Sparoidea (Sparidae, Centracanthidae, Lethrinidae, Nemipteridae), and Haemuloidea (Haemulidae, Inermiidae). He considered the relationships of the three superfamilies a particularly problematic area within the percoids relationships, finding no satisfactory evidence to relate them.

A second approach investigates single character complexes throughout a number of different hierarchical groupings (e.g. caudal skeleton, Monod 1968, Fujita 1990; branchiostegals, McAllister 1968; supernumerary median fin-rays, Patterson 1992; pelvic girdle, Stiassny and Moore 1992). However, a problem with the latter approach is that usually only a few 'typical' representatives of each family may have been examined.

Sparids are investigated here as a family in order to elucidate the internal relationships of genera, wherein the phylogenetically significant aspects of their morphology may be used for future studies of higher order relationships.

Sparid systematics

Sparids comprise a family containing 29 nominal genera and approximately 100 species (Nelson 1994; Plate 1.0). They have a broad geographical distribution and occur in tropical to temperate waters. Sparid classification has traditionally used dentition and external characterisitcs such as fin ray counts, scales and body colour to separate species. Dentition in particular has been used by many authors to distinguish genera (e.g. Cuvier 1817; Jordan and Fesler 1893; Smith 1938; Munro 1949; Akazaki 1962). Smith and Smith (1986) provide a subfamilial classification for the Sparidae, based primarily on dental morphology in accordance with their trophic specialization, erecting the following four subfamilies:

SPARINAE Jaws with bluntly rounded molars posteriorly; front teeth with 4-9 enlarged conical canines or compressed incisors.
DENTICINAE No molars; jaws with enlarged canines in front, smaller conical teeth behind.
PAGELLINAE Outer teeth small, conical; inner teeth small molars.
BOOPSINAE Outer teeth compressed, incisiform.

Previous morphological work on sparids includes an osteological review by Akazaki (1962), on what he termed sparifom fish (Sparidae, Nemipteridae and Lethrindae) of Japan. Johnson (1980) agreed with Akazaki's definition and subdivision of his 'spariform' fishes (Johnson's Sparoidea), finding additional evidence to support the monophyly of these families, to which Johnson added a fourth, the Centracanthidae, which contains five genera, with nine species

(Nelson 1994). However, no phylogenetic analysis of these families has been undertaken.

The phylogeny proposed by Akazaki places Nemipteridae as the most primitive sparoid group, whilst the Sparidae are considered to be intermediates between the Nemipteridae and the Lethrinidae. Johnson however, rejected this placement of the Sparidae citing sufficient evidence to indicate that the Nemipteridae and Lethrinidae are more closely related to each other, than to the Sparidae or Centracanthidae.

The Centracanthidae and Sparidae are considered to be more closely related to each other on the basis of a specialized premaxillary-maxillary articulation (Heemstra and Randall 1977, Johnson 1980). Johnson emphasizes this character as one of the osteological features supporting a possible sister group relationship between these families, prefering to retain the Centracanthidae as a separate family, rather than sub-family of the Sparidae pending further understanding of sparoid interrelationships. Morphological features supporting a possible sister group relationships between nemipterids and lethrinids include: identical dorsal-fin ray count (X, 9-10); well developed post-pelvic process and the absence of the specialized maxillary-premaxillary articulation that is unique to sparids and centracanthids.

There are indications that Johnson's Sparoidea and Haemuloidea (plus Gerreidae) may be related to the Pharyngognathi (Rosen and Patterson 1990). These authors include Carangidae, Centrarchidae, Gerreidae, Girellidae, Kyphosidae, Leiognathidae, Pomadasyidae, Sciaenidae, Scorpididae, Sparidae and some anabantoids as the non-pharyngognathi families which may collectively form a sister grouping to the Pharyngognathi of Müller (1844, 1845, 1846) and Günther (1862). The morphological features that suggest a relationship between pharyngognath and one or more of the non-pharyngognath families include characters from the neurocranium, jaws and palate. Rosen and Patterson (1990) list the following characters:

i) Two parasphenoidal processes: the rostral processes for the attachment of the adductor palatini muscle, while the caudal apophysis attaches to an articular process of the pharyngobranchial 3 (PB3) of the upper pharyngeal jaws (UPJ).
ii) long nasals firmly united with the frontals, which roof the fossa for the ascending process of the premaxilla,
iii) maxilla with a dorsal crest and sulcus for the palatine.

Gill arch features found in all or some labroid pharyngognaths have also been found to occur in other 'percoid' families. These are summarized following Rosen and Patterson (1990):

i) Absence of pharyngobranchial 2 dentition,
ii) first basibranchial ventral to axis of basibranchial series,
iii) posterior orientation of pharyngobranchial 2 and anterior epibranchials,
iv) a functionally median lower pharyngeal jaw,

v) teeth that are constricted proximally, and are capped by a conical, decurved tip of acrodin,
vi) the articulation of pharyngobranchial 3 with the parasphenoid apophysis is diarthrodial,
vii) absence of pharyngobranchial 4,
viii) absence of interarcual cartilage,
ix) oral margin of the first and/or second epibranchial is expanded.

Molecular studies

There are few published molecular phylogenies of sparid interrelationships. These studies include only a limited number of taxa, which are concentrated at the species level (e.g. Garrido-Ramos *et al.* 1995). In addition a study by Basagila (1990) using isozyme data for distance analysis (i.e. phenetic approach) presents the phylogenetic relationships of 15 species representing nine genera (figure 1.1). However, in none of these studies has rigorous cladistic analysis (using either maximum-likelihood or parsimony) been performed. More recently, Allegrucci *et al.* (1998) present a consensus tree, implementing both maximum parsimony and neighbour-joining for the cytochrome *b* gene for 15 species belonging to the Perciformes. Sparids are represented by three species which form the clade (*Dentex* (*Pagrus Boops*)). Research into sparid interrelationships using the molecular data (cytochrome *b*) is however, currently being carried out (Orrell 1999). The availability of both molecular and morphological data sets will provide an interesting opportunity to evaluate the relative contributions of these types of data to the classification of sparid fishes.

Aims of study

While some aspects of sparid morphology have been described and used to hypothesize about higher order relationships (e.g. Johnson 1980; Rosen and Patterson 1990), the intrarelationships of the Sparidae are poorly understood with no attempt to substantiate their monophyly using cladistic methodology. Thus, the main aim of this thesis is to provide a phylogenetic hypothesis for the Sparidae using cladistic methodology from detailed examination of comparative morphology. This thesis comprises six chapters that include the following themes: description of a presumed basal sparid and comparative morphology; phylogenetic inference; biogeography and ecology and the fossil record.

Chapter 2 represents the primary findings of this study by documenting morphological variation across the Sparidae with respect to related families. The following 29 sparid genera are included in this study: *Acanthopagrus*; *Archosargus*; *Argyrops*; *Argyrozona*; *Boops*; *Boopsoidea*; *Calamus*; *Cheimerus*; *Chrysoblephus*; *Crenidens*; *Cymatoceps*; *Dentex*; *Diplodus*; *Evynnis*; *Lagodon*; *Lithognathus*; *Oblada*; *Pachymetopon*; *Pagrus*, *Pagellus*, *Polyamblyodon*, *Polysteganus*, *Porcostoma*; *Rhabdosargus*; *Sarpa*; *Sparodon*; *Sparus*; *Spondyliosoma* and *Stentomus*. The monospecific genera: *Gymnocrotaphus*; *Petrus*; *Pterogymnus*; *Taius* and

Sparidentex are omitted from this study due to unavailability of specimens. However, as *Taius* and *Sparidentex* are considered to be subgenera of *Dentex*, their absence from this study is not detrimental for generic level analysis. It is worth noting that Nelson (1994) is incorrect listing *Pimelepterus* under Sparidae, as this genus belongs to the family Kyphosidae (Eschymeyer 1998).

Taxonomic problems associated at the generic level, due to overall similarities and key diagnostic features (Bianchi 1984), present uncertainty over the monophyly of these groupings. An example of this is the classification of *Sparus* and *Pagrus* that remains problematic due to the lack of external variation. This has led to their phylogenetic relationships remaining unresolved so that they have been alternatively grouped in a single genus (Bauchot *et al.* 1981; Basaglia 1992) or as separate genera (Bianchi 1984; Bauchot and Hureau 1986). For these reasons stated, where possible type species are used to code data.

This chapter is divided into two parts, with part 1 focusing on the osteology of the basal sparid *Dentex dentex,* for which a detailed description forms the basis for all subsequent descriptions of taxa in this thesis. In the second part of this chapter, I compare aspects of the morphology in the other sparid genera and thereby formulate a character list and data matrix for the phylogenetic analysis discussed in the next chapter.

Cladistics is one method of systematics, albeit a very powerful method, which attempts to provide an explanation to the classification and evolution of life (Mayr 1974). Cladistics is used here through the recognition of homologous structures, the theory and methodology of which is implemented and discussed in Chapters 3, 4 and 5.

Chapter 3 presents a number of evolutionary hypotheses for the Sparidae. Numerical phylogenetic analyses using parsimony is applied to the data matrix formulated in Chapter 2 in order to resolve the relationships of this family. In the first part of this chapter I aim to: 1) elucidate the interarelationships of the Sparidae and diagnose or challenge the monophyly of the group; 2) analyse the distribution of character state changes using both DELTRAN and ACCTRAN character optimizations; 3) assess data quality using permutation tail probabilities (PTP) tests; 4) assess the degree of confidence in the tree structure using Bremer support and Bootstrapping; 5) discuss support for the phylogenetic hypothesis. In this analysis all multistate characters are left unordered.

In the second part of this chapter, the data is analysed under a number of *a priori* and *a posteriori* assumptions to evaluate: 6) assessment of data quality using a compatibility approach of Le Quesne probability (LQP), and reanalysis of the data using only those characters with low LQP values; 7) exclusion of data partitions of particular character groups are used to assess their sensitivity on the tree topology, while partition homogenetiy tests provide a statistical measure for rejection of the null hypothesis of congruence; 8) influence of using a heterogeneous outgroup, by removal of one or more of the outgroups to assess their effect on tree stability; 9) the effects of ordering characters using the method of intermediates; 10) effects of coding, in which a

preliminary analysis is presented using non-applicable binary coding. Furthermore, I discuss the degree of confidence that can be assumed from the quality of the phylogenetic hypothesis.

In Chapter 4 the phylogenetic hypothesis presented in part 1 of Chapter 3 is used to infer questions pertaining to the biogeography and ecology of the Sparidae. In part 1, reconstruction of ancestral areas is examined through the application of three different methods of ancestral area analysis: 1) ancestral area analysis using irreversible parsimony (Bremer 1992, 1995), 2) ancestral area analysis using reversible parsimony (Ronquist 1994, 1995) and 3) dispersal-vicariance analysis or DIVA (Ronquist 1996, 1997). In the second part of this chapter phylogenetic perspectives of their feeding strategies are assessed in an evolutionary framework based on examination of the phylogenetic hypothesis.

In addition to elucidating the interrelationships of Recent sparids, the fossil record of sparids provides a temporal basis for the evolutionary hypothesis. However, I agree with Patterson (1993a:29-30) that 'no palaeontologist can place a fossil in a Recent taxon unless that taxon has some skeletal apomorphies, some characters that enable the palaeontologist to recognize its members.' Thus, with a proposed phylogenetic hypothesis, and cladistic taxonomy for Recent sparids, putative 'sparids' can be correctly identify and incorporated into a combined data matrix.

In Chapter 5, I review the fossil record of the Sparidae and focus on the earliest known members of the family from the early and middle Eocene. Morphological descriptions for each of these taxa are given and aspects of their ecology such as diet and locomotion are discussed. In the second part of this chapter a phylogenetic hypothesis is presented for the fossil sparids, further to which the fossil taxa are incorporated into the data matrix formulated in Chapter 2, in order to assess the influence of including fossils into Recent data sets and trace morphological systems through time to determine the development of complex morphologies.

Methods

It was necessary to clear and stain specimens for bone and cartilage to provide information of complex structures such as gill arches which are much less accessible in dry skeletons. The techniques used in this study are consistent with those performed by the Division of Fishes, Department of Zoology, The Natural History Museum London, following Pothoff (1983) and Taylor and Van Dyke (1985), omitting the destaining process used in Pothoff's procedure.

Specimens used for clearing and staining were counter stained to show bone and cartilage, using alizarin red S and alcian blue respectively. There is often varied success with staining cartilage, so that it may be faint or unobservable in certain specimens. This is probably due to the solvent in which the specimens were originally preserved. Specimens were then subsequently dissected, with particular attention being paid to the removal of the gill arches. In order to cause

minimal damage to the specimen only one side was dissected. The dissection consisted of the removal of the following anatomical complexes: i) the infraorbitals, ii) the palatine arch, iii) the lower and upper jaws as separate units by cutting through the mandibular tendons (figured in Schaffer and Rosen, 1961: 194, fig. c) and iv) the gill arches. The gill arches are covered by connective tissue in the mouth cavity, so it is important to gently dissect this away, in order to leave the other side of the fish intact. The connective tissue then needs to be separated in between the upper pharyngeals, so that the gill arches can be displayed two-dimensionally.

Specimens were dissected under a WILD M5 steromicroscope. Anatomical illustrations were drawn primarily with the aid of a camera-lucida mounted onto the microscope. A reducing lens (x0.3) was fitted for larger specimens such as dry skeletons and fossil material.

In many cases for both Recent and fossil specimens it was possible to examine several specimens; this allowed detailed morphological observations, and further enabled an assessment of the degree of intraspecific variation. However, some of the genera endemic to South Africa are represented by single specimens, as a consequence of their rarity. I am cautious about the observations from some of these specimens, as the morphology is recorded from a single specimen that due to its preservation has not always stained well. In these instances some morphological features may not always be obvious. Recording data from a single specimen also has implications as i) only juvenile characters are recorded (adult absent); ii) variation in species iii) a single specimen is not always adequate to observe all morphological features. The resultant coding will obviously influence the placement of these genera in the phylogenetic analysis proposed in Chapter 3 and I am aware that more specimens are desirable for further confidence in the relationships of these taxa.

Different techniques of preserving specimens can be advantageous for investigation of certain morphological systems, for example it is only possible to extensively survey gill arch morphology using cleared and stained specimens as noted previously. However, due to specimen avaliability some outgroup taxa are not represented by cleared and stained specimens of type species. As such the Centracanthidae: *Spicara smaris;* the Nemipteridae: *Scolopsis bilineateus* and the Lethrinidae: *Gymnocranius griseus* were used to code gill arch data (NB a list of all Recent specimens is given in the *specimen list* in the appendix).

Materials

Material examined during the course of this study includes: dry skeletons; alcohol; cleared and stained; radiographed and fossil specimens (both articulated and disarticulated material). Alcohol specimens were x-rayed using the facilities of the Department of Mineralogy, The Natural History Museum, London. A substantial proportion of the both Recent and fossil material examined during the course of this study is housed in the Departments of Zoology and Palaeontology at the Natural History Museum, London. Much of the South African material

examined was generously donated to the Natural History Museum from the J.L.B Smith Institute for the purpose of this study. All alcohol specimens lent for comparative investigation were subsequently stained with the permission of the institution

Institutional abbreviations

AMNH	The American Museum of Natural History, New York.
BMNH	The Natural History Museum, London (formerly The British Museum of Natural History).
CAS	Californian Academy of Sciences.
FMNH	Field Museum of Natural History, Chicago.
RUSI	JLB Smith Institute of Ichthyology, Grahamstown.
Bol.	Museo Civico di Storia Naturale, Verona
MNHN	Muséum National d'Histoire Naturelle
NMNH	National Museum of Natural History, Smithsonian Institution, Washington.
UF	Florida Museum of Natural History, Gainesville.

Anatomical nomenclature

Historically, biology follows a system for the naming of taxa, standardized by the International Code of Zoological Nomenclature, based on a Linnean binomial system of naming. Similarly, the International Anatomical Nomenclature Community has proposed a set of terms to refer to anatomical structures standardized in the Nomina Anatomica, used in medicine (human anatomy). Several other fields of biology have adopted the same convention: veterinary science, Nomina Anatomica Veterinara; embryology, Nomina Anatomica Embryologica and histology, Nomina Anatomica Histologica and recently for birds, Nomina Anatomica Avium.

While all systematists and taxonomists comply to the ICZN, using the Latinized/Linnean name given to a species, they do not generally adopt a standard for anatomical nomenclature. The majority of anatomical descriptions are written in English. The trend towards anglicising anatomy is mainly justified by accepting that English is a more accessible and therefore more easily accepted language.

Apart from historical priority in the literature anatomical nomenclature does not follow any clearly established rules. However, linguistic problems have emerged through the naming of anatomical structures, thus creating an inconsistency in the terminology used. The adoption of Latin, for its immutability, as the normative language of anatomical nomenclature is founded on several different levels of usage. Nomina Anatomica Avium, Baumel (1993) is a standard for avian anatomy, whereas Frey (1988) has applied terminologies that follow the same system of naming. A multilingual osteological dictionary Rojo (1991) includes Latin terms and Witmer (1997) has produced a standard of interpretation based on the inference of homology.

The use of latinized nomenclature is widely accepted for myological and/or neurological

structures, but rarely used for osteology descriptions in comparative anatomy literature. Early workers in ichthyology such as Allis (1897, 1898, 1903, 1919), Herrick, (1899a, 1899b) followed this preference. More recently the convention of using Latin terminology for myology, has been documented in Winterbottom's (1974) synonymy of striated muscles in the Teleostei, which is used as a standard for teleost myology.

While I do not regard it necessary to adopt an entirely Latinized terminology, as this adds unwarranted complexity, the application of a Latin terminology to certain anatomical structures does however provide a clearer definition as it describes the structure in question. I therefore disagree with Weitzman (1962: 18) '...that a name is merely a name, not a description.' An example of my preference of Latin terminology is for the complex structure such as the cranial part of the pelvic girdle. Current terminology for this structure in perciform fishes are referred to as 'wings' (Stiassny and Moore 1992). I therefore prefer to use the term superficies cranialis basipterygium; simply the cranial surface of the pelvic girdle, while the other faces are termed cranolateralis superficies or cranomedialis superficies. I therefore include a Latin terminology in the section of abbreviations for anatomical terminology.

Anatomical terminology followed

There may be more than one term used in the literature, for certain bones and anatomical structures, and that is often due to changing views of homologies. Most embryologists agree that the frontal of actinopterygians corresponds to the parietal of tetrapods (Jollie 1985), although for consistency the name frontal for actinopterygians is left unchanged. When describing a structure the anatomical terminology used is due to the author's belief in homology, thus, when evaluating what is homologous, the basic assessment must in the first instance involve topological and compositional similarity (de Pinna 1991; Hawkins *et al.* 1997).

As certain structures are liable to subjective terminologies, I adopt the terminology used by following authors: braincase, Patterson (1975); muscles, Winterbottom (1974); caudal skeleton, Fujita (1990); branchial skeleton, Nelson (1969); supraneural is used instead of predorsal (Mabee 1988), while the terminology for supernumerary fin-rays (Patterson 1992), uses radial in preference to pterygiophore (consisting of three parts, proximal, middle and distal).

Supraneural formula

Supraneural bones are given as a formula representing their relation to the neural spines. The formula was first introduced by Alstrom *et al.* (1976), as a modification from Smith and Bailey (1961), and has since been utilised by Johnson (1980, 1984). Each 0 represents a supraneural and each / a neural spine. The arabic numbers indicate the number of supernumerary fin spines associated with each radial. For the dorsal and anal fins, the finspines are denoted by roman numerals, and the soft rays are arabic numbers.

ABBREVIATIONS OF ANATOMICAL TERMINOLOGY

al.p.pm	alveolar process of the premaxilla	processus alveolus præmaxillare
amx	articular surface of maxilla	superficies articulatio maxillare
amyo	anterior myodome	
An	angular	os angulare
ap	adductor arcus palatini process on parasphenoid	processus adductor arcus palatini parasphenoideum
ar.p.pm	articular process of the premaxilla	processus articularis præmaxillare
arpr	articular process on UPJ (PB3)	processus articulars pharyngobranchialia 3
Art	articular	os articulare
ar.p.c	articular condyle of the premaxilla	condylus articularis premaxillare
arpl	articular surface for the palatine	facies articularis os palatinum
arvo	articular surface of the vomer	facies articularis os vomere
as.p.pm	ascending process of the premaxilla	processus ascendens præmaxillare
Bb	basibranchial	os basibranchiale
Bh	basihyal	os basihyale
Boc	basioccipital	os basioccipitale
Brr	branchiostegal ray	radii branchiostegi
Bsp	basisphenoid	os basisphenoideum
bsp.pd	basiphenoid pedicle	pediculum basisphenoidum
ca.b	area of cancellous bone	
Ce	ceratohyal	os ceratohyale
Cl	cleithrum	os cleithrum
Cor	coracoid	os coracoideum
cp	coronoid process	processus coronoideus
cp.pl	caudal process of the palatine	processus caudalis palatinum
cr.et.vo	dorsal crest of the ethmoid-vomerine region	crista os etmoideum+ vomere
cr.s	superior crest on the articular	crista articulare superior
Den	dentary	os dentale
df	dilatator fossa	fossa m. dilatator operculi
d.p.art	descending process of the articular	processus descendens os articulare
Ecp	ectopterygoid	os ectopterygoideum
Eh	epihyal	os epihyale
Enp	endopterygoid	os endopterygoideum

E1-4	epibranchials	os epibranchiale
Ep	epural	os epurale (plur: ossa epuralia)
Epi	epioccipital	os epioccipitale
Et	ethmoid	os ethmoidale
et.pr	ethmoid process	processus ethmoideum
ET2	second epibranchial toothplate	
Exa	extrascapular	os extrascapulare
Exo	exoccipital	os exoccipitale
exocc	exoccipital condyle	condylus exoccipialis
f.as.p.pm	fossa for the ascending process of the premaxilla	fossa processus ascendens præmaxillare
fbl	fossa for the attachment of Baudelot's ligament	fossa ligamentum baudelotinum
fc	frontal crest	crista frontalis
fdop	foramen for the m. dilatatori operculi	foramen m. dilatatori operculi
f.hm.a	anterior hyomandibular facet	facies hyomandibulare rostralis
f.hm.p	posterior hyomandibular facet	facies hyomandibulare caudalis
f.n.pt	formen n. pterygialis	formen n. pterygialis
fica	foramen of the internal carotid artery	foramen arteria interna carotidea
fm	foramen magnum	foramen magnum
fa.pa	facet for the palatine	facies palatinum
fpo	preorbital fossa	
fpr	foramen of the profundus	foramen n. profundus
fptd	fossa for the dorsal process of the posttemporal	fossa articularis posttemporalis dorsalis
fptv	fossa for the ventral process of the posttemporal	fossa articularis posttemporalis ventralis
Fr	frontal	os frontale
fse	sub-epiotic fossa	fossa sub-epioticum
fso	foramen of the superficial opthalmic branch of the V and VII	foramen superficialis opthalmicus V+VII
fsoc	foramen of the spinal-occipital nerve	foramen n. spino-occipitalis
Hd	dorsal hypohyal	os hypohyale dorsalis
Hv	ventral hypohyal	os hypohyale ventralis
Hm	hyomandibular	os hyomandibulare
Hy 1-5	hypurals	os hypurale
Hyb 1-4	hypobranchials	os hypobranchiale
hyp	hypurapophysis	hypurapophysis
IAC	interarcual cartilage	

Ic	intercalar	os intercalare
Ih	interhyal	os interhyale
Ino	interopercle	os interoperculum
Io 1-6	infraorbitals 1-6	os infraorbitale
lcom	lateral commisure	commisura lateralis
Le	lateral ethmoid	os ethmoideum laterale
LPJ	lower pharyngeal jaws	os pharyngeum inferior
l.p.mx	lateral process of the maxilla	processus lateralis maxillare
mcv	foramen of the middle cerebral vein	foramen venae medialis celebralis
mdc	dorsal crest on maxilla	crista dorsalis maxillare
mdp	dorsal maxillary process	processus dorsalis maxillare
Mpt	metapterygoid	os metapterygoideum
Mx	maxilla	os maxillare
mx.p.	maxillary process of the palatine	processus maxillaris palatinum
pmyo	posterior myodome	
Na	nasal	os nasale
occ	occipital condyle	condylus occipitalis
occr	occipital crest	crista occipitalis
Op	opercle	os operculum
Ops	opisthotic	os opisthoticum
Pa	parietal	os parietale
Pah	parhypural	os parhypurale
Par	parasphenoid	os parasphenoideum
parc	parasphenoid carina	carina parasphenoideum
PB 1-4	pharyngobranchials 1-4	os pharyngobranchiale
pc	parietal crest	crista paritale
Pcl.d	dorsal postcleithrum	os postcleithrum dorsalis
Pcl.v	ventral postcleithrum	os postcleithrum ventralis
pha	pharyngeal apophysis on basicranium	os pharyngeum apophysis basicranium
pj	pars jugularis	pars jugularis
pja	anterior opening of the pars jugularis	apertura pars jugularis rostralis
pjm	middle opening of the pars jugularis	apertura pars jugularis medialis
pjp	posterior opening of the pars jugularis	apertura pars jugularis caudalis
Pl	palatine	os palatinum
pl.ca	palatine carina	carina palatinum
plo	process for the m. levator operculi	processus m. levator operculi
pnlc	pore for nasal part of the laterosensory canal	

pmdc	premaxillary dorsal crest	crista dorsalis premaxillare
Pmx	premaxilla	os præmaxilla
pof	preorbial flange	os præorbitale
Pop	preoperculum	os preoperculum
Pro	prootic	os prooticum
ps	palatine sulcus	sulcus palatinum
pstpp	post-pelvic process	processus postbasipterygium
psym	symphysial process of the dentary	processus symphysis mandibularis
Pt	posttemporal	os posttemporale
ptc	pterotic crest	crista pteroticum
ptf	posttemporal fossa	fossa posttemporale
Pto	pterotic	os pteroticum
Q	quadrate	os quadratum
rafl	radials of the pectoral fin	ossa radialia pinnæ pectorales
Sc	scapula	os scapulum
Scl	supracleithrum	os supracleithrum
sef	subepioccipital fossa	fossa subepioccipitale
sfcl	superficies craniolateralis	superficies craniolateralis
sfcm	superficies craniomedialis	superficies craniomedialis
sha	sulcus of the hyoid artery	sulcus arteria hyoidea
Sn	supraneurals	
snlc	sulcus for the nasal part of the laterosensory canal	
Soc	supraoccipital	os supraoccipitale
Sop	subopercule	os suboperculum
so.s	subocular shelf	
Sph	sphenotic	os sphenoticum
sp.occ	spina occipitalis	spina occipitalis
St	supratemporal	os supratemporalis
stf	sub-temporal fossa	fossa sub-temporalis
subpp	sub-pelvic processes	processus sub-basipterygium
Sym	symplectic	os symplecticum
UP3,4	upper pharyngeal toothplate of third and fourth pharyngobranchial	
UPE2,3	upper pharyngeal toothplate of second or third epibranchial	
Uh	urohyal	os urohyal
UPJ	upper pharyngeal jaws	os pharyngeum superior
Ur	uroneurals	os uroneurale (plur: ossa uroneuralia)

Us	urostyle	urostylus
Vo	vomer	os vomere
I	foramen of olfactory nerve	foramen n. olfactori
Vmd	foramen of the mandibular branch of the trigeminale nerve (V)	formen ramus mandibularis n. trigeminal nerve
Vso	foramen of the ophthalmic branch of the trigeminal nerve (V)	foramen ramus opthalmicus n. trigeminale
VI	foramen of the abducens nerve	foramen n. abducens
VIIhm	foramen of the hyomandibular trunk of the facial nerve (VII)	foramen truncus hyomandibularis n. facialis
VII	foramen of the mandibular branch of the facial nerve	foramen truncus mandibularis n. facialis
VIIot	foramen for the otic branch of the facial nerve	foramen ramus oticus nervus facialis
IX	foramen of the glossopharyngeal nerve	foramen n. glosspharngei
X	foramen of vagus nerve	foramen n. vagi
IX+X	foramen of glossopharyngeal and vagus nerves	foramen n. glossophargei + vagi
CINPU4	interneural spine cartilage 4	
CIHPU4	interhaemal spine cartilage 4	
CIHPU3	interhaemal spine cartilage 3	
CPHPU2	posthaemal spine cartilages	
CPHY5	posthypural cartilage 5	

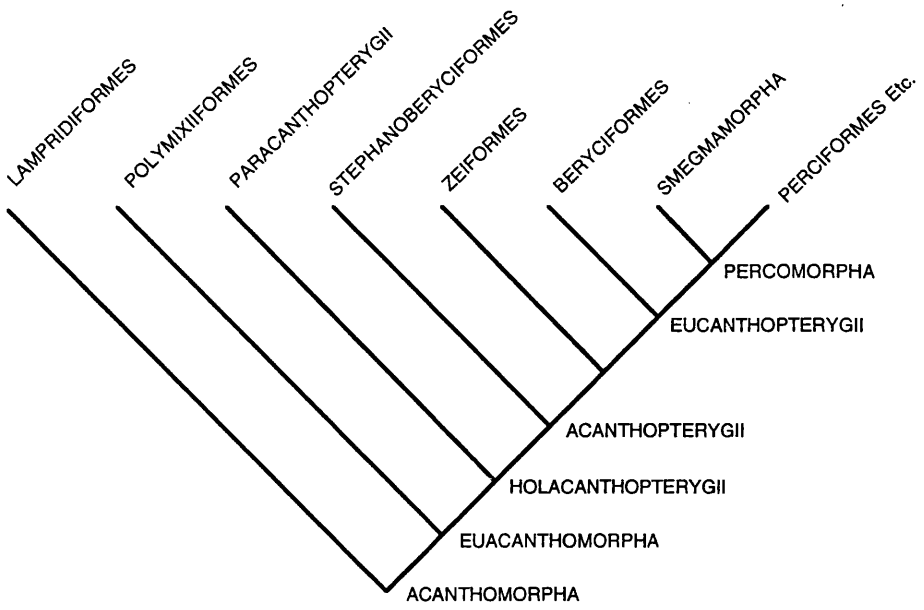

Figure 1.0 Cladogram redrawn after Johnson and Patterson (1993) summarizing acanthomorph interrelationships. The names on the axis are the major groups that have been proposed by the authors.

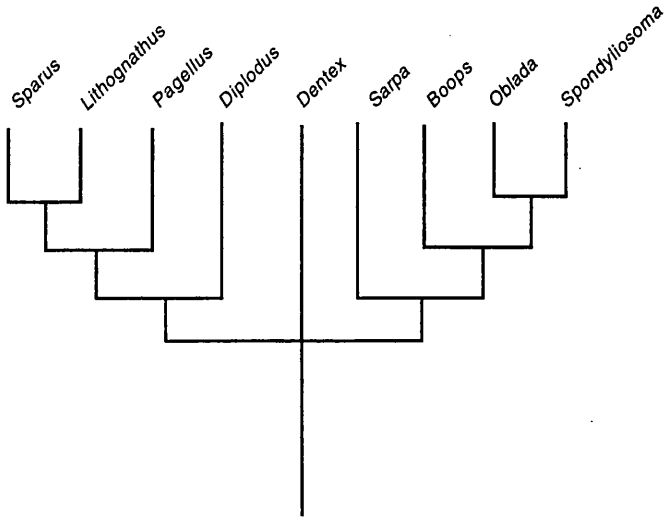

Figure 1.1 Phenogram of selected sparid genera based on isozyme data. Redrawn from Basagila (1991)

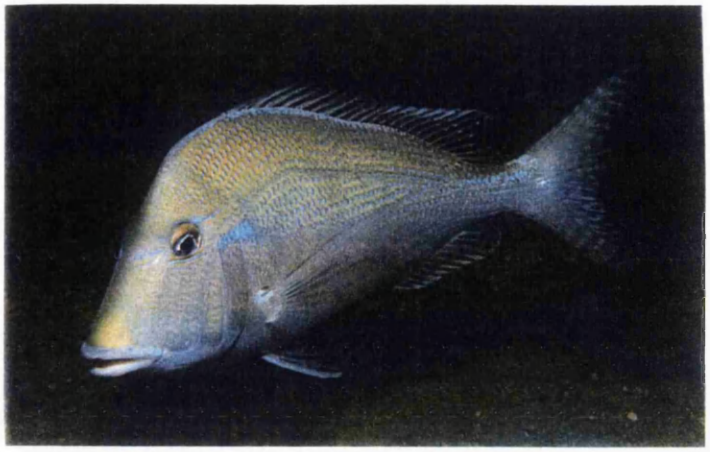

Calamus proridens

Archosargus rhomboidalis

Diplodus holbrooki

from P. Humann (1994)

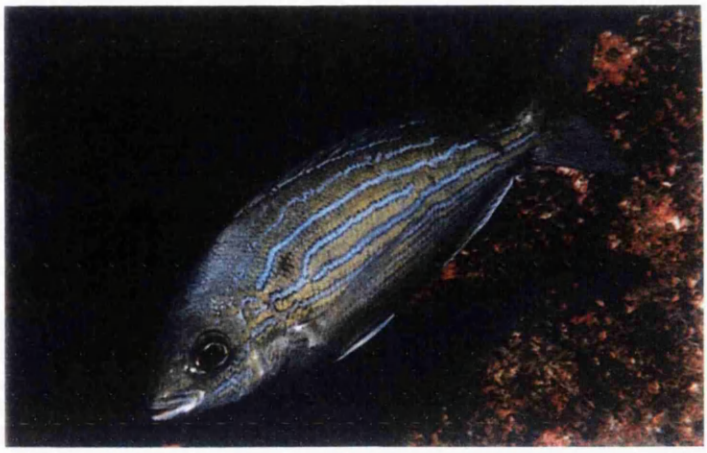

Lagodon rhomboides

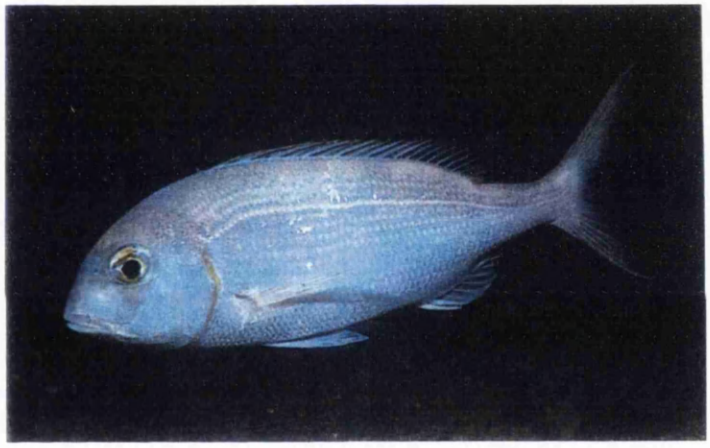

Pagrus pagrus

Archosargus probatocephalus

from P. Humann (1994)

CHAPTER 2

COMPARATIVE MORPHOLOGY OF THE SPARIDAE

"... good morphology lasts forever, whereas today's matrix and the cladograms it yields will soon be superseded."

Colin Patterson (1998)

Introduction

Sparids, like many families of the suborder Percoidei are poorly defined anatomically and as a consequence of this their relationships remain obscure (Johnson 1980). To answer questions concerning family interrelationships, and ultimately higher order relationships, it is necessary to elucidate variation at the family level. The aim of this chapter is to document the morphological variation across the Sparidae with respect to related groups.

This chapter is divided into two parts. Part one presents a detailed description of *Dentex dentex,* a basal member of the Sparidae, while the second part of this chapter examines the comparative morphology of 28 additional genera (listed on p 5) with reference to the initial description. The work presented here provides a comprehensive morphological review of the Sparidae, building on morphological studies of Akazaki (1962); Johnson (1980) and Rosen and Patterson (1990). In order to assume taxonomic validity for each genus the type species is examined where possible.

Observations from the other families of the superfamily Sparoidea: Centracanthidae, Lethrinidae and Nemipteridae, provide an opportunity to examine the morphological diversity of the Sparidae with regards to their closest allies, in addition to providing character polarity. Representatives of three other lower percoid families; Haemulidae, Lutjanidae and Centropomidae are included to provide further character polarization with respect to the ingroup.

Based on the comparative anatomy present here, a character list and data matrix are formulated for phylogenetic analysis which is discussed in the next chapter.

Part 1 OSTEOLOGY OF THE BASAL SPARID *Dentex dentex*

The genus *Dentex* (Cuvier, 1814) was chosen for the principal description as it represents a morphologically generalized sparid that can be used as a reference for interpreting variation of morphological features (characters) in other genera. A detailed morphological study of the osteology of *Dentex dentex* (Linnaeus, 1758) therefore provides a basis for further comparative work and phylogenetic analysis of the family Sparidae. *Dentex dentex* is chosen here as a representative of the genus *Dentex* due to its status as the type species.

SYSTEMATIC ZOOLOGY

Division TELEOSTEI sensu Nelson, 1969
Order PERCIFORMES Bleeker, 1859
Suborder PERCOIDEI Bleeker, 1859
Superfamily SPAROIDEA Johnson, 1980
Family SPARIDAE Bonaparte, 1852
Genus DENTEX Cuvier, 1814

Type species. Dentex dentex Linnaeus, 1758

Dentex dentex Linnaeus, 1758

1758 *Sparus dentex* Linnaeus: 281.
1830 *Dentex vulgaris* Valenciennes: 6: 220, pl. 153 in Cuv. & Val (1830).
1859 *Dentex vulgaris* Günther: 1: 366.
1893 *Dentex dentex* Linnaeus; Jordan & Fesler: 17: 505.
1969 *Dentex dentex* Wheeler: 350, fig. 117.
1971 *Dentex dentex* Fischer.
1973 *Dentex dentex* Tortonese: 407 in Hureau and Monod (1973).
1990 *Dentex dentex* Bauchot and Hureau: 793 in Quéro et al (1990).
1998 *Dentex dentex* Eschmeyer: 469.

Diagnosis (emended)

The body is oblong. The colour is metallic blue, speckled with darker blue spots and the sides may have a yellow/pink hue in older individuals.

External features include a row of caniniform teeth along the occlusal margin of the jaws, with two prominent recurved caniniform teeth anterolaterally and a medial field of villiform teeth.

The combination of morphological features ('C' numbers refer to character matrix given in

full later) that distinguish this genus include the following unambiguous character states: C39 (descending process of the articular is the same length as the ventral margin of the dentary), C41 (a superior crest is present on the articular) and C82 (anterior processes of the supraneurals are separate).

Habitat, distribution and diet

Littoral to sublittoral, benthopelagic down to a maximum depth of 200m, found mainly on rocky sea floors. Distribution encompassing the Mediterranean, Adriatic, Black Sea (rare), Atlantic, British Isles (rare), Madeira Islands, Canary Islands and along the coast of West Africa, north of Cape Blanc. Predominantly carnivorous, feeding on fish and soft-bodied invertebrates such as cephalopods.

Other species

Dentex (Cheimerius) canariensis Steindachner, 1881; *Dentex (Cheimerius) gibbosus* Rafinesque, 1810; *Dentex (Polysteganus) macrophthalmus* Bloch, 1791; *Dentex (Polysteganus) maroccanus* Valenciennes, 1830.

DESCRIPTION

CRANIUM

Braincase; Ethmoid region (Figures 2.0 - 2.3)

A third of the total length of the braincase is formed from the vomer (Vo), ethmoid (Et), parasphenoid (Par) and the lateral ethmoids (Le), which together form the anterior part of the braincase or snout. The vomer is sutured posterodorsally to the ethmoid and to the lateral ethmoids, while the posteroventral margin inserts into an anteroventral fossa in the parasphenoid, forming a sharp ventrally concave margin. The vomer is edentulous as in all sparid fish, with the ventral surface inclined at a shallow angle.

The ethmoid is long and narrow, separating the lateral ethmoids and is sutured anteriorly to the vomer and posteriorly to the frontals (Fr). The dorsal surface of the vomer and ethmoid form a median crest (Figure 2.0: *cr.et.vo*) that is confluent with the dorsal surface of the frontals. A small premaxillary facet (Figure 2.0: *arvo*) on the anterodorsal margin of the crest is the result of the articulation with the articular processes of the premaxilla.

The orbitonasal canal and anterior myodome (amyo) are confluent. The myodome runs between the lateral ethmoids, and is divided longitudinally to form two separate chambers, which contains the n. olfactores and houses the insertion of the musculi oblique attaching to the eye.

The maxillary process (mx.p) of the palatine is accommodated in a shallow concavity along the postero- and anterolateral margins of the vomer and lateral ethmoids respectively. Posteriorly,

an oval anterolaterally inclined facet, the long axis of which is orientated anteroposteriorly forms the articulation point between the palatine and ethmoid (Figure 2.0: *arpl*).

Posteriorly, the lateral ethmoids form a preorbital flange. The width of braincase at the level of the preorbital flange equals the width of braincase at contact of the dorsal limb of the posttemporal (Figure 2.1b: *fptd*). The preorbital fossa forms a moderately large, deep triangular depression, that is situated along the dorsal margin of the preorbital flange. The medial margin of the fossa contacts the anterolateral margin of the frontals, while anteriorly it is level with the posterior margin of the nasals (Na).

A shallow anteroposteriorly orientated sulcus is present on the ventral surface of the lateral ethmoids and anteroventral part of the frontals (Figure 2.1a: *snlc*). The sulcus is connected to the nasal part of the laterosensory canal that exits at the contact between the nasals and frontals.

The frontals occupy much of the roof of the braincase. They cover an area that extends from the lateral ethmoids to approximately the anterior margin of the sphenotic (Sph). Immediately anterior to the occipital crest (occr), the frontals are inclined anteroventrally at an angle of 20°, (the angled is measured from a horizontal trajectory parallel with the vertebral column). Posterior to the anterior margin of the occipital crest, the frontals are horizontal. The frontals are separated by the supraoccipital (Soc) posteromedially, and are sutured to the ethmoid anteriorly and the lateral ethmoids anterolaterally. In addition, they are attached by connective tissues to the nasals anteriorly and to the sixth infraorbital (dermosphenotic) laterally, along the posterior margin of the orbit. The suture between the frontals is straight. In dorsal aspect, the frontals have a fine cancellose texture, with spaces that are <1mm. Posterior to the occipital crest, however, the rest of the dorsal surface of the skull roof is smooth. The frontals form the anterior third of the frontal crest, and the anteriormost part (about 5%) of the occipital crest. These two structures are separate anteriorly. A number of small foramina or pores, anterior to the frontal crest and which occur along the dorsal margin of this crest, form the openings of the laterosensory canal.

Occipital region

The parietals (Pa) are small, hexagonal bones that form part of the skull roof. They are separated by the supraoccipital medially and are sutured to the frontals anteriorly, the pterotic (Pto) ventrolaterally and the epioccipital (Epi) posteriorly. The parietals form a third of the frontal crest that transects the central part of this bone.

The posttemporal fossae (ptf) are large, deep, conical cavities that widen posteriorly, forming most of the dorsal occipital region. The fossae slope at a slightly oblique angle posteroventrally to the deepest point on the pterotic. The fossae open dorsolaterally, and are bounded medially by the epioccipital and parietals, and laterally by the pterotic and sphenotic. Anteriorly, the fossae penetrate into the posterior margin of the frontals. The frontal (Figure 2.1b: *fc*) and paretial crests (*pc*) form the medial and lateral walls of the fossae, which in posterior view are nearly vertical. The floor of the fossa is concave and is formed largely by the pterotic, and to a

lesser extent by the sphenotic (Sph). The fossa receives the epaxial trunk muscles (Stiassny 1986).

The supraoccipital is a large bone that covers the median part of the posterior skull roof, forming a prominent medial crest. In dorsal aspect the supraoccipital is sutured to the frontals anteriorly, the parietals laterally and the epioccipitals posteriorly. In occipital aspect, the supraoccipital separates the exoccipitals medially by a ventral spur: the spina occipitalis (sp.occ). The occipital crest is a prominent feature of the neurocranium, extending over half the length of the skull. Anteriorly, it is level with the central point of the orbit, extending posteriorly so that the apex is level with the dorsal margin of the foramen magnum (fm). The length of the crest is greater than the height. The dorsal margin is convex whereas the posterior margin is gently concave. The increase in size of the occipital crest in acanthomorph fishes, has become a new site for muscle insertion, due to the anterior extension of the m. epaxialis (Stiassny 1986). The spina occipitalis initially described by Allis (1909) extends ventrally between the epioccipital and exoccipitals forming the dorsal margin to the foramen magnum (Figure 2.0: *sp.occ*) and is a character of acanthomorph fishes (Stiassny 1986: 432). A posterodorsal ridge extending from the base of the spina occipitalis either side of the occipital crest is presumably for strengthening the crest.

The exoccipitals cover much of the central part of the occipital region of the cranium. They are separated dorsomedially by the supraoccipital, whilst they are sutured dorsally to the epioccipital, laterally to the pterotic and ventrally to the basioccipital. The exoccipital condyles (exocc) contact medially, forming the ventral margin of the foramen magnum. The condyles are inclined posteroventrally, however, it is only the lateral semielliptical face that contacts the prezygapophyses. The ventral margin of the foramen magnum is horizontal, whereas the dorsolateral margin is convex. The height and width of the foramen magnum are approximately the same. In lateral aspect, the margin forming the foramen magnum and the exoccipital condyles extend posteriorly from the basioccipital (Boc) to a point which is equal to that of the posterior extremity of the occipital crest. Dorsolateral to the foramen magnum is the sub epioccipital fossa (Figure 2.2: *sef*), a shallow, oval, depression, the greater axis of which is orientated dorsoventrally. In lateral aspect, the exoccipitals contacts the prootic anteriorly, the pterotic dorsally and the basioccipital ventrally.

The foramen n.vagi (X) is large opening leading to a dorsomedially orientated canal. This foramen is situated anterolaterally to the exoccipital condyles. Just anterior to this foramen, is the smaller foramen n. glossopharngei (IX). The foramen n. spino-occipitalis is ovoid, the posterior canal of which is inclined lateroventrally. The long axis of this foramen extends along the lateral margin of the exoccipital condyles.

The basioccipital forms the posteroventral corner of the neurocranium. In lateral aspect the basioccipital narrows posteriorly to form the occipital condyle, the external margin of which becomes raised so that it articulates with the corpus of the first vertebrae. The occipital condyle (occ) is circular in posterior view with a diameter similar to that of the foramen magnum. Directly

dorsal to the occipital condyle is the exoccipital condyle.

In lateral aspect the basioccipital is bordered by the exoccipital dorsally, the prootic (Pro) anteriorly and the parasphenoid ventrally. A small, deep circular fossa situated just anterior to the occipital condyle is the site of origin of Baudelot's ligament (Figure 2.0: *fbl*). This ligament passes around a dorsal process on the cleithrum, and inserts on the medial face of the supracleithrum (Johnson and Patterson, 1993: 605-6). Ventrally, the basioccipital forms the roof of the posterior myodome (pmyo), which opens posteriorly. The myodome is floored anteriorly by the parasphenoid, while the basioccipital forms the floor to the cavum sinus imparis.

The foramen opticum is by far the largest opening in the skull, occurring in the posterior wall of the orbit. A medial sulcus on the ventral surface of the frontals extends from the dorsal margin of the foramen opticum to the anterior myodomes. The sulcus forms one third of the width of the skull roof. The foramen is deeply concave ventrally, its margins are formed from the basisphenoid posteriorly, prootics laterally and the frontals dorsally. There is no foramen n. oculomotori (III) so presumably it exits from the opticum foramen. The olfactory nerves emerge through a foramen (I) at the anterior end of the foramen opticum, and run anteriorly to the ethmoid region of the orbit.

Otic region (Figure 2.0-2.2)

The epioccipital forms the dorsoposterior corner of the braincase. In occipital aspect, the epioccipitals are separated ventromedially by the spina occipitalis, medially by the supraoccipital and are sutured ventolaterally to the pterotic. Laterally, the epioccipital borders the parietal anteriorly and the pterotic ventrally. The epioccipital contributes to the posterior third of the frontal crest. This crest extends posteriorly to form a shallow, dorsally orientated fossa that articulates with the dorsal process of the posttemporal (Figure 2.1b: *fptd*). A spine like projection extends posteromedially from the fossa to a point level with the margin of the foramen magnum.

The pterotic is sutured to the epioccipital dorsally, the sphenotic anteriorly, the intercalar (Ic) ventrally, the prootic anteroventrally, and the exoccipital posteromedially. The pterotic crest is present along the dorsal face of the bone, the posterior margin of which forms a small, shallow, fossa for the articulation of the ventral process of the posttemporal (Pt). The laterosensory canal enters the pterotic through a pore in the posterior margin of the pterotic crest, continuing along the thickened dorsal margin of the crest that is punctuated by approximately three additional pores. A large oval facet, that articulates with the posterior condyle of the hyomandibular (Hyo) is associated with both the pterotic dorsally and the intercalar ventrally. The suture between these bones bisects the centre of this facet. The facet is inclined lateroventrally; the long axis of which is orientated anteroposteriorly. Directly anterior to this facet, is a second facet that articulates with the anterior condyle of the hyomandibular.

The intercalar is a small, ventrally facing bone (Figure 2.1a: *Ic*), which is sutured to the prootics anteriorly, the exoccipitals posteroventrally and the pterotic dorsally. The posterolateral margin of the intercalar extends posteroventrally forming a narrow process for the attachment of

the m. levator operculi, the lateral margin of which is the surface of origin for this muscle (Figure 2.1a: *plo*). The lateral margin also forms the ventral part of the posterior hyomandibular condyle.

In ventral view the subtemporal fossa covers much of the ventral surface of the intercalar and the prootic (Figure 2.1a: *stf*). The fossa is shallow, with a straight medial margin and has a convex lateral margin.

In lateral aspect the sphenotic contacts the frontals anterodorsally, the parietals posterodorsally, the pterotic posteriorly, and the prootic ventrally. The sphenotic forms the anterolateral margin of the otic region, contacting the prootic medially. A circular, deep facet inclined ventrolaterally, articulates with the anterior condyle of the hyomandibular. The facet is situated on the anterolateral margin of the suture between the prootic and sphenotic. On the anterior face of the sphenotic is a small, centrally situated foramen for the otic branch of the facial nerve (VII).

The dilatator fossa (df) accommodates the m. dilatator operculi. The fossa extends anteriorly over approximately one third of the roof of the orbit and is limited anteriorly by the post-orbital process of the sphenotic and by the posterior margin of the pterotic (Figure 2.0: *df*). A circular foramen on the anterior face of the sphenotic and frontals, situated centrally over the suture between these bones allows the m. dilatator operculi to penetrate through and attach on the ventral surface of the frontals. The m. dilatator operculi originates from the frontals and inserts on the anterodorsal face of the opercular (Winterbottom 1974).

The prootics form much of the floor of the cranial cavity, and the roof of the posterior myodome. Below the sub-temporal fossa, the otic region narrows ventrally. However, dorsal to the pharyngeal apophysis the prootics become distended laterally. The ventral margin of the prootics are convex and are sutured to the parasphenoid ventrally, the basioccipital posteroventrally, the exoccipital posterodorsally, the sphenotic anterodorsally and the pterotic posterodorsally. Anteriorly, the prootics are separated by the basisphenoid, and form the lateral margins of the foramen opticum. The foramen that transmits the middle celebral vein occurs in the anterior wall of the prootic, near to the margin of the foramen opticum. However, the presence of this foramen appears to be inconsistent from specimen to specimen.

Trigemino-facialis chamber (Figure 2.3)

The trigemino-facialis chamber is a complex cavity, described here with reference to the works of Allis (1919) and Patterson (1964: 434-440; 1975). The cavity forms the anterolateral wall of the neurocranium, and is divided into the internal pars ganglionaris, which houses the ganglia of the profundus, trigeminal and facial nerves and the external pars jugularis. The pars jugularis (pj) is a horizontal canal running anteroposteriorly through the prootic, which is particularly short in perciform fishes (Patterson, 1964: 437).

The lateral commissure (lcom) carries the jugular canal, which enters and exits through the anterior and posterior openings of the pars jugularis. The commissure is divided into an anterior and posterior pillar, thereby giving rise to an anterior (pja), middle (pjm) and posterior (pjp)

opening (Figure 2.0). Patterson (1964: 435) noted that in all perciform skulls, the pars jugularis has two openings, except the families Scorpaenidae, Monodactylidae, Kyphosidae and Sparidae which have three openings, the latter condition also occurring in Beryciformes. The number of opening in the pars jugularis in the superfamily Sparoidea appears variable, with between three to four openings in Centracanthidae, three in Sparidae, while there are two openings in Nemipteridae and Lethrinidae (Johnson 1980).

The anterior opening in the pars jugularis carries the buccal branch of the facial nerve (VII) and the buccal branch of the trigeminal nerve (V) that link together to form a compound nerve. Similarly the superficial ophthalmic branch of the facial (VII) and the superficial ophthalmic branch of the trigeminal (V) also link together to form a compound nerve. The otic branch of the facial nerve (VII) and the profundus nerve also pass through the anterior opening of the pars jugularis. An obliquely inclined lateral flange extends from the posterior pillar of the lateral commisure, and is flush to the anterodorsal edge of the foramen on the medial face of the hyomandibular for transmission of the hyomandibular trunk of the facial nerve (VII). In all extant members (and presumably fossils) of the taxonomic groups mentioned in the above paragraph, the hyomandibular trunk of the facial nerve (VII) passes through the middle opening of the pars jugularis (Greenwood 1986). The posterior opening of the pars jugularis carries the hyoid branch and mandibular branch of the facial nerve (VII).

In the medial wall of the pars jugularis are two large foramina, the foramen trigeminale, which accommodates the trigeminal nerve and the buccal and otic branches of the facial nerve, and the foramen facialis, lying dorsal to the foramen trigeminale and housing the hyomandibular trunk of the facial nerve. The foramen for the superficial ophthalmic pierces the anterior face of the prootic dorsal to the foramen trigeminale. A narrow sulcus extends dorsally from this foramen to the lateral margin of the foramen opticum. Medial to this foramen and situated directly laterally to the precommisure bridge is the foramen profundus.

Posterior myodome

In teleosts the posterior myodome (Figure 2.1a: *pmyo*) is developed in the basisphenoid (Bsp) of the skull in teleosts, extending back to the basioccipital, due to the lengthened musculi recti externi and musculi recti interni (Goodrich 1930). The myodome is separated from the cranial cavity by the prootics dorsally. The parasphenoid and basioccipital form the anterior and posterior floor of the myodome, which opens posteroventrally. The myodome is divided into left and right entrances by the basisphenoid pedicel (Figure 2.0: *bsp.pd*).

The parasphenoid forms the ventral margin of the braincase. It is sutured to the vomer anteriorly, the basioccipital posteriorly, the prootics posterodorsally and to the basisphenoid pedicel dorsally. Along the contact between the parasphenoid and prootic is the foramen arteria interna carotidea. The ventral margin of the parasphenoid is concave narrowing ventrally to form the parasphenoid carina or keel (parc), the sides of which form the attachment site for the m. adductor arcus palatini.

Pharyngeal apophysis

On the otico-occipital region of the parasphenoid, a ventral median process, level with the anterior limit of the cranial cavity has also developed for the attachment of the m. adductor arcus palatini (Figure 2.0: *ap*). This process is laterally flattened, narrowing ventrally. Posterior to this process, and directly ventral to the convex margin of the prootic is the pharyngeal apophysis of the basicranium (Figures 2.0, 2.1a: *pha*). The apophysis attaches to an articular process of pharyngobranchial 3 (PB3) of the upper pharyngeal jaw (UPJ: Rosen and Patterson 1990). On the ventral (articulation) surface of the pharyngeal apophysis a v-shaped indentation is present, the point of which is continuous with the elevated part of the parasphenoid carina.

The basisphenoid is a small median bone that forms the ventral margin of the foramen opticum, and contacts the dorsal surface of the parasphenoid through the basisphenoid pedicel. The pedicel is a narrow, laterally flattened bone that in adult specimens develops a flange along the dorsal margin. Posterior to the pedicel is the foramen n. abducens (VI), which allows the n. abducens to enter the roof of the myodome and innervate the external rectus. The basisphenoid tapers posteriorly forming the anteroventral floor of the braincase, and is sutured with the prootics on all other margins.

Cephalic sensory canal (cranium)

The laterosensory canal enters the braincase through a large pore at the posterolateral margin of the pterotic crest. The pterotic crest is perforated along its dorsal margin anteriorly by pores for the passage of the otic canal, which joins the infraorbital canal, in addition to the supraorbital canal prior to entering the frontals just anterior to the occipital crest. The passage of the supraorbital canal through the dorsal surface of the frontals is evident by five small pores. The canals of the pores are orientated anteriorly, apart from the posterior most pore, the canal of which is orientated dorsally. The laterosensory canal exits from the frontals posterior to the contact between the nasals.

***Nasals** (figure 2.1b)*

The nasal is a long, slender, flat bone that tapers anteriorly. It is connected posteriorly by strong connective tissue to the anterior margin of the frontals. The nasal forms a tube, which contains the most anterior part of the supraorbital canal of the laterosensory system.

Oral jaws

Dermal upper jaw (Plate 2.0, Figure 2.4a)

The ascending process of the premaxilla (as.p.pm) is shorter in length than the alveolar process (al.p.pm). The distinction of which is, however, less apparent in younger individuals examined. The ascending processes of the premaxillae contact medially along a smooth, narrow symphysis, sheathed by connective tissue and the entire length of the articular process of the premaxilla is confluent with the posterior margin of the ascending process (Figure 2.4a: *ar.p.pm*).

The alveolar process is slender, tapering posteroventrally and is four-fifths as long as the maxilla. The dorsal margin of the alveolar process is straight. The distal end of the alveolar ramus is bifurcated forming a groove for the reception of the ventral margin of the maxilla.

The maxilla has a knob-like dorsal crest (Figure 2.0: *mdc*) which is separated from the articular condyle (ar.p.c) by an oblique, sulcus, the anterolateral margin of which extends to a point level with the first anterolateral tooth of the premaxilla (Figure 2.4a: *ps*). The sulcus is short, but fairly deep, and accommodates the maxillary process of the palatine. The articular condyle clasps the posterior margin of the articular process of the premaxilla (ar.p.pm), and exhibits a small facet on its medial surface from this contact. The condyle also contacts the vomer forming a distinct facet on the anterodorsal crest of the vomer (Figure 2.0: *arvo*). Extending laterally from the lateral margin of the palatine sulcus is a small process that is inclined posterolaterally. The posterior margin of the maxilla (Mx) is blunt, and extends beyond the premaxilla. The maxilla is tightly bound anteriorly to the ascending process of the premaxilla by connective tissues.

Mandible (Plate 2.0, Figure 2.4b)

The mandible comprises three bones, the dentary (Den), articular (Art) and angular (An). The dentary is a long, narrow bone forming about three quarters of the total length of the lower jaw. The symphysis is short, approximately a quarter of the total length of the dentary and is orientated vertically forming a small ventral symphyseal process (Figure 2.4b: *psym*). The rami are connected anteriorly along the smooth symphysis by connective tissue. Four, shallow oval fossae, the long axes of which run anteroposteriorly, occur along the lateroventral surface of the dentary. Foramina present in both margins of the fossae transmit the mandibular canal of the lateral sensory system that runs from the preopercle along the ventrolateral face of the articular, before entering the dentary. The articular fossa is a deep, triangular cavity in the posterior margin of the dentary.

The articular is triangular, its height is approximately two-thirds its length. The anterior ascending process of the articular inserts into the articular fossa, and is attached within the dentary by connective tissues. The articular has a high, narrow ascending posterior process that flares slightly dorsally and is the same height as the coronoid process. Along the posterior margin of the articular is the fossa for the articulation of the quadrate. Below the fossa, the descending process (Figure 2.4b: *d.p.art*) is confluent with the ventral margin of the dentary.

The angular is small and oval, occupying the ventrocaudal corner of the articular and forming the posterior margin of the descending process. Laterally, the bone reaches its maximum thickness above a dorsally concave ridge occurring along the central axis of this bone.

Dentition

The alveolar process of the premaxilla bears a single row of caniniform teeth along its ventral margin. There are two large anterolateral recurved caniniform teeth, or fangs which are much larger than those along the ventral margin. In addition, there is a band of villiform teeth along the entire medial margin of the premaxilla. The dentition of the dentary is similar to the

premaxilla. The teeth along the occlusal margin do not extend along the coronoid process.

Infraorbital region *(Plate 2.0, Figure 2.5b)*

There are six infraorbitals. The first and second infraorbitals are large, rectangular bones, while the remainder are tubular. Infraorbital I attaches to the braincase by a small ventrally inclined medial process along the posterior margin of the lateral ethmoid. It covers much of the anterior region of the maxilla and extends ventrally to the centre of the alveolar process of the premaxilla. Infraorbital II likewise covers the posterior part of the maxilla, extending as far as the ventral margin of this bone. Vertical ridges are prominent on these bones in adult specimens. Infraorbital III, bears a well developed subocular shelf, that extends anteriorly to a point level with the lateral ethmoid process of infraorbital I. The width of the subocular shelf covers three quarters of the cavity between the infraorbitals and the parasphenoid. The dorsal and anterior margin of infraorbital VI is freely suspended from the sphenotic.

The infraorbital branch of the laterosensory canal passes through the infraorbital bones close to the dorsal margin, branching ventrally along its length and terminating at the anterior margin of infraorbital I.

Hyo-palatine bones *(Plate 2.0, Figure 2.5a)*

The palatine (Pl) has a long anterior maxillary process (Figure 2.5: *mx.p*), that is laterally deflected and is accommodated by the palatine sulcus of the maxilla. An anteroventral facet has formed from the articulation of the maxillary condyle. This process is attached to the maxilla by connective tissue. A posteromedially inclined facet along the dorsal margin of the palatine articulates with the ethmoid. The posterior process of the palatine extends beyond this facet, and is level with the anterior margin of the orbit. The palatine forms a concave anterior margin, contacting the ectopterygoid (Ecp) posteriorly and tapering ventrally, where it contacts the endopterygoid (Enp).

The ectopterygoid is a long, thin, vertical bone that contacts the posterior margin of the palatine and the anterior margin of the quadrate (Q). The ectopterygoid does not extend as far as the quadrate condyle.

The endopterygoid is a small irregular sheet of bone, that contacts the ectopterygoid anteriorly, the palatine dorsally, the metapterygoid (Mpt) posteriorly and the quadrate ventrally.

The metapterygoid is a large sheet of bone that is medially concave, forming the central part of the palate. The anteroventral margin is slightly convex and is separated from the quadrate by a fontanelle, which is observed in both juvenile and adult specimens. The posterior margin is straight and contacts the anterior margin of the hyomandibular, the ventral margin contacts the symplectic (Sym)and preopercle (Pop).

The quadrate is shaped like a sector of a circle, the centre of which forms the bicondylar quadrate condyle. The lateral condyle is larger than the medial condyle. The ventral margin of the

quadrate extends over the ventral limb of the preopercle, forming a ridge confluent with the quadrate process, which flattens posteriorly. The quadrate contacts the ectopterygoid anteriorly, the metapterygoid dorsally and the symplectic posteriorly.

The symplectic is an anteriorly tapering rod-like bone that is posteriorly expanded. It is accommodated by the symplectic incisure, a narrow sulcus on the medial face of the quadrate. The posteroventral margin is expanded and lies against the metapterygoid.

The hyomandibular articulates with the otic region of the neurocranium, via a double condyle along the dorsal margin of the head. The hyomandibular is broad dorsally, while ventrally it forms a narrow rod that lies almost vertically against the anterior margin of the preopercle. The anterior hyomandibular condyle is circular and articulates with the sphenotic and prootic, whilst the posterior condyle is ovoid and articulates with the pterotic and intercalar. The opercular condyle is situated on the posterior margin of the hyomandibular, is short and also circular. The hyomandibular crest converges with the posterior process, continuing ventrally along the ventral process and terminating two-thirds of the way along its length. The dorsal and ventral parts of the crest lie 60° apart. Anterior to the crest and ventral to the posterior condyle the hyomandibular forms a triangular shaped sheet of bone, the ventral margin of which is in contact with the metapterygoid. The truncus hyomandibularis n. facialis enters the hyomandibular through the large foramen n. facialis hyomandibulare (VII) in the medial face, just posterior to the anterior process. The canal of this foramen is orientated posteroventrally to emerge on the lateral face (Figure 2.5a *VIImd*). Posterior to the crest is a shallow sulcus in which the anterior margin of the opercle rests. Along the anterior edge of this sulcus, are two foramen that open posteroventrally, through which presumably the ramus hyomandibularis n. facialis passes, feeding the preopercle and opercle (Op). The large, foramen n. mandibularis and its associated canal are orientated posteriorly. This foramen is situated on the posterolateral margin of the ventral process, directly ventral to the terminal point of the crest.

***Opercular bones** (Plate 2.0, Figure 2.5a)*

The preopercle is bent through about 52°, the dorsal limb of the bone being three times as long as the ventral limb. The dorsal limb of the bone is broad, and is of a similar length to the angle, while the ventral limb is significantly narrow, half that of the dorsal limb. The flange of the preopercle is greatly expanded at the angle to its maximum width, tapering dorsally to approximately two thirds of the total length of the dorsal limb, and is reduced to one third of the maximum width at the distal end of the ventral limb. The posterior margin is convex and is ornamented with a row of equally spaced faint ridges that are perpendicular to the posterior and ventral margins. The anterior margin of the dorsal limb of the preopercular is accommodated by the sulcus hyomandibularis forming a confluent ridge with the crista hyomandibularis. The ventral limb of the preopercular is overlain by the ventral margin of the quadrate.

The preoperculo-mandibular canal runs posteriorly through the dentary, continuing as a

short sulcus from the posterior margin of the dentary into the anterior margin of the articular, traversing the dermal tissues between the mandible and preopercle, before entering the latter (Allis 1903). Foramina on the medial face of the preopercle transmit branches of the externa n. mandibularis to innervate the laterosensory canal.

The opercle is broad dorsally narrowing ventrally. The anterior margin of the opercle is overlain by the dorsal limb of the preopercle, while the posteroventral margin overlaps the subopercle (Sop). A circular fossa on the medial margin is for the articulation of the opercular process of the hyomandibular. The posteriormost corner of the fossa is raised forming the highest point of an opercle crest. The crest runs across the widest part of the opercle in an anterodorsal-posteroventral orientation, extending a little way beyond the posterior margin as a short, stout projection. On the lateral face of the opercle, directly posterior from the fossa, is the foramen ramus n. vagus. A narrow sulcus joins this foramen and runs some way along the length of the bone.

The subopercle is a long, slender bone, which narrows dorsally. It is overlain dorsally by the opercle, and anteriorly by the interoperulum. Anteriorly, the long, pointed dorsal process lies against the medial contact between the hyomandibular and the opercle.

The interopercle is roughly oval in shape, overlain dorsally by the preopercle, and contacting the subopercle posteriorly. Anteriorly, the interopercle is connected to the mandible by connective tissues.

Lower part of the hyoid arch *(Figure 2.6a)*

The lower part of the hyoid arch comprises six bones. Two, small anterior bones: the dorsal hypohyal (Hd) and ventral hypohyal (Hv) are separated from each other by the cartilage surrounding their margins. The ventral hypohyal is the larger and bears a short ventral process on to which ligaments from the urohyal are inserted.

The ceratohyal (Ce) forms the central and largest bone of the hyoid arch. In juveniles, it is rectangular in shape, becoming expanded at the distal ends in adults. Along the anterodorsal margin of the ceratohyal a small process is present that contacts the dorsal hypohyal. The ceratohyal is sutured posteriorly to the epihyal (Eh). The suture between the ceratohyal and epihyal is straight on the lateral face, while on the medial face it is interdigitated.

The posteriormost element of the arch is the epihyal, which tapers to a knob-like process posteriorly. On the lateral face of the ceratohyal and epihyal, parallel to the dorsal margin is a sulcus receiving the hyoid artery (Patterson 1964). The sulcus is narrow anteriorly becoming posteriorly expanded (FIgure 2.6a: *sha*).

The interhyal (Ih) is a stout rod, that is attached by cartilage to the epihyal process dorsally, and to the ventral process of the hyomandibular medially.

The urohyal (Uh) is a medial element attached by ligaments via an anterior process to the hypohyals (Figure 2.6b). It is thickened ventrally, having a convex dorsal and ventral margin, and

a concave posterior margin. The posteroventral margin extends posteriorly as a short spine.

Branchiostegal rays

There are six branchiostegals that articulate with the ventral margin of the hyoid arch. The two anterior rays are slender, while the rest are much larger, having broad proximal heads. McAllister (1968) defined the shape of these branchiostegal rays as acinaciform (from the Latin *acinaces* or scimitar). Rays i-iv attach to the ceratohyal, ray v attaches to the interspace between the ceratohyal and epihyal and ray vi attaches to the epihyal (Figure 2.6a: *Br*).

Gill arches *(Figure 2.6c)*

The glossohyal (basihyal: Bh) is edentulous, and forms the anteriormost element of the hyoid arch. It is conical shaped, narrowing posteriorly and partly overlying the first basibranchial. There are four basibranchials arranged in line. The anterior three basibranchials are rod-like bones, whereas the fourth is a small triangular cartilage. Lateral to the basibranchials is hypobranchial 1 of the first gill arch, which connects to the contact between the first and second basibranchials. Hyobranchial 1 (Hyb 1) is long and slender with a small weakly developed anterior process mid-way along its length. Hyobranchial 2 (Hyb 2) connects to the dorsolateral margin of the third basibranchial and is also narrow. There are four dome-shaped gill rakers along the anterolateral margin. Hyobranchial 3 (Hyb 3) is connected to the ventrolateral margin of the third basibranchial. Unlike the first and second hypobranchials, this bone is dorsoventrally flattened and posteriorly expanded. Two dome-shaped gill rakers are present along the anterolateral margin of this bone.

Lateral to the hypobranchials are five pairs of ceratobranchials (Cb), which are long rod-like bones. There are 11 gill rakers on the anterolateral margin of ceratobranchial I that have the form of slender attenuated isosceles triangles. These elongate rakers become progressively larger distally. They are inclined anteriorly and have a narrow band of teeth covering the dorsomedial face. On the medial face of ceratobranchial 1 and on both margins of ceratobranchials 2- 4 small isolated dome-shaped rakers are present, the entire surface of which is covered with teeth. Each ceratobranchial has two pairs of 11 gill rakers orientated along the long axis of each bone.

Lower Pharyngeal Jaws (LPJ)

The lower pharyngeal dentition consists of an elongated tooth plate fused with the fifth ceratobranchial. The anterior halves of the tooth plates contact each other medially (Figure 2.6c) the plates have been pulled apart) forming the greatest dentigerous area. The tooth plates are gently concave dorsally, and are covered with posteriorly recurved isolated caniniform teeth, that become larger rostromedially. The fifth ceratobranchial forms a medial ventral keel, which extends anteriorly and posteriorly beyond the margin of the tooth plate.

Upper Pharyngeal Jaws (UPJ: Figure 2.7)

There are four pairs of epibranchials (E1-4)) that contact ceratobranchials 1-4. Epibranchials 1-2 are long, slender bones, of which epibranchial 1 is the longest. Dorsally,

epibranchial 1 has a uncinate process along the dorsal margin that attaches to the interarcual cartilage (IAC). This cartilage has a long cyclindrical form, which is approximately one-fifth or less of the total the length of epibranchial 1. There are eight rakers along the anterior margin and three rakers on the posterior margin of the first epibranchial, while there are a further three rakers along the anterior margin of the second epibranchial. The lateral two rakers on the first epibranchial are elongate in form, whereas the other rakers on the first and those on the second epibranchial are dome-shaped. The medial and lateral margins of epibranchial 2 are a similar size, with distinctive central flanges on the anterior and posterior margins of the bone. Epibranchials 3 and 4 are considerably shorter and stouter than the first two epibranchials with a single uncinate process (defined as having a cartilage tip) along their posterior margins. The uncinate processes are shorter than the distance from the process to the distal margin of the epibranchial.

The upper pharyngeal dentition consists of four tooth plates. The anterior most tooth plate is fused with the second pharyngobranchial (PB2), associated with a cartilage forming the anterior, medial and posterior margins. Directly behind this tooth plate is the smaller autogenous second epibranchial toothplate (ET2: Johnson 1980). Posteriomedial to these toothplates is a much larger tooth plate that is fused with the third pharyngobranchial (PB3). Directly posterior to PB3, is the small cartilage PB4 that appears to be separate, rather than attached to PB3. The upper pharyngeal tooth plate 4 (UP4) forms the posterior-most tooth plate of the UPJ. The tooth plates PB2 and ET2 are narrow in this genus, their lateral and medial margins forming a constant width. In contrast the tooth plates PB3 and UP4 are larger, the lateral margin of UP4 forming a greater width than the medial margin of PB3. The pharyngeal apophysis in relation to PB3 is described as being amphiarthrosis (Rosen and Patterson, 1990) i.e. having a mixed articulation, so that the dorsal gill arch muscle and connective tissue intervene between PB3 and the bony pharyngeal apophysis of the basicranium. There is a definite articular facet on the dorsal surface of PB3 is present in this taxon as in all other sparids examined (Figure 2.7: *ARPR*). The ventral surface of the tooth plates are covered with unicuspid caniniform teeth, that are larger on PB2 and PB3, than those on UP4 which are villiform. Distally these teeth are capped by a conical, decurved tip of brown or umber coloured acrodin (Rosen and Patterson 1990).

POST-CRANIAL SKELETON

Pectoral girdle and fin *(Figure 2.8a and b)*

The posttemporal (Plate 2.0) is characterized by the usual anteriorly orientated dorsal and ventral processes. The dorsal process is dorsoventrally flattened and slightly longer than the ventral process, articulating with the dorsal fossa of the epioccipital (Figure 2.1b *fptd*). The ventral process articulates with a posterior fossa on the pterotic, just above the process for the attachment of the m. levator operculi. A large, smooth posteriorly convex flange extends above the posterior margin of the dorsal process. Ventrally, the posttemporal contacts the supracleithrum by a ventrally inclined facet occurring at the junction of the two processes.

There are three extrascapular (Exa 1-3), that together form a narrow Y- shaped, tubular series lying anterolaterally to the post-temporal, although they are much thinner bones than the latter. The ventral process of the extrascapular is short and contacts the posterior margin of the epioccipital. The long dorsal process extends rostromedially, above the epioccipital and supraoccipital, meeting over the mid-line of the occipital crest and carrying the supratemporal commissure canal.

The supracleithrum (Scl) is elongate, tapering dorsally, and is thickened anteriorly. Its ventral margin lies lateral to the cleithrum.

The cleithrum (Cl) is the largest bone of the pectoral girdle. The ventral limb is inclined anteroventrally at an angle of 34° from the dorsal limb, which is only a quarter of the total length of the former. The dorsal limb contacts the supracleithrum medially, and extends dorsally as a spine. A posterior flange extends from the dorsal limb to just below the angle, forming a small, rounded projection ventrally. A medial crest runs vertically along the ventral limb, extending ventrally as a spine.

The scapula (Sc) contacts the cleithrum along its dorsal and anterior margins, while contacting the coracoid ventrally. It is wider than it is deep, with the large, oval foramen n. pterygialis (Allis 1903) lying in the centre of the bone. Along the posterior margin are three of the four shallow fossa for the articulation of the proximal radials.

The main body of the coracoid is a thinner bone than the scapula, although it is of a similar size. The anterior process is slender, and attaches to the ventral limb of the cleithrum. The fossa for the attachment of the fourth ray is situated along the posterior margin on the interspace between this bone and the scapula.

The dorsal postcleithrum (Pcl.d) lies against the medial face of the posterior margin of the cleithrum. It is thickened anteriorly, has a dorsally convex posterior flange, and narrows ventrally to a point. The ventral postcleithrum (Pcl.v) is a long, narrow bone that contacts the ventral edge of the medial face of the dorsal postcleithrum.

The four radials at the base of the pectoral fin, increase in size ventrally and articulate with approximately 15, soft pectoral fin rays.

Cephalic sensory canal system

On the lateral surface of the posttemporal, between the dorsal and ventral processes is a foramen, the associated canal of which opens anteriorly, in addition to a large, oval foramen situated posteriorly from the former. Both foramina are linked by an anterodorsally inclined canal that passes along the dorsal process into the extrascapular, the function of which is to convey the lateral line. There are also foramina on the surface of the ventral process of the posttemporal that carry the canal into the braincase via the pterotic.

Pelvic girdle and fin *(Figure 2.8b)*

The pelvic girdle is a two-dimensional structure in the median plane, embedded in the

hypaxial and carinal musculature. It is attached to the ventral process of the ventral postcleithrum a third of the way up its length by a ligament, and is inclined dorsally (Johnson and Patterson 1993). Pelvic girdles in percomorphs are convoluted structures with enlarged internal and external 'wings' that are strongly inclined dorsomedially (Stiassny and Moore 1992). The girdle is sutured cranially to two triangular sheets of bone (termed here as superficies cranialis), that contact each other medially. The superficies cranialis is divided centrally between a medial (Figure 2.8: *sfcm*) and a lateral superficies (*sfcl*). The superficies craniomedialis is inclined dorsally at approximately 40°. A ventral, medially orientated keel runs anteroposteriorly along a mid-sagittal plane of each superficies cranialis. The superficies cranolateralis is also dorsally inclined, but is much narrower than the superficies cranomedialis.

The subpelvic (subpp) and postpelvic processes (pstpp) are median pairs of prong-like processes on the ventral face of the girdle extending anteriorly and posteriorly respectively (Matsubara 1943). Johnson (1980) observed that in sparids the postpelvic process is well developed (Figure 2.8b: *pstpp*). In percomorphs they function as a partial attachment site for the m. infracarinalis anterioris as well as the m. abducens superficialis in some of the higher percomorphs (Yabe 1985).

The pelvic fin consists of five segmented soft rays and a large lateral pelvic spine.

***Vertebral column** (Plate 2.1)*

The total number of vertebrae is 24 (10 abdominal +14 caudal), including the last articulated vertebra, termed urostyle, following Gosline (1961). The centra are amphicoelous, thus limited motion is permitted in any direction (Hildebrand 1995). The anterior face of the first centrum is inclined anteroventrally, at an angle of 35° from the horizontal plane. The first two vertebrae are anteroposteriorly compressed, so that the neural arch of the second centrum overlaps the neural arch of the first centrum. The neural spines of the first and second centra are approximately two-thirds of the length of the suceeding spines. Eight pairs of ribs are associated with the third through tenth abdominal vertebrae, in addition to twelve pairs of intermusculars (epineurals), which start on the first vertebra. The 'neoneural' ligaments (Patterson and Johnson 1995: 41) are present throughout the superfamily Sparoidei, and related families.

***Dorsal fin** (Plate 2.1)*

The formula for the supraneurals and dorsal fin is 0/0+0/2+1/1/ (see Chapter 1 for construction of this formulae). The three supraneurals are strut-like bones with expanded anterodorsal process. The dorsal processes are separate from each other and do not overhang the preceding supraneural. However, the expansion of the anterodorsal process of the first supraneural is much greater, so that it overhangs the dorsal margin of the foramen magnum, but does not overhang the dorsal margin of the occipital crest.

The dorsal fin comprises XI + 12 fin rays. The spines of the dorsal and anal fins are

supported by bisegmental radials, in the'chain-link' articulation of Bridge (1896). The anteroventral margin of the first proximal middle radial bears two complete bony loops, each of which traverses a foramen at the base of the spine. The two spines articulate with the head of the first proximal radial, hence, two supernumerary fin spines are present. There is a general trend towards the reduction of dorsal supernumerary. Within the Perciformes, a single dorsal supernumerary spine is assumed to be derived (Patterson 1992). The suceeding spines are supported by the distal segment of each radial being tightly attached to the proximal radial. A hook-like process extends posteriorly and is connected by a ligament to a bony tubercle on the dorsocranial margin of the preceeding proximal radial. Thus, each spine is supported by two radials. The soft-rays do not exhibit the chain-link articulation of the spines, however, they do have a dual support (Johnson 1980: 35-36). The spinous rays are much longer than the soft rays, which are segmented and bifurcate in comparison. The fin membrane is continuous.

Anal fin *(Plate 2.1)*

The anal fin configuration is similar to the dorsal fin (Johnson 1980). The formula for the anal fin is III + 9. The first radial of the anal fin supports two spines, thus, two supernumerary fin spines is present, as in the dorsal fin. This radial is much larger than the others, as it is buttressed anteriorly, due to the attachment of both the first and second fin spines and extends to a point level with the last haemal arch. The second and third fin spines are greater in length than the first, being approximately twice as long.

Caudal fin skeleton *(Figure 2.9)*

There are five hypurals (HY1-5) associated with the last vertebra, which is formed by the fusion of the first ural and preural centra ('urostyle'; Gosline, 1961). All hypurals are autogenous, as is the parahypural and the haemal arch of the second and third preural centrum. The hypurals are separate from each other and there are no flanges on the dorsal and ventral margins of hypurals 2 and 3 respectively. Hypural 1 and 4 are twice the width of hypurals 2, 3 and 5. The hypurapophysis is well developed, extending posterodorsally to a point level with the anterior margin of hypural 2. The neural spine of the second preural centrum is reduced to a neural crest, which is a similar height to the crest upon uroneural 1 (Ur1).

The two uroneurals are autogenous. Uroneural 1 has a large anterodorsal crest that contacts the posterior margin of the neural crest of the second preural centrum. Uroneural 2 (Ur2) by contrast is a narrow rod-like bone. Both the parahypural (Pah) and the haemal spine of the second preural centrum have large anterior flanges that extend three quarters of the length of the bone. There is also a smaller cranial flange associated with the neural spine of the third preural centra.

There are three epurals (Ep1-3), lying between the neural spine of the third preural centra and uroneural 1. The epurals are elongated bones, the first of which is the largest of the series, extending ventrally so that the ventral margin is in close proximity to the dorsal margin of the

crest of the second preural centra.

The rays are segmented and branched; the inner principal rays also have small anterolateral flanges. The principal caudal fin ray formula is 9:8, in addition there are nine dorsal and ten ventral procurrent rays. The procurrent spur (Johnson 1975, 1980) is absent in all sparid fish.

Fujita (1990) recently described both the osteological and cartilaginous elements of the posterior fin skeleton. Interneural spine cartilage 4 (CINPU4) and interhaemal spine cartilage 4 (CIHPU4), directly anterior to the neural and haemal spines of the third preural centrum, are large, irregular ovoid cartilages. Interhaemal spine cartilage 3 (CIHPU3) is situated in between the haemal spine of the third preural centrum and the haemal spine of the second preural centrum. It is convex and elongated dorsally, whereas the ventral margin is straight. There are two, small posthaemal spine cartilages (CPHPU2), that lie just behind the haemal spine of the second preural centrum. Posthypural cartilage 5 (CPHY5) forms a narrow ovoid lying directly behind the posterior margin of the fifth hypural. Cartilage is also present along the posterior margins of the epurals, hypurals, parahypural, the haemal spines of the second and third preural centrum, and the neural spine of the third preural centrum.

Part 2 **COMPARATIVE MORPHOLOGY**

The second part of this chapter includes a comprehensive morphological review of sparid genera, so that skeletal variation between genera can be assessed with regards to character formulation. Comparative material is described with reference to characters throughout the text, which are written in parenthesis, and refer the reader to the character list and data matrix at the end of this chapter.

CRANIUM

Braincase

The overall form of the braincase differs remarkably among sparids, which display a great variation of morphological features and are biometrically disparate. Compared to the braincases of *Diplodus* or *Calamus* for example (Figures 2.10-2.12), the braincase described for *Dentex* (Figures 2.0-2.1) may be seen as conservative, differing little in overall shape from lutjanids, regarded as primitive percoids (Johnson 1980).

Ethmoid region

There is considerable variation of the ethmoid region among sparid genera, due to the reduction in length of the vomer, ethmoid and lateral ethmoids. Although hard to quantify, the use of different features on the cranium can help to solve this problem. In taxa such as *Dentex* and *Lithognathus* this region forms one third of the total length of the skull, as does the orbital and otico-occipital regions of the braincase. In contrast, this region in taxa such as *Diplodus, Lagodon*

and *Rhabdosargus* becomes dramatically reduced to approximately one sixth of the total length of the skull. While the distinction between these two extremes may be obvious, the intermediate constructions are variable and harder to quantify. The skull dimensions in *Calamus* are unique in that the ethmoid region forms two-fifths of the total length of the skull.

The vomer forms approximately two-thirds of the total length of the ethmoid region (or snout) and one-quarter of the total length of the braincase in *Dentex* and *Lithognathus* for example (measured along the ventral margin of the braincase). For the same measurements, taxa such as *Diplodus* and *Rhabdosargus* show that the vomer forms the total length of the snout, but approximately only one-sixth of the total length of the neurocranium. To quantify this difference in shape as a character, the suture between the vomer and parasphenoid is taken as a landmark and mentally projected vertically. In the former taxa mentioned, the suture is in the same plane as the posterior facet of the ethmoid for the articulation of the palatine and the anterior margin of the frontals, whereas in the latter taxa the anterior margin of the orbit is also in the same plane (character 1). In taxa with the latter construction, the snout also becomes inclined ventrally, with the vomer, ethmoid and particularly the lateral ethmoids becoming anteroposteriorly flattened, thus contributing to a reduction in snout length.

The median dorsal crest of the vomer and ethmoid present in *Dentex* occurs to varying degrees in other sparids. In taxa such as *Pagellus*, with a well developed dorsal crest (Figure 2.14a), a maxillary articulation surface develops on the anterodorsal margin, which is due to the articular process of the premaxilla articulating against the crest as the jaws open. The crest is greatly reduced in taxa where a depression has developed in the dorsal margin of the ethmoid for the ascending process of the premaxilla and as such, no articulation between the crest and articular process (character 2).

The development of a depression in the form of either a fossa or foramen is present along the dorsal margin of the ethmoid in taxa where the ethmoid-vomerine crest is weakly developed, covers an area directly anterior to the ethmoid-frontal suture. It is typically shallow in *Archosargus*, where the structures consists of two oval depressions either side of the midline, whereas it occurs as a deep, circular depression in *Calamus* (Figure 2.12). A posteroventrally inclined foramen is developed through the ethmoid-frontal suture in *Diplodus* (Figures 2.10-2.11), *Lagodon* and *Rhabdosargus* (character 3).

The ventral surface of the vomer is edentulous in sparoid fishes, but dentigerous in centropomids and lutjanids (character 4). Fine, villiform teeth cover the entire ventral surface of the vomer in centropomids, where as the total dentigerous area in lutjanids is smaller. The shape of the vomerine tooth patch may also differ. de Neer (1987) described four different shapes of tooth patch, the posterior margin of which may be straight, concave, convex or pointed. However, the shape of the tooth patch appears to variable and therefore has little taxonomic significance

The posterior ethmoid facet for the articulation of the palatine is inclined anterolaterally, with its long axis orientated anteroposteriorly in genera that have an elongated snout region. In

genera with a reduced snout, such as *Acanthopagrus, Diplodus*, *Lagodon* and *Sargus* (Figure 2.13) the facets face anteriorly, with the long axis orientated dorsoventrally (character 5).

The width of the preorbital flange of the lateral ethmoids is a variable measurement. This structure is very prominent in *Calamus,* extending laterally as horn-like projections (Figure 2.12b), while in *Sarpa* for example the flange is weakly developed (Figure 2.14b). In order to quantify a continuous variable such as this structure, the width of the flange is measured against landmarks such as the point of contact between the dorsal and ventral limbs of the posttemporal with the braincase, by inferring a horizontal trajectory. Thus, the width of the braincase at the level of the preorbital flange equals the width of the braincases at the contact of the dorsal limb of the posttemporal as found in *Dentex, Cymatoceps, Polysteganus*, or the width of the braincase at the level of the preorbital flange extends level to or beyond the width of the braincase at the contact of the ventral limb of the post-temporal, as in *Calamus*. An intermediate width also occurs, and may be described by the width of the braincase at the level of the preorbital flange being greater than the width of the braincase at the contact of the dorsal limb of the posttemporal, but less than the width of the braincase at the contact of the ventral limb of the posttemporal (character 6).

The dorsal fossa of the preorbital flange is present in all sparoids but is absent from lutjanids and centropomids. It is always a roughly triangular depression, the size of which appears to be dependent on the size of the preorbital flange (character 7). The extension of the preorbital flange, also accounts for the enlargement of the lateral margin of the anterior myodomes, which have a more pronounced concave margin than in centropomids or lutjanids.

In taxa where a depression for the ascending process of the premaxilla is present, an ethmoidal process forms at the ethmoid-frontal suture extending anteriorly (Figure 2.12a). The dorsal surface is flat for support of the posterior part of the nasals. The process may be short with a semi-elliptical dorsal surface, or extended in form of a parabolic curve (character 8).

On the ventral surface of the lateral ethmoids the shallow sulci that connect to the nasal part of the laterosensory canal may be present as more extensive structures than those described for *Dentex* (Figure 2.1a), or as less well developed structures. In taxa such as *Lithognathus* and *Diplodus* (Figure 2.12a), the sulci extend into the frontals, to approximately the mid-point of the orbit, while the sucli are only just visible in *Archosargus* and *Calamus* (Figure 2.12b; character 9).

The frontals occupy a similar percentage of the skull roof in all genera, however, the inclination of the frontals anterior to the occipital crest is variable. In taxa such as *Dentex* and *Lithognathus* the inclination of the frontals is relatively shallow at 20°, whilst in *Diplodus* the frontals are inclined at 45°, which is the maximum angle measured for the family. In this latter genus the angle of the frontals and occipital crest are the same, making the dorsal margin of the skull continuous. The inclination of the frontals becomes increasingly steep as the skull shortens, thus a shallow angle is measured in taxa with a long ethmoid region. Intermediate conditions

occur between these two variables.

The total area which the frontals occupy of the occipital crest is variable, although there appears to be little or no continuity amongst genera. The suture between the frontals and the supraoccipital is one sixth of the way along the dorsal margin of the crest in *Archosargus* and *Calamus,* occupying approximately 15° of the total area of the crest, compared to as little as 5° total surface area in taxa such as *Dentex* and *Lithognathus*.

A cancellose texture (ca.b) on the dorsal surface of the frontals anterior to the occipital crest and frontal sagittal crest occurs in some genera. The texture may be fine as observed in *Dentex* and *Archosargus,* or coarse, which is particularly notable in *Diplodus* (Figure 2.10, 2.11; character 10). The frontals in *Lithognathus* for example are smooth, however, unlike most other genera which have smooth frontals the foramina for laterosensory canal cause the surface to be convoluted. The frontals in some taxa including *Argyrozona* and *Pagellus* are anteriorly protuberant, so that they extend over the posterior margin of the ethmoid and lateral ethmoids (character 11).

Occipital region

The parietal bones are a similar size and shape throughout the family, however, the cancellose texture present on the frontals of some genera may also be found on the parietals and the posteroventral surface of the supraoccipital, as in *Archosargus* and *Calamus* (Figure 2.12a; character 12). The frontal sagittal crest may vary in height, so that it is deeper in *Diplodus* compared to *Dentex*, becoming laterally flattened in *Calamus*.

The posttemporal fossae are open in all sparoid fish, although the size of the cavity may vary, as it tends to be deeper in *Calamus* and wider in *Diplodus* for example, than that described for *Dentex.* The fossae are semi-closed anteriorly in centropomids suggesting a primitive condition.

The occipital crest, formed largely from the supraoccipital, is a prominent feature of the braincase in percoid fishes. In taxa such as *Argyrozona*, *Dentex* and *Lithognathus* where the overall shape of the skull is elongate, the crest is greater in length than height, whereas in taxa with a much shorter skull the height and length of the crest maybe equal, or the height is greater than the length, as observed in *Diplodus* and *Calamus* (Figures 3.10a, 3.12a; character 13). The dorsal margin of the crest may also vary from convex to straight, and may or may not overhang the posterior margin of the foramen magnum.

The frontal sagittal crest and the occipital crest are separate structures in most genera, but in some taxa such as *Diplodus* (Figure 2.11b), they meet anteromedially (character 14).

The orientation of the exoccipital condyles provides a usual measure of the inclination of the otico-occipital part of the braincase. The inclination of the ventral margin of the otico-occipital region of the braincase ranges from approximately 12° in *Calamus* to angles as high as 40-45° in *Diplodus*. The inclination itself is hard to quantify as it appears to be a continuous variable, a problem that is not solved by gap coding. However, the condyles are either orientated

posteroventrally as in *Dentex*, or are orientated posteriorly as observed in taxa such as *Boops, Diplodus* and *Sarpa* (character 15). The latter condition occurs when the ventral margin of otico-occipital part of the braincase is inclined to 40° or more.

The exoccipital condyles also vary in their extent of medial separation at the ventral margin of the foramen magnum. They may contact along the midline, as in *Diplodus* or they are separate to varying degrees in taxa such as *Dentex*, *Calamus* and *Lithognathus* (character 16). The significance of the medial separation is unclear but not unique, being recorded in other percoid families such as centropomids (Otero 1997), as well as other vertebrate groups, where a similar condition is found in caecilians (Wilkinson and Nussbaum 1997).

The opisthotic, generally associated with more primitive fish, is a small bone on the ventral surface of the braincase, adjacent to the prootic, pterotic and exoccipital. It is present in centropomids, lutjanids and haemulids as that of type II Tomiyama (1931), and in nemipterids as type I Tomiyama (1931). However, Johnson (1980) observed the opisthotic to be absent from other sparoid families (character 17).

The separation or coalescence of the foramen n. glossopharyngei and foramen n. vagi is variable at the generic level. In taxa where the foramen are separate, the foramen n. vagi has a considerably larger diameter than the foramen n. glossopharyngei. Most sparid genera appear to have a single foramen e.g. *Sparus* (Figure 2.13) for the combined glossopharyngeal and vagus nerves, the associated canal of which is orientated posteriorly (character 18). This character is however, difficult to observe in stained juvenile specimens, as often the bone is not completely ossified.

Otic region

The shape of the dilatator fossa in lateral aspect, is roughly triangular and is inclined anterodorsally, varying in shape according to the anterior extension of the muscle it houses, so that in some taxa the fossa is squat, whereas in others it is elongate. However, the observation that the m.dilatator opercul may or may not pierce the anterior wall of the sphenotic and frontal provides a discrete character that is considered more desirable for cladistic analysis (character 19). The confinement of the muscle within the fossa, so that it does not pierce the anterior wall of the sphenotic is observed in taxa such as *Argyops Sparus* and *Pagellus* (Figure 2.14a). Conversely, the presence of a foramen bisecting the suture between the sphenotic and frontal allows the muscle to pierce through the anterior wall of the dilatator fossa and attach to the ventral surface of the frontals. The diameter of the foramen appears to be variable. Where there is no lateral margin to the foramen, the structure is termed a fossa. The fossa enables a larger block of muscle to attach to the roof of the braincase and is also variable in size. In anterior aspect, the shape of the fossa is semi-circular in *Diplodus*, whereas in *Lithognathus* and *Calamus* for example (Figure 2.12a), the fossa is more elongate. In the latter genus the fossa extends some way anteriorly, so that the site of attachment to the frontals is a third of the width of the orbit, compared to a quarter of the width in *Diplodus*. In *Calamus* the dilatator fossa is narrow and

dorsally elongate, which is presumably why, unlike most taxa examined, the hyomandibular facets are of a similar size. The anterior and posterior hyomandibular facets are usually disparate in size, as described for *Dentex.* The attachment site of the m.dilatator operculi in sparids appears to be on the frontals, even when the dilatator fossa is totally enclosed (e.g. *Sparus*). However, in lutjanids, where the dilatator fossa is also enclosed, the site of attachment is apparent on the sphenotic or extends as far anteriorly as the suture between the frontals and sphenotic.

The pars jugularis

The pars jugularis in most sparids is constant in having three openings, as described in *Dentex* (see Figure 2.3), however, some such as *Boops* and *Sarpa* for example may have more openings (Figure 2.14b). The number of openings is also variable within Sparoidea; nemipterids generally have two openings, although four are present in *Pentapodus* (Johnson 1980), lethrinids also have two openings, while centracanthids have between three and four openings (character 20). The lateral commisure of the pars jugularis in *Argyops*, *Calamus* and *Sparus*, differs from that described for *Dentex*, as it extends in an anteroposterior direction along the parasphenoid and is greatly extended laterally, which is particularly apparent in *Calamus*. The anterior foramen of the pars jugularis in these genera is ovoid, the long axis of which is orientated dorsoventrally, compared to the circular foramen found in taxa with an unextended commisure, i.e. the commisure is strut-like and level to the anterior margin of the braincase (character 21).

The pharyngeal apophysis

The process for the m. adductor arcus palatini of the parasphenoid and the pharyngeal apophysis of the basicranium are present in all sparoids. These processes are also present in haemuloids, but are absent in centropomids and lutjanids. The process for the m. adductor arcus palatini is weakly developed in some taxa, including *Dentex*, *Diplodus* and *Sarpa* (Figure 2.0, 3.10, 3.13b) or alternatively it may be well developed extending beyond the ventral margin of the parasphenoid as in *Lethrinus, Acanthopagrus, Archosargus, Argyops Sparus* and *Calamus* (Figure 2.12a, 2.13; character 22). The pharyngeal apophysis may also be weakly developed, forming a semi-circular process in lateral view in *Acanthopagrus, Archosargus, Diplodus, Sarpa* and *Pagellus* (Figure 2.10, 3.14), or well developed where it forms a stalk-like process, as in *Argyops, Rhabdosargus* and *Calamus* (Figure 2.12; character 23). The process for the m. adductor arcus palatini is generally observed to extend further ventrally than the pharyngeal apophysis.

The parasphenoid carina is absent from some taxa where the m. adductor arcus palatini and pharyngeal apophysis are weakly developed, as in *Sarpa*, *Oblada* and *Sarpa* (Figure 2.14b). The carina is weakly developed in *Dentex* and *Lithognathus*, however, if one or both processes are strongly developed, then the carina is generally observed to be well developed, as in *Acanthopagrus, Archosargus, Rhabdosargus* and *Calamus* (Figure 2.12a). Furthermore, while the two processes are well developed in *Arygops*, the parasphenoid carina is weakly developed (character 24).

Nasals

The nasals may be long and slender as those described for *Dentex*, and other taxa where the ethmoid region is elongate

such as *Arygrozona* and *Lithognathus*. In taxa with a reduced ethmoid region, such as *Sarpa, Diplodus* and *Lagodon* the nasals are considerably shorter and have a wider posterior margin. The posterior margin of the nasals in these taxa attaches to both the anterior margin of the frontals and preorbital fossa of the lateral ethmoids (character 25).

Oral jaws

The jaws, like the braincase, show considerable variation in morphology and dental types. A number of constructs are identified here, which are summarized at the end of this section.

Dermal upper jaw

The height and length of the ascending and alveolar processes of the premaxilla vary in their proportions with respect to each other. The ascending process of the premaxilla may be shorter than the alveolar process as described for *Dentex* (see my remark p. 27). This condition is also observed in *Lutjanus, Nempiterus* and *Arygrozona* for example, or it is approximately equal in length to the alveolar process (to within 5mm) as in *Acanthopagrus, Archosargus* and *Pagellus* (Figure 2.17a). The ascending process may also be longer than the alveolar process as in *Calamus, Lithognathus, Lagodon, Rhabdosargus* and *Diplodus*, (Figure 2.18a), or is found be approximately double the length of the alveolar process, as observed in *Centracanthus* (Figure 2.16a) and *Lethrinus* (character 26). An additional observation is that the ascending process is rounded distally in *Sarpa* (Figure 2.19a), unlike the usual condition in which it tapers.

As the jaw becomes fully retracted during feeding the ethmoid depression provides the necessary cavity for the accommodation of the ascending process (Rognes 1973: 13, figures 6-10). The proportions of the ascending and alveolar processes are therefore directly correlated with the presence or absence of a fossa on the dorsal surface of the ethmoid. In taxa where the processes are equivocal in height and length the ethmoid depression is found to be a fossa, whereas if the dimension of the ascending process is greater, a foramen is present. However, while these structures form a functional unit, and thus characters three and 26 are dependant on each other, the concern of over weighting is lessened as the characters are split into four ethmoidal states, compared to three premaxillary states.

The dorsal margin of the alveolar process, as described for *Dentex* and observed in taxa such as *Crenidens, Oblada* and *Sarpa* may be straight (Figures 2.4a, 2.19a), or is convex to varying degrees. If the dorsal margin is convex then it is regarded as maxillary crest, which has presumably developed as greater support for the lever arm of the maxilla. The presence of this crest is observed in more taxa than by its absence. Observations of the position and shape of the maxillary crest are also found to vary among taxa. The position of the maxillary crest is central in the outgroup taxa *Centropomus* and *Lutjanus,* as well as in some sparid taxa, such as *Argyops.*

However, the shape of the maxillary crest in the former taxa are pinched inwards at the base, widening dorsally, with a flattened dorsal margin, while the crest of the latter taxon is convex, being continuous with the dorsal margin of the alveolar process. The maxillary crest in sparids is more commonly observed as a well developed convex structure in a sub-terminal position, as in *Archosargus, Calamus*, *Rhabdosargus, Pagellus* and *Diplodus* for example (Figure 2.18a, 2.18a). In these taxa the alveolar process is often substantially reduced, so that the maxillary process forms most of its length. (character 27).

The alveolar process in all sparid taxa examined bifurcates posteroventrally, the lateral process of which extends posteriorly, providing support for the maxilla (character 28). The specialized jaw articulation (Figure 2.15) of the premaxilla and the maxilla is unique to both sparids and centracanthids (Figure 2.16a: Johnson 1980:48), contary to the statement of Carpenter and Orrell (1999) that it is previously undescribed. Other sparoids have a typical percoid articulation (Figure 2.16,b and c).

The articular process of the premaxilla serves as a fulcrum for the head of the maxilla in its outward movement i.e. when the mouth opens (Rojo 1991). Johnson (1980) observed that the articular process is separate from the ascending process of the premaxilla in centropomids and partially separate in lutjanids and nemipterids. The two processes are entirely fused in sparids, lethrinids and haemulids, whereas the articular process is absent from centracanthids (character 29).

The maxillary crest (forming the dorsolateral margin of the palatine sulcus) varies in magnitude, and is directly correlated to the length of the lever arm of the maxilla. Thus, a maxilla that has a low dorsal crest, as described in *Dentex* (Figure 2.4a) will also have a long, narrow lever arm. In this construction the fulcrum of the maxilla and lever arm are horizontal. Conversely, in taxa where the maxilla has a more developed dorsal crest, the lever arm will likewise be shorter, as observed in taxa such as *Archosargus, Rhabdosargus*, *Sparus* and *Diplodus* (Figure 2.18b; character 30). In taxa with a dorsal maxillary crest, the fulcrum and lever arm may or may not be horizontal with respect to one another. The latter condition is true in *Diplodus*, in which the fulcrum and lever arm are bent through nearly 90°, although this angle may be less in other taxa, compared to *Calamus* and *Pagellus* in which the maxilla is straight (Figure 2.16b).

The palatine sulcus is found to be extended in taxa that have the construct of a well developed dorsal crest and short lever arm. This is particularly acute in taxa such as *Acanthopagrus, Diplodus* and *Rhabdosargus* where the sulcus extends to the anterior margin of the ascending process of the premaxilla (character 31). It is in these taxa that the fulcrum and lever arm of the maxilla form a steep angle with respect to each other.

The lateral maxillary process, described in *Dentex*, is present throughout the Sparidae. The process is absent from centropomids and lutjanids, but appears to be present in haemulids, lethrinids, centracanthids and nemipterids. It is most commonly observed as the small knob-like

process, but may also occur as a stalk-like projection as in *Calamus* (character 32).

A foramen piercing the lateral face of the maxillary fulcrum and palatine sulcus occurs in some taxa, such as *Diplodus* and *Rhabdosargus*, and presumably accommodates one of the maxillary ligaments (character 33).

Mandible

The proportions between the dentary and articular (plus angular) differ, so that the articular forms approximately half of the total length of the mandible in centropomids and lutjanids, whilst in taxa such as *Lithognathus, Dentex* and *Pagellus* (Figures 3.4b, 3.14c) the articular forms a third of the total length. The articular may account for even less than one-third of the total length of the mandible, as *Calamus*, *Rhabdosargus*, *Diplodus* and *Sarpa* (Figures 3.15c, 3.16b; character 34).

The symphysis is short in those taxa with a long, narrow mandible, such as *Argyrozona, Dentex* and *Spondyliosoma,* with the symphysial process positioned anteriorly. The length of the symphysis increases in *Pagrus* and *Pagellus* for example (Figure 2.16c), extending to a quarter of the total length of the dentary, while in some taxa, such as *Calamus* and *Diplodus* the symphysis extends to as much as half of the length of the dentary, so that the length and height of the dentary are almost equal (Figure 2.18b; character 35). In taxa with a shortened mandible, the mandibular sensory canal may form a double row of foramina as observed in *Calamus, Diplodus*, and *Sparus* (character 36). Some of these taxa may also have a dorsal facet on the coronoid process, rather than the tapering form described for *Dentex* (character 37).

The depth of the articular fossa may be determined by the shape of its lateral and medial margins. If these margins are V-shaped, then the fossa is considered deep, whilst a fossa with concave margins is shallow. Those taxa with long mandibles appear to have deep articular fossae. As the mandible becomes progressively shorter the medial margin only tends to be concave, while in taxa with a considerably reduced mandible, such as *Calamus*, both lateral and medial margins are observed as concave in outline (character 38). Accordingly, the articular has the form of an isosceles triangle in taxa where the mandible is elongate, where as in taxa with a shortened mandible the articular is more compressed to that equilateral dimensions.

There is both variation of the depth of the descending process of the articular and the position of the angular on this process. The ventral margin of the descending process and dentary are flush as in *Centropomus, Lutjanus, Argyrozona* and *Dentex.* Alternatively, the descending process may extend beyond the ventral margin of the dentary, but not below the symphysal process as observed in *Pagellus,* or the process may extend beyond the ventral process of the symphysis as in *Calamus* (character 39).

In taxa where the ventral margin of the descending process is flush with that of the dentary, the angular may form the posteroventral corner of the descending process as in *Centropomus* and *Lutjanus,* or it may form the posterior margin of the descending process as in *Dentex.* Where the descending process extends beyond the ventral margin of the dentary, the angular forms the central part of the posterior margin of this process, directly below the articular facet for

articulation of the condylar surface of the quadrate (character 40).

On the lateral surface of the articular both a superior and inferior crest, present along the dorsal and ventral margins respectively is present in the basal percoids: *Centropomus* and *Lutjanus*. The superior crest observed in *Dentex* (Figure 2.4b), is also found in other genera, such as *Argyrozona, Oblada* and *Spondyliosoma*, although it is more usual for the lateral face of the articular to be smooth and gently convex as in the majority of sparid genera (Figure 2.18c; character 41).

Dentition

The dentition in the premaxilla and dentary shows a wide variation of morphologies among sparid genera. Historically, dentition has been used as an important characteristic in defining sparid subfamilies (Smith and Smith 1986) or genera (Akazaki 1962 and Smith and Smith 1986), as well as other percoid families (Johnson 1980).

Sparid dentition comprises four main tooth morphologies that are found in association or separately. Villiform dentitions are composed of numerous small, close-set teeth, which may form an entire tooth field in some taxa such as *Centropomus* and *Spondyliosoma,* or are present in varying proportions along the medial or anteromedial occlusal margins of the jaws as in *Dentex* or *Calamus* for example (character 42).

Caniniform teeth occur as a single row, with prominent anterolateral fangs in taxa such as *Argyrozona*, *Lutjanus* and *Dentex* (Figure 2.4) as well as in association with conical or molariform morphologies, where they occur along the anterior margin only (character 43).

Conical teeth represent a morphology intermediate between caniniform and molariform teeth, as observed in *Pagellus* (Figure 2.17), and maybe found in association with molariform teeth, occurring on the lateral occlusal margin (character 44).

Durophagy characterizes a number of genera such as *Acanthopagrus, Calamus, Sparus* and *Diplodus* (Figure 2.18). Large molariform teeth occupy several rows, becoming progressively larger posteromedially (character 45). The premaxilla tends to have an additional row of teeth if two or more rows are present in the dentary. In these taxa, the anterior margin of the jaw may contain either caniniform or incisiform teeth. It is more common to find caniniform teeth associated with molariform teeth as in *Calamus* and *Sparus*, than incisisifom teeth as observed in *Diplodus*. Taxa with molariform teeth have a much bigger occlusal area, however, not all taxa that exhibit this morphology have a dorsal facet on the coronoid process of the dentary. The facet appears to occur in those taxa that have up to three or four rows of molariform teeth, whereas as it is absent from those with two or fewer rows of teeth. The number of tooth rows is also included as a potential character (character 47).

Incisiform morphologies occur as previously mentioned in association with molariform teeth, however, this morphology also occurs, albeit in a different form, in a number of taxa. This additional morphology is described as crenulate, as the occlusal margin is characterized by small serrations, as observed in the following taxa: *Boops, Crenidens, Lagodon, Pachymetopon,*

Polyamblydon and *Sparodon* (character 46). These teeth of these taxa are roughly diamond shaped in both upper and lower jaws, however, the monospecific genus *Sarpa*, is unique in having an interlocking occlusal surface with no serrations (Figure 2.18). The tooth morphology of upper jaw is again diamond shaped, while the teeth of lower jaw are bicuspid.

Infraorbitals

The morphology of the infraorbital series in sparids and centracanthids is the same as that described for *Dentex*. In nemipterids and lethrinids infraorbitals I and II are also enlarged, but differ from the sparid condition as the height and width of these bones have similar dimensions (Figure 2.20b). The infraorbitals of sparoids therefore differ to those of lutjanids and haemulids in which only infraorbital I is enlarged (character 48).

Johnson (1980) identified the subobcular shelf as well developed in lutjanids, sparids and nemipterids, whilst it is reduced in centracanthids and lethrinids, and absent in haemulids (character 49).

Hyo-palatine bones

The shape of the palatine arch is dependant on whether the ethmoid-vomerine region is reduced or elongate. Thus, the palatine arch is likewise reduced or elongate accordingly, although in the former state the arch is strongly concave laterally so that in some taxa, such as *Calamus* the deepest point of the arch is level with the lateral margins of the palatine.

The maxillary process of the palatine in those taxa where the ethmoid-vomerine region is elongate is well developed and deflected laterally, so that the distal ends of this process are facing. In taxa such as *Boops* (Figure 2.20a), *Calamus* and *Sparus* taxa in which the ethmoid-vomerine region is considerably reduced, the maxiallary process is short and orientated horizontally (character 50).

The posterior process of the palatine, defined as extending beyond the dorsal ethmoid process, is observed in taxa that may have an elongated maxillary process as *Dentex* and *Lithognathus* or in taxa in which the maxillary process is short as in *Calamus*. The process is however, absent from taxa where the maxillary process is elongate (character 51).

The ventral margin of the ectopterygoid extends to the anterodorsal margin of the quadrate in all sparoid families except nemipterids, where the ectopterygoid extends as far the condylar surface of the quadrate (character 52).

The ventral margin of the quadrate may form a continuous ridge with the preopercle depending on the asymmetry of the bicondylar process of the quadrate. If the lateral condyle is significantly larger than the medial condyle then the ventral margin of the quadrate forms a prominent ridge that is confluent with preopercle, as observed in a number of genera such as *Archosargus, Calamus* and *Sparus*. When the condyles are of a similar size the ventral margin is initially flat before forming a confluent ridge with the preopercle as observed in *Dentex* (character

53).

Johnson (1980) observed that the metapterygoid in sparoids is without a lamina (character 54), articulating along an anteriorly extended broad sheet-like area of bone of the hyomandibular, as well as along the ventral process, leaving no interosseous space. He further noted that the symplectic in these fish are expanded posteriorly, overlapping both the metapterygoid and preopercle (character 55), a configuration which was not observed in any other group of percoids.

Opercular bones

The angle of the dorsal and ventral processes of the preopercle vary from 52° in *Dentex* to approximately 80° in *Boops* (Figure 2.20a), whilst the angle measured for the outgroup taxon *Lutjanus* at 42°, is significantly shallower than the lowest angle measured for any sparid taxon. The angle corresponds to whether the braincase is elongated or reduced, so that in taxa where the angle is shallow the construction of the braincase is thus elongate, and likewise the reverse is true. However, as measurements of this angle form a continuous series rather than discrete clusters, as would be suitable for gap coding (see chapter 3), it is not used for further cladistic analysis.

Faint parallel ridges perpendicular to the posterior margin of the preopercular angle are observed in all sparids examined in this study. In centropomids, lutjanids and haemulids numerous serrations occur along the length of the posterior and ventral margins, which are particularly well developed at the angle (character 56).

The opercle, subopercle and interopercle generally become narrower (anteroposteriorly) in those taxa where the braincase is reduced. The opercle is also a thicker bone in some taxa such as *Acanthopagrus* and *Archosargus* as it is convex medially, rather than the usual sheet-like bone described for *Dentex*.

Lower part of the hyoid Arch

The arrangement of bones in the lower part of the hyoid arch is similar in the percoid families used in this study, however, there are several variable structures. In centropomids a 'beryciform' foramen is present near the dorsal margin of the ceratohyal through which the hyoid artery passes (Greenwood 1976). Whilst, in Haemulinae (exception *Anisotremus*) and Lutjanoidea a sulcus accommodates the hyoid artery (Johnson 1980), which is present on the lateral face of the ceratohyal extending posteriorly into the epihyal. The hyoid artery sulcus is also present in some sparids such as *Chrysoblephus*, *Dentex* (Figure 2.6a) and *Polysteganus*, however it appears to be absent from many genera, including *Archosargus*, *Boops*, (Figure 2.21a), *Calamus* (Figure 2.21b), *Lithognathus* and *Pagellus* (character 57).

The ceratohyal is generally straight, with slightly enlarged distal margins. The small anterodorsal process described for *Dentex* becomes greatly enlarged in some taxa as in *Archosargus* and *Calamus* (Figure 2.21b), so that the anterior margin of the ceratohyal becomes strongly bifurcated. In these latter taxa a separate anterior and dorsal process contact the ventral

and dorsal hypohyals respectively. In those taxa where the hyoid arch is anteriorly bifurcate, the ceratohyal is considerably stouter (character 58).

The posteroventral projection of the urohyal occurs in two states as a single or bifid spine. In the latter state, the spines maybe weakly bifid as in *Pagrus* (Figure 2.21d) so that in ventral aspect the base of the urohyal is of equal width, which is the same as in the single spine condition. Conversely, when the spines are strongly bifid, as in *Sparus* (Figure 2.21e), the base of the urohyal widens posterolaterally so that the spines are further from the midline. The spines also extend further posteriorly (character 59). In the majority of sparid taxa the posterior margin of the urohyal is concave and it is usual for the deepest point to occur ventrally; however, in a few taxa including *Lutjanus* and *Dentex* the deepest point is situated centrally (character 60).

Branchiostegal rays

In centropomids, lutjanids and haemulids the number of branchiostegal rays totals seven, whereas in sparoids the number of rays totals six (character 61). The articulation of these rays also differs between the former families compared to sparoids. Rays i-v articulate with the ceratohyal while vi and vii articulate with the epihyal in centropomids, lutjanids and haemulids. All sparoids, with the exception of nemipterids, have the same configuration of rays so that rays i-iv articulate with the ceratohyal, while v articulates with the interspace between the ceratohyal and epihyal and vi attaches to the epihyal. In nemipterids rays i-v articulate with the ceratohyal, and vi articulates with the interspace between the ceratohyal and epihyal (character 62). The rays in all these families are acinaciform in shape.

Gill arches

The branchial arches in sparoids show considerable variation in the number, form and arrangement of gill rakers on the hypobranchials and ceratobranchials; the size and shape of epibranchials; number of uncinate processes on epibranchials II, III and IV and the size of the tooth patches and tooth morphology of the upper pharyngeal jaws. However, the number of bones and there arrangement is similar to that described for *Dentex.*

Lower pharyngeal jaws

The number and form of the rakers on the anterior margin of the first ceratobranchial is variable, with between 14-15 rakers in *Boop* and *Spicara* (Centracanthidae) while there are 7-12 in all other sparids (Figure 2.22a and b) as well as *Lutjanus*, while as few as five are present in *Gymnocranius* (Lethrinidae) and *Scolopsis* ([Nemipteridae, Figure 2.22c] character 63). The form of the rakers is triangular, with the exception of the latter two genera where the rakers are dome-shaped (character 64). The size of the triangular rakers varies from highly attenuated in taxa such as *Boops* and *Lagodon* to much shorter forms as in *Arygrozona, Dentex* and *Lutjanus* for example. In *Centropomus* and *Lutjanus* the rakers on the posterior margin of the first ceratobranchial and both anterior and posterior margins of ceratobranchials 2-4 are dome-shaped yet irregular in their overall form, while in sparoid fish these rakers are circular (character 65).

Hypobranchial 1 is a narrow rod-like bone with a weakly developed anterior process in *Cymatoceps, Dentex, Evynnis* and *Polysteganus*, however, this process is absent in *Centropomus* and *Lutjanus*. The anterior process is well developed in some taxa such as *Boops, Pachymetopon* and *Spicara* to form 'horn-like' projections that extend as far as the posterior margin of the dorsal hypohyal. In these taxa hypobranchial 1 is a much shorter, stouter bone. In *Calamus* (Figure 2.22a), *Gymnocranius*, *Lagodon* and *Sparadon* for example, hypobranchial 1 is roughly square shaped (character 66).

Gill rakers are present on both the anterior and posterior margins of hypobranchial 1 in *Boopsoidea, Pachymetopon* and *Spicara*, or are present only on the anterior margin. Dome-shaped rakers may instead be present along the anterior margin for example in *Evynnis, Lagodon, Polyambydon* and *Porcostoma,* while rakers are absent from some taxa such as *Calamus, Cheimerius, Gymnocranius* and *Scolopsis* (character 67). Dome-shaped rakers may also occur on the anterior margin of either hypobranchial 2 and/or 3. Rakers are usually present on the anterior margin of hypobranchial 2 (Figure 2.22b), with the exception of some taxa such as *Calamus* (Figure 2.22a), *Gymnocranius* and *Scolopsis* (Figure 2.22c) where they are absent (character 68). In contrast, it is observed that rakers are usually absent from hypobranchial 3 (character 69). The number of rakers on the anterior margins of hypobranchial 2 and 3 varies between one and four.

Upper pharyngeal jaws (see Figure 2.20)

An interarcual cartilage (IAC) is present in sparids, contrary to Johnson (1980:22). The cartilage does not fully span the distance between the first epibranchial and second pharyngobranchial, unlike the IAC in lutjanids and haemulids that is particularly well developed. The length of the IAC appears to be reasonably constant in sparids, so that it may be used to quantify the length of the first epibranchial that varies in length. In taxa such as *Dentex, Evynnis* and *Porcostoma* the IAC is approximately a fifth of the total length of the first epibranchial, where as in taxa such as *Diplodus* and *Calamus* the IAC is a third of the length of this bone (character 70).

The number, position and length of rakers, as in the UPJ are also variable. Those attached to the epibranchials may be present on both anterior and posterior margins on the first, second and third epibranchials, or they are present on the first and second epibranchials. In *Haemulon, Lethrinus* and *Nemipterus* rakers are present on the first epibranchial only (character 71). The length of the rakers on the first epibranchial are considerably longer in taxa such as *Boops* (Figure 2.23c) and *Centracanthus*, than in *Dentex* (Figure 2.7). In taxa such as *Sparus* the rakers are dome-shaped (Figure 2.23b), while they are absent from others such as *Calamus* (Figure 2.23a).

Uncinate processes are small projections tipped with cartilage for the attachment of gill arch muscles. Their occurance is not, however, constant on epibranchial II and IV. In all observed sparid taxa either a medial flange (as described for *Dentex*, Figure 2.7*: E2*) or an uncinate process is present (character 72). The presence of a medial flange is the more common modification of epibranchial II and is also observed in *Smaris, Lethrinus* and *Haemulon*, but is absent from

Nemipterus.

A single uncinate process is present on epibranchial III and is the usual condition for epibranchial IV. However, in nearly all sparid taxa examined, with the exception of *Dentex* and *Cymatoceps,* two uncinate processes are present on epibranchial IV. This observation maybe unique to sparid fish as it has not been observed in any other percoid family (G. D. Johnson, pers. comm.). The double uncinate process is also observed in the taxa *Smaris*. The second process is situated directly above the first and is reduced in size so that it is noticable largely due to its cartilage tip (character 73).

Variation in the size of the margins of PB3 and ET2 may vary from that described for *Dentex*. In the taxa *Calamus* and *Diplodus* for example, the lateral margin of PB3 is expanded compared with the medial margin of ET2 (character 74), while PB3 is absent from *Nemipterus* (Johnson 1980). Similarily, the medial and lateral margins of toothplates PB3 and UP4 may also vary in their dimensions with respect to each other. Unlike the condition observed in *Dentex*, these margins in taxa such as *Archosargus, Calamus* and *Diplodus* are a constant width (character 75). Potential characters may also be found from the cartilage associated with PB2, which differs from that observed in *Dentex*, as in *Calamus* this cartilage is found only on the anterior and posterior tips of this bone. Furthermore, the attachment of PB4 is observed to vary, as in *Boops* it appears to be more closely attached to PB3, whereas in *Dentex* this cartilage is more separate. The latter condition is regarded as the more usual (G. D. Johnson, pers.comm.).

The occlusal surface of the tooth plates are usually covered with small isolated recurved caniniform type dentition. However, some taxa such as *Calamus*, *Diplodus* and *Sparus* have numerous isolated teeth covering the dentigerous surface, most of which have constricted tips in which the acrodin cap is of smaller diameter than the supporting tooth (Figure 2.23b; character 76).

The upper pharyngeal dentition consists of four tooth plates. The anterior most tooth plate is fused with the second pharyngobranchial (PB2), associated with a cartilage forming the anterior, medial and posterior margins. Directly behind this tooth plate is the smaller autogenous second epibranchial toothplate (ET2: Johnson 1980). Posteriomedial to these toothplates is a much larger tooth plate that is fused with the third pharyngobranchial (PB3). Directly posterior to PB3, is the small cartilage PB4 that appears to be separate, rather than attached to PB3. The upper pharyngeal tooth plate 4 (UP4) forms the posterior-most tooth plate of the UPJ. The tooth plates PB2 and ET2 are narrow in this genus, their lateral and medial margins forming a constant width. In contrast the tooth plates PB3 and UP4 are larger, the lateral margin of UP4 forming a greater width than the medial margin of PB3.

POST-CRANIAL SKELETON (Plates 2.1 - 2.11)

Pectoral girdle and fin

The pectoral girdle appears to be quite conservative throughout the Sparoidea; although

there are some variations between families as well as subtle generic differences.

The posttemporal is ornamented by faint ridges running perpendicular to the posterior margin in sparoids, which are however, serrated in centropomids and lutjanids (character 77).

The angle between the dorsal and ventral limbs of the cleithrum give rise to a range of quantitative data similar to that measured for the angle of the preopercle. The range of inclination measured is from 30° - 55°, so that those taxa where the dorsal and ventral limbs are furthest apart (lowest angles) likewise have shallow preopercle angles, while those taxa with dorsal and ventral limbs that are closer together have steeper preopercle angles.

The medial margin of the cleithrum appears to vary in degree of convolution, which is particularly prominent in taxa such as *Calamus, Oblada* and *Pagellus*, absent from *Lutjanus*, whilst there is some convolution along this margin as described for *Dentex*. Highly convoluted structures may help to strengthen this area of the girdle.

The insertion of radial iii on the scapula and iv onto the interspace between the scapula and corocoid occurs in basal percoids such as centropomids, lutjanids, in addition to haemulids, and sparoids, with the exception of nemipterids. In this latter family, the arrangement differs so that radials i-ii insert onto the scapula, while iii inserts onto the interspace and iv inserts onto the coracoid (character 78).

Pelvic girdle and fin

The pelvic girdle and fin changes little throughout the Sparoidea and therefore the reader is referred to this section in the description of *Dentex*. However, variation in the development of the post-pelvic and subpelvic processes, in particular the former process is observed to vary (Johnson 1980). The post-pelvic process is greatly reduced or absent in sparids and centracanthids, while it is well developed in the other two sparoid families; nemipterids and lethrinids, as well as in haemulids and lutjanids (character 79).

Vertebral column

The total number of vertebrae 10 + 14, is constant throughout sparoids and is frequently found amongst other percoid families. Higher counts are often recorded, such as in haemulids (11 + 16), although lower counts are uncommon (23 is present in *Mene, Priacanthus* and *Scatophagus* (Johnson 1980, after Regan 1913).

In sparoids and lutjanoids the first two vertebrae are generally compressed, with reduced neural spines, compared to the rest of the vertebral column. The anterior surface of the first centrum faces anteriorly in taxa where the ventral margin of the otico-occipital region of the braincase is close to the horizontal. Whereas in those taxa in which this region is steeply inclined the centrum is inclined anteroventrally, so that in lateral aspect it is wedge-shaped.

While there are consistently eight pairs of pleural ribs in those families used in this study, the number of intermusculars varies, with 7-8 pairs in lutjanids, haemulids and nemipterids; 11

pairs in lethrinids; 12-13 pairs in sparids and 15 in centracanthids (character 80).

Dorsal and anal fins

The supraneural formula described for *Dentex* as 0/0+0/2+1/1 is also found in all other sparid genera, with the exception of *Boops* and *Sarpa*, in which the formula 0/0/0+2/1+1 is the same as that counted in *Lutjanus*. The formula of the centracanthids and lethrinids examined in this study is also the same as that of *Dentex*, while a reduction of supraneurals from three to two is present in nemipterids 0/0/2+1/1/. Two supraneurals are considered to be the derived condition, apparently due to secondary loss (Johnson 1980), while three supraneurals are assumed to be the primitive configuration (character 81).

The anterior processes of the supraneurals may be separate from each other as observed in *Boops* and *Sarpa*, or as in most taxa the processes overlie the preceding supraneural. In taxa where the anterior processes are separate, the over all shape of the fish is elongate, whereas those taxa in which the processes overlap tend to be deeper bodied forms (character 82).

The dorsal fin spines are generally similar in length in most taxa. However, the first few dorsal fin spiness in *Argyops* and *Stenotomus* are greatly elongated (see Plate 2.3), so that they are approximately four times the length of the subsequent spines (character 83).

The first radial of the anal fin is generally strut-like and buttressed anteriorly in most taxa, although in *Boops, Oblada* and *Sarpa* the radial is a considerably more slender structure. Smith-Vaniz *et al.* (1988) used robustness of fin-spines as a character in groupers, although remarked, however that it is difficult to quantify. The first radial in *Calamus* and *Stenotomus* is, however, remarkably different as the radial forms a cone that opens anteriorly (Plate 2.5, character 84). This structure has evolved to receive the swimbladder, although it is not unique to these taxa, as it is also found in *Lateolabrax, Malakichthys elegans* (Percichthyidae), *Acropoma* (Acropomatidae) and *Eucinostomus* (Gerreidae; Tominaga *et al.* 1996).

The number of trisegmented radials in the dorsal and anal fins varies within and between families, so that for sparids there are 1-3, centracanthids have 1-4, lethrinids 2-3, nemipterids appear to have only one, while haemulids have no trisegmented radials (character 85). In beryciforms each radial supporting the dorsal and anal fins is trisegmented, whilst in perciform fishes there is a trend for the proximal and medial elements to become fused. However, the posteriormost radials in some percoid families may retain the trisegmented structure, thus the lack of fusion is regarded as a primitive characteristic (Gosline 1966; Johnson 1980).

Caudal fin skeleton

The caudal fin skeleton described for *Dentex* is that of a generalized percoid type that Monod (1968) refers to as 'sciaeno-sparidien banal'. The reader is referred to Gosline (1961), Patterson (1968: 87); Monod (1967, 1968); Fujita (1990) for a fuller discussion on the caudal skeleton of perciform fishes.

There is little variation in the basic plan of the caudal fin skeleton within the Sparidae. However, fusion between the associated hypurals 1-2 and 3-4 may occur in some taxa, such as *Boops* and *Sarpa*. Hypural fusion often occurs in species that are more active swimmers, and is therefore associated with strengthening the tail. In most taxa the hypurals are usually separate or semi-fused, i.e. attached for only part of their length (character 86). The depth of the gape of the tail between hypurals 2 and 3 may also vary, as the dorsal and ventral margins of these bones in some taxa, may have additional flanges. These flanges cause the gape to become much shallower, which appears to be consistent with those taxa where the hypurals are fused, whereas deep gapes, extending to the urostyle are associated with separate or semi-fused hypurals.

The formula of principal rays for sparoids is 9:8, the same as for Lutjanids. The following counts of procurrent rays do however vary within the sparoids: sparids, 7-11; centracanthids, 9:10; lethrinids 7:9 and nemipterids 8:11 (Johnson 1980).

The length of the hypurapophysis may form a short process extending to a central point of the first hypural, or is well developed extending to the medial margin of hypural 2 (character 87).

The arrangement of posterior cartilages described in *Dentex*, are similar to those observed in other sparid genera, however, variation may be more prevalent as Fujita (1990) observed that CIHPU3 in *Pagrus* is divided into a larger posterior and smaller anterior element. The arrangement of CIHPU4 and CINPU4 does however, differ among sparoids, as they form moderately sized irregular ovoids in sparids and nemipterids, whereas in lethrinids they are small and circular. In centropomids the cartilages are divided so that they form a larger anterior and a smaller posterior cartilage, whilst in lutjanids they appear to be absent (character 88). In *Lutjanus* the CIHPU3 and CPHPU2 form a single large cartilage, dorsal to which is a smaller additional CPHPU2. The CIHPU3 and CPHPU2 forms a single cartilage in sparids and *Scolopsis*, whilst an additional separate posterior CPHPU3 is present in *Nemipterus*. In *Lethrinus* the CPHPU3 and CPHPU2 occur as single cartilages (character 89).

Discussion

Examination of comparative material shows that sparids are a morphologically diverse assemblage. The cranium is especially character rich, in particular the braincase, jaws and gill arches, while the post-cranium appears to be much more conservative. A plethora of dentitions are observed through out the group, and are associated with particular cranial constructions. A cursory examination of other sparoid families shows that they are not as morphologically diverse as sparids, which is perhaps unsurprising considering that these groups do not contain nearly as many genera. The implications of the morphological diversity of this family are discussed fully in Chapter 5.

Sparids are one of the percoid groups considered to be closely related to the Pharyngognathi (Rosen and Patterson 1990). However, only certain members have been examined, whereas this study provides a comprehensive review of the morphology of the family.

Many of those characters outlined in Chapter 1, that may be used to align certain families to the Pharyngognathi, are identifiable within the Sparidae. These characters are summarized below, where an asterisk indicates a character found in all sparids that I have examined:

i) the teeth of the pharyngeal jaws are capped by a conical decurved tip of acrodin*

ii) reduction of the IAC compared to basal percoid families*

iii) strong ventral carina of the parasphenoid

iv) ventral extension of the median carina of the parasphenoid in the form of a triangular process, directly level with the posterior margin of the orbit, forming an adductor process from which the posterior fibres of the adductor muscle arise. The adductor process in *Boops* for example is all that remains of the ventral keel, while this process is particularly well developed in some taxa such as *Calamus**

v) development of a V-shaped pharyngeal apophysis on the parasphenoid, which in sparids is situated in an anterior position on the otico-occipital region of the parasphenoid. The articulation with PB3 is ampiarthrotic rather than diarthrotic as in labroids, sparids include species that have a definite articular facet dorsally on PB3 (Rosen and Patterson 1990)*

vi) maxilla with a well developed dorsal crest

vii) long slender articulo-ascending process of the premaxilla, with an alveolar process half the length of the former process

viii) nasals firmly united with the frontals providing roofing for ascending process fossa

However, further comprehensive studies are required of other families suggested as possible sister groups to the Pharyngognathi, in order to identify characters that are robust enough to support these associations in phylogenetic analysis.

CHARACTER ANALYSIS

CRANIUM

Braincase

1. The length of the vomer along the ventral margin of the braincase extends to a point level with the middle of the orbit (0), to a point level with the ethmoid-frontal suture (1), or the posterior margin of the vomer is level with both the ethmoid-frontal suture and the anterior margin of the orbit (2).

2. Anterodorsal facet on the medial dorsal crest of the vomer is present (0), or absent (1).

3. Absence of a depression along the dorsal margin of the ethmoid (0), presence of a shallow fossa for the ascending process of the premaxilla (1), presence of a deep fossa for the ascending process of the premaxilla (2),or presence of a foramen for the ascending process of the premaxilla (3). **Ord.**

4. Vomer is dentigerous (0), or not (1).

5. The ethmoid facets for the articulation of the palatine are orientated anterolaterally (0), or anteriorly (1).

6. Width of braincase at level of preorbital flange equals width of braincase at contact of the dorsal limb of the posttemporal (0), or is greater than the width of the braincase at contact of the dorsal limb of the posttemporal, but less than the width of the braincase at the contact of the ventral limb of the posttemporal (1), or the width of the braincase at level of preorbital flange extends level to or beyond the width of the braincase at the contact of the ventral limb of the posttemporal (2).

7. Preorbital fossa of the lateral ethmoid is absent (0), or present (1).

8. The lateral ethmoidal process is absent (0), semi-elliptical (1), or extended anteriorly (2). **Ord.**

9. The sagittal ventral sulcus of the lateral ethmoids and frontals are absent (0), occur on the lateral ethmoids only (1), or extend into the frontals (2).

10. Cancellose texture on the dorsal margin of the frontals anterior to the occipital crest and the pterotic sagittal crest is absent (0), or present (1).

11. Dorsal margin of frontals is flat (0), or protuberant anterior to the occipital crest (1).

12. Cancellose texture on the supraoccipital and epioccipital is absent (0), or present (1).

13. Length of the occipital crest is greater than the height (0), is approximately equal to the height (1) or is less than the height (2). **Ord.**

14. The frontal sagittal crest and the occipital crest remain separate (0), or meet anteromedially (1).

15. The exoccipital condyles are inclined posteroventrally (0), or posteriorly (1).

16. The exoccipital condyles contact along the midline (0), or show varying degrees of medial separation (1).

17. Opisthotic is present (0), or absent (1).

18. Separate foramina for the n. vagus and n. glossopharyngeal (0), or single foramen n vagus + n. glossopharyngeal (1).

19. No extension of the m. dilatator operculi beyond the dilatator fossa (0), m. dilatator operculi piercing a foramen in the anterior margin of the sphenotic (1), or m. dilatator operculi piercing a fossa in the anterior margin of the sphenotic (2). **Ord.**

20. The pars jugularis has 2 openings (0),or 3 or more openings (1).

21. Lateral commisure is strut-like, and is level with the posterior margin of the orbit (0), or is laterally inflated extending anteroventrally to the mid-point of the orbit (1).

22. A process for the m. adductor arcus palatini is absent (0), weakly developed (1) or extended (2). **Ord.**

23. Pharyngeal apophysis of the basicranium is absent (0), present as a dome-shaped process (1), or as a stalk-like process (2). **Ord.**

24. Parasphenoid carina absent (0), weakly developed (1), or well developed (2). **Ord.**

Nasals

25. The nasal is attached to the anterior margin of the frontal (0), or to both the anterior margin of the lateral ethmoid and frontal (1).

Jaws

Upper jaw

26. The height of the ascending process of the premaxilla in adults is less than the length of the alveolus process (0), the height of ascending process is the same as the length of the alveolar process (1), the height of the ascending process is greater than the length of the alveolar process (2), or the height of the ascending process is double that of the alveolar process (3). **Ord.**

27. Dorsal maxillary crest of the premaxilla is central with a flat dorsal margin (0), is central with a convex dorsal margin (1), sub-terminal with a convex dorsal margin (2), or absent (3). **Ord.**

28. Articulation between the premaxilla and the maxilla is simple (0), or specialized (1).

29. The articular process is separate from the ascending process of the premaxilla (0), part of anterior margin only is fused to the ascending process (1), the articular process is fused to the ascending process (2), or is absent (3). **Ord.**

30. The dorsal crest of the maxilla is knob-like (0), weakly developed (1), or well developed, so that the dorsal margin of the crest is as long as the lever arm of the maxilla (2). **Ord.**

31. The palatine sulcus of the maxilla is short (0), or extended to the anterior margin premaxilla (1).

32. The lateral maxillary process is absent (0), present as a weakly developed knob (1), or stalk-like (2). **Ord.**

33. A foramen developed through the dorsal crest and palatine sulcus of the maxilla is absent (0), or present.

The mandible

34. The combined length of the articular and angular forms half the total length of the lower mandible (0), forms a third of the total length (1), or less than one third of the total length (2). **Ord.**

35. The symphysal process of the dentary is anterior (0), extends to a quarter of the total length of the dorsal process of the dentary (1), or extends to a half of the total length of the dorsal process of the dentary (2). **Ord.**

36. The mandibular sensory canal opens by a single row of pores throughout the length of the jaw (0), or a double row anteriorly (1).

37. Facet on the dorsal margin of the coronoid process is absent (0), or present (1).

38. The lateral and medial margins of the articular fossa are V-shaped (0), the medial margin only is concave (1), or both medial and lateral margins are concave (2). **Ord.**

39. Descending process of the articular is the same length as the ventral margin of the dentary (0), or extends below the ventral margin but not beyond the ventral process (1), or extends below the ventral process (2). **Ord.**

40. The angular forms the posteroventral corner of the articular (0) or the posterior margin (1).

41. A superior and inferior crest are present on the lateral face of the articular (0), a superior crest only is present (1), or both crests are absent (2). **Ord.**

Dentition

42. A villiform dentition is present on the occlusal surface of the premaxilla and dentary (0), occurs only on the medial margin of the occlusal surface of the premaxilla and the dentary (1), or along the anteromedial margin of the occlusal surface of the premaxilla and dentary (2), or absent (3). **Ord.**

43. Caniniform teeth absent (0), or present (1).

44. Conical teeth absent (0), or present (1).

45. Molariform teeth absent (0), or present (1).

46. Incisiform teeth absent (0), present (1), or crenulated (2). **Ord.**

47. Tooth field present (0), one tooth row present (1), or more than one row present (2).

Infraorbitals

48. Infraorbital I only is enlarged (0), infraorbital I and II are enlarged (1), or infraorbital I and II are deeper than wide (2). **Ord.**

49. The subocular shelf is well developed so that it extends medially over the parasphenoid (0), is reduced (1), or is absent (2). **Ord.**

Palatine arch

50. The maxillary process of the palatine is deflected medially (0), or is straight (1).

51. Posterior process of the palatine is present (0), or absent (1).

52. The ventral margin of the ectopterygoid extends to the articular condyle of the quadrate (0), or contacts the anterodorsal margin of the quadrate (1).

53. A confluent ridge along the ventral margin of the quadrate and the preopercle is absent (0), or present (1).

54. Metapterygoid with lamina (0), or without (1).

55. Symplectic is simple (0), or expanded both dorsally and ventrally to overlap the metapterygoid and preopercle (1).

Opercular bones

56. The posteroventral margin of the preopercle has well developed serrations (0), small serrations (1), or faint ridges (2).

Lower part of the hyoid arch

57. Beryciform foramen, through which the hyoid artery passes is present in the ceratohyal (0), sulcus arcus hyoideus is present along the lateral face of the ceratohyal and epihyal (1), or is absent (2). **Ord.**

58. Dorsal process on ceratohyal is absent (0), weakly developed (1), or well developed (2). **Ord.**

59. The base of the urohyal is of equal dimension (0), or is triangular in shape (1).

60. The deepest point of the concavity along the posterior margin of the urohyal is central (0), or ventral (1).

61. Number of branchiostegals totals 7 (0), or 6 (1).

62. Branchiostegal rays i-v attach to the ceratohyal, whilst rays vi-vii attach to the epihyal (0), rays i-iv attach to the ceratohyal, ray v attaches to the interspace between the ceratohyal and the epihyal and ray vi attaches to the epihyal (1), or rays i-v attach to the ceratohyal and ray vi attaches to the interspace between the ceratohyal and the epihyal (2). **Ord.**

Branchial arches

Lower pharyngeal jaws

63. The number of rakers on the first ceratobranchial are between 14-15 (0), 7-12 (1), or 5 (2). **Ord.**

64. Rakers on the anterior margin of the first ceratobranchial are elongate (0), or dome-shaped (1).

65. Irregular dome-shaped rakers on the posterior margin of the first ceratobranchial and both anterior and posterior margins of the ceratobranchials two-four (0), or circular dome-shaped rakers are present (1).

66. The anterior process on hypobranchial one is absent (0), weakly developed (1), well developed (2) or hypobranchial one is square shaped (3). **Ord.**

67. Rakers on hypobranchial one are elongate (0), dome-shaped (1), or absent (2).

68. Rakers on hypobranchial two are present (0), or absent (1).

69. Rakers on hypobranchial three are present (0), or absent (1).

Upper pharyngeal jaws

70. The length of the interarcual cartilage is a fifth of the length of the first epibranchial (0), or a third of the length (1).

71. Rakers present on anterior and posterior margins of the first, second and third epibranchials (0), rakers present on the anterior and posterior margins of the first and second epibranchials (1), or are present on the first epibranchial only (2). **Ord.**

72. Process on second epibranchial is absent (0), medial flange present (1), or uncinate process present (2). **Ord.**

73. Fourth epibranchial has one uncinate process (0), or two (1).

74. The lateral and medial margins of tooth plates PB2 and ET2 have similar dimensions (0), PB2 is expanded with respect to ET2 (1), or are absent (2).

75. The lateral margin of UP4 is greater in width than the medial margin of PB3 (0), or they form a similar width (1).

76. The dentition of the upper pharyngeal tooth plates are recurved caniniform (0), or the teeth have restricted tips in which the acrodin cap is of smaller diameter than the supporting tooth (1).

POST-CRANIAL SKELETON

Pectoral girdle

77. The posterior margin of the posttemporal is serrated (0), or is smooth (1).

78. Insertion of radials i-iii on the scapula and iv on the interspace between the scapula and corocoid (0), or radials i-ii on the scapula, iii on the interspace and iv on the corocoid (1).

79. Post-pelvic process is well developed (0), or reduced/absent (1).

Axial skeleton

80. Intermusculars total 7-8 (0), 11-13 (1), or 15 (2).

Dorsal and anal fins

81. The supraneural formula is 0/0/0+2/1+1 (0), or 0/0+0/2+1/1/ (1), or 0/0/2+1/1 (2).

82. Anterior processes of the supraneurals are separate (0), or overlap (1).

83. Dorsal fin spines are the same length (0), or the initial spines are considerably longer (1).

84. The first radial of the anal fin is strut-like (0), or conical (1).

85. Number of trisegmental radials total between 1-7 (0), 1-3 (1), or 0 (2).

Caudal fin

86. Hypurals 1+2 and 3+4 are separate (0), fused for part of their mutual length (1) or fused (2). **Ord.**

87. Parahypophysis extends to hypural 1 (0), or extends to the ventral margin of the second hypural (1).

88. CINPU4 and CIHPU4 each form a double cartilage (0), a single, medium sized oval cartilage (1), or a single, small circular cartilage (2).

89. CIHPU3 and CPHPU2 form a single cartilage with an additional separate CPHPU2 dorsally (0), a single/double CIHPU3 and double CPHPU2 (1), or a single CIHPU3 and a single CPHPU2 (2).

All characters are treated as unordered, however, note that characters with Ord. in bold denote those that are only ordered in the subsequent ordered analysis performed in Chapter 3.

Table 2.0 Multistate data matrix

CHARACTER

TAXA	1	2	3	4	5	6	7	8	9	10	11	12	13	14	15	16	17	18	19	20	21	22	23	24	25	26	27	28
Centropomus	0	0	0	0	0	0	0	0	0	0	0	0	0	0	0	0	0	0	0	0	0	0	0	0	0	0	0	0
Lutjanus	0	0	0	0	0	0	0	0	0	0	0	0	0	0	0	0	0	0	0	0	0	0	0	0	0	0	0	0
Haemulon	1	0	1	1	0	2	1	0	2	0	0	0	0	0	0	0	0	1	0	0	0	1	1	1	0	2	3	0
Centracanidae	2	0	0	1	0	0	1	0	2	0	0	0	0	0	0	0	1	1	2	1	0	1	1	0	0	3	2	1
Lethrindae	1	0	1	1	0	1	1	0	1	1	0	0	1	0	0	0	1	1	0	0	0	2	1	1	0	3	3	0
Nemipteridae	1	0	0	1	0	0	1	0	0	0	0	0	0	0	0	0	0	1	2	0	0	1	1	1	0	0	0	0
Archosargus	2	1	2	1	1	1	1	1	2	0	0	1	1	0	1	1	1	1	2	1	0	2	2	2	1	1	2	1
Acanthopagrus	2	1	2	1	1	1	1	1	2	0	0	1	1	0	1	0	1	1	2	1	0	2	2	2	1	1	2	1
Argyops	1	1	2	1	1	1	1	2	2	0	1	0	1	0	0	0	1	1	0	1	1	2	2	2	1	1	1	1
Argyrozona	1	0	0	1	0	1	1	1	1	0	1	0	0	0	0	1	1	1	1	1	0	1	1	1	0	0	3	1
Boops	2	0	0	1	1	0	1	0	1	0	0	0	0	0	1	0	1	1	2	1	0	1	1	0	1	0	3	1
Boopsoidea	1	0	2	1	0	1	1	0	2	0	0	0	0	0	1	?	1	0	0	1	0	1	1	1	1	0	3	1
Calamus	1	1	2	1	1	2	1	2	0	0	0	1	2	0	0	1	1	1	2	1	1	2	2	2	1	2	2	1
Cheimerus	1	0	0	1	0	1	1	0	2	0	0	0	0	0	0	0	1	0	0	1	0	1	1	1	0	1	0	1
Chrysoblephus	1	1	1	1	0	1	1	0	1	0	0	0	0	1	0	0	1	0	0	1	0	1	1	1	1	1	2	1
Crenidens	1	1	2	1	1	1	1	0	2	0	0	0	0	0	1	0	1	1	1	1	0	1	1	1	1	1	2	1
Cymatoceps	1	0	0	1	0	1	1	0	1	0	0	0	0	0	0	0	1	0	0	1	0	1	1	1	0	0	0	1
Dentex	1	0	0	1	0	1	1	0	1	0	0	0	0	0	0	0	1	0	1	1	0	1	1	1	0	0	3	1
Diplodus	2	1	3	1	1	2	1	0	2	1	0	0	2	1	1	0	1	1	2	1	0	1	1	1	1	2	2	1
Evynnis	1	0	2	1	0	1	1	0	2	1	0	0	0	1	0	0	1	1	0	1	0	1	1	1	1	1	1	1
Lagodon	2	1	2	1	1	1	1	0	2	0	0	0	0	0	1	1	1	1	2	1	0	1	1	1	1	2	2	1
Lithognathus	1	0	0	1	0	1	1	0	2	0	0	0	0	0	0	1	1	0	2	1	0	1	1	1	0	2	2	1
Oblada	2	0	0	1	1	0	1	0	2	1	0	0	0	1	1	0	1	1	2	1	0	1	1	0	1	1	3	1
Pachymetopon	2	1	?	1	0	1	1	0	2	0	0	0	0	0	0	0	1	1	2	1	0	1	1	0	1	2	1	1
Pagrus	1	0	2	1	0	1	1	0	2	0	0	0	0	0	0	1	1	1	0	1	0	1	1	1	0	1	2	1
Pagellus	1	0	2	1	0	1	1	0	2	0	0	0	0	1	0	0	1	0	0	1	0	1	1	1	0	1	2	1
Polyamblyodon	2	1	1	1	1	1	1	0	1	0	0	0	0	0	0	0	1	1	1	1	0	1	1	0	1	1	1	1
Polysteganus	1	1	1	1	0	1	1	0	1	0	0	0	0	0	0	0	1	1	0	1	0	1	1	1	1	1	?	1
Porcostoma	1	1	1	1	0	1	1	0	1	0	0	0	0	0	0	0	1	1	0	1	0	1	1	1	0	0	3	1
Rhabdosargus	2	1	3	1	1	1	1	0	1	0	0	0	2	1	1	0	1	1	2	1	0	1	2	2	1	2	2	1
Sarpa	2	0	0	1	1	0	1	0	2	0	0	0	0	0	1	0	1	1	1	1	0	1	1	0	1	1	2	1
Sparodon	2	1	2	1	1	1	1	0	2	0	0	0	0	0	1	0	1	1	2	1	0	1	1	1	1	2	2	1
Sparus	1	1	2	1	1	1	1	0	2	1	0	0	1	1	0	0	1	1	0	1	1	2	2	1	1	1	2	1
Spondyliosoma	1	1	0	1	0	1	1	0	2	0	1	0	0	0	1	0	1	1	2	1	0	1	1	1	0	1	2	1
Stenotomus	1	1	2	1	0	1	1	1	2	0	0	0	0	1	0	0	1	1	1	1	0	2	1	1	1	2	2	1

TAXA	29	30	31	32	33	34	35	36	37	38	39	40	41	42	43	44	45	46	47	48	49	50	51	52	53	54	55	56
Centropomus	0	0	0	0	0	0	0	0	0	0	0	0	0	0	0	0	0	0	0	0	0	0	0	0	0	0	0	0
Lutjanus	1	0	0	0	0	0	0	0	0	0	0	0	0	1	1	0	0	0	1	0	0	0	0	0	0	0	0	0
Haemulon	2	1	1	1	0	1	0	0	0	0	0	0	1	2	1	0	0	0	1	0	2	0	0	1	0	0	0	0
Centracanidae	3	1	0	1	0	1	0	0	0	2	0	0	2	1	1	0	0	0	1	1	1	0	1	1	1	1	1	2
Lethrindae	2	1	0	1	0	2	0	0	0	0	1	0	0	1	1	1	0	0	1	1	2	0	0	1	0	1	1	2
Nemipteridae	1	1	0	1	0	1	0	0	0	0	1	0	2	1	1	0	0	0	1	1	0	1	1	0	0	1	1	2
Archosargus	2	2	1	1	0	2	2	1	1	2	1	1	2	3	0	1	1	1	2	2	0	1	0	1	1	1	1	2
Acanthopagrus	2	2	1	1	0	2	2	1	1	1	2	1	2	3	1	1	1	0	2	2	0	1	0	1	1	1	1	2
Argyops	2	2	0	2	0	2	1	0	1	1	1	1	2	3	1	1	1	0	2	2	0	0	0	1	1	1	1	2
Argyrozona	2	1	0	1	0	1	0	0	0	0	0	0	1	1	1	0	0	0	1	2	0	0	0	1	0	1	1	?
Boops	2	1	0	1	0	1	0	0	0	1	0	0	1	3	0	0	0	2	1	2	0	0	1	1	1	1	1	2
Boopsoidea	2	0	0	1	0	1	0	0	0	0	0	0	1	1	1	0	0	0	1	2	0	0	0	1	1	1	1	2
Calamus	2	2	1	2	0	2	2	1	1	1	2	1	2	2	1	1	1	0	2	2	0	1	0	1	1	1	1	2
Cheimerus	2	0	0	1	0	1	0	0	0	0	0	0	2	1	1	0	0	0	1	2	0	0	0	1	1	1	1	2
Chrysoblephus	2	1	0	1	0	1	0	0	0	0	1	0	2	1	1	0	0	0	1	2	0	0	0	1	1	1	1	2
Crenidens	2	1	1	1	0	2	1	0	0	1	1	0	2	3	0	0	1	2	2	2	0	0	1	1	1	1	1	2
Cymatoceps	2	0	0	1	0	1	0	0	0	0	1	0	2	1	1	0	0	0	1	2	0	0	0	1	1	1	1	2
Dentex	2	0	0	1	0	1	0	0	0	0	0	0	1	1	1	0	0	0	1	2	0	0	0	1	0	1	1	2
Diplodus	2	2	1	1	1	2	2	1	1	2	2	1	2	3	0	0	1	1	2	2	0	1	1	1	1	1	1	2
Evynnis	2	1	0	1	0	1	0	0	0	0	1	0	2	1	1	0	0	0	1	2	0	0	0	1	1	1	1	2
Lagodon	2	1	1	2	0	2	1	0	0	1	1	0	2	3	0	0	0	2	2	2	0	0	1	1	1	1	1	2
Lithognathus	2	2	1	2	0	2	0	0	1	1	2	1	2	2	1	0	1	0	2	2	0	0	0	1	1	1	1	2
Oblada	2	1	0	1	0	1	0	0	0	1	0	0	1	3	1	0	0	2	1	2	0	0	0	1	1	1	1	2
Pachymetopon	2	1	0	1	0	1	0	0	0	0	0	0	2	1	0	0	0	2	1	2	0	0	0	1	1	1	1	2
Pagrus	2	2	0	1	0	2	1	0	1	0	1	1	2	2	1	1	1	0	2	2	0	0	0	1	1	1	1	2
Pagellus	2	2	0	1	0	2	0	0	1	0	1	1	2	2	1	1	0	0	2	2	0	0	0	1	1	1	1	2
Polyamblyodon	2	1	0	1	0	1	1	0	0	1	1	0	2	3	0	0	0	2	2	2	0	1	1	1	1	1	1	2
Polysteganus	2	1	0	1	0	1	0	0	0	0	1	0	2	1	1	0	0	0	1	2	0	0	0	1	1	1	1	2
Porcostoma	2	1	0	1	0	1	1	0	0	0	1	0	2	1	1	0	0	0	1	2	0	0	0	1	0	1	1	2
Rhabdosargus	2	2	1	1	1	2	2	1	1	1	2	1	2	3	1	1	1	0	2	2	0	1	0	1	1	1	1	2
Sarpa	2	1	0	1	0	1	1	0	0	2	1	0	2	3	0	0	0	2	1	2	0	0	1	1	1	1	1	2
Sparodon	2	2	1	2	0	2	2	1	0	2	2	1	2	3	0	0	0	2	2	2	0	1	1	1	1	1	1	2
Sparus	2	2	0	1	0	2	1	0	1	1	2	1	2	3	1	1	1	0	2	2	0	0	0	1	1	1	1	2
Spondyliosoma	2	1	0	1	0	1	0	0	0	0	0	0	1	0	1	0	0	0	0	2	0	0	0	0	0	1	1	2
Stenotomus	2	2	1	1	0	2	0	0	1	0	1	1	2	2	1	0	1	0	2	2	0	1	0	1	1	1	1	2

Table 2.0 cont.

TAXA	CHARACTERS																															
	57	58	59	60	61	62	63	64	65	66	67	68	69	70	71	72	73	74	75	76	77	78	79	80	81	82	83	84	85	86	87	88	89
Centropomus	0	0	0	0	0	0	0	0	0	0	0	0	0	0	0	0	0	0	0	0	0	0	0	0	0	0	0	0	0	0	0	0	0
Lutjanus	1	0	0	0	0	0	1	0	0	0	0	0	0	0	0	0	0	0	0	0	0	0	0	0	0	0	0	0	0	0	0	?	0
Haemulon	1	1	1	1	0	0	1	0	1	1	0	0	0	1	2	1	0	1	1	1	0	0	?	0	1	1	0	0	2	0	1	?	0
Centracanthidae	2	2	1	1	1	1	0	0	1	2	0	0	0	0	1	1	1	1	1	0	1	0	1	2	1	0	0	0	1	2	1	?	?
Lethrinidae	1	1	0	1	1	1	2	1	1	3	2	1	1	1	2	1	0	1	1	0	1	0	0	1	1	1	0	0	1	1	1	2	2
Nemipteridae	2	0	0	0	1	2	2	1	1	1	2	1	1	0	2	0	0	2	1	0	1	1	0	0	2	0	0	0	1	1	1	1	1
Archosargus	2	2	1	1	1	1	1	0	1	3	2	1	1	1	1	2	1	1	1	1	1	0	1	1	1	1	0	0	1	1	1	1	1
Acanthopagrus	2	2	1	1	1	1	1	0	1	3	2	1	1	0	1	1	1	0	1	0	1	0	1	1	1	1	0	0	1	0	0	1	1
Argyops	2	2	1	1	1	1	1	0	1	3	2	1	1	1	1	2	1	1	1	1	1	0	1	1	1	1	1	0	1	0	0	1	1
Argyrozona	?	?	1	1	1	1	?	?	?	?	?	?	?	?	?	?	?	?	?	1	0	1	1	1	?	0	0	1	1	1	1	1	1
Boops	2	1	1	1	1	1	0	0	1	2	0	0	0	1	0	1	1	1	1	0	1	0	1	1	0	0	0	0	1	2	1	1	1
Boopsoidea	1	1	1	1	1	1	1	0	1	1	0	0	0	1	1	1	1	1	1	0	1	0	1	1	1	1	0	0	1	0	0	1	1
Calamus	2	2	1	1	1	1	1	0	1	3	2	1	1	1	1	2	1	1	1	1	1	0	1	1	1	1	0	1	1	0	1	1	1
Cheimerus	1	1	1	1	1	1	1	0	1	0	2	0	1	1	0	1	1	1	1	0	1	0	1	1	1	1	0	0	1	0	0	1	1
Chrysoblephus	1	1	0	1	1	1	1	0	1	2	2	0	1	0	0	1	1	1	1	0	1	0	1	1	1	1	0	0	1	0	0	1	1
Crenidens	2	2	1	1	1	1	1	0	1	3	2	0	0	1	1	1	1	1	1	1	1	0	1	1	1	1	0	0	1	0	0	1	1
Cymatoceps	1	0	0	1	1	1	1	0	1	0	2	0	1	0	0	1	0	0	0	0	1	0	1	1	1	1	0	0	1	0	0	1	1
Dentex	1	1	0	1	1	1	1	0	1	1	2	0	0	0	0	1	0	0	0	0	1	0	1	1	1	0	0	0	1	0	0	1	1
Diplodus	2	2	1	1	1	1	1	0	1	3	2	0	1	1	1	2	1	1	1	1	1	0	1	1	1	1	0	0	1	1	0	1	1
Evynnis	1	1	0	1	1	1	1	0	1	1	1	0	0	0	1	1	1	1	1	0	1	0	1	1	1	1	0	0	1	0	0	1	1
Lagodon	2	2	1	1	1	1	1	0	1	3	1	0	0	1	1	1	1	1	1	0	1	0	1	1	1	1	0	0	1	0	0	1	1
Lithognathus	2	2	1	1	1	1	1	0	1	2	0	0	0	1	1	2	1	1	1	1	1	0	1	1	1	0	0	0	1	0	1	1	1
Oblada	2	1	1	1	1	1	0	0	1	2	0	0	0	1	0	1	1	0	1	0	1	0	1	1	1	0	0	0	1	2	0	1	1
Pachymetopon	2	1	1	1	1	1	1	0	1	2	0	0	0	0	0	1	1	1	1	0	1	0	1	1	1	1	0	0	1	0	0	1	1
Pagrus	2	2	0	1	1	1	1	0	1	3	1	0	0	1	1	1	1	1	1	0	1	0	1	1	1	1	0	0	1	1	1	1	1
Pagellus	2	2	0	1	1	1	1	0	1	2	0	0	0	1	0	1	1	1	1	0	1	0	1	1	1	1	0	0	1	1	1	1	1
Polyamblyodon	2	2	1	1	1	1	1	0	1	2	1	0	1	1	1	2	1	1	1	1	1	0	1	1	1	1	0	0	1	1	1	1	1
Polysteganus	1	1	0	1	1	1	1	0	1	1	1	0	0	1	0	1	1	1	1	0	1	0	1	1	1	1	0	0	1	0	0	1	1
Porcostoma	1	1	0	0	1	1	1	0	1	1	1	0	0	0	0	1	1	1	1	0	1	0	1	1	1	1	0	0	1	0	1	1	1
Rhabdosargus	2	2	1	1	1	1	1	0	1	3	2	0	1	1	1	2	1	1	1	1	1	0	1	1	1	1	0	0	1	0	0	1	1
Sarpa	2	1	1	1	1	1	1	0	1	2	0	0	0	1	0	1	1	1	1	1	1	0	1	1	0	0	0	0	1	2	1	1	1
Sparodon	2	2	1	1	1	1	1	0	1	3	2	0	1	1	1	1	1	1	1	1	1	0	1	1	1	1	0	0	1	0	1	1	1
Sparus	2	2	1	1	1	1	1	0	1	3	2	1	1	1	1	1	1	0	1	0	1	0	1	1	1	1	0	0	1	2	1	1	1
Spondyliosoma	2	2	0	1	1	1	1	0	1	2	0	0	0	1	0	1	1	0	1	0	1	0	1	1	1	1	0	0	1	1	1	1	1
Stenotomus	2	2	1	1	1	1	1	0	1	3	1	0	0	1	0	1	1	1	1	1	1	0	1	1	1	1	1	1	1	1	1	1	1

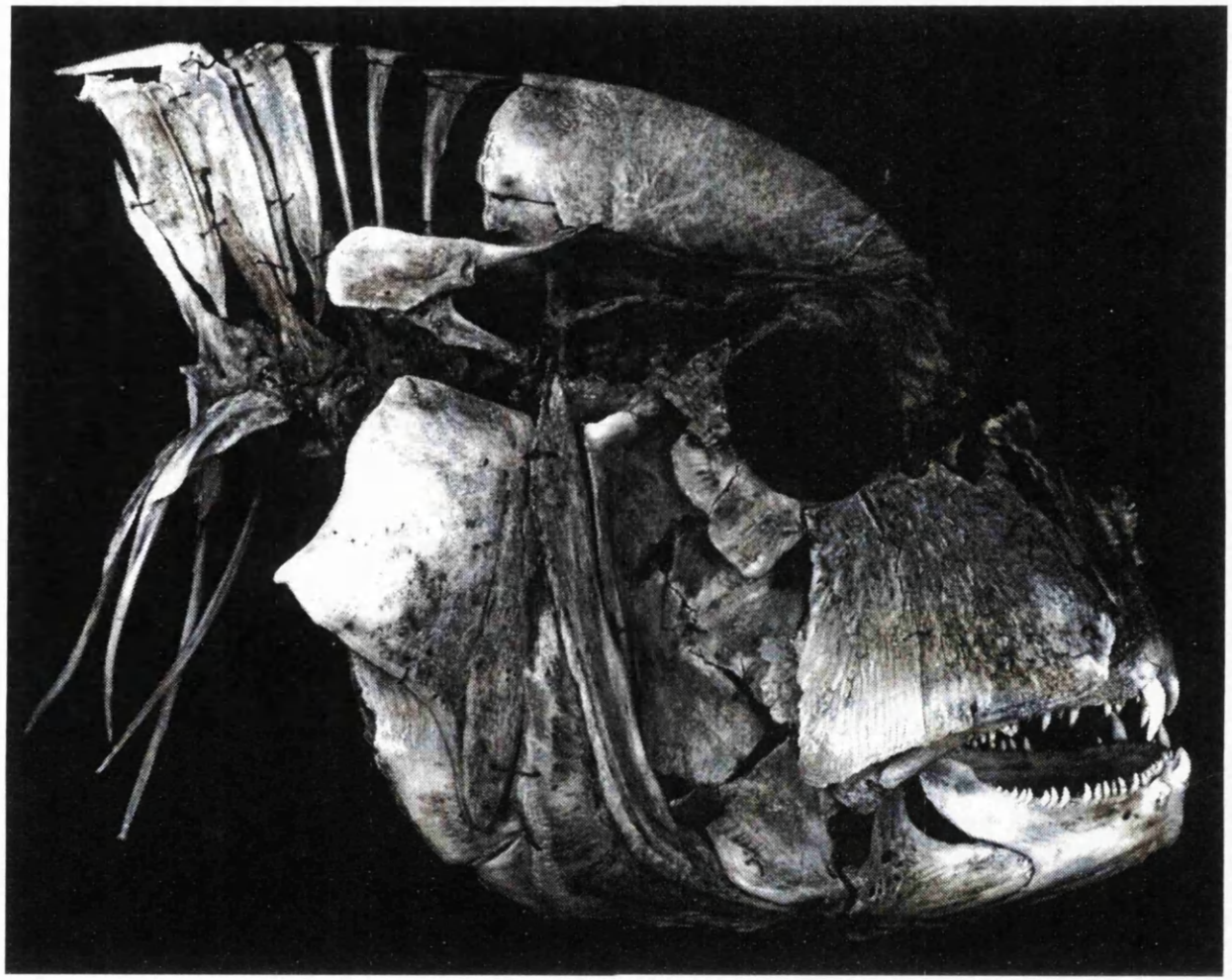

Plate 2.0 *Dentex dentex* BMNH 1910.4.19 (Length of braincase 148mm)

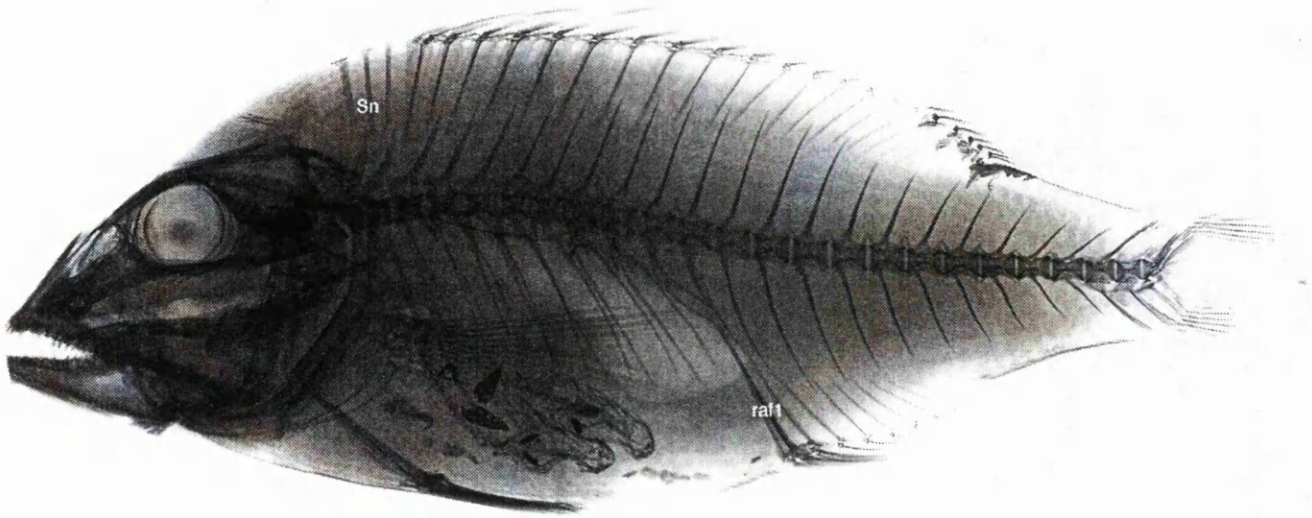

Plate 2.1 *Dentex dentex* BMNH 1988.2.3 (SL 131mm)

FIGURE 2.0 ***Dentex dentex*** **BMNH 1845.6.22**

Camera lucida drawing of the braincase in lateral view. Length of braincase 43mm (see Chapter 1 for abbreviations of anatomical terminology)

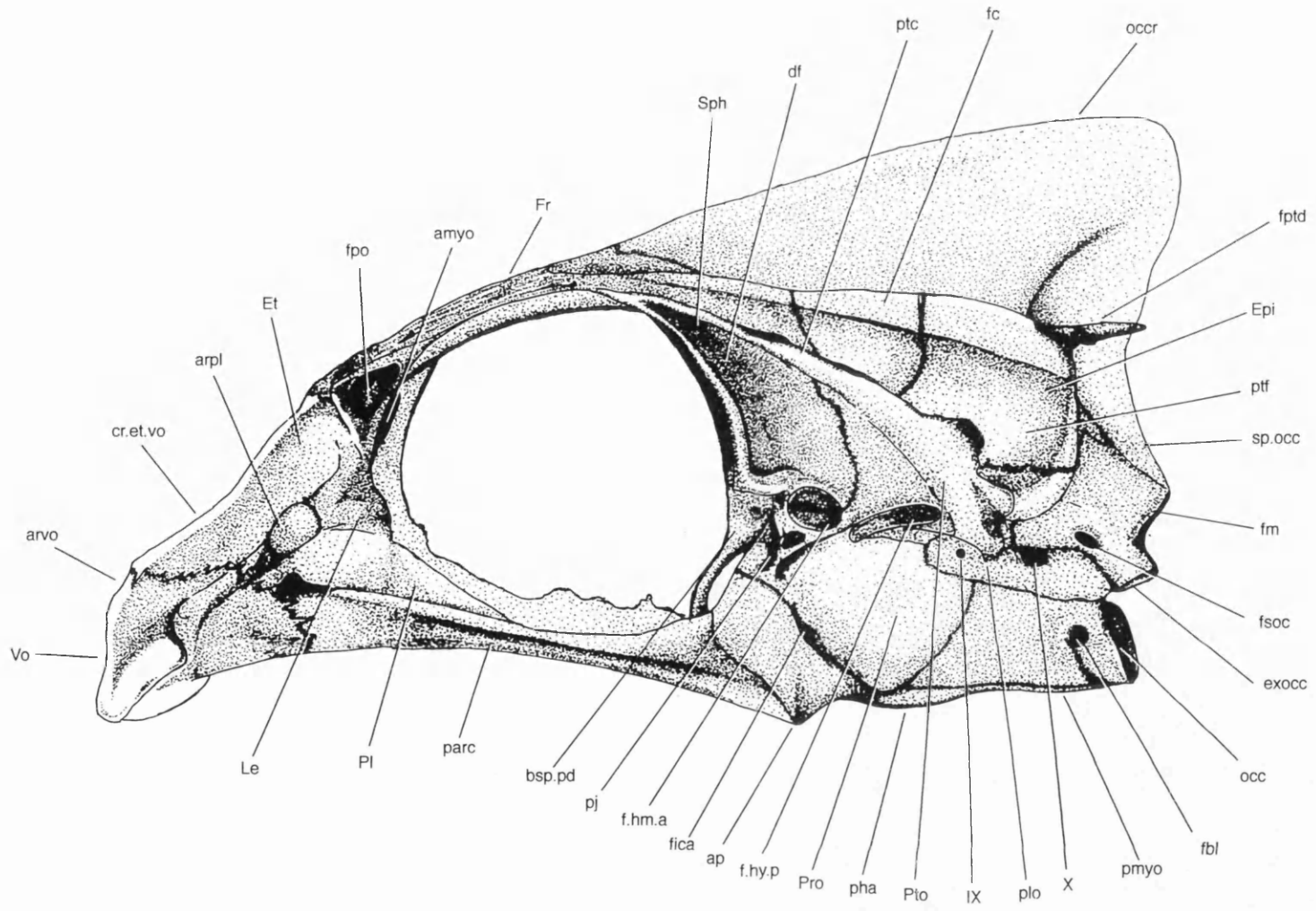
ptc
fc
occr
df
Sph
Fr
amyo
fpo
Et
arpl
cr.et.vo
arvo
Vo
fptd
Epi
ptf
sp.occ
fm
fsoc
exocc
occ
fbl
pmyo
X
plo
IX
Pto
pha
Pro
f.hy.p
ap
fica
f.hm.a
pj
bsp.pd
parc
Pl
Le

FIGURE 2.1 ***Dentex dentex*** **BMNH 1845.6.22**

Camera lucida drawing of the braincase:

a. ventral view

b. dorsal view

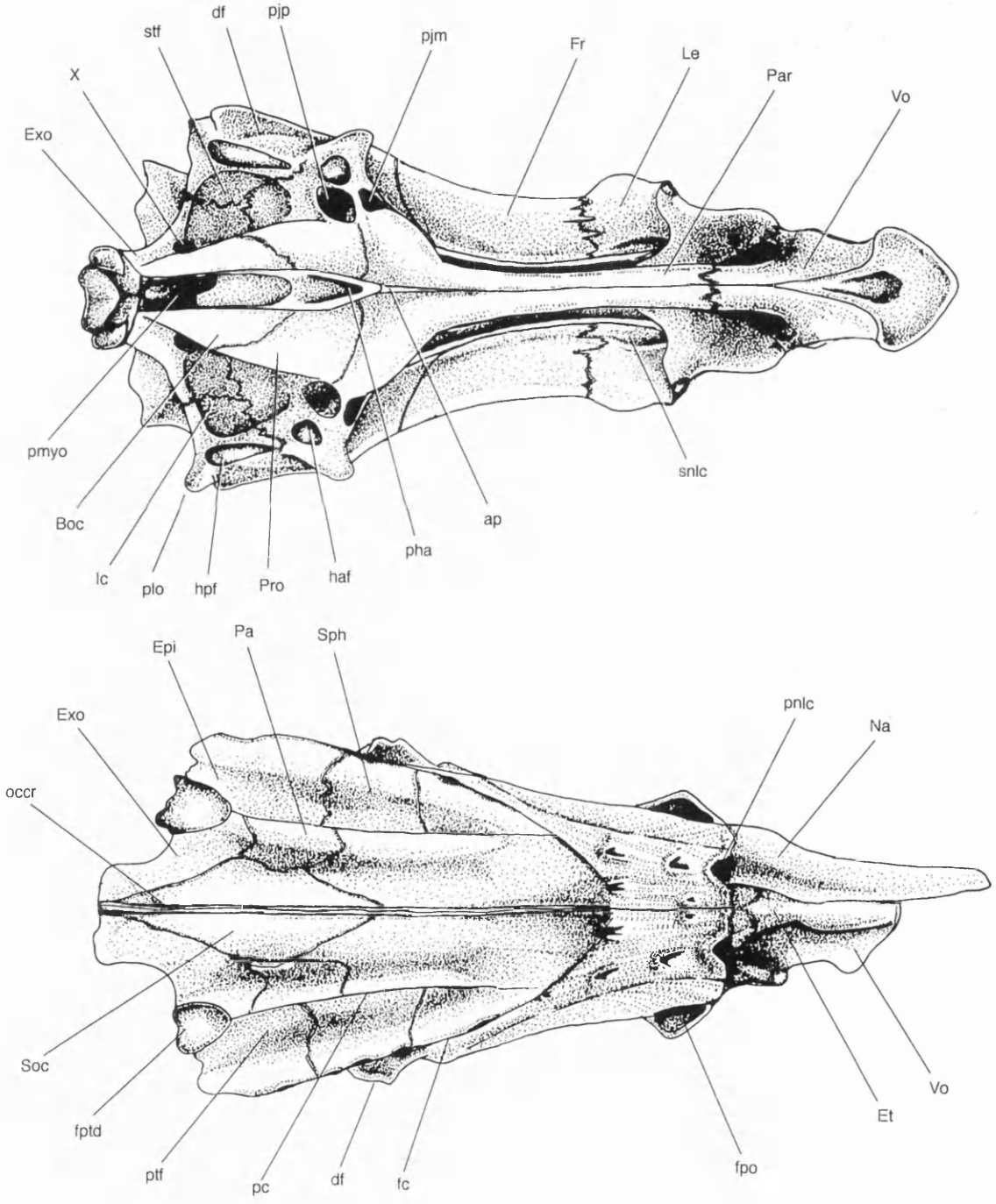
df
pjp
stf
pjm
Fr
Le
X
Par
Vo
Exo
pmyo
snlc
Boc
ap
pha
lc
plo
hpf
Pro
haf
Epi
Pa
Sph
Exo
pnlc
Na
occr
Soc
fptd
ptf
pc
df
fc
fpo
Et
Vo

FIGURE 2.2 ***Dentex dentex*** **BMNH 1845.6.22**

Camera lucida drawing of the braincase in occipital view

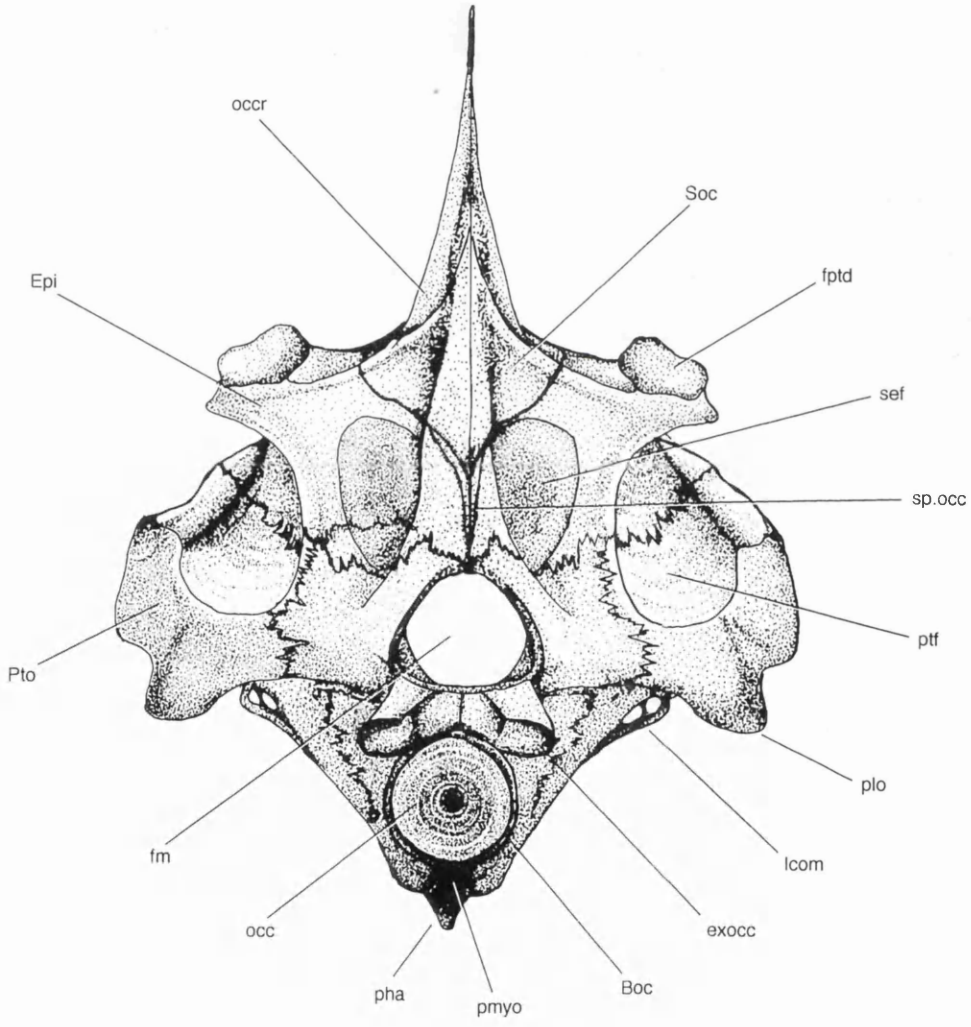
occr
Soc
Epi
fptd
sef
sp.occ
ptf
Pto
plo
fm
lcom
occ
exocc
pha
pmyo
Boc

FIGURE 2.3 ***Dentex dentex*** **BMNH 1845.6.22**

Camera lucida drawing of the trigemino-facialis region of the braincase in oblique view

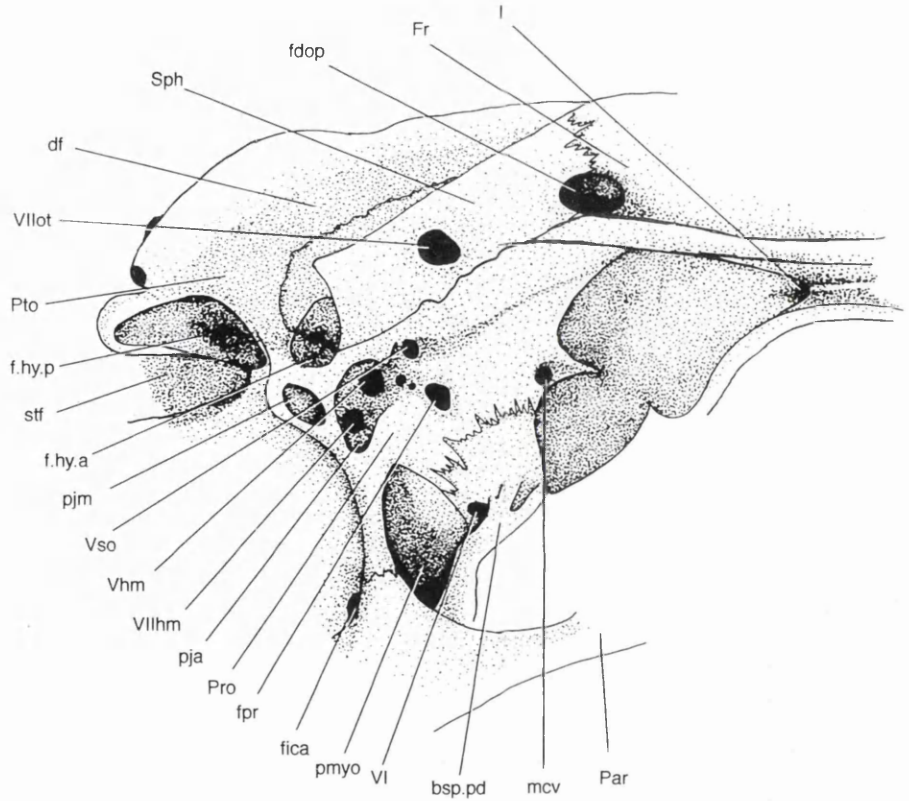
I
Fr
fdop
Sph
df
VIIot
Pto
f.hy.p
stf
f.hy.a
pjm
Vso
Vhm
VIIhm
pja
Pro
fpr
fica
pmyo
VI
bsp.pd
mcv
Par

FIGURE 2.4 ***Dentex dentex*** **BMNH 1845.6.22**

Camera lucida drawing of the jaws in lateral view:

a. premaxilla and maxilla

b. mandible

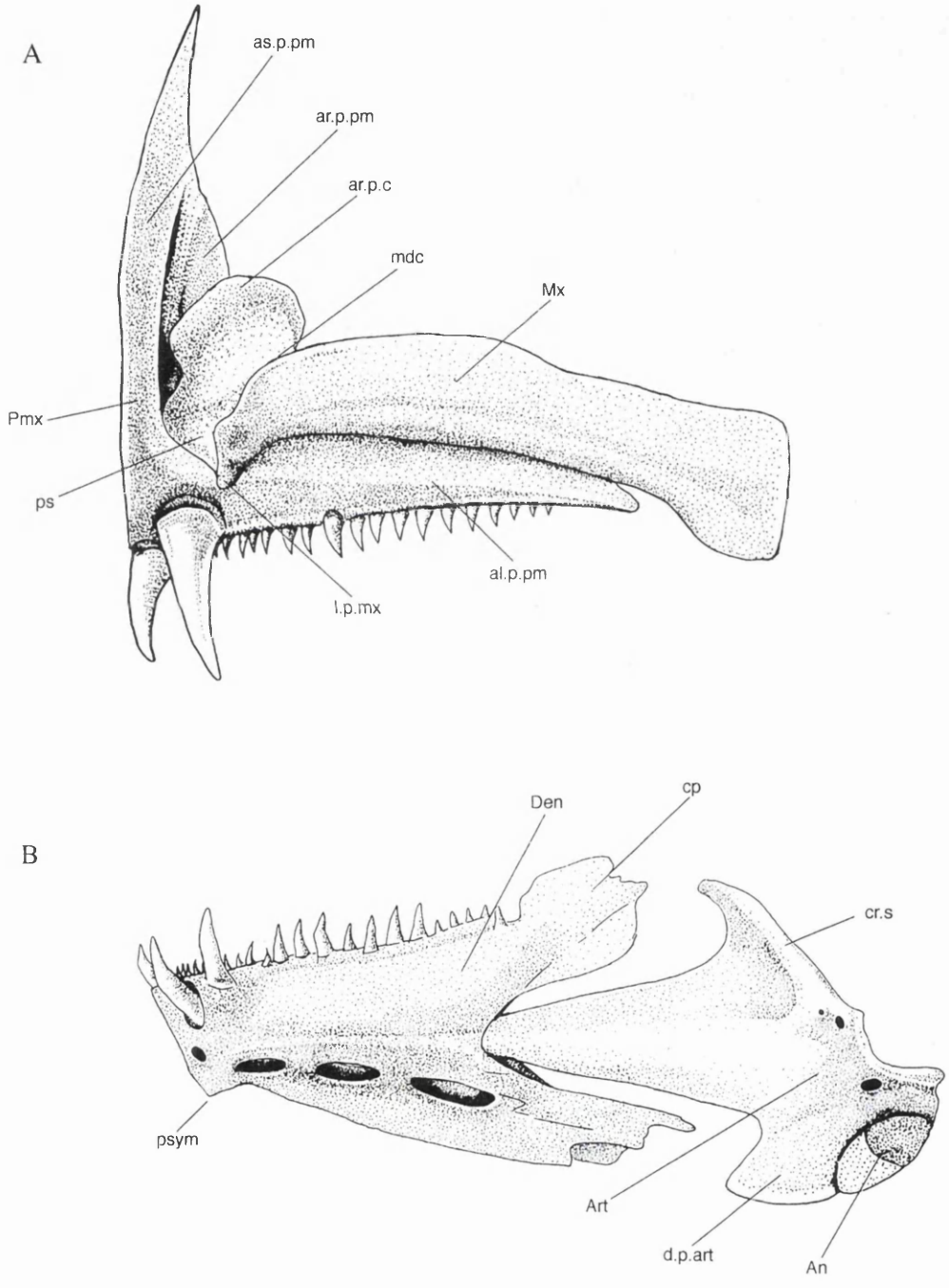
A
as.p.pm
ar.p.pm
ar.p.c
mdc
Mx
Pmx
ps
al.p.pm
l.p.mx
B
Den
cp
cr.s
psym
Art
d.p.art
An

FIGURE 2.5 ***Dentex dentex*** **BMNH 1845.6.22**

Camera lucida drawing of:

a. palatine arch

b. infraorbitals

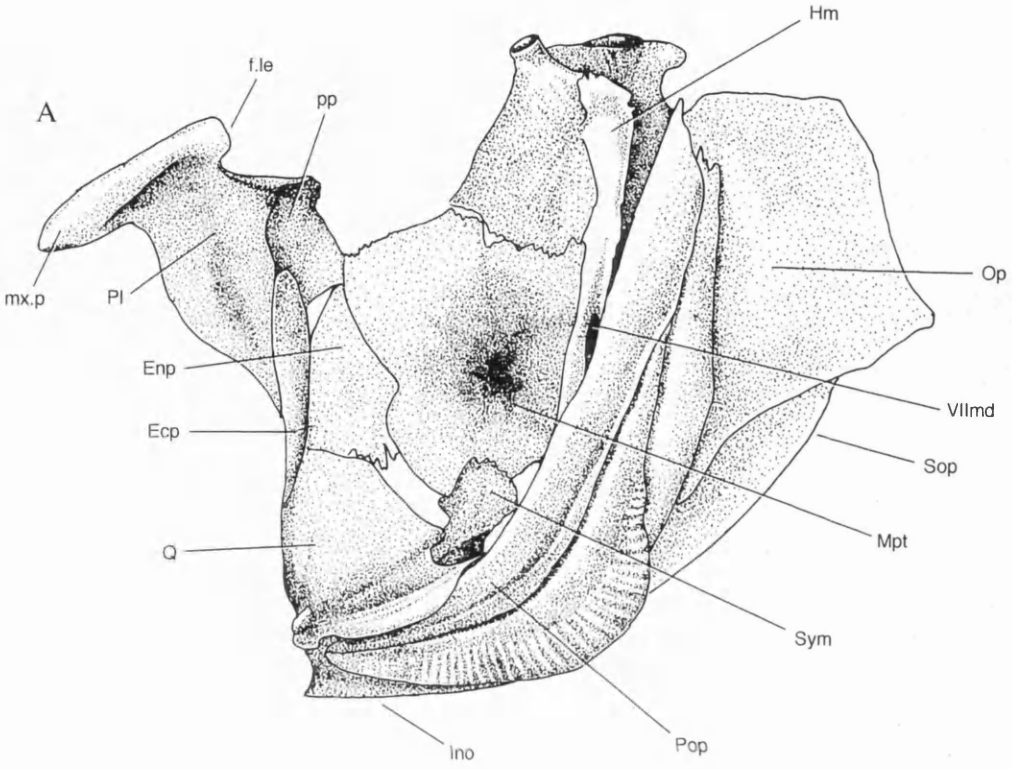
A
Hm
f.le
pp
Op
mx.p
Pl
Enp
VIImd
Ecp
Sop
Mpt
Q
Sym
Ino
Pop

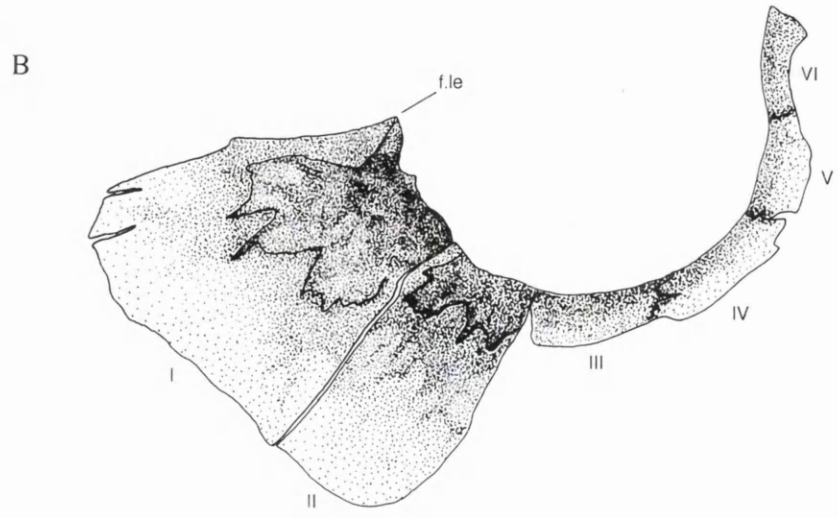
B
f.le
VI
V
IV
III
I
II

FIGURE 2.6 ***Dentex dentex*** **BMNH 1845.6.22**

Camera lucida drawing of:

a. the lower part of the hyoid arch

b. urohyal

c. gill arches, minus the upper pharyngeal jaws

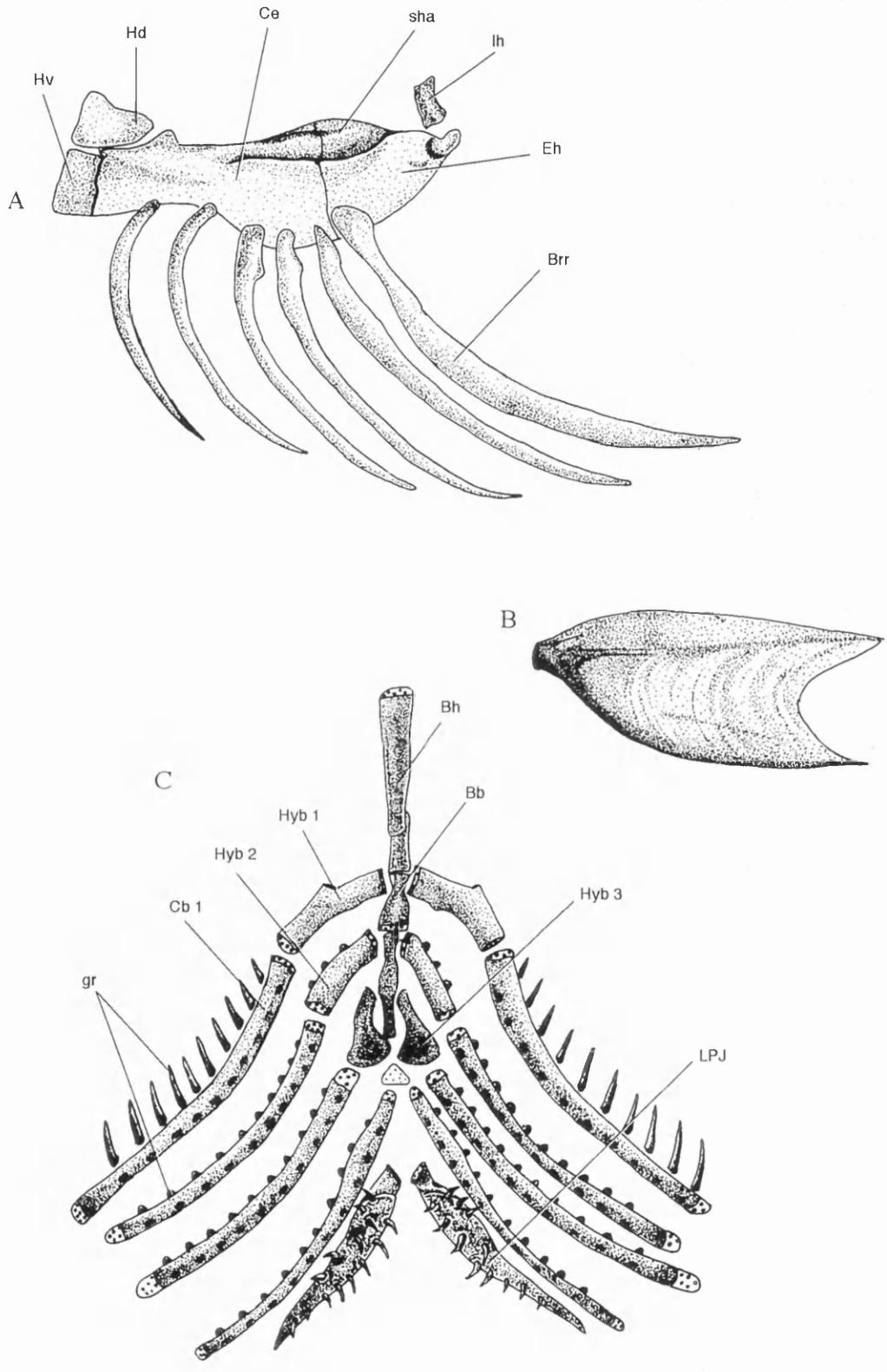
A
Hv
Hd
Ce
sha
Ih
Eh
Brr
B
C
Bh
Bb
Hyb 1
Hyb 2
Cb 1
Hyb 3
gr
LPJ

FIGURE 2.7 ***Dentex dentex*** **BMNH 1845.6.22**

Camera lucida drawing of the upper pharyngeal jaws drawn in dorsal and medial aspect

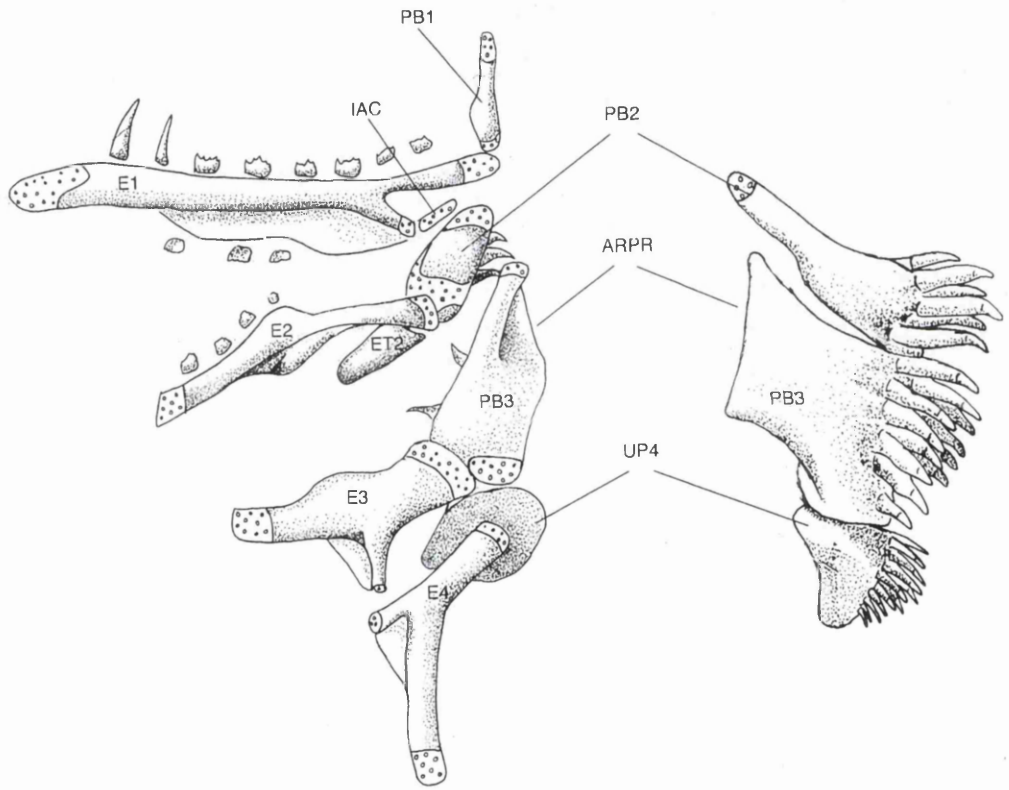
PB1
IAC
PB2
E1
ARPR
E2
ET2
PB3
PB3
UP4
E3
E4

FIGURE 2.8 ***Dentex dentex*** **BMNH 1845.6.22**

Camera lucida drawing of:

a. pectoral girdle in lateral aspect

b. posttemporal and supratemporal in lateral aspect

c. pelvic girdle in ventral aspect

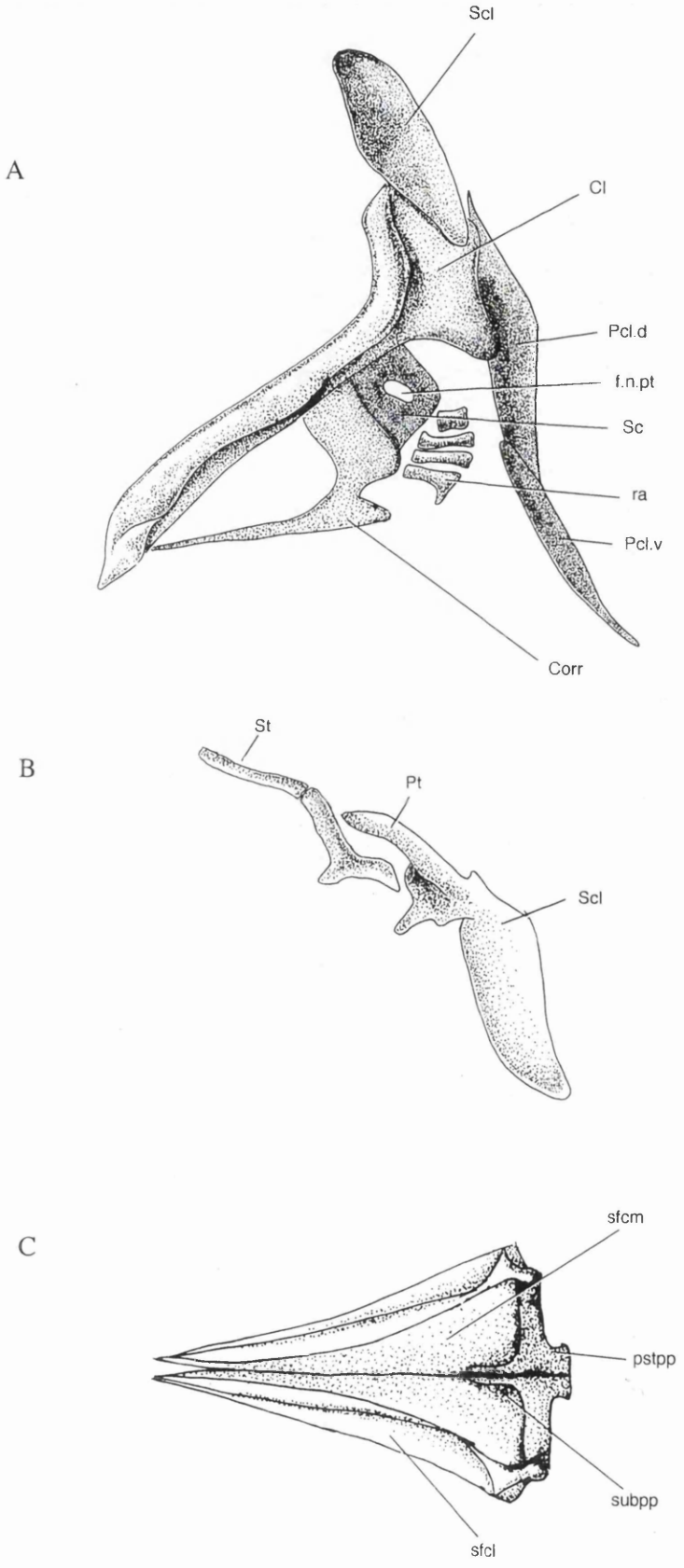
A
Scl
Cl
Pcl.d
f.n.pt
Sc
ra
Pcl.v
Corr
B
St
Pt
Scl
C
sfcm
pstpp
subpp
sfcl

FIGURE 2.9 ***Dentex dentex*** **BMNH 1845.6.22**

Camera lucida drawing of the caudal fin skeleton. Arrows indicate the limit of the principal rays

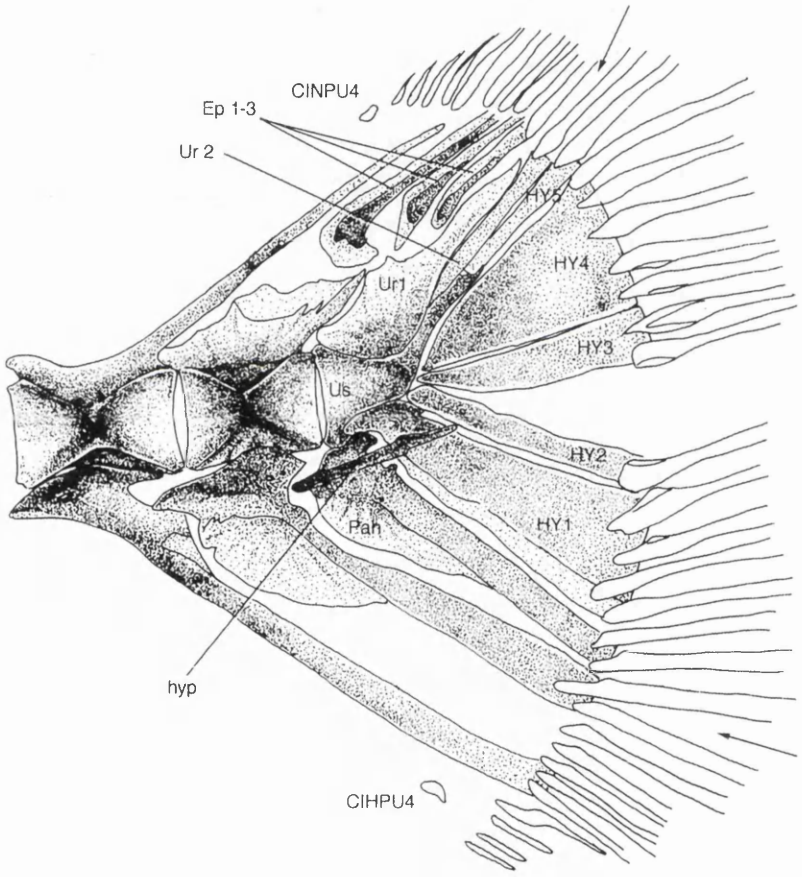
ClNPU4
Ep 1-3
Ur 2
HY5
HY4
Ur1
HY3
Us
HY2
Pah
HY1
hyp
ClHPU4

FIGURE 2.10 ***Diplodus rondeletii*** **BMNH 1890.6.29**
Camera lucida drawing of the braincase in lateral view

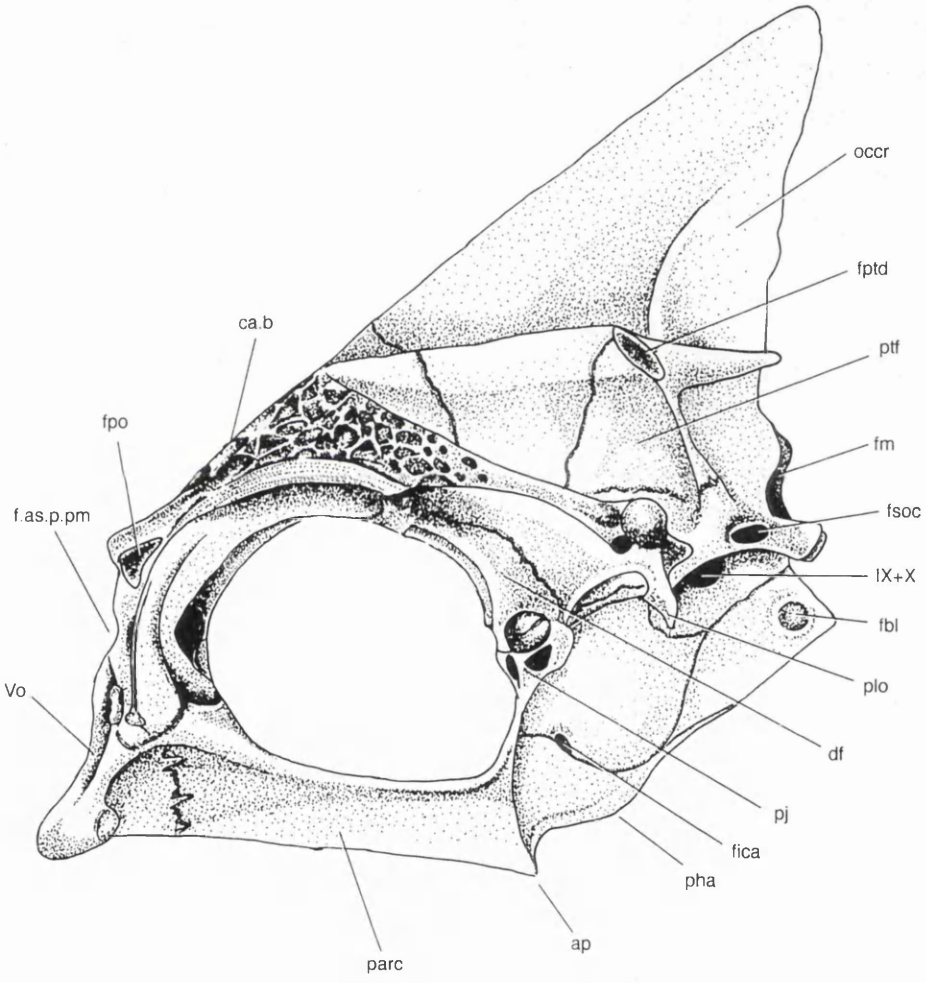
occr
fptd
ca.b
ptf
fpo
fm
f.as.p.pm
fsoc
IX+X
fbl
plo
Vo
df
pj
fica
pha
ap
parc

FIGURE 2.11 ***Diplodus rondeletii*** **BMNH 1890.6.29**

Camera lucida drawing of the braincase:

a. ventral view

b. dorsal view

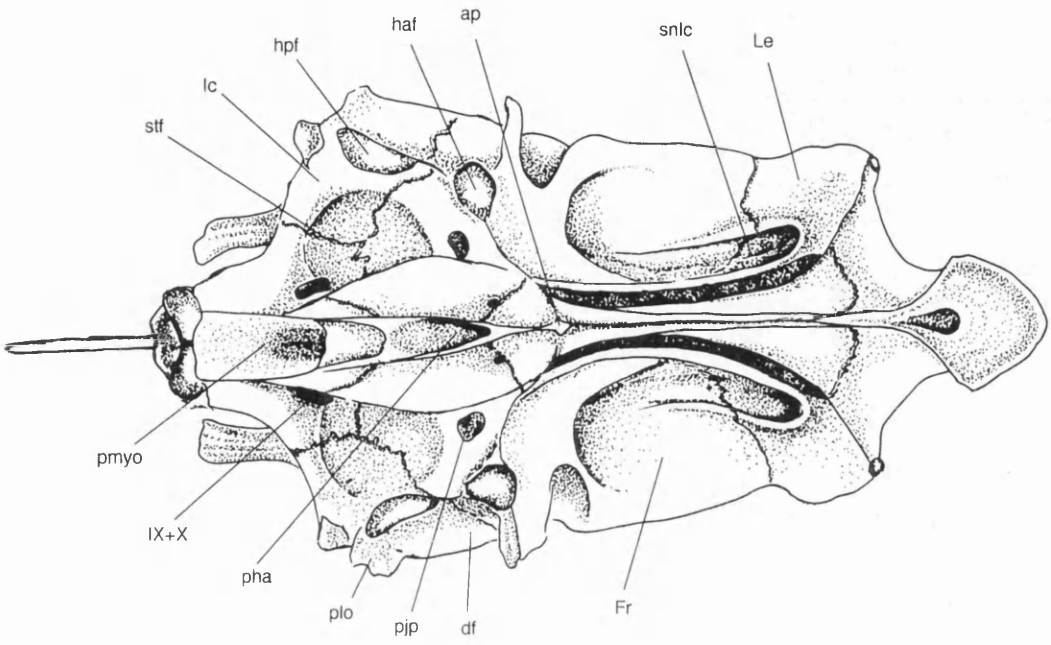
haf
ap
hpf
snlc
Le
lc
stf
pmyo
IX+X
pha
plo
pjp
df
Fr

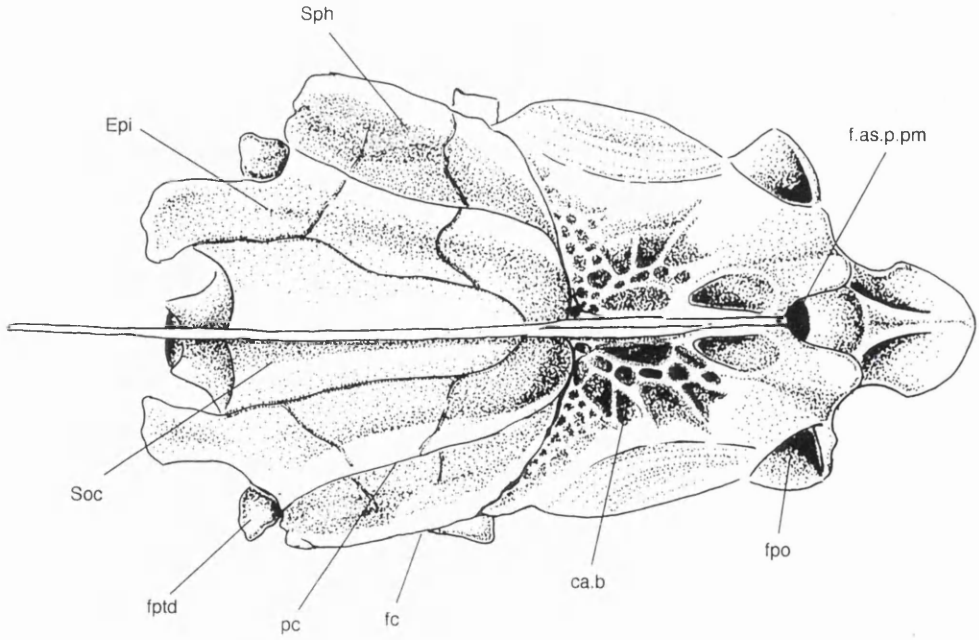
Sph
Epi
f.as.p.pm
Soc
fptd
pc
fc
ca.b
fpo

FIGURE 2.12 ***Calamus calamus*** **BMNH 1905.3.19**

Camera lucida drawing of the braincase:

a. lateral view

b. ventral view

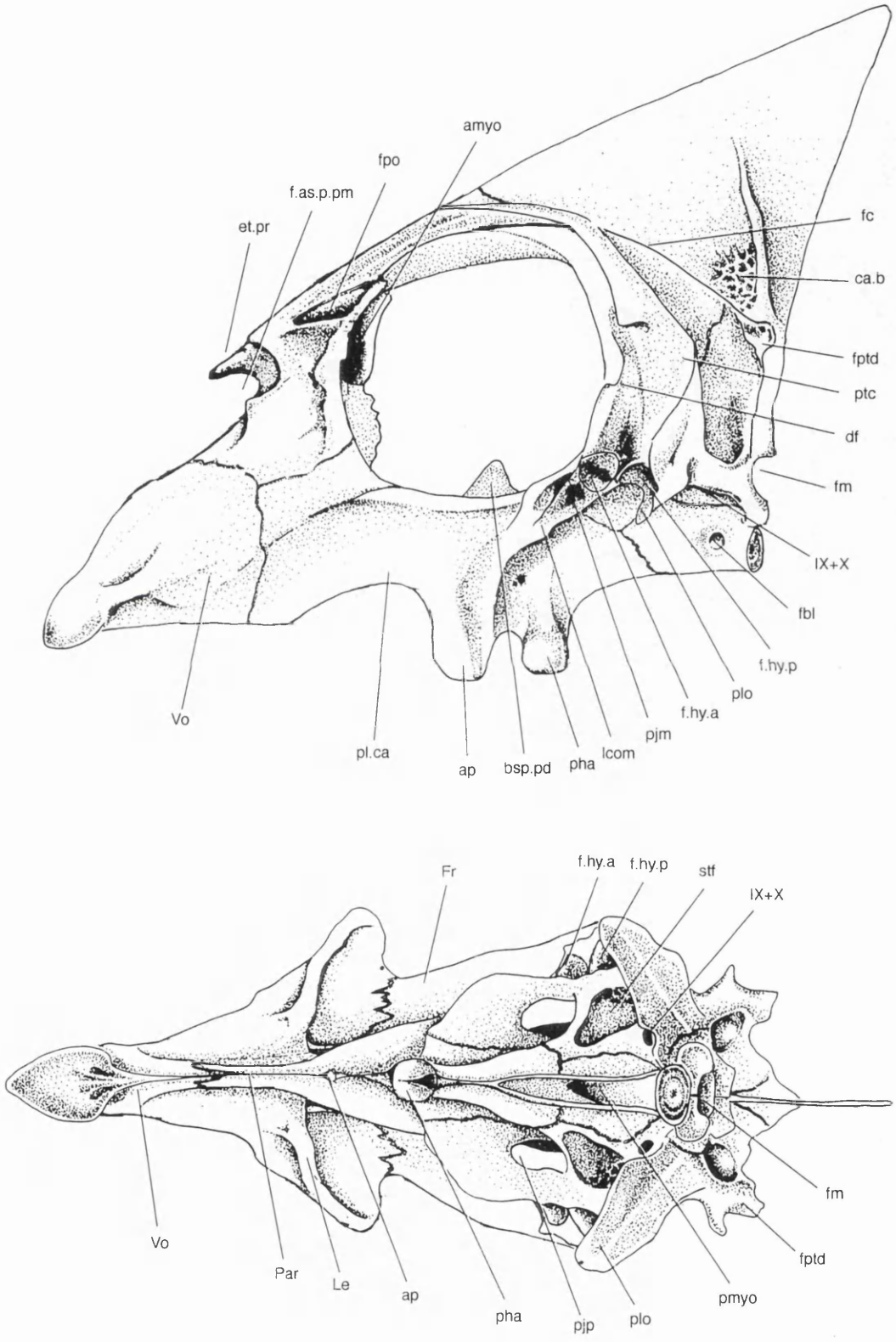
amyo
fpo
f.as.p.pm
et.pr
fc
ca.b
fptd
ptc
df
fm
IX+X
fbl
f.hy.p
plo
f.hy.a
pjm
lcom
pha
bsp.pd
ap
pl.ca
Vo
Fr
f.hy.a
f.hy.p
stf
IX+X
fm
fptd
pmyo
plo
pjp
pha
ap
Le
Par
Vo

FIGURE 2.13 *Camera lucida* drawing of the braincases:

a. Lateral view of *Pagellus erythrinus* BMNH 1982.5.10

b. Lateral view of *Sarpa salpa* BMNH 1859.5.4

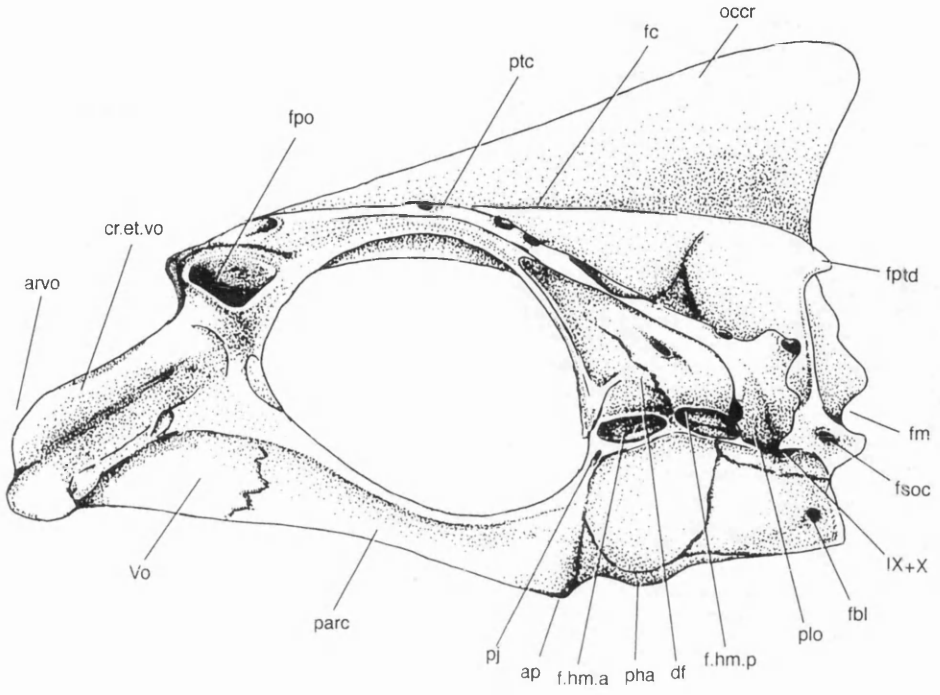
occr
fc
ptc
fpo
cr.et.vo
arvo
fptd
fm
fsoc
IX+X
fbl
plo
Vo
parc
pj
ap
f.hm.a
pha
df
f.hm.p

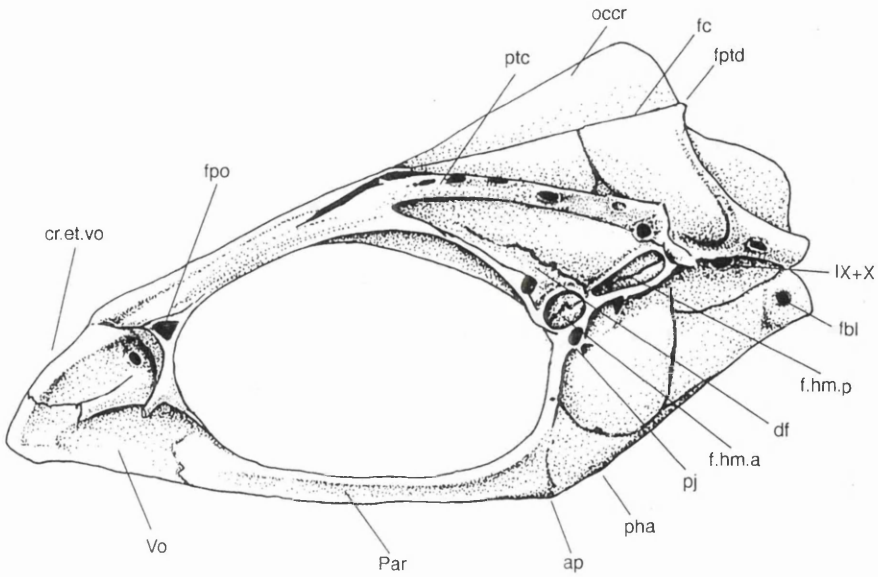
occr
fc
ptc
fptd
fpo
cr.et.vo
IX+X
fbl
f.hm.p
df
f.hm.a
pj
pha
Vo
Par
ap

FIGURE 2.14 ***Sparus auratus*** **AMNH 093436**
Camera lucida drawing of the braincase in occipital view

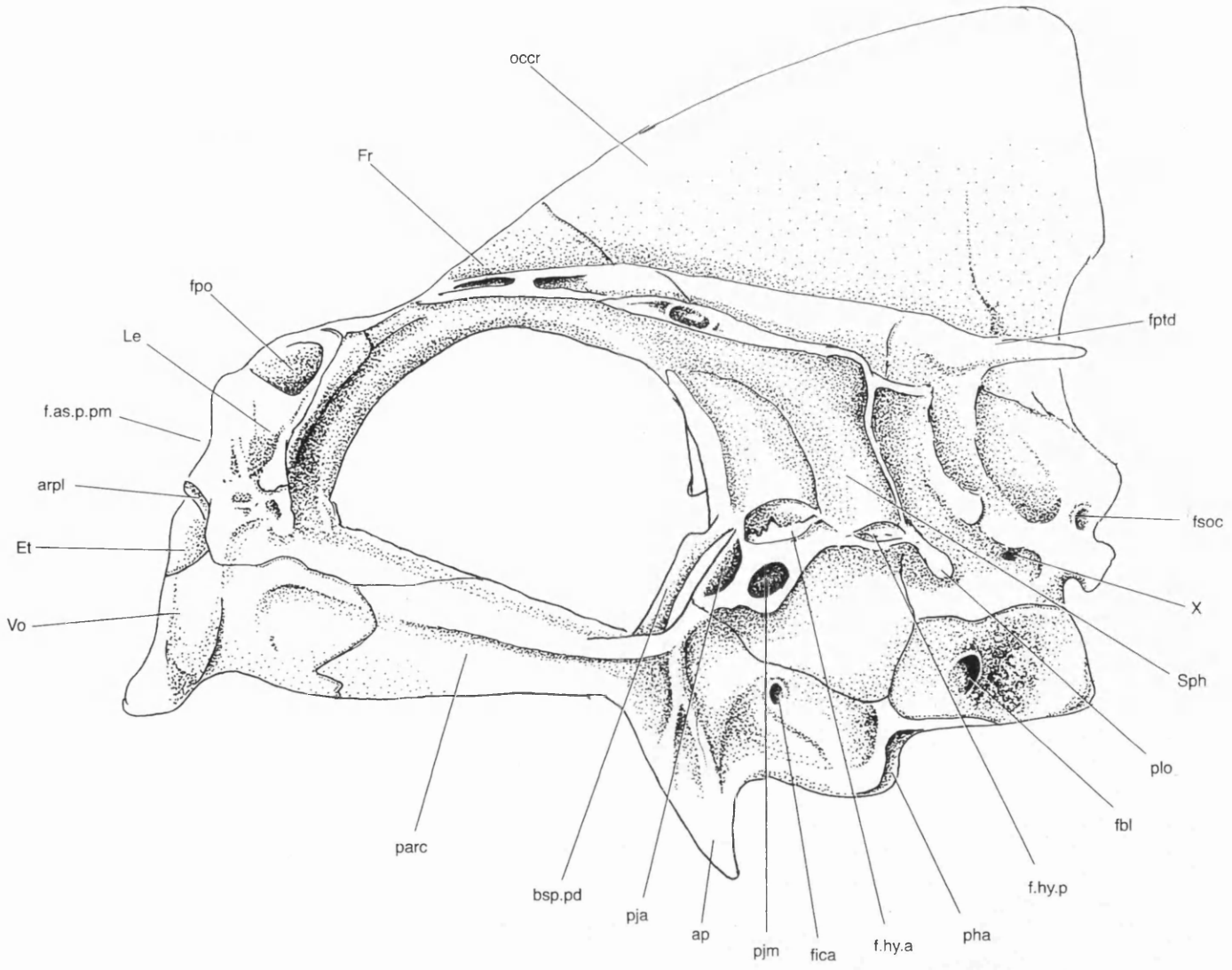
occr
Fr
fpo
Le
f.as.p.pm
arpl
Et
Vo
fptd
fsoc
X
Sph
plo
fbl
f.hy.p
pha
f.hy.a
fica
pjm
ap
pja
bsp.pd
parc

FIGURE 2.15 *Stenotomus caprinus* **USNM 155372**

a..*Camera lucida* drawing of the jaw in lateral view

b. *Camera lucida* drawing showing the specialized articulation between the premaxilla and maxilla

c. same as b, but with the maxilla draw behind the premaxilla

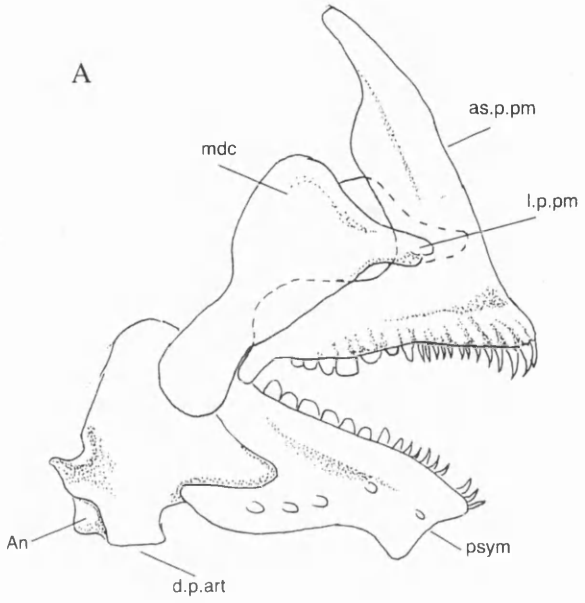
A
as.p.pm
mdc
l.p.pm
An
psym
d.p.art

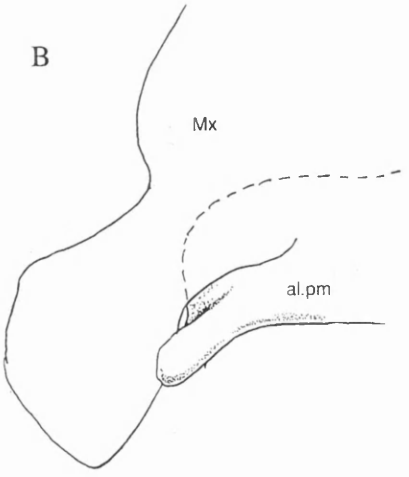
B
Mx
al.pm

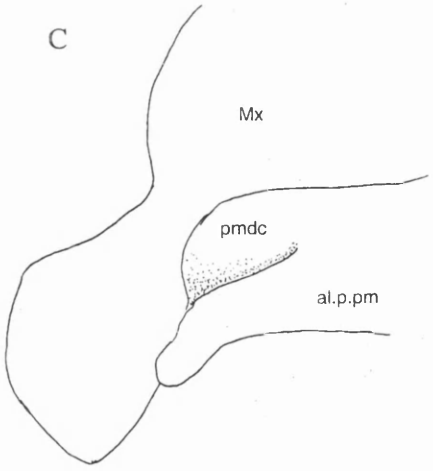
C
Mx
pmdc
al.p.pm

FIGURE 2.16 ***Camera lucida drawing of the jaws*:**

a. Lateral view of *Spiraca smaris* USNM 290493

b. Lateral view of *Gymnocranius griseus* USNM 290494

c. Lateral view of *Scolopsis bilineatus* USNM 290482

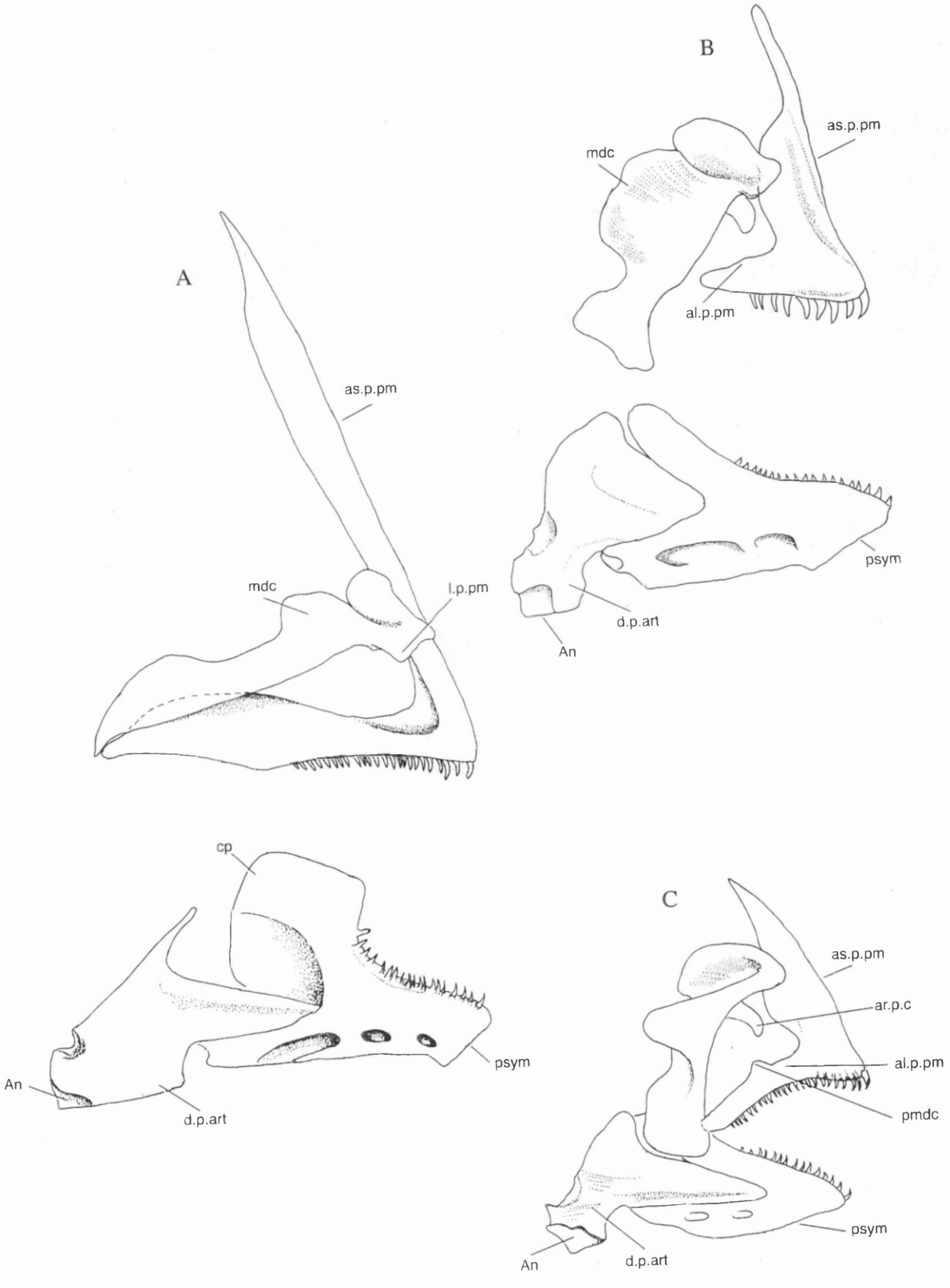
A
as.p.pm
mdc
l.p.pm
B
as.p.pm
mdc
al.p.pm
psym
d.p.art
An
cp
An
d.p.art
psym
C
as.p.pm
ar.p.c
al.p.pm
pmdc
psym
An
d.p.art

FIGURE 2.17 ***Pagellus erythrinus*** **BMNH 1982.5.10**

Camera lucida drawing of the jaws in lateral view

a. premaxilla

b. maxilla

c. dentary

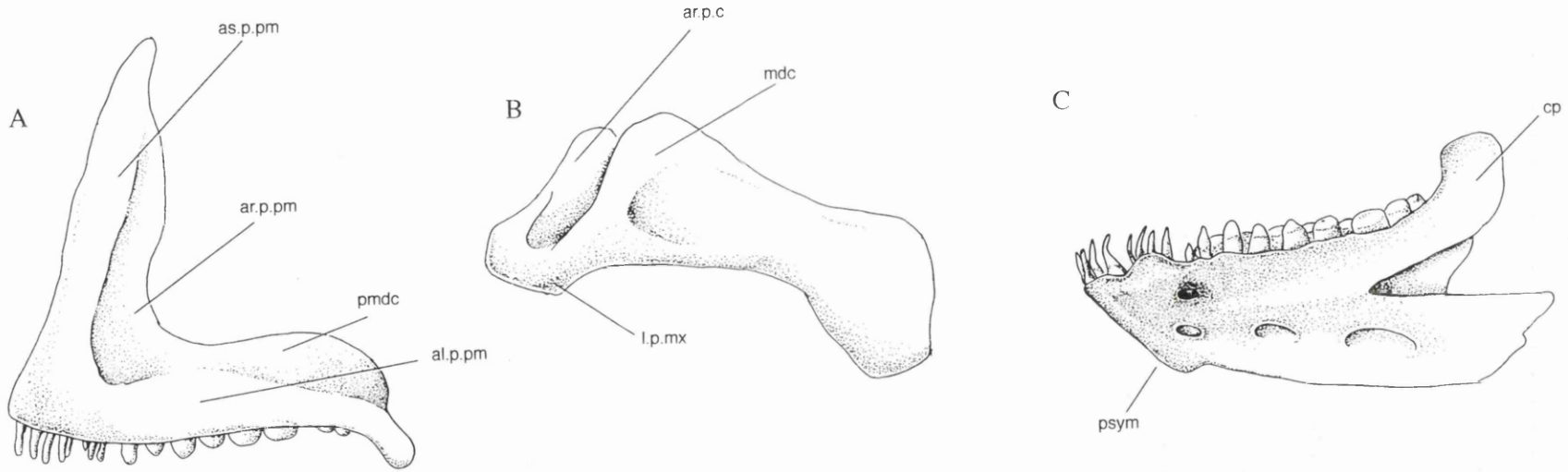
A
as.p.pm
ar.p.pm
pmdc
al.p.pm
B
ar.p.c
mdc
l.p.mx
C
cp
psym

FIGURE 2.18 ***Diplodus rondeletii*** **BMNH 1890.6.29**

Camera lucida drawing of the jaws in lateral view

a. premaxilla

b. maxilla

c. mandible

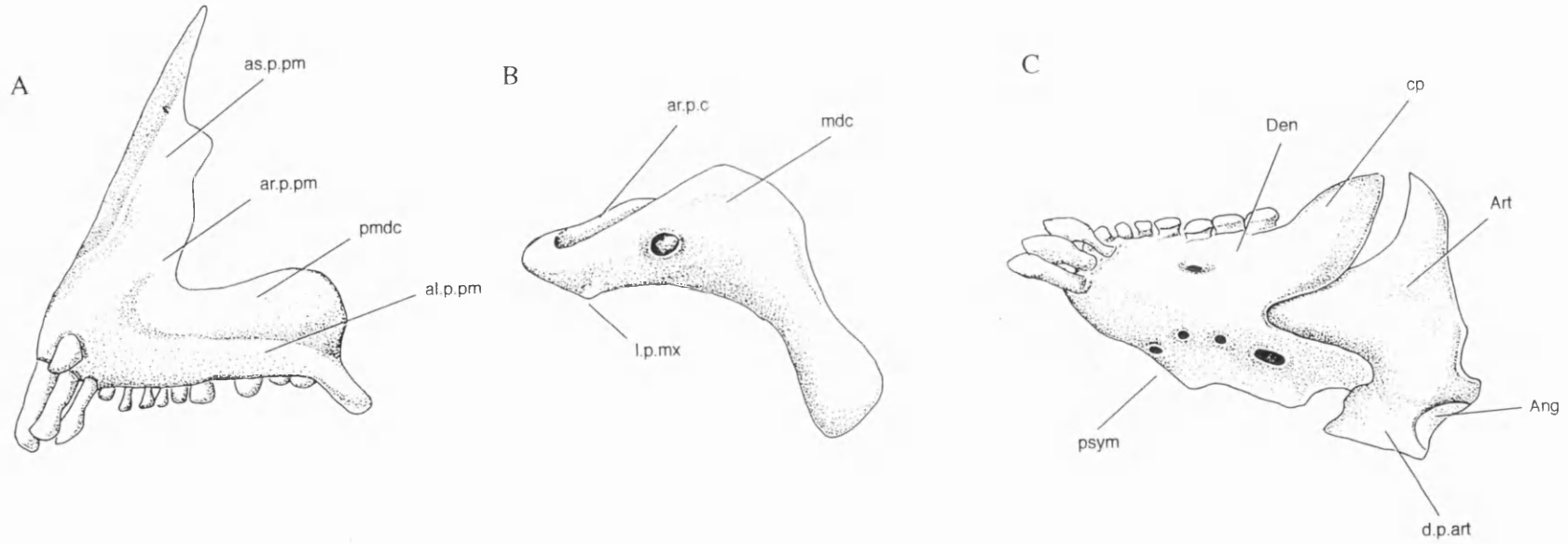
A
as.p.pm
ar.p.pm
pmdc
al.p.pm
B
ar.p.c
mdc
l.p.mx
C
cp
Den
Art
Ang
psym
d.p.art

FIGURE 2.19 *Sarpa salpa* BMNH 1859.5.4

Camera lucida drawing of the jaws in lateral view

a. premaxilla and maxilla

b. dentary

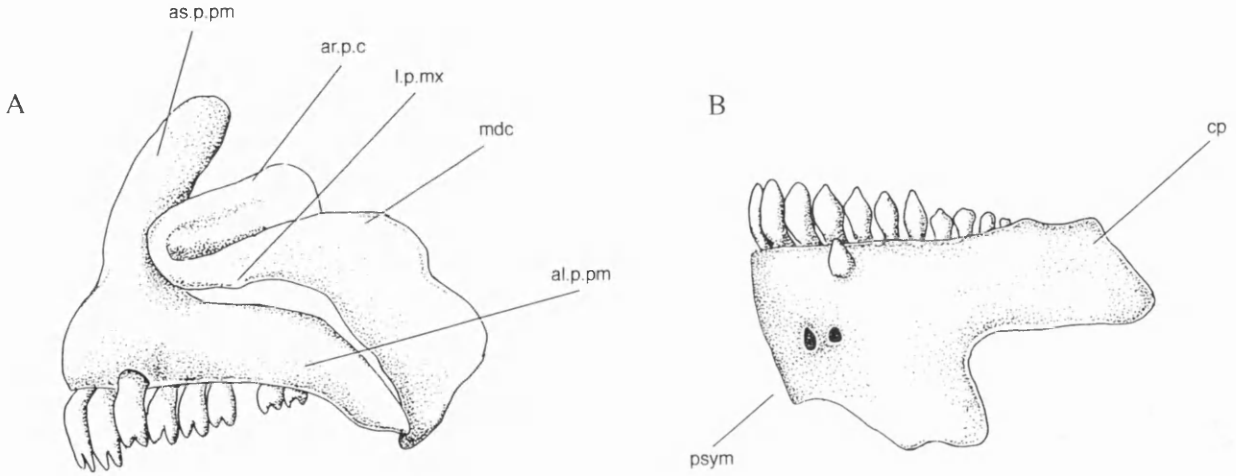
A
as.p.pm
ar.p.c
l.p.mx
mdc
al.p.pm
B
cp
psym

FIGURE 2.20 *Camera lucida* drawing

a. Palatine arch of *Boops boops* BMNH 1982.5.10 in lateral view

b. Infraorbital series of *Gymnocranius griseus* USNM 290494 in lateral view

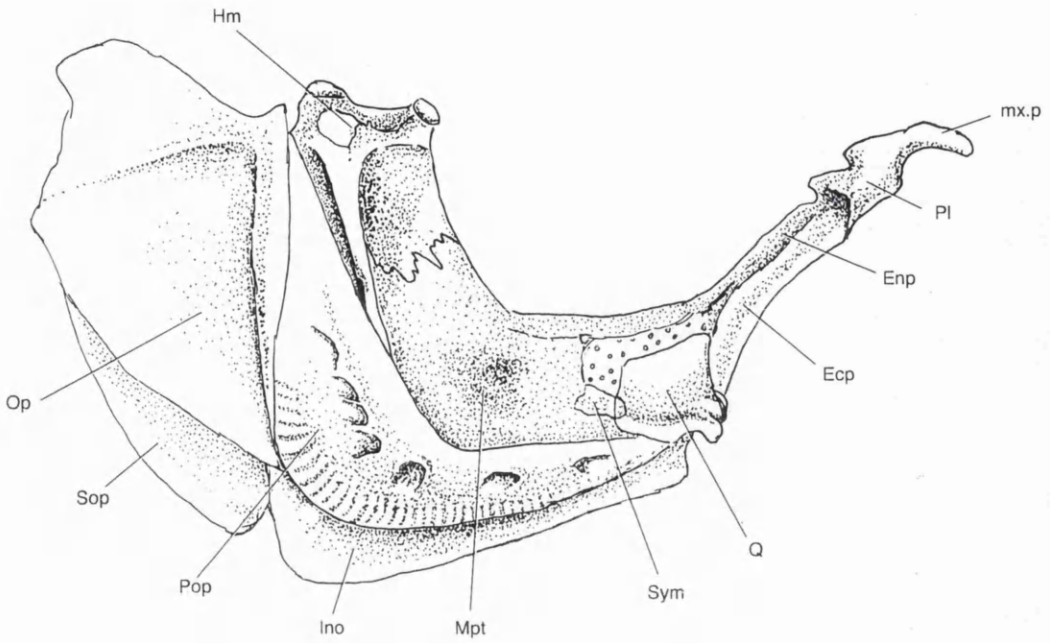
Hm
mx.p
Pl
Enp
Ecp
Op
Sop
Pop
Ino
Mpt
Sym
Q

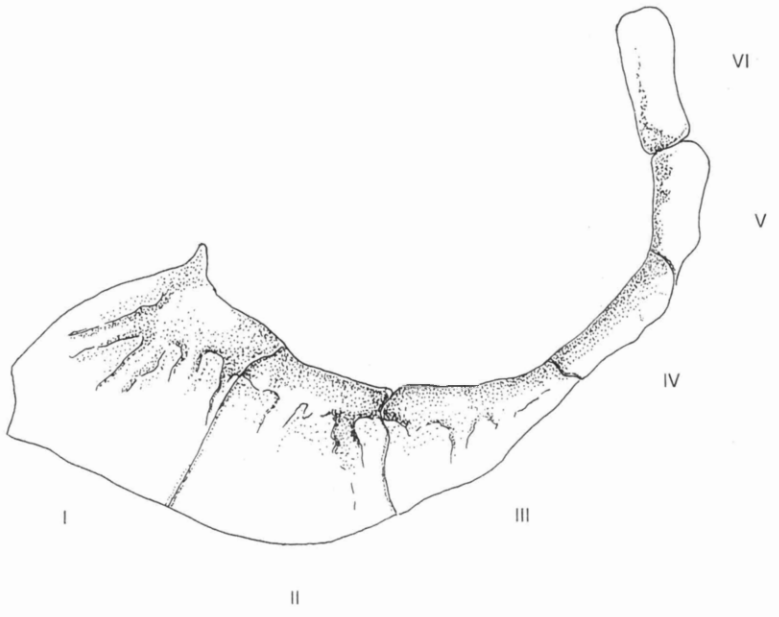
VI
V
IV
I
III
II

FIGURE 2.21 *Camera lucida* drawing

a. lower part of the hyoid arch of Boops boops BMNH 1982.5.10 in lateral view
b. lower part of the hyoid arch of *Calamus penna* BMNH 1985.7.16 in lateral view
c. gill arches of *Calamus penna* BMNH 1985.7.16 in lateral view
d. urohyal of Sparus aurauts USNM 347127 in lateral view
e. urohyal of Pagrus pagrus BMNH 1997.9.18 in lateral view

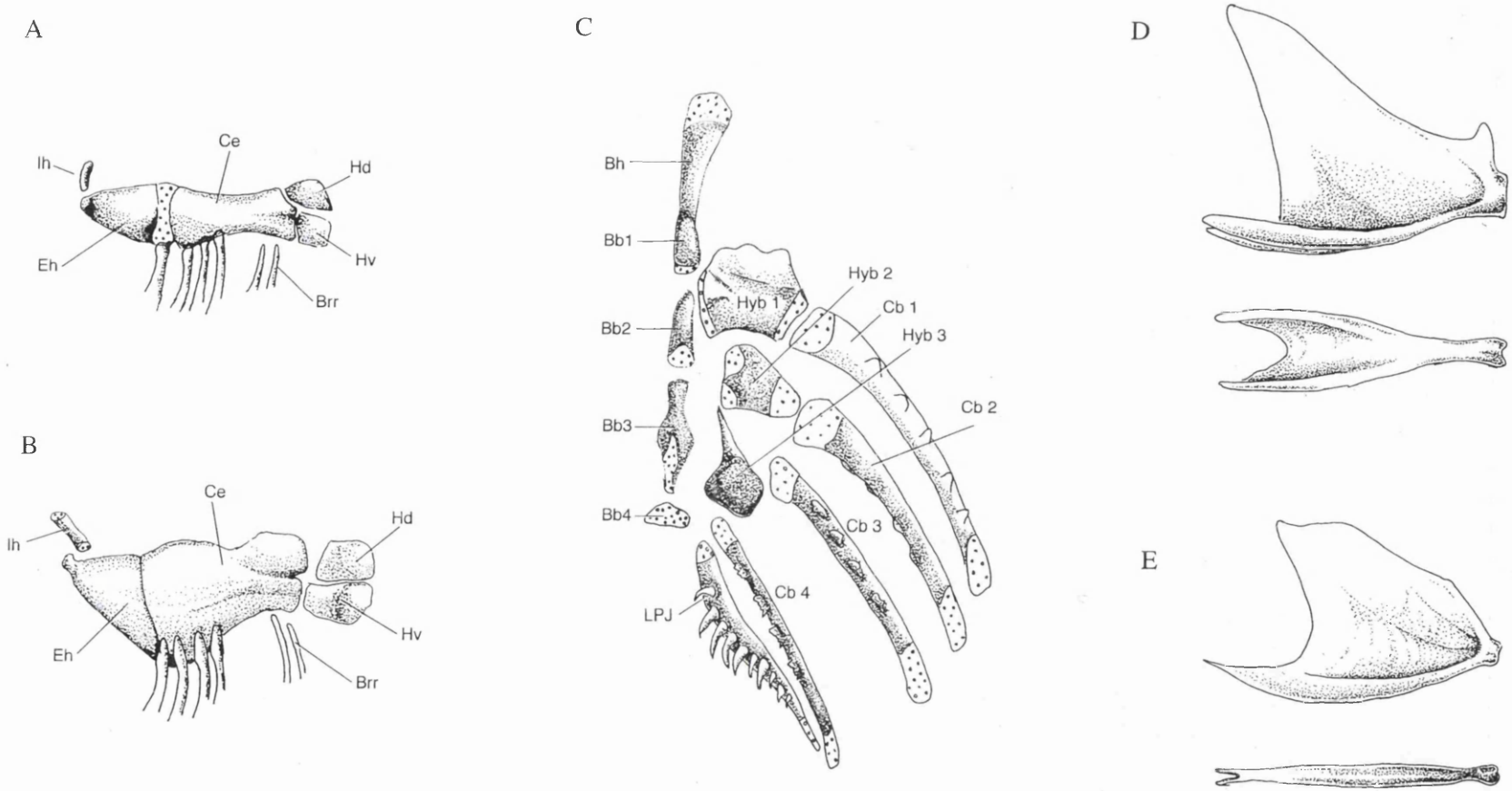
A
Ih
Ce
Hd
Eh
Hv
Brr
B
Ih
Ce
Hd
Eh
Hv
Brr
C
Bh
Bb1
Bb2
Bb3
Bb4
Hyb 1
Hyb 2
Hyb 3
Cb 1
Cb 2
Cb 3
Cb 4
LPJ
D
E

FIGURE 2.22 *Camera lucida* drawing of the ceratobranchial and hyobranchials:

a. *Calamus penna* BMNH 1985.7.16 in dorsal view

b. *Diplodus cervinus hottentotus* BMNH 1997.9.81 in dorsal view

c. *Scolopsis bilineatus* USNM 290482 in dorsal view

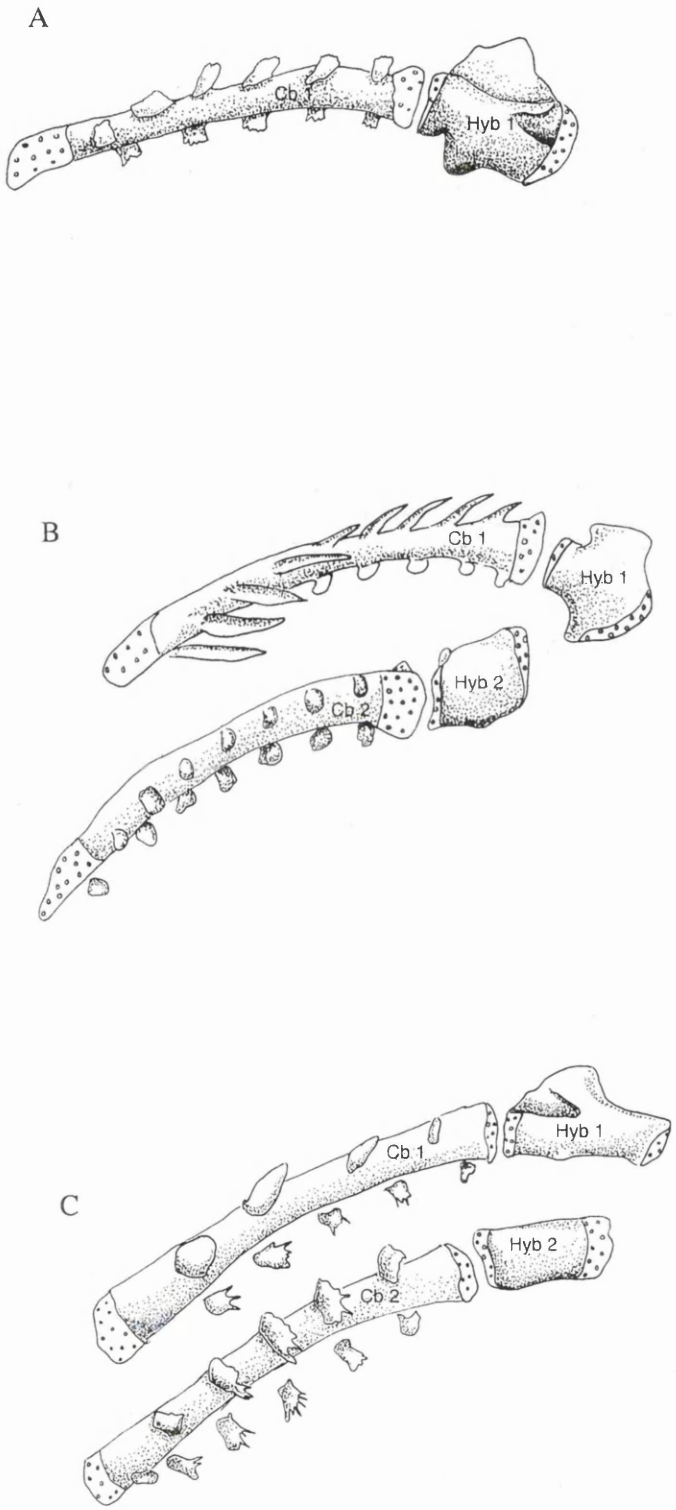
A
Cb 1
Hyb 1
B
Cb 1
Hyb 1
Hyb 2
Cb 2
C
Hyb 1
Cb 1
Hyb 2
Cb 2

FIGURE 2.23 *Camera lucida* drawing of the upper pharyngeal jaws:

a. *Calamus penna* BMNH 1985.7.16 drawn in dorsal aspect

b. *Sparus auratus* USNM 347127 in dorsal and medial aspect

c. *Boops boops* USNM 347127 in drawn in dorsal aspect

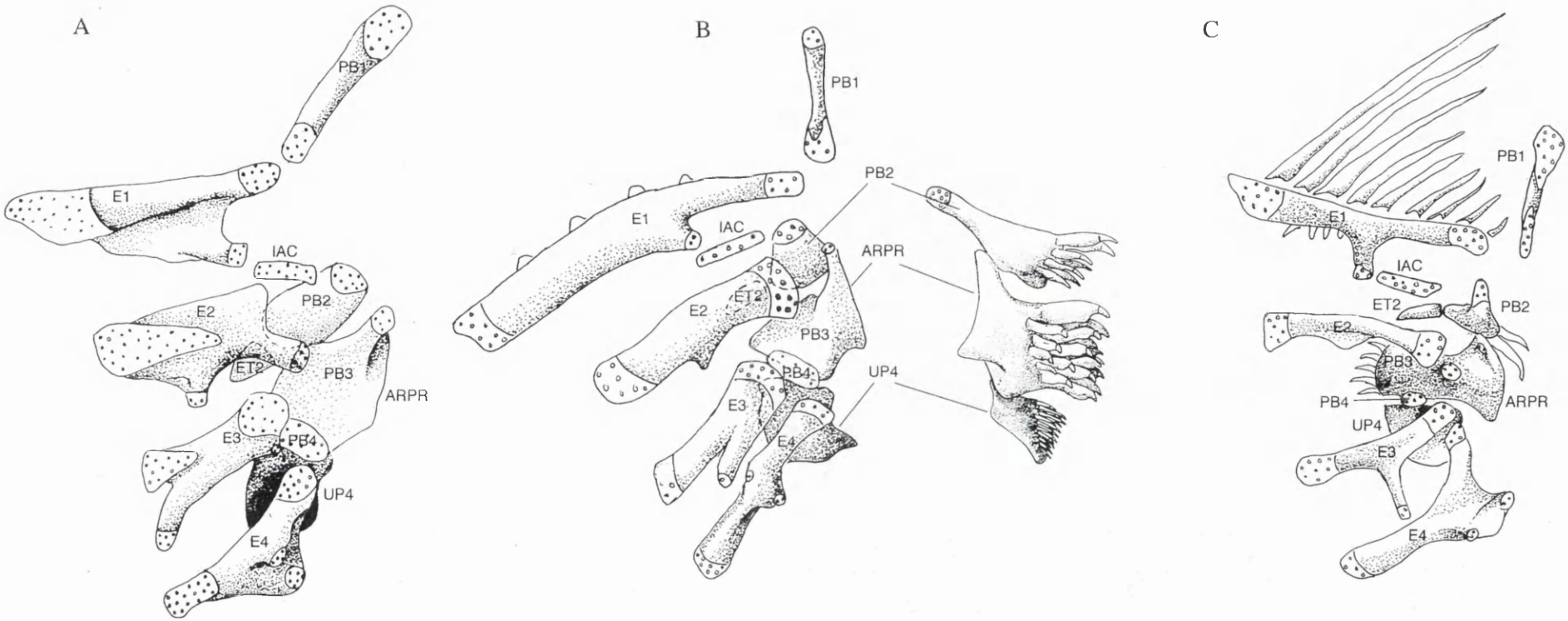
A
PB1
E1
IAC
E2
PB2
ET2
PB3
ARPR
E3
PB4
UP4
E4
B
PB1
PB2
E1
IAC
ARPR
E2
ET2
PB3
PB4
UP4
E3
E4
C
PB1
E1
IAC
ET2
PB2
E2
PB3
PB4
ARPR
UP4
E3
E4

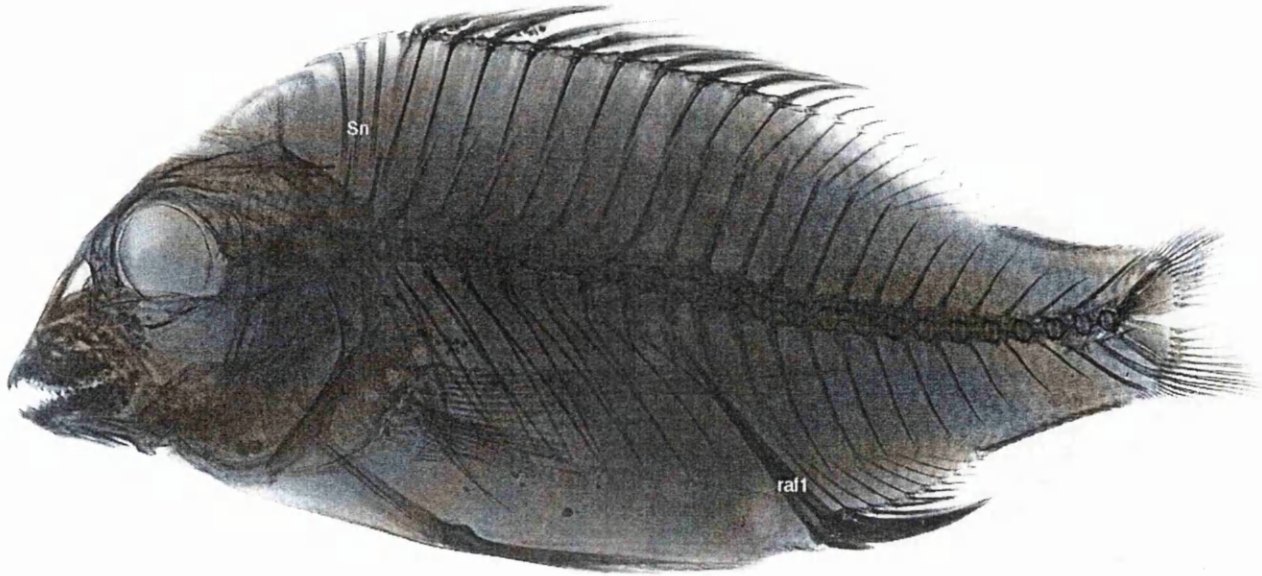

Plate 2.2 *Acanthopagrus latus* BMNH 1987.2.12 (SL 83mm)

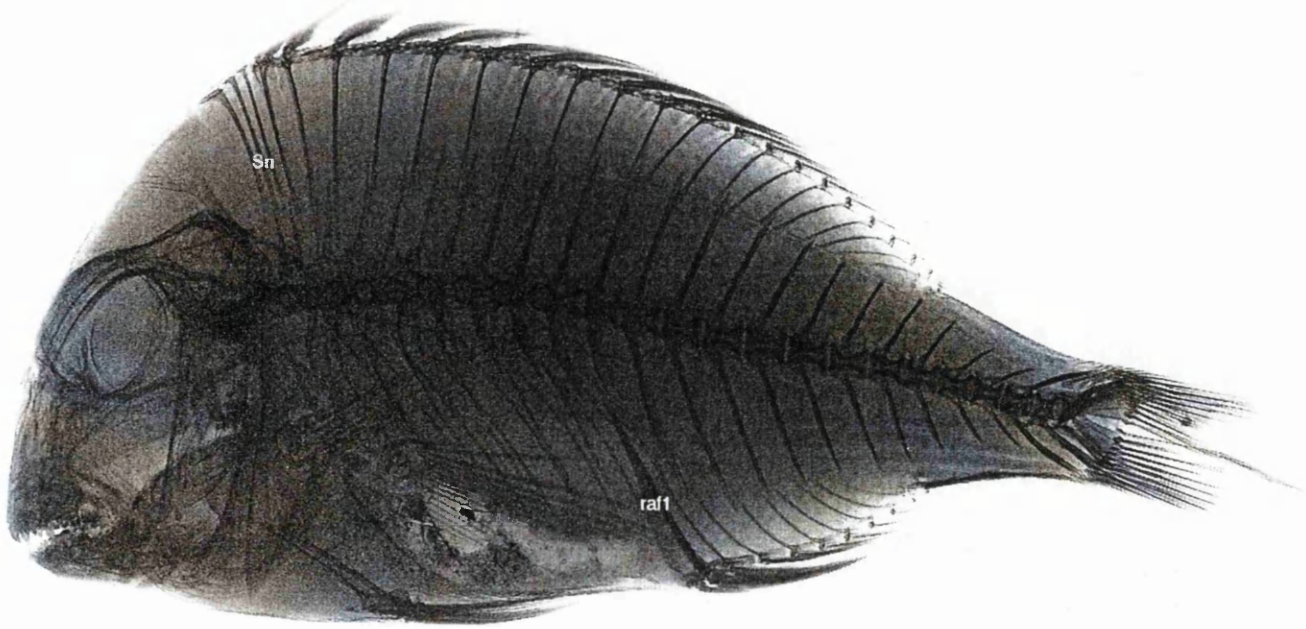

Plate 2.3 *Argyops spinfer* BMNH 1979.3.23 (SL 113mm)

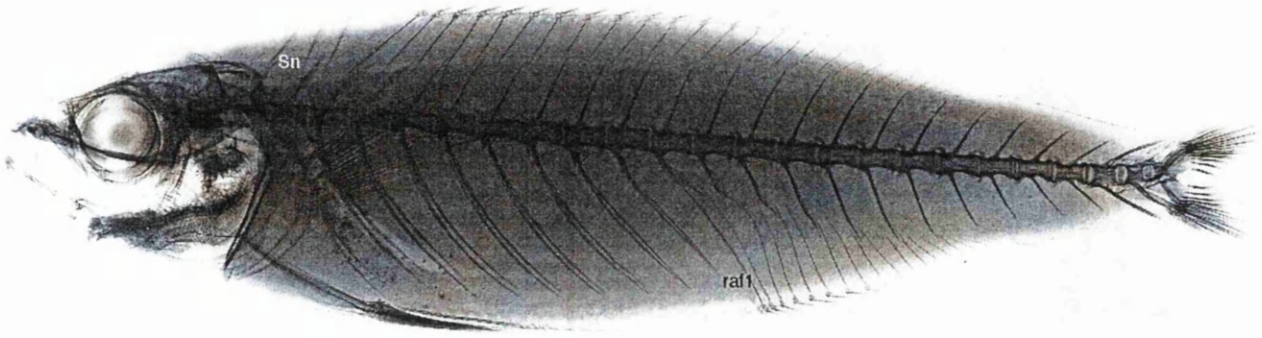

Plate 2.4 *Boops boops* BMNH 1964.8.6 (SL 280)

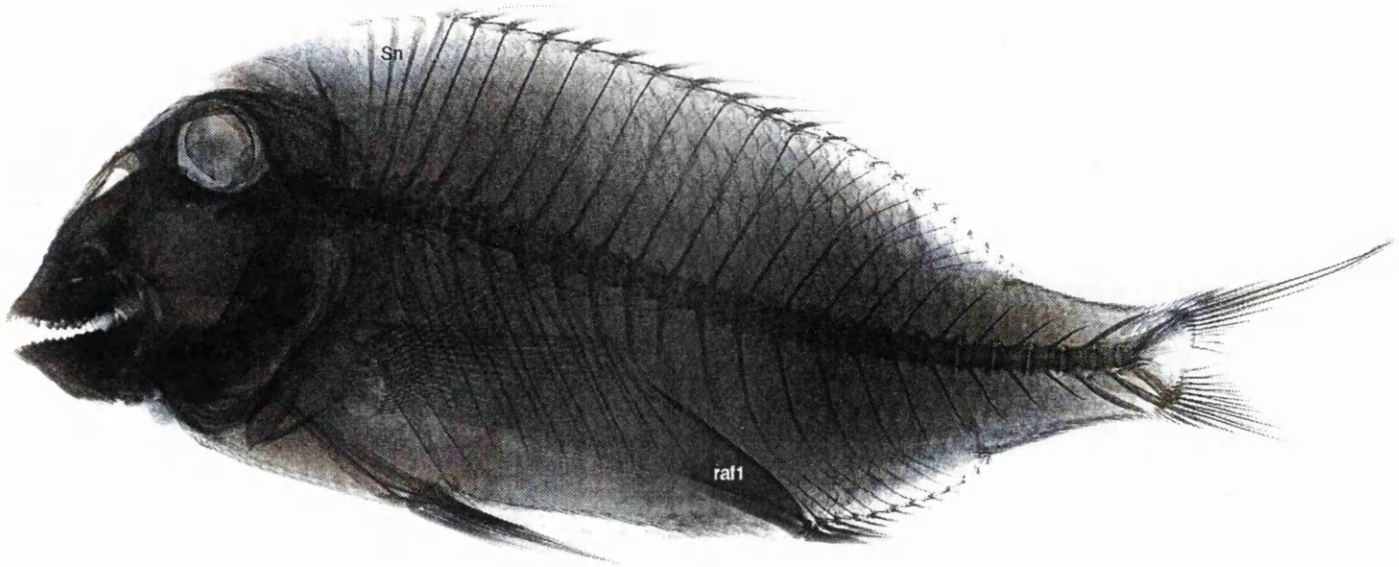

Plate 2.5 *Calamus arctifrons* BMNH 1884.7.7 (SL 177mm)

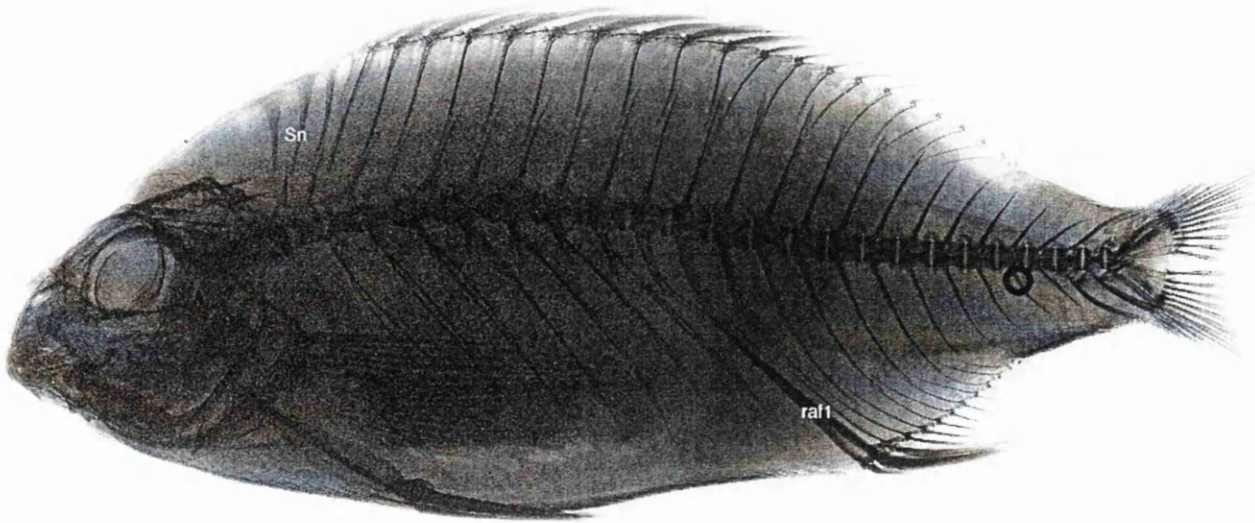

Plate 2.6 *Crenidens crenidens* BMNH 1984.2.13 (SL 176mm)

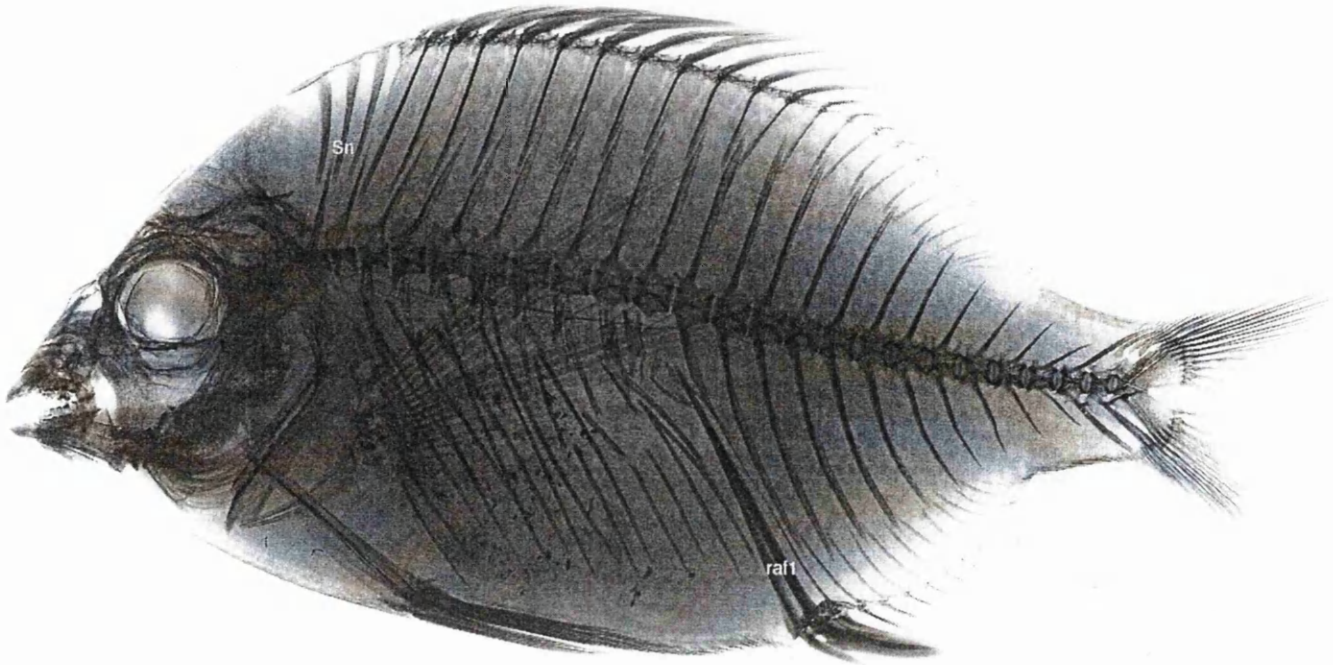

Plate 2.7 *Diplodus holbrookei* BMNH 1933.10.12 (SL 173mm)

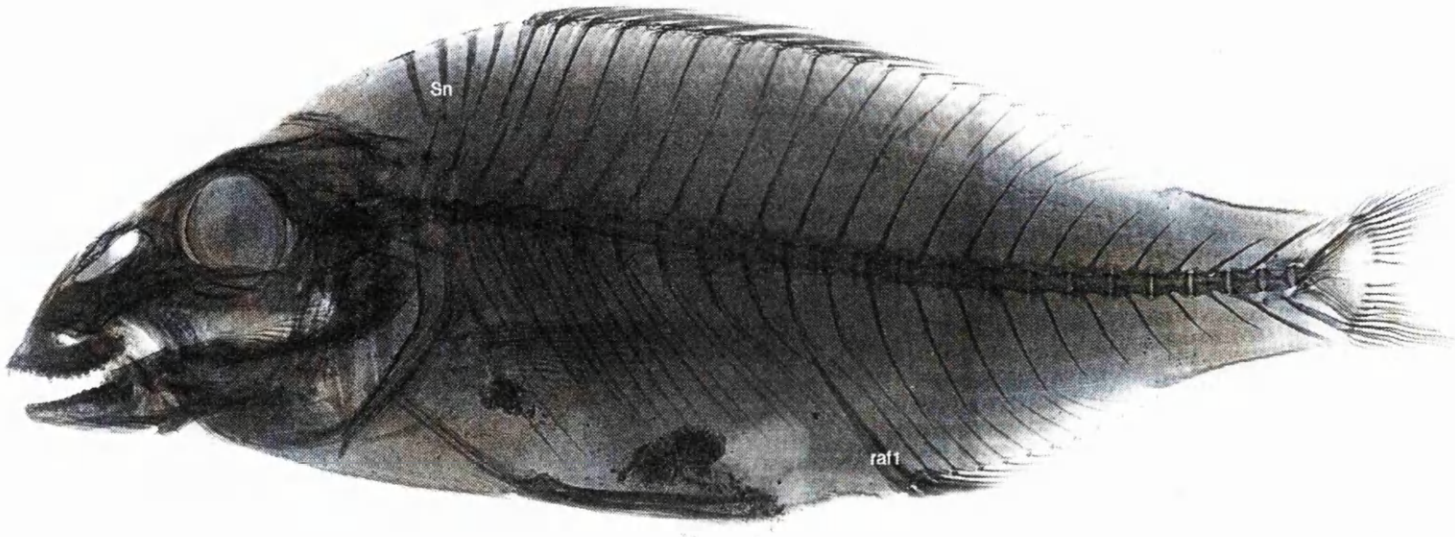

Plate 2.8 *Lithognathus mormyrus* BMNH 1983.10.11 (SL 132mm)

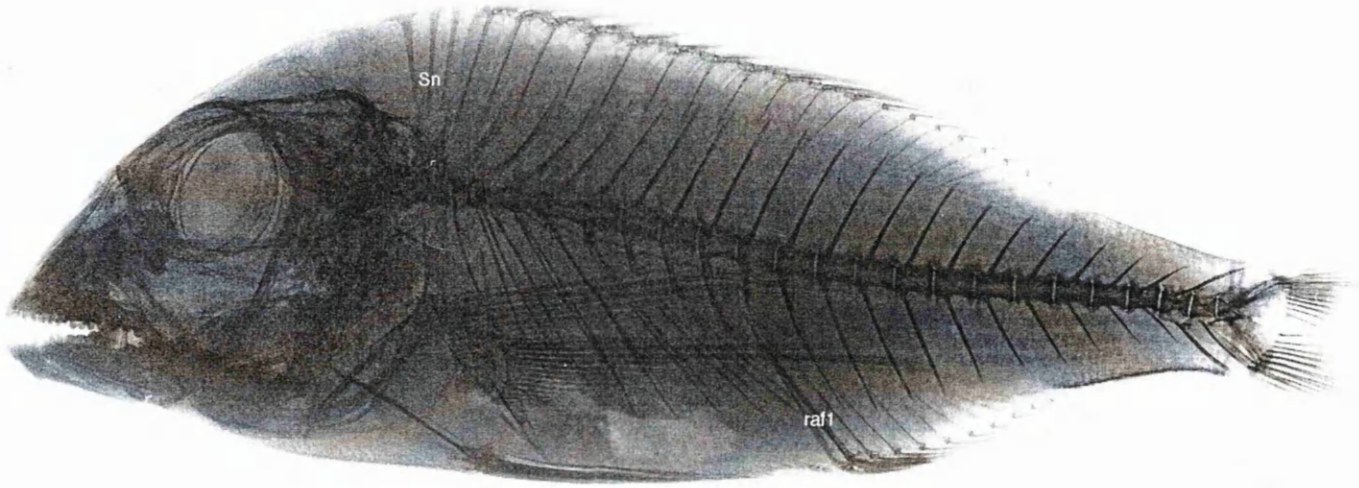

Plate 2.9 *Pagellus erythrinus* BMNH 1935.3.5 (SL 161mm)

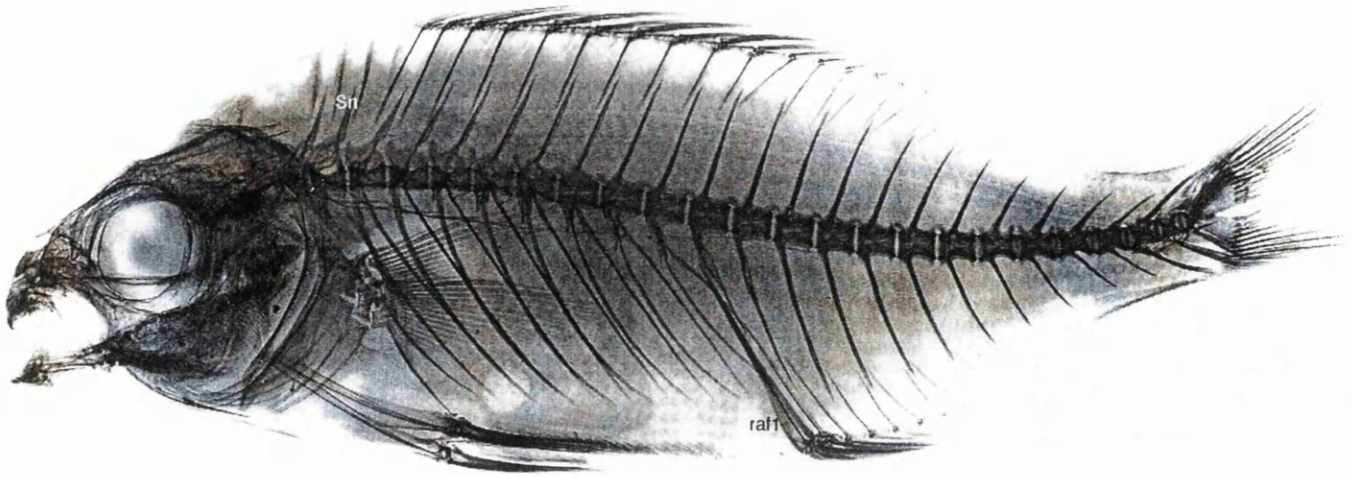

Plate 2.10 *Sarpa salpa* BMNH 1872.12.13 (SL 115mm)

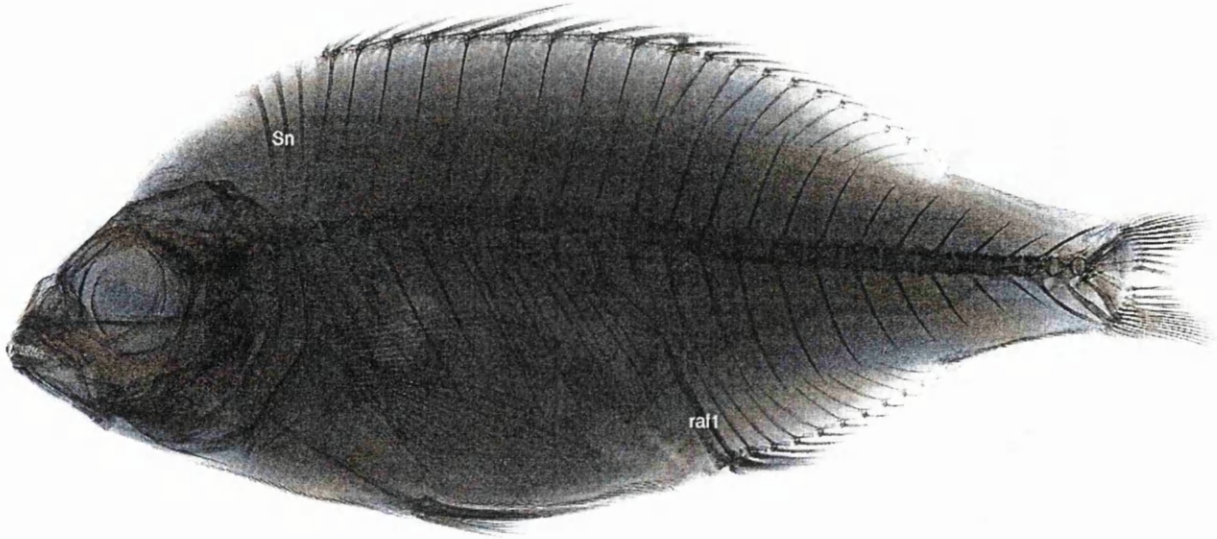

Plate 2.11 *Spondyliosoma cantharus* BMNH 1983.10.11 (SL 125mm)

CHAPTER 3

PHYLOGENETIC RELATIONSHIPS OF THE SPARIDAE

"The real purpose of scientific method is to make sure Nature hasn't misled you into thinking you know something you don't actually know."

Robert M. Pirsig (1974)
Zen and the Art of Motorcycle Maintenance

Introduction

Cladistic analysis, accepted by many systematists as the most rigorous method for reconstructing phylogeny (Smith 1994), has not previously been applied to the Sparidae. Using parsimony analysis, the interrelationships of the Sparidae are investigated based on the data matrix assembled from morphological characters of Chapter 2.

In part 1 of this chapter a phylogenetic hypothesis is presented for the Sparidae, for which an analyses of the distribution of character state changes is discussed under both DELTRAN and ACCTRAN character optimizations. In this analysis all characters are left unordered and equally weighted. Data quality is measured using permutation tail probabilities (PTPs) to assess whether it is phylogenetically informative and the quality of the phylogenetic hypothesis for the most parsimonious trees are assessed though Bremer support (decay index) and bootstrapping. The distribution of characters are discussed with reference to other teleost data sets (see table 3.1), while their distribution may also be used as a basis in support of the phylogenetic hypothesis.

In the second part of this chapter, I aim to analyse the data under a number of *a prior* and *a posteriori* assumptions to assess variables such as taxon stability, character quality and congruence in phylogenetic inference. A series of phylogenetic analyses presented here include: 1) the assessment of character quality using a compatibility-based approach (Le Quesne probability), with subsequent analysis performed using only those characters with low Le Quesne values; 2) data partitioning by the removal of character groupings (systems) is used to ascertain the sensitivity of these characters on the phylogenetic hypothesis. Partition-homogenetiy tests

provide a statistical measure as to whether the null hypothesis of congruence can be rejected for each data partition; 3) the influence of outgroup taxa on ingroup topology; 4) the effects of ordering character data, through the method of intermediates is also presented and evaluated with respect to the original parsimony run using unordered characters and 5) An alternative method of coding is also presented here, with the multistate data set recoded using non-additive binary coding

Cladistic theory

Homology and systematics

The cladistic method initially formulated by Hennig (1950, 1966), is used to establish relationships between taxa into 'natural' (monophyletic) classifications. The approach represented a fundamental shift in the perception concerned with the concept of evolution in systematics. Hennig recognized that similarities form the central component of any taxonomic study and differentiated between primitive similarity (plesiomorphy) and advanced similarity (apomorphy). He assumed that evolution had occurred and that shared characters were the direct result of inheritance, thus, only shared derived characters (synapomorphies) are evidence of common ancestry.

Central to the theory of phylogenetic systematics is homology; which Patterson (1982), defines in terms of monophyly, thus homologous features are those which characterize monophyletic groups (clades).

The concept of homology may be traced back to Aristotle (Russell 1916) and Belon (1555), who depicted the skeleton of both a man and a bird, the bones of which are labelled as he thought equivalent. The concept is also implicit in the works of Goethe, Carus and Oken (Panchen 1994), however, no concise definition was presented until Owen (1843) attempted to distinguish between homology and analogy:

> ANALOGUE A part or organ in one animal which has the same function as another part or organ in a different animal. (Owen 1843:374).
> HOMOLOGUE (Gr. *homos: logos* speech.) The same organ in different animals under every variety of form and function (Owen 1843:379).

Owen's definition of homology does not refer to phylogeny (Wagner 1994), as he perceived the two structures in different animals as being derivations of those found in the archetype. It was not until Darwin's (1859) reinterpretation of homology, which relates that homologous characters are inherited from a common ancestor, that an historical aspect was introduced. Thus, in its simplest form, homology allows for the validity of comparative information, so that comparisons between similarities (homologies) are meaningful in the hierarchical context, whereas comparisons between differences are not (de Pinna 1991).

The importance of specifying the hierarchical level at which structures are homologous can be exemplified by two groups of animals; birds and pterosaurs, both of which use powered flight (the former observed, while the latter is inferred). At one hierarchical level the forelimbs of these animals are homologous to each other as the forelimbs of tetrapods. However, the manus in these groups clearly shows different modifications to the digits, so that in birds digit 3 is extended while the rest are reduced, compared to pterosaurs where digit 4 is extended (Kardong 1995: 345). Thus, the structure at a lower hierarchical level shows the forelimbs to be analogous.

It is accepted by many scientists that the cladistic methodology equates homology and synapomorphy, a concept generally attributed to Patterson (1982). However, the equivalence between these notions had been noted by previous authors (cf. Patterson 1982: 29), e.g. Wiley (1975, 1976); Bonde (1977); Bock (1977); Szalay (1977); Platnick and Cameron (1977); Nelson (1978); Cracraft (1978); Patterson (1978); Platnick (1979); Gaffney (1978). More recent reviews such as Janvier (1984); Patterson (1988); Rieppel (1988, 1992); de Pinna (1991); Panchen (1992) continue to accept this concept.

Eldredge and Cracraft (1980: 36) conceptualize homology as synapomorphy, (including symplesiomorphy). The inclusion of symplesiomorphies within this idea is also noted by Patterson (1982: 33) who states that '*symplesiomorphies are also synapomorphies*'. However, he considers symplesiomorphies as irrelevant because they encompass a group whose generality is wider than the specific problem in question. If homologous features and conditions are acquiescent to the taxonomic hierarchy of groups (Bock 1963: 268), it is then synapomorphies and symplesiomorphies which are in hierarchical relation to one another (Patterson, 1982).

dePinna (1991), concluded that there are two steps in the assessment of homology, which he termed as primary and secondary homology. To determine whether a structure is homologous the initial phase or *primary* homology, is to postulate that similar individual characters, based on their structure and anatomical position are the same, and thus represent evidence of grouping. Once the primary homology has been resolved, *secondary* homology uses cladistic analysis to characterize a monophyletic group using parsimony.

Brower and Schawaroch (1996), have attempted to further define de Pinna's primary homology, by assuming two steps before identifying homology using congruence based on cladogram topology. They use the term *topographic identity* from Jardine (1969), to describe characters that are in the same topological position and thus are not inferring homology before individual character states or *character state identity* may be conjectured as homologous. Character state identity can be defined as the process of partitioning characters and scoring character states for a single taxon to form one column of the data matrix. Thus, the data matrix may be viewed as a set of primary homology statements Hawkins *et al.* (1997). The hypothesis of primary homology should be considered as the most important stage of any analysis, i.e. defining characters and potential character states and thus the formulation of the data matrix (Brady 1983; Bryant 1989).

I agree with Brower and Schawaroch (1996) in that it is important not to invoke homology at the initial stage of any phylogenetic analysis (observational stage) when looking for similarities, but as automaton machines it is hard or in fact impossible not to infer homology a priori from the beginning of study. It may be reasonable to produce a hypothesis of homology in terms of identifying topographic identity and character state identity, but in reality these steps are processed as one in the human brain. When elucidating lower taxonomic relationships, such as at the family level, similarities between anatomical structures are easier to identify. Moreover, when inferring higher level relationships, similarities become harder to quantify, therefore it would become more important to try and conceptualize the two distinctions of topographic identity and character state identity. However, it is probably correct to assume that most researchers whilst compiling their data matrices are already predicting the outcome.

Tests of homology

Patterson (1982) defined three tests of homology: congruence, similarity, and conjunction. In modern systematics it is congruence only which can serve as a test in the strict sense (de Pinna 1991), as congruence equates homology to synapomorphy (Smith 1994). Hypothezised homologies which are shown to arise once on the cladogram pass the test of congruence, while those characters that do not, are assumed to be the result of convergent or parallel evolution and are thus homoplastic in origin.

It is generally assumed that the more characters used, the more stringent the test they provide of homologous statements, which is important because it maintains that the hypothesis of homology should be evaluated on total evidence available (Kluge 1998). Advocacy for total evidence concedes that if all synapomorphies available are used when testing phylogenetic hypothesis, a statement describing the results of multiple tests "will be less probable than a statement describing only some of the tests" (Popper 1992: 247-248); if a multiple test result is therefore improbable, it is accordingly more severe than its component tests (Kluge 1998). For a review on the advantages and disadvantages of total evidence see Huelsenbeck *et al.* (1996).

Character partitioning and coding in cladistic analysis

Characters and character states

The 'character' is one of the most ill-defined concepts in cladistics, as it is used with a multiplicity of meanings (Thiele 1993). The distinction and definition of the terms character and character state are often downplayed in the literature (see also de Pinna 1991; Hawkins *et al.* 1997; Pimentel and Riggins 1987). The importance of recognizing that there is a clear distinction between character and character state, and that the two terms should not be confused, is discussed here. Recently, Hawkins *et al.* (1997) have redressed the importance of the distinction between characters and character states which they regard as essential to the operational task of constructing a data matrix. Many authors who have attempted to provide a definition between the term character and character state, however, often do not make a conclusive distinction between

the *character* and the *character state* such as Smith (1994: 37) that "characters are observed variations which provide diagnostic features for differentiation amongst taxa". I would prefer to postulate that characters are conjectured topographical similarities and agree with Hawkins *et al.* (1997) that the character *states* are the variation, through the application of parsimony which are used to provide cladogenic resolution. This is the basis for Hawkins *et al.* (1997) to fundamentally disagree with authors who assume that the character and character state are the same thing. Platnick (1979: 542) regards that "a character consists of two or more different attributes (character states) found in two or more specimens that, despite their differences can be considered alternate forms of the same thing (the character)", while Patterson (1988: 604) found the distinction between characters and character states "...neither necessary nor useful." I would propose that *the character should be regarded as a structure(s) occurring as variation in topographic correspondence in two or more taxa, which can then be partitioned into character states*. It is the partitioning of morphological variation into discrete characters which is the fundamental step to the understanding of secondary homology. Thus, a character is a collective that unites a set of variables (states), as Jardine's (1969) definition of characters as *nouns* and character states as *adjectives* suggests. I would therefore disagree with Popper (1962: 14) that "definitions do not play any very important part in science" a statement which becomes a paradox in comparative biology as definitions by default are all we have to define terminology.

Character independence

Darwinism is based on an atomistic background, that views the organism as being composed of an aggregation of fundamentally variable constitutional elements (Rieppel 1988). The structure and function of which, may be viewed in isolation, thus for parsimony analysis one assumption is that characters should be logically independent of one another (Felsenstein 1982, Farris 1983, Pimental and Riggens 1987, Smith 1994). Independence of characters is, however, problematic especially when using morphological data, where characters are generally part of a functional unit, and are therefore dependent on one another. Furthermore, functional character complexes are dependent on one another, since the organism itself is a functional unit. However, this is a holistic way to viewing organisms, and therefore it is important to treat all morphological characters as independent. The importance of character independence in phylogenetic inference is recognised by Wilkinson (1995a) in that "...characters are generally interpreted as providing independent evidence of relationships." Thus, it is important to define characters as objectively as possible, so that the same morphological state is not scored as two independent characters and therefore overweighted.

Wilkinson (1995a), distinguishes between two kinds of independence in what he terms 'biological' and 'logical'. He suggests that *biological* independence (structure/function) is when transformations in one character are coupled to transformations in the other. Likewise, two characters are not *logically* independent if some underlying variation is coded in two different

ways. A simple test to see if a character is logically independent is if knowledge of coding for one character reveals something about the other character e.g. a process which is coded as simply present/absent, also has a variable shape. The shape of the process is not initially taken into account and would be coded separately, thus, it would not be logically independent.

Discrete and continuous characters

Characters may be divided into *continuous* variables (quantitative) or *discrete* variables (qualitative). Most cladistic characters are discrete, occurring as a small number of states, the most objective of which exists as simply absence/presence. However, a great many so-called discrete characters are really quantitative. For example, the character leaf round or leaf square may initially appear to be discrete, but exactly how round does the leaf have to be before being regarded as round? (see Thiele 1993). Continuous characters refer to metric variables such as shape parameters (morphometric data), linear ratios and density information.

Discrete characters are less ambiguous and are undoubtedly more reliable in producing a good 'fit' to the shortest cladogram. Continuous characters have often been ignored in the past; regarded as unsuitable for cladistic analysis, as there are no valid criteria for dividing quantitative data into discrete states, as being inherently continuous (Pimentel and Riggins 1987; Felsenstein 1988; Mickevich and Weller 1990; Garland and Adolph 1994; Bookstein 1994). Objections to coding morphometric data are concerned with what Thiele (1993) terms 'overlapping' data. This is when the range of individual varieties for any given taxon may overlap the range of another taxon (Rae 1998; Swiderski *et al* 1998). However, apart from the obvious 'more data is better' (Chappill 1989, Donoghue and Sanderson 1992); Rae (1998) suggests that based on theoretical foundations continuous characters should not be excluded as they exist as homologous character states and can be coded for non-arbitrarily.

In vertebrate groups such as mammals; particularly primate and anthropoid studies (Rae 1995 1998) morphology is such that discrete variables are few, whilst the majority of variation can only be substantiated metrically. If we want to understand the relationships of these groups then it is imperative that continuous coding is used. The inclusion of continuous characters in phylogenetic analysis has become more evident in recent years from studies such as: Chappill (1989), Thiele (1993), Zelditch *et al.* (1995), Rae (1998), Swiderski *et al.* (1998), Van Velzen *et al.* (1998).

Character coding

Overview

Whilst there is literature enough on how we analyse characters, there appears to be a paucity of theoretical studies focusing solely on character coding; which considering the importance of this stage of the analysis; namely that of primary homology assessment, is surprising. Recent theoretical studies include Pimentel and Riggins (1987); Lipscomb (1992);

Scotland and Williams (1993); Meier (1994); Pleijel (1995); Wilkinson (1995a); Forey and Kitching (in press), in addition to coding procedures that are included into the framework of a particular group under study e.g. Wake (1993, 1994); Wilkinson (1997). I outline a brief summary only of coding methods, and refer the reader to the relevant literature in each instance for more comprehensive discussions.

The importance of defining and partitioning characters as previously discussed is one of the most important steps in the construction of the data matrix. Character construction leads directly into the way in which primary observations are coded, a step which can produce dramatically different phylogenetic results.

There is considerable variation in the cladistic literature as regarding the different approaches used in coding. The two main methods of coding are those of multistate coding and binary (absence/presence) coding. Essentially, multistate and non-additive binary coding are the product of the application of two fundamentally different philosophies of systematics; phylogenetic systematics, which focuses on evolutionary processes, and transformed cladistics, which is concerned with patterns of character distribution (Ruta 1998). The difference between multistate and binary coding centres around the issue of transformation between character states (Wilkinson 1995a). Thus, in using multistate coding, characters should be treated as a transformational series, in which hypotheses of adjacency between character states should be coded as *a priori* in the character state matrix (Kitching *et al.* 1997).

Multistate coding

The most frequent and indeed least conflicting way to code a character is when it is coded as simply presence/absence; a structure is either present or not, it exists as a square or a circle, or it is red or blue etc. However, as 'morphological structures are likely to undergo more than a single change during the course of evolution' (Hauser and Presch 1991), it would seem reasonable that some structures should not be coded as simply absent/present. Thus, problems in coding arise when certain traits are linked either logically and/or biologically (Wilkinson 1995a), resulting in the multistate character.

Many authors (I include myself here), prefer the rationale behind multistate coding to that of binary coding, and as a consequence it is by far the more prevalent method of coding in the literature. Pimentel and Riggins (1987) consider that all cladistic characters should be treated as multistate, as '...in denying multistate characters, some aspects will either be ignored, combined, or treated as independent characters'. In addition, they suggest that by treating character states as separate individual characters, it may be presumed that any character state can be transformed into any other, and that the analysis of such data can lead to multiple, equally parsimonious solutions. Meier (1994) rejected binary coding on the basis that such analyses would result in less parsimonious or 'pseudoparsimonious' trees, and that it produces 'homoplasy bias', a criticism also noted by Pimentel and Riggins (1987). Thus, the advantage of the multistate character is that

it avoids the possibility that false homologies will obscure true phylogenetic signal (Pleijel 1995).

Complex morphological features, will inherently lead systematists to apply different coding methods when constructing characters. Thus, there are alternative ways of coding morphological multistate characters, which may result in different phylogenetic conclusions (Forey and Kitching in press). An example of how coding complex structures may lead to different phylogenetic outcomes has emerged from a study by Wake (1993) in her use of unconventional morphological characters in caecilian phylogeny. The composition of the hypoglossal nerve was coded by Wake to form nine states, each state representing a particular combination of 'wires'. Problems associated with the complexity of this type of coding are discussed by Wilkinson (1995a) and Forey and Kitching (in press).

Using characters from my own data, I attempt to illustrate alternative coding methods. Character 27 (dorsal maxillary crest) from data matrix 2.0, exemplifies a character that has been coded using composite coding (or concealed coding Wilkinson 1995a). This character is problematic, as three variables need to be considered: the presence or absence of the crest; the position of the crest and shape of the crest.

Composite coding distinguishes that all variables of a feature are subsequently coded in different combinations of that feature. Hawkins *et al.* (1997), however, favour the method of contingent coding, where observations regarding the variation of a feature, such as shape and position of the dorsal crest in the case of C27 should be coded separately, in addition to the absence/presence of a feature.

Contingent coding brings the problem of non-applicable data, as if the feature is not there, then subsequent characters describing that feature will be entered as a '?' in the data matrix. Inapplicable characters are problematic as they cannot be scored as any of the optional character states, and as a consequence of this, PAUP or any of the other parsimony programmes, will assign one of the alternative states to the unknown variable in the data matrix. Inapplicable data can therefore lead to phylogenetic hypothesis which rely on spurious optimizations (Maddison 1993). To avoid this problem, Smith (1994) advocates in these instances combining binary states into a single multistate character. Forey and Kitching (in press) suggest that it may be argued that in the case of contingent coding, it may not be necessary to include the absence/presence of a feature as the non-applicable coding in that the further two characters describing attributes of a feature imply absence.

Reductive coding (Wilkinson 1995a), which is not, however, the same as the presence/absence coding of Pleijel's (1995) as Forey and Kitching state (in press), partitions the variation of a character complex into simpler characters, which describe the variation in a particular component of that character complex. This is exemplified when Wake's (1993) multistate composite character of eye musculature, which is spilt into six characters through the application of reductive coding (Wilkinson 1995a, 1997). Reductive coding, differs from absence/presence coding as it is still accessible to multistate coding, albeit that which describes

only single features: e.g. the superior oblique eye muscles exists in three states; present, attenuate and absent.

To assess whether composite or reductive coding should be applied, features that are not biologically independent justify the use of composite coding, as reductive coding may cause overweighting of underlying variation, whereas, if features are biologically independent then reductive coding is justified, in that composite coding may cause underweighting. An additional criticism of composite coding is that unlike reductive coding, homoplasy may be concealed (Wilkinson 1995a).

A further method of coding a multistate character is to use a Sankoff coding or stepmatrix (Forey and Kitching in press; Wilkinson 1995a). Sankoff coding attempts to quantify distance between observations, and is regarded by these authors as the preferred method of coding where theories of character transformation are concerned. The reader is referred to the latter reference for a fuller discussion and implementation of this method.

While each method of coding is not without faults, problems associated with coding morphologically complex features can be avoided by carefully selecting a method to suit the problem in hand. Thus, the methodology used to construct each character should be scrutinised by comparing it with alternative methods.

There are plenty of instances in the literature in which authors prefer the rational of binary coding. In the Part 2 of this Chapter, the multistate character list of Chapter 2 is recoded into absence/presence coding to determine what effects this may have to the hypothesis of relationships presented in Part 1 of this chapter.

Ontogeny Criterion

Analysis of ontogenic series enabling determination of character polarity (see Nelson 1978), was beyond the scope of this thesis, primarily due to lack of sufficient specimens. If ontogenic information is available then ordering multistate characters is certainly advantageous (Forey and Kitching in press), however, as there is no ontogenetic evidence available, characters remain unordered in the main analysis.

Selection of taxa and outgroups

Ingroup taxa

Nelson (1994) lists 29 nominal genera of sparids, however, a further six genera are described from the FAO regional guides (see p 5), although *Sparidentex* and *Viridentex* are probably subgenera of *Dentex.* In this study 29 genera, including 63 species were dissected and/or examined from osteological preparations (see appendix 1.0).

Outgroup taxa

Use of outgroup(s) to determine character polarity is the most frequent and advocated method to root trees (Forey *et al.* 1992; Barriel and Tassy 1998; Kitching *et al.* 1998). It is

generally advised that multiple outgroups are the best way to root trees, the reasons for this practice are outlined by Barriel and Tassy (1998) in that i) it precludes a possible unfortunate choice of outgroup; ii) it raises the level of generality; and iii) it serves as a test for the alleged monophyly of the ingroup.

The outgroup taxa used in this study were selected on the basis of previous work on sparoid interrelationships (e.g. Johnson 1980). The closest relatives of the Sparidae; Centracanthidae, Lethrinidsae and Nemipteridsae are included, in addition to more basal percoids such as Centropomidae, Lutjanidae and Haemulidae. The taxon *Centropomus* has all characters coded as zero and is therefore referred to an 'all-zero outgroup', which is equivalent to an artificial all-plesiomorphic outgroup. As there is heterogeneity among the outgroup taxa, state zero may not be assumed *a priori* to be the plesiomorphic state for the ingroup (Nixon and Carpenter 1993).

However, when a set of heterogeneous outgroups are used, it is often found that they may greatly alter ingroup topology (Smith 1994; Kitching *et al.* 1998). Furthermore, multiple outgroups may also effect the outcome of the pattern of outgroups and the optimization of character states at basal nodes, if the resulting ingroup is not monophyletic Barriel and Tassy (1998).

Part 1 **PHYLOGENETIC ANALYSIS**

Cladistic analysis is accepted by most systematists as the most effective method available for reconstructing phylogeny (Forey *et al.* 1992; Smith 1994; Kitching *et al.* 1998).

Cladograms are constructed from the principle that the number of changes from one character state to the next are minimized. The axiom that requires fewer assumptions is the rule of parsimony. With the advent of computer-implemented algorithms, such as Hennig 86 (Farris 1988) and PAUP (Phylogenetic Analysis Using Parsimony; Swofford 1993), the search for the most parsimonious or minimum-length cladogram has been dramatically speeded up.

For this analysis data matrices were processed using PAUP* (Swofford 1998) on a Power Macintosh G3. In addition, the initial run was also processed using Hennig 86 (Farris 1988) for comparison or conformation of results.

The data was processed using a heuristic method of search, rather than an exhaustive or branch and bound search due to the size of the data set. However, a heuristic search does not necessarily guarantee that the most parsimonious tree will be found, as it does not examine all the possibilities resulting from rearrangements of taxa (Kitching *et al.* 1998). In this analysis and all subsequent analyses, unless otherwise stated all characters were unordered. The outgroup was set to the option making the ingroup monophyletic and the outgroup paraphyletic with respect to the ingroup. A random stepwise addition sequence based on 10 replicates and tree-bisection and reconnection branch swapping (TBR) algorithm was used, with steepest descent option in effect.

The MULPARS option enabled PAUP* to save all minimal trees. Characters were optimized using both ACCTRAN (accelerated transformations) and DELTRAN (delayed transformations) options, which are only available using PAUP.

Character distribution

The initial matrix was assembled using 89 characters (see Chapter 2; table 2.0), of which 40 are coded as multistate characters. The matrix was constructed using MacClade version 3.0.1 (Maddison and Maddison 1992).

To assess which areas of the skeleton are more susceptible to morphological modification, it is useful to look at the distribution of characters for different functional/anatomical units (see table 3.0). The most morphological variation, with regards to the total number of characters scored is observed in the skull, which accounts for 76 characters (85%), compared with only 13 characters (15%) from the post-cranium. The distribution of characters can further be assigned to character groups or functional units, in order to assess which particular areas of the skeleton are most variable. From table 3.0, it is notable that the braincase, jaws and dentition and gill arches are areas in which a high percentage of characters were scored.

As the skull is a complex structure, it is reasonable to assume that there is more possibility for variation, particularly in fishes, than in the post-cranial skeleton. This appears to hold true for many data sets, however, by comparing the percentage of characters scored for the cranium versus post-cranium (see table 3.1), the number of characters scored for the cranium is significantly higher for Sparidae and for the labroid family Scaridae than the other groups. The differing proportions of characters may well be genuine fluctuations in areas of morphological variability. However, it is as well to be cautious in estimating which areas are more susceptible to morphological variation as this may be an artefact of the expertise of the investigator, or the type of material used.

Missing values

In this matrix there are 3115 entries, 27 of which are represented by missing entries. The total proportion of missing entries is low at 0.86%, as would be expected from a Recent morphological data set. The dispersion of missing entries across characters results in 65 characters having no missing entries, 23 characters having one missing entry and one character (character 88) having three missing entries. The proportion of missing entries for each taxon are as follows: *Argyrozona* 20.22%; *Centracanthus* 2.25%; *Haemulon* 2.25%; *Boopsoidea* 1.12%; *Lutjanus* 1.12%; *Pachymetopon* 1.12%; *Polysteganus* 1.12%

Missing entries in the data set of Recent taxa may represent either unknown information if anatomical features are missing (the relatively high percentage of missing data for the taxon *Argyrozona* is due to the lack of gill arch data) or uncertain character-state assignment ,due to the quality of stained specimens, where certain anatomical features remain indistinct. None of

Table 3.0 *Character distribution*

Skull: braincase 25 (28%), jaws and dentition 22 (24.7%) [of which jaws 16 (18%), dentition 6 (6.7%)], infraorbitals 2 (2.2%), palatine arch 6 (6.7%), opercular series 1 (1.1%), lower hyoid arch 6 (6.7%), gill arches 14 (15.7%)

Post-cranium: pectoral girdle 3 (3.4%), axial skeleton 1 (1.1%), dorsal and anal fins 5 (5.6%), posterior fin 4 (4.5%)

Table 3.1 *Comparison of character distribution*

Data set	Total	Cranium	Post-cranium
Sparidae	**89**	**76 (85%)**	**13 (15%)**
Scaridae (Bellwood 1994)	133	106 (80%)	27 (20%)
Cheilinini (Westneat 1993)	86	41 (62%)	25 (38%)
Centropomidae (Otero 1997)	35	21 (60%)	14 (40%)
Aulopiformes (Baldwin & Johnson 1996)	118	53 (54%)	45 (46%)
scombroids (Johnson 1986)	48	24(50%)	24(50%)
Epinephelinae (Baldwin & Johnson 1993)	46	17 (36%)	29 (63)

(note that the total number of characters used here are based on those which can be readily spilt into cranial and post-cranial characters).

the missing entries in this matrix are due to non-applicable character states (see section on coding for further discussion on non-applicable coding).

Safe Taxonomic Reduction

When taxa have a high proportion of missing entries, they may be responsible for increased numbers of most parsimonious trees (MPT). Safe taxonomic reduction (STR) is a method for reducing numbers of MPTs by eliminating taxa which include question marks, but which have non-unique combinations of character states (Wilkinson 1995b, 1996) of the real data. Using $TAXEQ_2$ (Wilkinson 1995c) to determine whether STR need be implemented for this data set, the results show, as expected for a matrix with a low proportion of missing entries, that there is no equivalence, thus each taxon has its own set of unique character states. For further use of STR see Chapter 5.

Tree statistics

Measures of character fit

This analysis produced three equally parsimonious trees (figure 3.0). Homoplasy signifies discordance of character distribution within a particular cladogram and can be measured by the indices CI and RI These indices indicate how well a tree describes a data set. CI is used as an indicator of the level of homoplasy in data, as CI = 1 for a given data set when there is no homoplasy, decreasing as homoplasy increases (Siebert 1992). RI can be regarded as the proportion of similarities on a tree interpreted as synapomorphy (Farris 1989), thus RI may be considered as a better measure of group support than CI. RI is high when state changes occur on internal nodes and low when changes are concentrated on branches leading to terminal taxa (Siebert 1992).

Lower case ci refers to the proportion of homoplasy per character. All trees have 21 characters (23.4%) with a ci value of 1, whilst 46 characters (51%) have a ci value between 1 and 0.500.

Two additional methods of testing whether a matrix is informative or not, may be resolved by using the formulas: CI_{random} index (Klassen *et al.* 1991) and $CI_{expected}$ index (Sanderson and Donoghue 1989). The CI_{random} index = $2.937 \times n^{-0.9339}$ (where n represents the total number of taxa), pertains that if the value of CI deriving from the data set is greater than that for the CI_{random} value of a matrix consisting of an equal number of taxa, then an assumption that the matrix has structure can be presumed. For 35 taxa, $CI_{random} = 0.12$, therefore as this value is much lower than the CI value, the matrix can be considered to contain phylogenetic information. The $CI_{expected}$ index = $0.9 - 0.0022 \times n + 0.000213 \times n^2$ is based on the supposition that because the CI varies directly with the number of taxa, then this number affects the level of homoplasy for a given data set, more than the number of characters present. Thus, for 35 taxa the $CI_{expected}$ = 0.40, which is similar to the obtained CI value of 0.572, again demonstrating that this matrix is

informative.

Pairwise compatibility permutation tail probability (PCPTP)

The value of the PTP is used to assess the degree of cladistic structure in the data. The PTP test simply randomizes the data to see if the incompatibility count for the original data falls outside the random data , in which case the data contains cladistic structure. If the incompatibility count falls within the random data, then the data is no better than if it had been randomly selected and should therefore be rejected.

The PCPTP test employs similar rationale, and provides a fast way to measure the quality of the data. Wilkinson (1992) and Alroy (1994) both developed a similar test independently, however, due to availability of software the PCPTP programme (Wilkinson 1995d) is implemented here. The PTP test was computed using this option in PAUP*. The values for the parsimony and pairwise incompatibility PTPs are 0.01 and 0.001 respectively (see table 3.2 for PCPTP output), which is the minimum possible for the number of random permutations. As the null hypothesis states that data should be rejected at the 0.05% level, the value of 0.001 is the lowest possible value for the number of randomly permuted data, allowing for the rejection of the null hypothesis that the data is no more congruent than for random data. The data presented here therefore contains cladistic structure beyond that due to chance.

Table 3.2 *Statistics from PCPTP output*

incompatibility count for original data = 2170
PCPTP = 0.001
mean = 2782.716 ± 21.475
normal deviate = 28.532
95% cutoff = 2749
incompatibility excess ratios:
IER_1 = 0.220
IER_2 = 0.208

Some authors do not consider the PTP test to place meaningful confidence on cladistic data. Carpenter (1992) regards it is "...a misapplication of statistics", while Kitching *et al.* (1998: 138) view cladistic characters to be intrinsically hierarchical, thereby denoting that "...all methods of using a random model as a null hypothesis are fundamentally flawed". However, as Wilkinson (pers. comm.) pointed out, it would appear that Kitching *et al.* (1998) are happy to use the PTP test to indicate whether a data set contains significant cladistic structure, but because they regard cladistic data to be hierarchical, data that does not pass the PTP test is not rejected. This creates a paradoxical situation, as if the test verifies the data it is used to denote confidence, while if it does

not then the data is preferred to the test.

Tree topology

The overall shape of the MPTs produced from the original parsimony run are pectinate (figure 3.0). The trees differ only in the position of two taxa; *Chrysoblephus* and *Polysteganus.* Sparid genera from *Evynnis* to *Argyrops* are abbreviated here to the monophyletic group A. In tree 3 *Chrysoblephus* is basal to *Polysteganus,* represented in parenthetical notion as (*Chrysoblephus* (*Polysteganus* (A))), whereas in tree 2 the reverse is true, (*Polysteganus* (*Chrysoblephus* (A))). Tree 1 differs to trees 3 and 2 in that *Polysteganus* and *Chrysoblephus* are sister groups, thus (A (*Polysteganus Chrysoblephus*)).

Character optimizations

The distribution of characters are important because they define clades, and potentially allow us to say something about character evolution within the group. Character distribution is thus evaluated here at the various nodes for the MPTs. The characters are described using both accelerated transformations (ACCTRAN; Swofford and Maddison 1987; Swofford 1990) and delayed transformations (DELTRAN; Swofford and Maddison 1987; Swofford 1990) options. Characters optimized under ACCTRAN 'favour the acquisition of a character, with subsequent homoplasy accounted for by a reversal', whilst those under DELTRAN describe parallel changes and therefore 'favour independent gains of a state rather than acquisition and reversal' (Kitching *et al.* 1998).

In this section I discuss which characters define the monophyly of the superfamily Sparoidea and the family Sparidae, in addition to those that support the internodes (figure 3.1). The ci value of a particular character is only included if it is >0.500. However, a list of apomorphies (see appendix)for both ACCTRAN and DELTRAN optimizations describes the consistency index for each character as well as the relative character state change.

Monophyly of Sparoidea

When DELTRAN is in effect, 11 characters support the monophyly of sparoids, these include C39 (descending process of the articular), C54 (metapterygoid without lamina; ci = 1), C55 (symplectic is expanded so that it overlaps both the metapterygoid and preoperculum; ci = 1), C56 (faint ridges occur on the posteroventral margin of the preopercle; ci = 1), C61 (number of branchiostegal rays totals six; ci = 1), C62 (branchiostegal rays are absent from, or ray vi only, is attached to the epihyal; ci = 1), C67 (presence or absence of rakers on hypobranchial 1), C77 (posterior margin of the posttemporal is smooth; ci = 1), C85 (number of trisegmental radials total three or less; ci = 1), C88 (posterior cartilages, CINPU4 and CIHPU4 are singular in form; ci = 1) and C89 (there is no additional separate CPHPU2; ci = 1). Under ACCTRAN, there is an increase of characters, so that 13 changes support this node. These additional characters include C17

(opisthotic absent; ci = 0.500), C41 (absence of a superior crest), C48 (infraorbitals I and II are both enlarged; ci = 0.667), C80 (intermusculars total 11+; ci = 0.667). Thus, there is good support for a monophyletic Sparoidea, as nine unambiguous character state changes (39, 54, 55, 56, 61, 62, 67, 77 and 89) support branch 0 (figure 3.1), seven of which are synapomorphies (ci = 1), coming from all categories of character types (table 3.2) except braincase, jaws, dentition and axial skeleton.

Monophyly of Sparidae

Node 1 when DELTRAN is in effect, Sparidae is supported by nine character state changes, which pertain to C6 (width of braincase at level of preorbital flange), C9 (sagittal ventral sulcus of the lateral ethmoids and frontals), C17 (opisthotic is absent; ci = 0.500), C20 (pars jugalaris has three or more openings; ci = 1), C28 (articulation between the premaxilla and maxilla is specialized; ci = 1), C41 (superior crest only is present), C48 (infraorbitals I and II are deeper than wide; ci = 0.667), C79 (post-pelvic processes are reduced or absent; ci = 1), C80 (intermusculars total 11-13; ci = 0.667).

Under ACCTRAN the monophyly of Sparidae is supported by the six character state changes: C20, C28, C48, C71 (distribution of rakers on epibranchials I, II and II), C79 and C87 (hypurapophysis extends to hypural 1).

Thus, a monophyletic Sparidae, is supported by three unambiguous character state changes, including: the presence of three or more openings in the pars jugularis (C20), a specialized premaxilla/maxilla articulation (C28) and the post-pelvic processes are reduced or absent (C79). However, C48 (infraorbitals I and II are deeper than wide) which is reversed in *Centracanthus,* warrants further investigation in adult specimens as this may indeed prove to be an additional synapomorphy. The synapomorphies of the group come from four of the nine categories of character types (see table 3.3).

Ingroup taxa

The characters supporting the clade (*Dentex Cymatoceps*), node 2 include four unambiguous character state changes: C18 (separate foramina for IX and X nerves), C30 (dorsal crest of the maxilla is knob-like), C74 (the lateral and medial margins of tooth plates PB2 and ET2 have similar dimensions) and C75 (lateral margin of UP4 is greater in width than the medial margin of PB3; ci = 0.500). Under ACCTRAN an additional character C3 (absence of any depression along the dorsal margin of the ethmoid) unites this clade.

Unambiguous characters supporting *Dentex*, include C39 (descending process of the articular is the same length as the ventral margin of the dentary), C41 (a superior crest only on the articular is present), C82 (anterior process of the supraneurals are separate). While those of *Cymatoceps* include: C27 (dorsal maxillary crest of the premaxilla is central with a flat dorsal margin), C53 (presence of a confluent ridge along the ventral margin of the quadrate and

preoperculum), C58 (dorsal process on the ceratohyal is absent) C66 (anterior process on hypobranchial one is absent) and C69 (rakers on hypobranchial three are absent).

When DELTRAN is in effect, node 5 supporting *Porcostoma* as the sister group to all higher taxa include C3 (presence of a shallow fossa for the ascending process of the premaxilla), C67 (rakers on hypobranchial 1 are dome-shaped), C73 (two uncinate processes are present on epibranchial IV; ci = 1), whereas under ACCTRAN C2 (anterodorsal facet on the medial dorsal crest absent) replaces C3.

Characters supporting *Porcostoma* include: C35 (symphysal process of the dentary extends to a quarter of the total length of the dorsal process of the dentary), C60 (deepest point of the concavity along the posterior margin of the urohyal is central) and C87 (hypurapophysis extends to the medial margin of the second hypural).

The characters supporting node 7 under DELTRAN include: C25 (nasal attached to the anterior margin of the lateral ethmoid and frontal), C26 (height of the ascending process is the same length as the alveolar process) and C53 (confluent ridge along the ventral margin of the quadrate and preoperculum present), while under ACCTRAN a fourth character, number 27 (dorsal maxillary crest is central with a convex dorsal margin) also supports this node.

Character state changes supporting node 11, *Evynnis* as the sister group to all higher taxa, under the DELTRAN optimisation include C3 (presence of a deep fossa for the ascending process of the premaxilla) and C9 (sagittal ventral sulcus extends into the lateral ethmoids and frontals). While under ACCTRAN C2 (absence of a anterodorsal facet on the dorsal crest of the vomer) also supports this association.

Character states changing along branch to *Evynnis* include: C10 (cancellose texture on the the dorsal margin of the frontals anterior to the occipital crest and the pterotic sagittal crest), C14 (the frontal and occipital sagittal crests meet anteromedially) and C71 (rakers are present on the anterior and posterior margins of the first and second epibranchials).

The characters supporting node 13, is supported by three character state changes under DELTRAN: C39 (descending process of the articular is the same length as the ventral margin of the dentary), C59 (bifid posteroventral spine of the urohyal) and C67 (rakers on hypobranchial 1 are elongate). While under ACCTRAN, C14 (frontal sagittal crest and the occipital crest remain separate) and C70 (IAC is a third of the length of the first epibranchial) also support this node.

Characters supporting the sister group pairing (*Cheimerus* + *Boopsoidea*), under ACCTRAN include C18 (separate foramina for nerves IX and X), C27 (dorsal crest of the maxilla is central with a flat dorsal margin), C30 (dorsal crest of the maxilla is knob-like), whilst under DELTRAN C70 (IAC is a fifth of the length of the first epibranchial) supports this clade with the exclusion of C27.

Character state changes leading to *Cheimerus* include: C3 (absence of a depression along the dorsal margin of the ethmoid), C25 (nasals attached to the frontals), C66 (anterior process on hypobranchial is absent), C67 (rakers on hypobranchial one are absent) and C69 (rakers on

hypobranchial three are absent). Whilst autapomorphies supporting *Boopsoidea* includes: C15 (exoccipitals are oriented posteriorly), C26 (the height of the ascending process is less than the length of the alveolar process), C41 (superior crest is present) and C71 (rakers present on the anterior and posterior margins of the first, second and third epibranchials).

Under both optimizations, node 17 supporting *Pachymetopon* as the sister group to cladistically derived taxa include the following character state changes: C19 (m. dilatatori operculi pierces a fossa in the anterior margin of the sphenotic) C57 (sulcus arcus hyoideus absent; ci = 0.667) and C66 (well developed anterior process of hypobranchial 1).

The six character state changes supporting *Pachymetopon* include: C1 (posterior margin of the vomer is level with both the ethmoid-frontal suture and the anterior margin of the orbit), C2 (anterodorsal facet on the dorsal crest of the ethmoid is absent), C24 (parasphenoid carina is absent), C26 (the height of the ascending process is greater than the length of the alveolar process), C43 (caniniform teeth are absent) and C46 (incisiform teeth are crenulate).

Node 19, under DELTRAN is supported by six character state changes support including: C25 (attachment of the nasals to the frontals), C27 (dorsal maxillary crest of the premaxilla is sub-terminal), C58 (dorsal process of the ceratohyal is well developed), C70 (IAC is a third of the length of the first epibranchial), C86 (hypurals 1+2 and 3+4 are fused for part of their mutal length), C87 (hypurapophysis extends to the medial margin of the second hypural), whereas C70 is absent under ACCTRAN.

The clade ((*Pagellus Pagrus)* (*Stenotomus Lithognathus*)), node 20, is united by seven character state changes under DELTRAN, including: C30 (dorsal crest of the maxilla is well developed), C34 (combined length of the articular and angular form less than one third of the total length of the mandible; ci = 0.500), C37 (facet on the dorsal margin of the corocoid process is present; ci = 0.500), C39 (descending process of the articular extends below the ventral margin of the dentary but not below the ventral process of the dentary), C40 (angular forms the posterior margin of the articular; ci = 0.500), C42 (villiform dentition occurs along the anteromedial margin of the premaxilla and dentary; ci = 0.500) and C47 (more than one tooth row is present; ci = 0.500). Under ACCTRAN, an addition character; C45 (presence of molariform teeth) also supports this association.

Character state changes under both optimizations uniting the clade (*Pagellus Pagrus*) pertain to: C19 (no extension of the m. dilatatori operculi beyond the dilatator fossa), C44 (presence of conical teeth) and C59 (urohyal has a single spine).

Character state changes supporting *Pagellus* include: C14 (frontal and occipital crest meet anteromedially) and C18 (separate foramina for the nerves IX and X), whilst those supporting *Pagrus* include: C16 (exoccipital condyles show varying degrees of medial separation), C35 (symphysal process of the dentary extends to a quarter of the total length of the dorsal process of the dentary), C66 (hypobranchial one is square-shaped), C67 (rakers are dome-shaped) and, C71 (rakers present on the anterior and posterior margins of the first and second epibranchials).

The clade (*Stenotomus Lithognathus*) is supported by four character state changes under DELTRAN, including: C26 (height of the ascending process is greater than the length of the alveolar process), C31 (palatine sulcus of the maxilla extends to the anterior margin of the premaxilla), C45 (molariform teeth are present) and C76 (teeth have restricted tips in which the acrodin cap is of a smaller diameter than the supporting tooth), whilst under ACCTRAN C45 is excluded.

Eleven character state changes support *Stenotomus* which include: C2 (anterodorsal facet on the dorsal crest of the vomer is absent), C8 (the lateral ethmoidal process is semi-elliptical), C14 (the frontal sagittal crest and the occipital crest meet anteromedially), C19 (m.dilatatori operculi piercing a foramen in the anterior margin of the sphenotic), C22 (process for the m. adductor arcus palatini parasphenoideum is extended), C25 (nasal is attached to both the frontals and the anterior margin of the lateral ethmoid), C50 (maxillary process of the palatine is straight), C66 (hypobranchial one is square shaped), C67 (rakers on hypobranchial one are dome-shaped), C83 (initial dorsal finspines are longer than proceeding ones) and C84 (first radial of the anal fin is conical). While the autapomorphies supporting *Lithognathus* include to C3 (absence of a depression along the dorsal margin of the ethmoid), C16 (exoccipital condyles show varying degrees of medial separation), C18 (separate foramina for the IX and X), C32 (lateral maxillary process is stalk-like), C38 (the medial margin only of the articular fossa is concave), C39 (descending process of the articular extends below the ventral margin of the dentary), C71 (rakers present on the anterior and posterior margins of the epibranchials I and II), C72 (uncinate process present on epibranchial II), C82 (anterior processes of the supraneurals are separate) and C86 (hypurals are separate).

With either optimization in effect, node 27 is only supported by C3 (absence of a depression along the dorsal margin of the ethmoid) and C82 (anterior process of the supraneurals are separate), both of which have very low ci values.

The clade (*Spondyliosoma Argyrozona*) is united by C11 (dorsal margin of the frontals are protuberant anteriorly; ci = 0.500), C41 (superior crest only is present) and C53 (confluent ridge along the ventral margin of the quadrate and the preoperculum is absent). However, an additional fourth character, C74 (the lateral and medial margins of tooth plates PB2 and ET2 have similar dimensions) supports this relationship when ACCTRAN is in effect.

Character state changes supporting *Spondyliosoma* include: C2 (anterodorsal facet on the dorsal crest of the vomer is absent), C15 (exoccipital condyles are orientated posteriorly), C42 (villiform dentition present on the occlusal surface of the premaxilla and dentary), C47 (tooth field present), C52 (ventral margin of the ectopterygoid extends to the articular condyle of the quadrate) and C59 (posteroventral spine of the urohyal is single). The autapomorphies supporting *Argyrozona* come solely from the cranium and jaws and include: C8 (lateral ethmoid process is semi-elliptical), C9 (sagittal ventral sulcus occurs on only on the lateral ethmoids), C16 (exoccipital condyles show varying degrees of medial separation), C19 (m. dilatatori operculi

pierces a foramen in the anterior margin of the sphenotic), C26 (height of the ascending process is less than the length of the alveolus process) and C27 (dorsal maxillary crest of the premaxilla is absent).

The node supporting a sister group relationship between *Centracanthus* and cladistically more derived sparids is supported by the following characters: C1 (posterior margin of the vomer is level with both the ethmoid-frontal suture and the anterior margin of the orbit), C6 (width of braincase at the level of the preorbital flange equals the width of the braincase at the contact of the dorsal limb of the posttemporal), C24 (absence of parasphenoid carina), C51 (posterior process of the palatine is absent) and C86 (hypurals are fused). In addition, under ACCTRAN C38 (medial margin only of the articular fossa is concave) and C63 (number of rakers on the first ceratobranchial total 14-15; ci = 0.500) also support this association.

The character state changes supporting *Centracanthus* include: C26 (height of the ascending process is double that of the alveolar process of the premaxilla), C29 (articular process is absent; ci = 0.750), C38 (margins of the articular fossa are concave), C48 (infraorbitals I + II have the same dimensions; ci = 0.667), C49 (subocular shelf is reduced; ci = 0.667), C70 (IAC is a fifth of the length of epibranchial I), C71 (rakers present on the anterior and posterior margins of ceratobranchials I and II) and C80 (intermusculars total 15; ci = 0.667). When DELTRAN is in effect C63 also supports this node.

Unambigious characters supporting the clade (*Oblada Boops*) include: C27 (dorsal maxillary crest of the premaxilla is absent), C41 (articular has a superior crest only). when deltran is in effect a further two character state changes support this node: C58 (dorsal process on the ceratohyal is weakly developed), C63 (number of rakers on the first ceratobranchial are 14-15; ci = 0.500).

Character state changes supporting *Oblada* include C10 (cancellose texture on the dorsal margin of the frontals anterior to the occipital crest and the pterotic sagittal crest), C14 (frontal and occipital sagittal crests meet anteromedially), C51 (posterior process of the palatine is present), C74 (medial and lateral margins of tooth plates PB2 and ET2 of have similar dimensions) and C87 (hypurapophysis extends to hypural 1), while those supporting *Boops* include C9 (sagittal ventral sulcus occurs on the lateral ethmoids only), C26 (height of the ascending process of the premaxilla is less than the length of the alveolar process) and C81 (supraneural formula is 0/0/0+2/1+1).

Node 37 is supported by the five unambiguous character state changes which include: C2 (anterodorsal facet on the medial dorsal crest of the vomer is absent), C6 (width of the braincase at the level of the preorbital flange is greater than the width of the braincase at contact of the dorsal limb of the posttemporal, but less than the width of the braincase at the contact of the ventral limb of the posttemporal), C47 (more than one tooth row is present; ci = 0.500), C71 (rakers present on the anterior and posterior margins of epibranchials I and II) and C82 (anterior processes of the supraneurals overlap). Under ACCTRAN character state changes also include C58

(dorsal process of the ceratohyal is well developed), C67 (rakers on hypobranchial I are dome-shaped) and C86 (hypurals are separate).

The taxon *Sarpa* is supported by the following character state changes: C38 (medial and lateral margins of the articular fossa are concave) and C81 (supraneural formula is 0/0/0+2/1+1; ci = 0.500).

Under DELTRAN, character state changes supporting *Polyambyodon* as the sister group to cladistically more derived taxa (node 39) include: C19 (m. dilatatori operculi pierces a foramen in the anterior margin of the sphenotic) C35 (symphysal process of the dentary extends to a quarter of the total length of the dorsal process of the dentary), C39 (descending process of the articular extends below the ventral margin, but not below the ventral process of the dentary), C43 (caniniform teeth are absent), C76 (teeth of the upper pharyngeal tooth plates have restricted tips in which the acrodin cap is of a smaller diameter then the supporting tooth), Under ACCTRAN C43 is replaced with C63 (number of rakers on the first ceratobranchial totals 7-12; ci = 0.500).

Character state changes supporting *Polyamblyodon* include: C9 (presence of a sagittal ventral sulcus in the lateral ethmoids), C15 (exoccipital condyles are oriented posteroventrally), C27 (dorsal maxillary crest of the premaxilla is central with a convex dorsal margin), C50 (maxillary process of the palatine is straight), C69 (rakers on hypobranchial III are absent), C72 (uncinate process present on epibranchial II) and C86 (hypurals are fused for part of their mutual length).

Character state changes supporting *Crenidens*as the sister grouping to higher taxa (node 41) include the following seven characters state changes: C3 (presence of a deep fossa for the ascending process of the premaxilla), C24 (parasphenoid carina is weakly developed), C31 (palatine sulcus of the maxilla is extended to the anterior margin of the premaxilla), C34 (length of the articular and angular is less than one third of the total length of the mandible; ci = 0.500), C66 (anterior process on hypobranchial I is square-shaped), C67 (rakers on hypobranchial I are absent) and C87 (hypurapophysis extends to hypural 1). When DELTRAN in effect C86 (hypurals are separate) aslo supports this relationship.

Two character state changes support *Crenidens* under both optimizations include: C1 (posterior margin of the vomer is level with the ethmoid-frontal suture) and C45 (molariform teeth are present).

Character state changes supporting *Lagodon* as the sister group to more cladistically derived taxa include: C19 (m.dilatatori operculi pierces a fossa in the anterior margin of the sphenotic) and C26 (the height of the ascending process of the premaxilla is greater than the length of the alveolar process). An additional character C32 (stalk-like lateral maxillary process) supports this relationship with ACCTRAN in effect.

The following character state changes supporting *Lagodon* include: C16 (the exoccipital condyles show varying degrees of medial separation), C67 (rakers on hypobranchial I are domed-shaped) and, C76 (dentition of the upper pharyngeal tooth plates are recurved caniniform).

The character state changes that support the *Sparodon* (node 45) as the sister group to cladistically more derived taxa include: C30 (dorsal crest of the maxilla is well developed), C35 (symphysis extends to half of the total length of the dorsal process of the dentary), C36 (mandibular canal consists of a double row of pores; ci = 0.500), C39 (descending process of the articular extends below the ventral process of the dentary), C40 (angular forms the posterior margin of the articular; ci = 0.500), C50 (maxillary process of the palatine is straight) and C69 (rakers on hypobranchial III are absent). When ACCTRAN in effect C38 (medial and lateral margins of the articular fossa are concave) also supports this node.

A single unambigious character; C87 (hypurapophysis extends to the medial margin of the second hypural) supports *Sparodon,* however, under DELTRAN, C32 (lateral maxillary process is stalk-like) and C67 (rakers on hypobranchial I are absent) also support this node.

Four character state changes support *Diplodus* as the sister group to cladistically more derived taxa (node 47) which include: C13 (height of the occipital crest is greater than length ; ci = 0.500), C37 (presence of facet on corocoid; ci = 0.500), C45 (presence of molariform teeth) and C72 (uncinate process on second epibranchial). When ACCTRAN is in effect, an additional five characters support this node, including: C3 (presence of a foramen for the ascending process of the premaxilla), C14 (frontal and the occipital sagittal crests meet anteromedially), C32 (lateral maxillary process is a weakly developed knob), C33 (foramen present through the dorsal crest and palatine sulcus of the maxilla; ci = 0.500) and C46 (presence of incisiform teeth).

Character state changes supporting *Diplodus* include: C6 (width of the braincase at level of preorbital flange extends level to or beyond the width of the braincase at contact of the ventral limb of the posttemporal), C10 (cancellose texture on the dorsal margin of the frontals anterior to the occipital crest and the pterotic sagittal crest), C46 (presence of incisiform teeth), and C86 (hypurals are fused for part of their mutual length)

The following six characters support *Rhabdosargus* as the sister group to cladistically higher taxa (node 49) include: C23 (pharyngeal apophysis is stalk-like; ci = 1), C24 (parasphenoid carina is well developed), C43 (caniniform teeth present), C44 (presence of conical teeth), C51 (posterior process of the palatine is present). When DELTRAN in effect this node is also supported by C46 (absence of incisiform teeth), whereas under the ACCTRAN optimization C38 (medial margin of the articular fossa is concave) supports this node.

Only one unambiguous character state change: C9 (sagittal ventral sulcus occurs on the lateral ethmoids) supports Rhabdosargus. However, under the DELTRAN optimization the additional characters: C3 (presence of a foramen for the ascending process of the premaxilla), C14 (frontal and occipital crests meet anteromedially) and C33 (foramen developed through the dorsal crest of the palatine sulcus of the maxilla) also support this node.

The following six character state changes support the *Acanthopagrus* as the sister grouping to cladistically more derived taxa (node 51) pertain to: C8 (lateral ethmoid process is semi-elliptical), C12 (cancellose texture on the supraoccipital and epioccipital; ci = 0.500), C13 (length

of the occipital crest is the same as the height; ci = 0.500), C22 (process for the m. adductor arcus palatini parasphenoideum is extended; ci = 0.500), C26 (height of the ascending process is the same as the length of the alveolar process), C68 (rakers on hypobranchial II are absent; ci = 0.500). When ACCTRAN is in effect an additional three characters support this node which include: C3 (deep fossa present in the dorsal margin of the ethmoid for the ascending process of the premaxilla), C14 (frontal and occipital sagittal crests are separate), C33 (absence of a foramen through the dorsal crest and palatine sulcus of the maxilla; ci = 0.500).

The taxon *Acanthopagrus* is supported by the following character state changes: C70 (IAC is a fifth of the length of epibranchial I), C72 (medial flange present on epibranchial II), C74 (PB2 is expanded with respect to ET2) and C76 (dentition of the upper pharyngeal tooth plates are recurved caniniform).

Node 53 supporting *Archosargus* as the sister group to cladistically higher taxa is weakly supported with only a single ambiguous character: C87 (extension of the hypurapophysis to the ventral margin of hypural II). An addition character; C16 (exoccipital condyles show varying degrees of medial separation) occurs under the ACCTRAN optimization.

The character state changes supporting *Archosargus* include: C38 (both margins of the articular fossa are concave), C39 (descending process of the articular extends below the ventral margin of the dentary, but not below the ventral process), C43 (caniniform teeth are absent), C46 (presence of incisiform teeth) and C86 (hypurals are fused for part of their mutual length).

Support for *Calamus* as the sister group to cladistically higher taxa (node 55) includes four character state changes: C1 (the posterior margin of the vomer is level to the ethmoid-frontal suture), C8 (the lateral ethmoidal process extends anteriorly), C15 (exoccipital condyles are oriented posteroventrally) and C21 (the lateral commisure is laterally inflated extending anteroventrally to the mid-point of the orbit; ci = 1). Under the ACCTRAN optimization an addition character 32 (lateral maxillary process is stalk-like) also supports this association.

Unambiguous character state changes supporting *Calamus* include C6 (width of the braincase at the level of the preorbital flange extends beyond the width of the braincase at the contact of the ventral limb of the posttemporal); C9 (ventral sulcus of the lateral ethmoids is absent); C13 (length of the occipital crest is less than the height; ci = 0.500); C26 (height of the ascending process is greater than the length of the alveolar process); C42 (villiform teeth present along the anterolateral margin of the occlusal surface of the premaxilla and dentary; ci = 0.500); C84 (the first radial of the anal fin is conical; ci = 0.500). A further two character state changes support this taxon under DELTRAN: C16 (exoccipital condyles show varying degrees of medial separation) and C32 (lateral maxillary process is stalk-like).

Node 57 supporting the clade (*Sparus Argyops*) include the following characters: C12 (absence of cancellose texture on the supraoccipital and epioccipital ; ci = 0.500), C19 (no extension of the m.dilatatori operculi beyond the dilatator fossa), C31 (palatine sulcus of the maxilla is reduced), C35 (symphysal process of the dentary extends to a quarter of the total length

of the dorsal process of the dentary), C36 (mandibular sensory canal is single; ci = 0.500) and C50 (maxillary process of the palatine is deflected medially). When ACCTRAN in effect C16 (exoccipital condyles contact along the midline) also supports this relationship.

Character state changes supporting *Argyops* include: C11 (dorsal margin of frontals are protuberant anterior to the occipital crest; ci = 0.500), C27 (dorsal maxillary crest is central, with a convex dorsal margin), C39 (descending process of the articular extends below the ventral margin of the dentary, but not below the ventral process), C83 (the initial dorsal finspines are greater in length than the proceeding ones; ci = 0.500) and C87 (hypurapophysis extends to hypural 1).

Character state changes supporting *Sparus* include: C8 (lateral ethmoidal process is absent), C10 (cancellose texture on the dorsal surface of the frontals), C14 (the frontal and occipital sagittal crests meet anteromedially), C24 (parasphenoid carina is weakly developed), C72 (medial flange present on epibranchial II), C74 (lateral and medial margins of tooth plates PB2 and ET2 have similar dimensions), C76 (dentition of the upper pharyngeal tooth plates are recurved caniniform) and C86 (hypurals are fused).

Unresolved taxa

The ambiguous placement of *Chrysoblephus* and *Polysteganus* at the base of the tree (figure 3.2), arises due to character conflict. Tree 1 supports the association of the clade (*Polysteganus Chrysoblephus*) as the sister group of more cladistically derived taxa. This hypothesis is supported by C2 (absence anterodorsal facet on the dorsal crest of the vomer) under DELTRAN or C27 (sub-terminal dorsal maxillary crest) under ACCTRAN. In tree 2, a single character under the ACCTRAN optimization; C14 (frontal and occipital sagittal crests meet anteromedially) supports *Polysteganus* is the sister group to *Chrysoblephus* and cladistically more derived taxa. In tree 3 the reverse relationship of tree 2 exists, with *Chrysoblephus* as the sister group of *Polysteganus* and cladistically more derived taxa. Character state changes supporting this hypothesis include: C67 (rakers on hypobranchial I are dome-shaped) under DELTRAN or C70 (IAC is a third of the length of the epibranchial I) under ACCTRAN.

The following character state changes supporting *Chrysoblephus* under both optimizations in each MPTs: C14 (frontal and occipital sagittal crests meet anteromedially), C66 (anterior process on hypobranchial I is well developed) and C69 (rakers on hypobranchial I are absent). In tree 1 and tree 2 characters leading to *Polysteganus* under both optimizations involve C70 (IAC is a third of the length of the epibranchial I), whereas in tree 3 this branch is delimited by the DELTRAN optimization only.

Tree support

Bootstrap

Bootstrap analysis is used to evaluate phylogenetic inferences by randomly sampling

characters from the original data set with replacement, thus forming a pseudoreplicate data set of the same dimensions. The most parsimonious cladograms for each pseudoreplicate are found and the degree of conflict among them are conventionally assessed by a majority-rule consensus tree of the bootstrap trees (Kitching *et al.* 1998).

To test the robustness of branch support a bootstrap analysis was performed using PAUP*. The analysis was based on 100 replicates to which a heuristic search was applied. The support is reasonable for a monophyletic Sparidae, with the inclusion of *Centracanthus* deep within the sparids (figure 3.3), but is mainly minimal for resolution within the ingroup. However, there are serious limitations with the use of bootstrap, as clades are generally supported by only a few characters, which contrasts to the expectation of bootstrapping which is that clades will be supported by large numbers of characters that will be recovered frequently by random sampling of characters and receive high scores on a majority-rule consensus. If the characters are homoplastic then clades are not expected to be recovered very often, if at all. Thus, a clade may be supported by a single character on the most parsimonious cladogram yet fail to be recovered in a bootstrap analysis, and therefore be excluded from the majority-rule consensus. Other factors lead to over estimates or underestimates of confidence, which includes size of data set, efficiency of the heuristic search, cladogram topology and differential rates of character change among branches (Kitching *et al.* 1998).

The low bootstrap percentages can be attributed to the large amount of homoplastic character state changes at each node, in addition the lack of synapomorphies supporting these nodes. The percentages of nodes that are entirely unsupported by synapomorphies is high (see figure 3.1). The character state changes along the internodes of the ingroup, have fairly low ci values, which explains why the bootstrap values discussed in this section are not particularly high.

Bremer support using decay index values

Branch support, more commonly referred to as Bremer support was first applied to a parsimony analysis by Bremer (1988; see also Bremer 1994) and aims to evaluate the support of tree branches through perturbation (modification) of the original analysis. The programme Autodecay Version 3 (Eriksson and Wilström 1995) was used to calculate the Bremer support for the consensus of the MPTs (figure 3.3) and is a test that determines the number of extra steps needed to collapse a clade. Thus, higher numbers of steps imply a more robust clade. Where there are multiple equally parsimoniously solutions, then at least one clade will have zero Bremer support (Kitching *et al.* 1998), as is the case with the clade containing the taxa *Polysteganus* and *Chrysoblephus*. Very few of the basal clades display a decay index value which is greater than one, however, the decay indices for crown group taxa have values ranging from 1-4, thus, there is fairly good support for the most cladistically derived members (i.e. from *Polyamblyodon* to *Sparus*). Bremer support is probably a better measure of support here since no randomisation of data is involved. This is particularly advantageous where synapomorphy support for individual

nodes is low.

Inclusion of Centracathidae within the the Sparidae

The family Centracanthidae is regarded as a separate family from the Sparidae, rather than a sub-family, on the basis of morphological specializations associated with a planktivorous mode of life (Johnson 1980). However, in the analysis performed here, Centracanthidae nests deeply within sparids. The morphology and placement of , Centracanthidae in the MPTs suggests that this taxon is closely related to *Boops* and *Oblada*. Subsequent phylogenetic analyses (see part 2 of this Chapter) show that this association is relatively stable. To assure confidence of the inclusion of the 'Centracanthidae' within Sparidae, further systematic investigation is undoubtedly required, with greater taxon sampling of the Centracanthidae Without this knowledge, I would therefore tentatively assign centracanthids within this grouping. However, recent molecular studies into sparid interrelationships (Orrell 1999) have found similar results supporting this placement.

Support for the phylogenetic hypothesis

If all characters supporting the basic framework of the tree all belong to one anatomical system, then we can assume that this system is important to a particular group of organisms. However, if a diversity of characters are found supporting a group of organisms then there is greater support for the phylogenetic hypothesis. This is because it is harder to invoke a simple story for why features in different anatomical systems have changed at one time, in which case there would be more chance of convergence. If characters are associated with more than one system, it suggests that, if the tree is correct, there has been some adaptation.

To assess the quality of the phylogenetic hypothesis table 3.3 classifies unambiguous character states for tree 1 into functional systems (character types). Partitioning characters into morphological systems may be somewhat artificial, as some functional association between characters of different systems will certainly exist (e.g. diarthrosis between the third pharyngobranchial and the pharyngeal apophysis of the basicranium in pharynognath fishes). This mirrors a similar problem of partitioning character complexes, that are also functionally dependent on each other, into characters and character states. However, by partitioning characters into 'systems' it provides a useful picture of the differences between morphological systems most affected by evolutionary changes occurring on different branches (Wilkinson and Nussbaum 1999).

Four of the ten character types listed in table 3.3, support a monophyletic Sparidae. Three of these characters are associated with the cranium, which is unsurprising considering that 85% of the total characters are scored from this region (see table 3.0). As the characters supporting node 1 are not represented by any one character type, a degree of confidence can be assumed in that these distributions imply support for the phylogenetic hypothesis. Partitioning characters into functional

units also provides an opportunity to see the type of characters supporting particular clades. Character types supporting nodes 20 and 45 for example (see figure 3.1) are jaw-related characters and these clades are thus represented by taxa with particular specialized jaw adaptations. These adaptations are discussed fully in Chapter 6.

Part 2 FURTHER ANALYSES OF THE DATA

Character quality

Direct evidence of homoplasy in individual characters, can be determined from a compatibility analysis. Character compatibility analysis is based on the assumption of Le Quesne's (1969) that if two characters each with two states, both evolve without homoplasy, then three combinations at most of the character states will be present in the taxa. If all four possible combinations of character states are present , then at least one of the characters is homoplastic, and therefore shows incompatibility (Meacham 1994).

The Le Quesne probability (LQP) of Wilkinson (1992) is used here as a randomisation test of the null hypothesis that a particular character is no less incompatible with the rest of the data than is a random character. Wilkinson (1992) and Meacham (1994) both independently developed similar tests, however LQP focuses on incompatibility, whereas Meacham's test termed Frequency of Compatibility Attainment focuses on compatibility. LQP test is analogous to the randomization and permutation tests of Archie (1989) and Faith and Cranston (1991), but differs in that it is a test of individual characters rather than entire data sets.

The incompatibility results for individual characters (see appendix, table 3.3), were determined using DNALQP (Wilkinson 1995d), approximation by 999 random permutations. All characters are assumed to be independent in this data set. Characters with a LQP greater than 0.05 and those greater than 0.1 are excluded from further analyses due to high incompatibility.

Character deletion following Le Quesne probability

Those characters with the highest LQP ($p > 0.05$) show no less incompatibility than random characters and were therefore excluded from the first analysis (A_1). This analysis excluded 50 characters, leaving 39 characters in total, of which 15 were coded as multistate. A second analysis (A_2) when $p > 0.1$, excluded 35 characters, leaving 54 characters.

Characters with low LQP are summarized according to character type for both $p > 0.05$ and $p > 0.1$ in Table 3.4. When $p > 0.05$ the skull, as for the original data set has a greater proportion of characters with low LQPs than the post-cranium. The braincase and jaws provide the most informative characters from the skull, although the mandible has the highest number of compatible characters. When $p > 0.1$, all anatomical units, apart from the jaws show a greatly increased number of compatible characters. However, using LQP when $p > 0.05$ could be

undoubtly informative regarding the relationships of ingroup taxa.

Table 3.4 *Numbers and percentages of characters excluded from A_1 ($p > 0.05$) and A_2 ($p > 0.1$) calculated for different morphological systems of the skeleton (see appendix, table 3.3).*

NChar		A_1 ($p > 0.05$)	A_2 ($p > 0.1$)
skull	76	41 (54.0%)	29 (38.2%)
braincase	24	13 (37.5%)	9 (37.5%)
jaws	16	5 (31.3%)	same
upper jaw	8	4 (50%)	same
mandible	8	1 (12.5%)	same
infraorbitals	2	2 (100%)	1 (50%)
palatine arch	8	6 (75%)	3 (37.5%)
hyoid arch	7	3 (42.9%)	1 (14.2%)
gill arches	14	8 (57.1%)	7 (50%)
post-cranial	13	9 (69.2%)	6 (46.2%)

Analysis 1

A strict component consensus (figure 3.4.0a) of the MPTs shows that Sparidae are monophyletic, however, the tree structure differs from the original parsimony run. The major difference between this consensus and that of the original parsimony run is that the clade (*Stenotomus* (*Pagrus* (*Pagellus Lithognathus*))) nests in a cladistically more derived position forming a dichotomy with the most cladistically derived taxa (*Argyops* (*Sparus* (*Calamus* (*Sparodon, Rhabdosargus, Diplodus, Acanthopagrus, Archosargus*)))). Other differences include the more derived placement of the taxon *Pachymetopon* so it forms a sister grouping to the unresolved node between *Boops* and *Oblada* and cladistically more derived taxa. The position between *Lagodon* and *Crenidens* is also reversed. The base of the tree is collapsed, with the relationships of 11 taxa remaining unresolved.

After reweighting using the rescale consistency index, a single MPT was found (figure 3.4.0b). The differences between this tree and the MPTs of the original parsimony run are similar to that described for the equally weighted run, however, *Centracanthus* forms a sister grouping to the clade (*Oblada* + *Boops*) and cladistically more derived taxa, while the taxa (*Evynnis* (*Polysteganus, Chrysoblephus*)) form a clade rather than part of the pectinate series found in the original parsimony run.

Analysis$_2$

The second analysis excluded characters using LQP when p >0.1 (figure 3.5.1a). The base of the tree as in analysis$_1$ is collapsed, although fewer taxa. are unresolved than in the previous analysis. The tree structure resolves two major clades with the taxa *Stenotomus*, *Pagrus*, *Pagellus* and *Lithognathus* forming a pectinate series with cladistically more derived taxa.. The clade (*Argyozona*, *Spondyliosoma*) and *Centracanthus* form an unresolved node at the base of this clade. Furthermore, the taxa (*Pachymetopon* (*Oblada* (*Boops* (*Sarpa* (*Polyamblyodon* (*Lagodon Crenidens*) form a clade that is basal to that previously described.

A reweighted analysis found 2 MPTs, with a similar structure to that described for A_1 (figure 3.4.1b). The major difference between these analyses is that *Centracanthus* forms a sister grouping with the clade (*Arygrozona, Spondyliosoma*).

Summary

The assessment of character quality using the compatibility approach of LQP is a useful approach to determine characters and character groups that are considered to be phylogenetically informative. It is found from these analyses that characters from the braincase and jaws are most phylogenetically informative, while those from the infraorbitals and palatine arch are least informative. Analyses performed with the exclusion of those characters that have the highest LQP values i.e. when the p value is >0.05 or >0.1, show that while relationships for more cladistically derived taxa are congruent, the relationships of those taxa more basal are incongruent. Thus the exclusion of these characters reveals that the relationships at the base of the tree are supported by homoplastic characters.

Data partitions

Partitioned analysis resulting in a number of separate analyses often yield conflicting results to those obtained through using combined analyses or 'total evidence' approach (e.g. Barrett *et al.* 1991; Wilkinson 1997). However, agreement between separate analyses provides strong evidence in support of the phylogenetic hypothesis. Huelsenbeck *et al.* (1996), suggest that if data sets are constructed from significantly heterogeneous sources e.g. nuclear genes versus mitochondral genes versus non coding genes, then separate analyses should be implemented. This is because the different types of data operate under different evolutionary rules. Further to which a consensus of these analyses, may reveal which parts of the cladogram are congruent or not.

While the data used in this study is predominately osteological, data partitioning between the different character groups outlined in tables 3.0 and 3.4, provides an opportunity to assess taxonomic congruence, in addition to the effect particular character groupings have on taxon stability.

Exclusion of post-cranial characters

The exclusion of post-cranial characters, which account for 15.0% of total characters, collapse the base of the tree and render sparids paraphyletic (figure 3.5a). The topology of the top of the tree is relatively unaffected from the exclusion of these characters, however, the polytomy between *Archosargus* and *Acanthopagrus*, is caused from the loss of the single character which supports this node in the MPTs of the original parsimony run. Interestingly, the clade (*Argyrozona Spondyliosoma*) is also paraphyletic in this analysis.

Exclusion of braincase characters

Exclusion of braincase characters again collapses the base of the tree, so that both *Lethrinus* and *Nemipterus* fall inside sparids. However, it also effects the relationships towards the top of the tree (figure 3.5b). A major change in tree structure is the clade (*Stenotomus* (*Pagellus* (*Pagrus Lithognathus*))) forming a sister grouping to *Sparus* or *Argyops* and cladistically derived taxa. The relationships between the clade (*Argyrozona Spondyliosoma*), *Boops* and *Oblada* are also unresolved.

Exclusion of jaw and dental characters

The exclusion of these characters retains the monophyly of the Sparidae, but causes the base of the ingroup to collapse, although the relationships of cladistically more derived taxa remain unaffected (figure 3.5c). An interesting difference is the taxa forming the clade ((*Stenotomus Lithognathus*)(*Pagellus Pagrus*)) in the original parsimony run is relatively stable in other analyses performed here, although the internal relationships may alter. However, due to the high proportion of jaw characters supporting this node (see table 3.2), the relationships of these taxa are unresolved apart from the placement of *Lithognathus*, which here forms a sister grouping to the clade (*Pachymetopon* (*Centracanthus* (*Oblada* (*Boops Sarpa*))).

Exclusion of hyoid arch characters

The exclusion of the hyoid arch characters causes instability in the most basal nodes, but does not effect relationships of more cladistically derived taxa (figure 3.5d).

Exclusion of gill arch characters

The exclusion of these characters results (figure 3.5e) in a different arrangement of taxa at the base of the tree relative to the original parsimony run, with (*Cymatoceps* (*Dentex* (*Cheimerus Boopsoidea*))) forming a basal clade. The relationships between the clades (*Argyrozona Spondyliosoma*) (*Boops Oblada*) (*Lithognathus Stenotomus*) *Pagrus Pagellus*) and the taxa *Centracanthus*, *Sarpa* and *Pachymetopon* are unresolved, while the relationships of the more cladistically derived taxa remain unaffected

Exclusion of hyoid and gill arch characters

The exclusion of all gill arch characters has a significant effect on the relationships of the ingroup (figure 3.5f). With the exception of the clade (*Boops Oblada*) and the clade (*Stenotomus, Pagellus, Pagrus, Lithognathus*) the relationships of the ingroup taxa are unresolved, however they remain monophyletic.

Exclusion of palatine arch characters

The exclusion of this data once again has a detrimental affect to the base of the trees in terms of lost resolution (figure 3.5g). However, there is more cladogenic structure at the base of these trees than in the other partition analyses. Whilst there is more structure, the relationships are different to those observed in the MPTs of the original parsimony run. Sparoidea is paraphyletic due to the taxon *Haemulon* falling between *Lethrinus* and *Nemipterus*, while the clade (*Dentex Cymatoceps*) is no longer basal in this analysis.

Summary

Reanalysis of the data with the exclusion of a particular data partition was found to have a detrimental effect to the base of the tree or those nodes supported by a particular character type. In particular, the exclusion of the character set containing gill and hyoid arch characters was found to cause signifcant loss of resolution to the overall tree structure.

Partition homogeneity test

To asses the significance of incongruence between data sets, the homogeneity test option using PAUP* is applied to each data partition. This test follows the principals set out following Farris *et al.* (1995) using the null hypothesis of congruence. The null distribution is obtained through random partitioning, which due to the size of the matrices was set at 99 partitions.

The value *p* for a particular data partition gives the incongruence length difference between the combined length of both matrices (partitions = P) and the length (L) of each partition to give the observed value for which:

$$p = L_{(P1+P2)} - (L_{P1} + L_{P2})$$

The critical value for rejecting the null hypothesis is usually 5%, so that the chance of rejecting incorrectly is no greater than the desired significance level (Farris *et al.* 1995). For the partitions (see table 3.5) where the *p* value is greater than 0.05 the null hypothesis of congruence can be rejected as the measure of incongruence is significantly larger than if the data is no more incongruent than for random partitions. Where the *p* value is less than 0.05, the partitions do not allow the null hypothesis to be rejected as the data is no more incongruent than for random partitions.

Table 3.5 *Partition homogeneity test with heuristic search*

Character partition	$p = 0.05$
post-cranial (C77-78)	0.212
braincase (C1-25)	0.151
jaw and dentition (C26-49)	0.020
hyoid arch (C57-62)	0.010
gill arches (C63-76)	0.890
hyoid and gill arches (C57-76)	0.030
palatine arch (50-55)	0.808

Where the null hypothesis of congruence cannot be rejected, those data partitions that show a conflicting signal include: jaws and dentition; hyoid arch and the hyoid and gill arches. However, randomization tests suggest that the data is significantly non-random, as the values for parsimony incompatibility PTPs for each of these partitions are 0.01, allowing for the rejection of the null hypothesis.

As the data used in these partitions is not random data, the conflicting signal may be attributed to misleading evidence of relationships because of homoplasy. However, the incongruence in the gill and hyoid arch partition is not surprising if the phylogeny for this data set (see figure 3.5f) is considered, as the ingroup without these characters is completely unresolved. Small partitions such as the hyoid arch, may have low p values due to homoplasy in a few characters, causing overall conflict. Using the output of Le Quesne probabilities from table 3.3 (see appendix), half of the characters for the lower part of the hyoid arch have high LQP ($p >$ 0.05), that do not allow for the rejection of the null hypothesis that they show no less incompatibility than random characters.

Deletion of outgroups

General remarks

When heterogeneous outgroup taxa are used, it is frequently found that the exclusion of one or more of these taxa markedly alters ingroup topology (Kitching *et al.* 1998). In this section I aim to assess the stability of the ingroup, by the exclusion of an outgroup or combination of outgroups. In all analyses, with the exception of *Centracanthus*, the deletion of an outgroup(s) caused the basal nodes of the trees to become unstable and collapse, thus, providing little or no information for the relationships of these taxa. The deletion of *Haemulon* in particular has an extreme effect on the base of the tree, causing the basal taxa to collapse to a single node and rendering the ingroup polyphyletic with the inclusion of both *Lethrinus* and *Nemipterus*. The relationships of the more cladistically derived taxa (*Centracanthus* - *Sparus*: referred to here as

group B) appear to be robust with respect to the deletion of outgroup taxa, and are only affected by the removal of *Centracanthus*, which causes two areas of instability among these taxa.

Deletion of Lethrinus

With the exclusion of *Lethrinus*, sparoids no longer form a monophyletic grouping, as *Nemipterus* is basal to *Haemulon,* however, Sparidae remains monophyletic (figure 3.6a). The major difference between this analysis and that of the original run is that the basal taxa form a discrete clade rather than the pectinate arrangement, with *Boopsoidea* as the most basal member. The taxon *Pachymetopon* is nested in a more derived position, as it forms a sister grouping with either *Centracanthus* or the clade (*Oblada Boops*) and cladistically more derived taxa. The topology of group B remains unaffected from the exclusion of *Lethrinus*, retaining an identical topology to the MPTs of the original analysis.

Deletion of Nemipterus

The exclusion of *Nemipterus* has no effect on tree topology, which remains identical to the MPTs of the original analysis (figure 3.6b).

Deletion of Centracanthus

With the deletion of *Centracanthus* (figure 3.6c), the basal taxa fall into similar positions as in the MPTS, however, the taxon *Evynnis* forms a polytomy with *Chrysoblephus*, *Polysteganus* and cladistically more derived taxa. The relationships of the taxa forming group B are similar to those described for the MPTs from the original analysis, apart from the relationships between *Sarpa, Oblada and Boops* and those of *Lagodon* and *Crenidens* which in this analysis are unresolved. The major difference between the MPTs of this analysis and that of the original analysis is the placement of *Pachymetopon* which forms the sister taxon to group B.

Deletion of Lethrinus and Nemipterus

With the exclusion of both *Lethrinus* and *Nemipterus* a single difference was found between this analysis and the MPTs of the original analysis (figure 3.6d). The topology of the basal taxa (*Evynnis* (*Porcostoma Polysteganus Chrysoblephus*) form a clade that is cladistically more derived than the taxa *Boopsoidea* and *Cheimerus*.

Deletion of Centracanthus, Lethrinus and Nemipterus

The exclusion of all sparoid outgroups (figure 3.6e) causes the base of the tree to become unstable, apart from the unresolved clade (*Porcostoma, Polysteganus, Evynnis, Chyrsoblephus*), while the rest of the tree forms the same topology as that described for the deletion of *Centracanthus* (see figure 3.6c).

Deletion of Haemulon

The deletion of *Haemulon* from this analysis has a considerable effect on the base of the tree, causing the ten basal nodes to completely collapse (figure 3.6f). However, the exclusion of this taxon does not effect the rest of the tree, which remains the same as that described for the MPTs of the original analysis.

Deletion of Centracanthus, Lethrinus, Nemipterus and Haemulon

This analysis (figure 3.6g) produces a very similar consensus tree to that of figure 3.6e, although in this analysis the relationships between the most basal taxa are resolved.

Summary

From the analyses excluding those outgroup taxa considered to be closely associated with sparids, it was found that certain taxa have a greater influence on ingroup topology than others. In particular, the taxon *Haemulon* has the most marked effect on ingroup topology in terms of polarising characters and stabilising the base of the tree, while the exclusion of *Lethrinus* alters the relationships of basal taxa due to the effects of character polarity. In contrast the exclusion of *Nemipterus* has the no effect on ingroup topology. Due to the more derived position of *Centracanthus* in the MPTs of the original analysis, the exclusion of this taxon consequently destabilises associated nodes, in addition to having some effect on character polarisation.

Phylogenetic analysis using ordered characters

Ordered characters

The treatment of multistate characters as to whether they should be ordered or unordered in phylogenetic inference concerns the effects of these hypotheses on cladogenic structure, resolution and length. Ordered characters differ from unordered characters in that transformations between any two non-adjacent states costs the sum of the steps between their implied adjacent steps (Kitching *et al.* 1998). Characters may be ordered using the method of intermediates or any other method to order character states, the former of which is closely associated with Hennig's auxiliary principle (Wilkinson 1992). If the character is ordered by the method of intermediates, then it explains the similarity between a subset of character states in terms of synapomorphy, while unordered characters in contrast ignore this similarity. Characters ordered following the method of intermediates, are therefore more explanative than those left unordered (Wilkinson 1992). The treatment of characters is a topic that is still under much debate (see also Mickevich and Weller 1990 and Hauser and Presch 1991). It is however, most sensible following the suggestion of Hauser and Presch (1991) that where characters are treated as ordered, comparison with an unordered analysis is desirable so that results may be compared for any variation.

Ordered analysis

Multistate characters were ordered following the method of intermediates (Wilkinson 1992) where appropriate, otherwise they were left unordered. For a review of which characters have been treated as ordered see the character analysis of Chapter 1. The data was analysed using the heuristic methods previously outlined in this chapter.

The ordered analysis found 3 MPTs, with a length of 410 steps. CI = 0.332; RI = 0.642; RC = 0.213 (figure 3.7a). This analysis found the same number of MPTs as the original parsimony analysis, however, tree length as expected for an ordered analysis is longer, while the C.I. is lower than for the original analysis. A randomization test using parsimony incompatibility PTP is 0.01, thus allowing for the rejection of the null hypothesis that the data is no more congruent than random data.

The major difference between the ordered and unordered analyses is the placement of some of the basal taxa, in particular the position of *Argyrozona* (figures 3.7a and b). In the ordered analysis, this taxon forms a sister grouping with *Dentex*, at the base of the Sparidae, whereas when the characters are unordered this taxon forms a clade with *Spondyliosoma* in a more cladistically derived position (figure 3.7a and b). The trees also differ in the position of *Cymatoceps*, which in the ordered analysis forms a sister grouping with *Cheimerus*, whereas in the unordered analysis this taxon forms a sister grouping with *Dentex*, while *Cheimerus* forms a sister grouping with *Boopsoidea*. The only area of conflict between the 3 MPTs in this analysis is the position of the clade (*Chrysoblephus* (*Cymatoceps Cheimerus*)) and the taxon *Polysteganus*.

A comparison of the tree lengths for only those characters whose lengths vary over trees (table 3.6), shows that when characters are unordered three more steps are required to obtain the ordered tree, whereas when the characters are ordered only one step is needed to obtain the unordered tree. The distribution of characters whose lengths vary over the trees is universal between the two trees. When characters are left unordered, 16 characters were found to differ in length, six of these preferring the unordered tree, while nine prefer the ordered tree. After ordering characters, an additional two characters were found; C3 and C41, with eight preferring the unordered tree, while 10 prefer ordered tree. By far the largest group of these characters, are those from the gill arches.

The differences in the position of the taxa between the unordered and ordered trees, are areas in which confidence of relationships is low. The incongruence between the MPTs found from each analysis may equate to certain functional complexes not evolving independently, so that there has been a certain amount of adaptive convergence between taxa.

Effects of coding in phylogenetic inference

Binary coding

As discussed previously in this chapter, character coding is a contentious issue, that may markedly effect the outcome of a cladistic analysis. Coding is a subjective procedure, which is

wholly dependent on the choice of characters and the coding methodology that is implemented by the investigator. In this analysis, I aim to employ a different technique of coding, namely absence/presence or binary coding of Pleijel (1995), to that used in all previous analyses. While I do not advocate this method, the results produced from reanalysis of the data when recoded as binary provide interesting discussion due to the different philosophy which each coding method employs.

The main criticism of multistate coding comes from Pleijel's (1995) work, who advocates the use of absence/presence (a/p) coding for phylogenetic reconstruction. Non-additive binary coding or a/p coding (Pleijel 1995), provides a different way in viewing homology in that it aims to maximize congruence of all possible observed features, by treating each condition of a complex structure in isolation. Thus, a/p coding avoids questionable assumptions regarding both ordered versus unordered observations, and has the advantage in that missing entries due to inapplicable characters are also avoided.

The argument that coding morphologically complex structures as multistate, results in characters with a large number of states (Pleijel 1995; Ruta 1999), is however, somewhat insubstantial. As previously discussed this problem can be avoided by the application of an alternative coding method such as reductive coding (see Wilkinson 1995a). Likewise, the dilemma of non-applicable data may also be avoided.

The two main approaches of binary coding, i.e. that of non-additive binary coding versus additive binary coding fundamentally differ from each other, in that the latter approach is considered equivalent to any ordered multistate character (Farris *et al.* 1970), whereas, non-additive binary coding is not synonymous to the unordered multistate character (see Wilkinson 1995a).

To exemplify a non-composite multistate character (see section on multistate coding for a defination) expressed as alternative formats of binary coding, character 9 (see character analysis from Chapter 2) is used here:

Multistate coding

Sagittal ventral sulcus of the lateral ethmoids and frontals is absent (0), occurs on the lateral ethmoids only (1), or extends into the frontals (2)

Binary coding

1i) *Non-additive binary coding*

ventral sulcus is absent (0), or present (1)

ventral sulcus of the lateral ethmoids is absent (0), or present (1)

ventral sulcus of the frontals is absent (0), or present (1)

ii) *Non-additive binary (variation of 1ii)*

ventral sulcus on the ethmoids is absent (0), or present (1)

ventral sulcus on the ethmoids and frontals is absent (0), or present (1)

2) *Additive binary coding*

ventral sulcus on the ethmoids is absent (0) or present (1)

ventral sulcus on the ethmoids and frontals is absent (0), or present (1)

Results from binary analysis

The binary matrix (see Appendix; table 3.6) was assembled using the original matrix (Chapter 2; table 2.0) which was recoded into the non-additive binary format, producing 181 characters. After processing this matrix using the same techniques as outlined in part 1 of this chapter, 120 MPTs were found with a length of 604 steps. CI = 0.295; RI = 0.607; RC = 0.179). The strict component consensus of these trees (figure 3.8a), shows a number of topological differences to the MPTs of the original parsimony run. Ten nodes at the base of the tree have collapsed, however, the top of the tree, like many of the analyses performed in the second part of this chapter is similar to the original MPTs. The relationships of those taxa that are most cladistically derived remain unresolved, although *Argyops* and *Sparus* are sister taxa as in the original MPTs. The taxon *Spondyliosoma* here forms a sister grouping to the clade (*Lithognathus* (*Pagellus* (*Pagrus Stenotomus*)), the internal relationships of which also differ from that of the original MPTs. While the position of *Pachymetopon* in this analysis is cladistically more derived. The most notable difference of this analysis is however, the sister grouping of the outgroup taxa *Haemulon* with *Lethrinus*, causing Sparoidea to become paraphyletic. It also apparent that the CI is very much lower in this analysis to the original MPTs and is infact lower than all other analyses conducted throughout this chapter.

After reweighting using rescale consistency index, 3 MPTs were found. The topology of the derived part of the tree is similar to the original MPTs (figure 3.8b), although (*Calamus* (*Argyops Sparus*) forms a separate clade to (*Archosargus Acanthopagrus*). The taxon *Spondyliosoma* forms the same grouping as described above, while *Argyrozona*, which is closely associated with *Spondyliosoma* in the original analysis is now placed in a considerably more basal position. In this analysis the taxon *Pachymetopon* forms a sister grouping to C*entracanthus* and cladistically more derived taxa. The outgroup taxa *Haemulon* and *Lethrinus* group basally within the ingroup, thus causing the Sparidae to become paraphyletic.

The results of this analysis are indeed interesting, if somewhat disquieting when compared with the MPTs of the unordered and ordered analyses. The results are not considered further here, however, future work on this data set will aim to investigate the rationale as to why a different outcome is preferred when binary coding is implemented.

Discussion

The initial analysis where multistate characters were left unordered, supports a monophyletic Sparidae that is well resolved but only relatively well supported. The data has a fairly high level of homoplasy, which is not inconsistent with other similar data sets of perciform fishes formulated from morphological characters. However, randomization tests for this data set using both parsimony and pairwise incompatibility PTPs give the lowest possible value for the number of randomly permuted data., allowing for the rejection of the null hypothesis that the data is no more congruent than would be expected for random (phylogenetically uninformative) data. In addition tree statistics for the MPTs are also consistent that the data is phylogenetically informative. The analysis found 3 MPTs that differed only between a single node regarding the placement of the taxa *Chrysoblephus* and *Polysteganus.* Support for internal relationships considered from both Bootstrap proportions and Bremer support, show that relationships within the 'higher' sparids are better supported than for those branches at the base of the tree.

Subsequent analysis of the data through exclusion of outgroups or characters, greatly influence the base of the tree, causing little or no resolution between taxa, whilst relationships at the top of the tree remained largely congruent with the initial analysis. The instability at the base of the tree suggests that the available data is not compelling in support of a phylogenetic hypothesis for basal sparids that is well supported, and consequently confidence in these relationships is limited.

Character quality is assessed using the compatibility approach of Le Quesne probability (LQP), so that only those characters where the LQP is greater than 0.05 or 0.1 are included Review of the values from this analysis found that the characters with the lowest LQP, i.e. characters which are considered to be phylogenetically informative, are concentrated particularly in the braincase and jaws, while the palatine arch and infraorbitals contain characters with the highest LQP values, so that 75% and 100% respectively of these characters are excluded when $p = >0.05$.

The partitioning of characters into character types may be considered artifical as previously discussed. However, these character grouping are used to define data partitions. The exclusion of these partitions tends to effect the resolution at the base of the tree or those nodes which are supported by particular character groups. The values given for partition homogeneity tests show that for the character systems: postcranial, braincase, gill arches and palatine arch, the data is significantly more phylogenetically informative than would be expected for random partitions, allowing for the rejection of the null hypothesis that the data is no more incongruent than for random partitions. However, while the following partitions: gill and hyoid arch; jaws and dentition and hyoid arch, are considered to be phylogenetically uninformative, because the data is no more incongruent than random; randomization tests confirm that this data is significantly non-random. As the data of these partitions is not random, the conflict is therefore attributed to homoplasy. It is, however, clear from the results of these analyses that the data of certain

character sets is considered more phylogenetically informative than others.

A separate analysis performed where some of the multistate characters are ordered through the method of intermediates, produced a similar 'tree' to that of the initial analysis where all mulitstate characters are unordered. The major difference between the ordered analysis when compared to the unordered analysis is the shift in position of the taxon *Argyrozona,* from a central position to a basal one. In addition, the taxa *Cheimerus* and *Cymatoceps* form slightly different groupings at the base of the tree. The areas of disagreement between the two hypotheses presented here using unordered and ordered characters, implies that not much confidence can be placed in the relationships of these taxa.

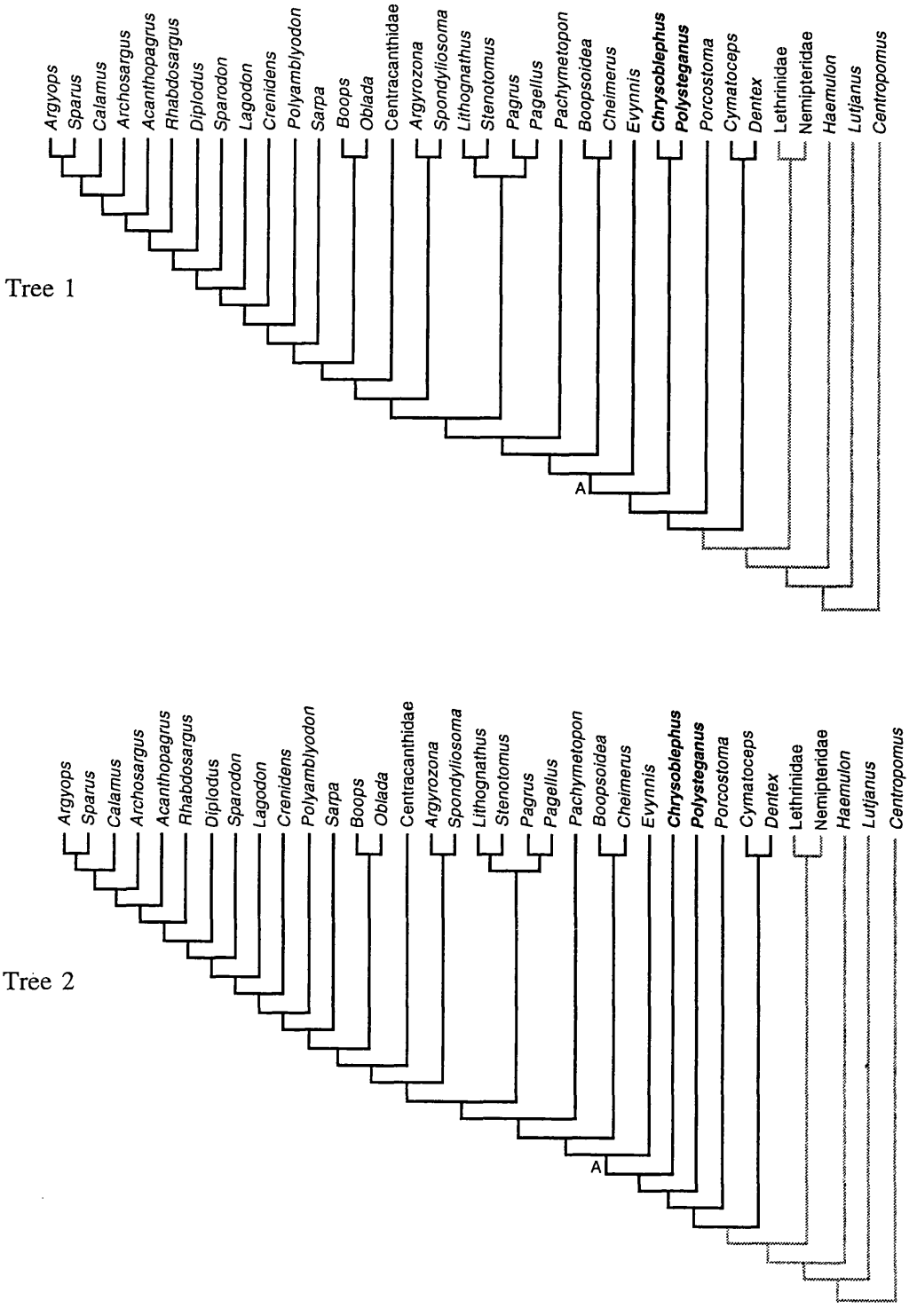

Figure 3.0 MPTs of the initial parsimony run using equally weighted, unordered multistate characters. CI = 0.72; RI = 0.804; RC = 0.460; L = 384. Bold text indicates conflicting taxa while grey branches represent outgroup taxa.

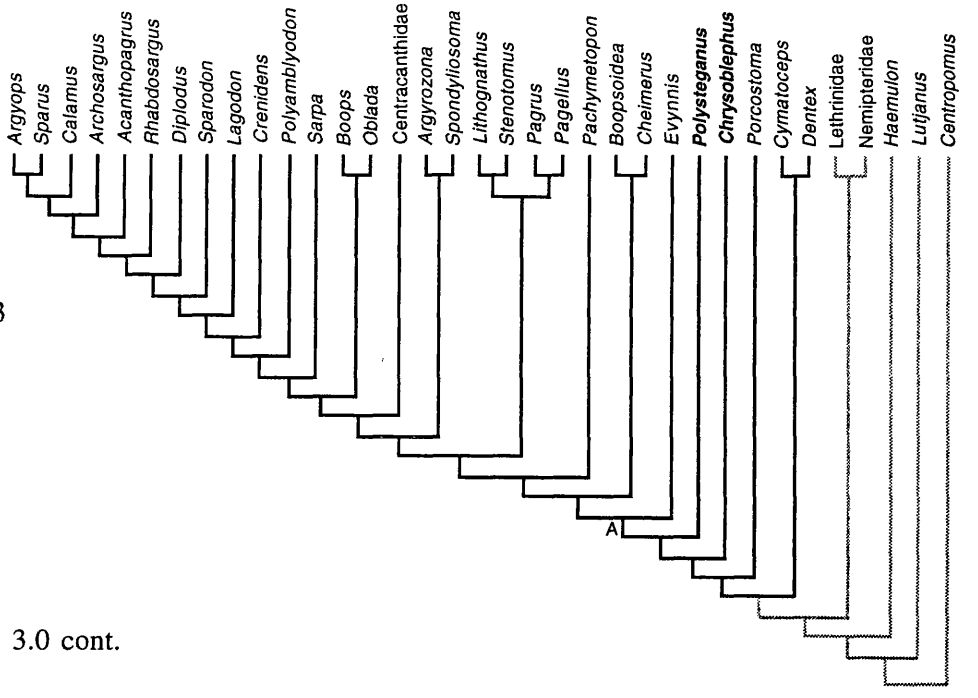

Tree 3

Figure 3.0 cont.

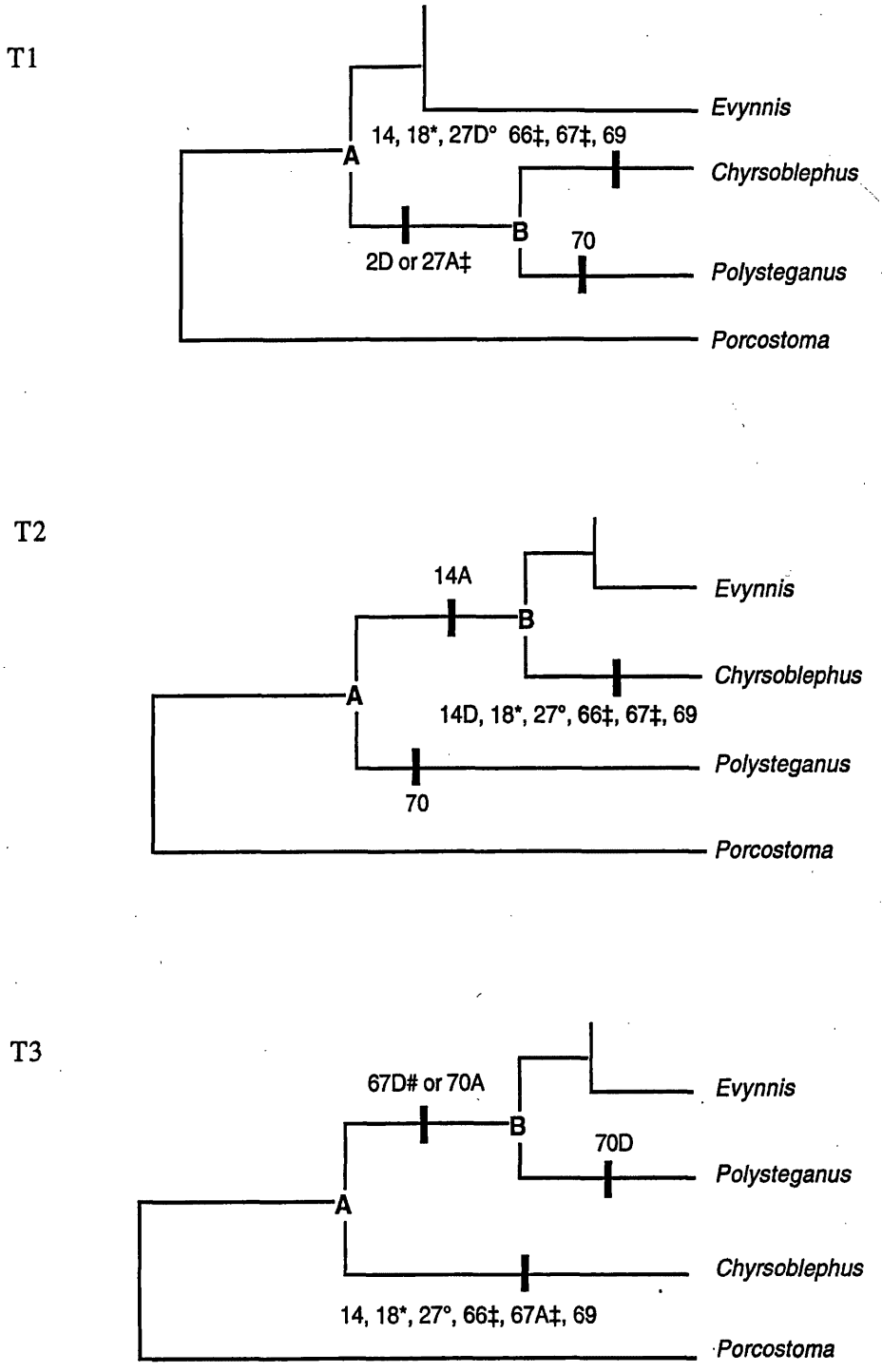

Figure 3.2 Ambiguous character state changes for the unresolved taxa *Chyrsoblephus* and *Polysteganus* in the three most parsimonous trees. Characters with no parenthetical notation are supported by both optimizations, otherwise A = ACCTRAN or D = DELTRAN optimizations. Superscript symbols as in figure 3.1.

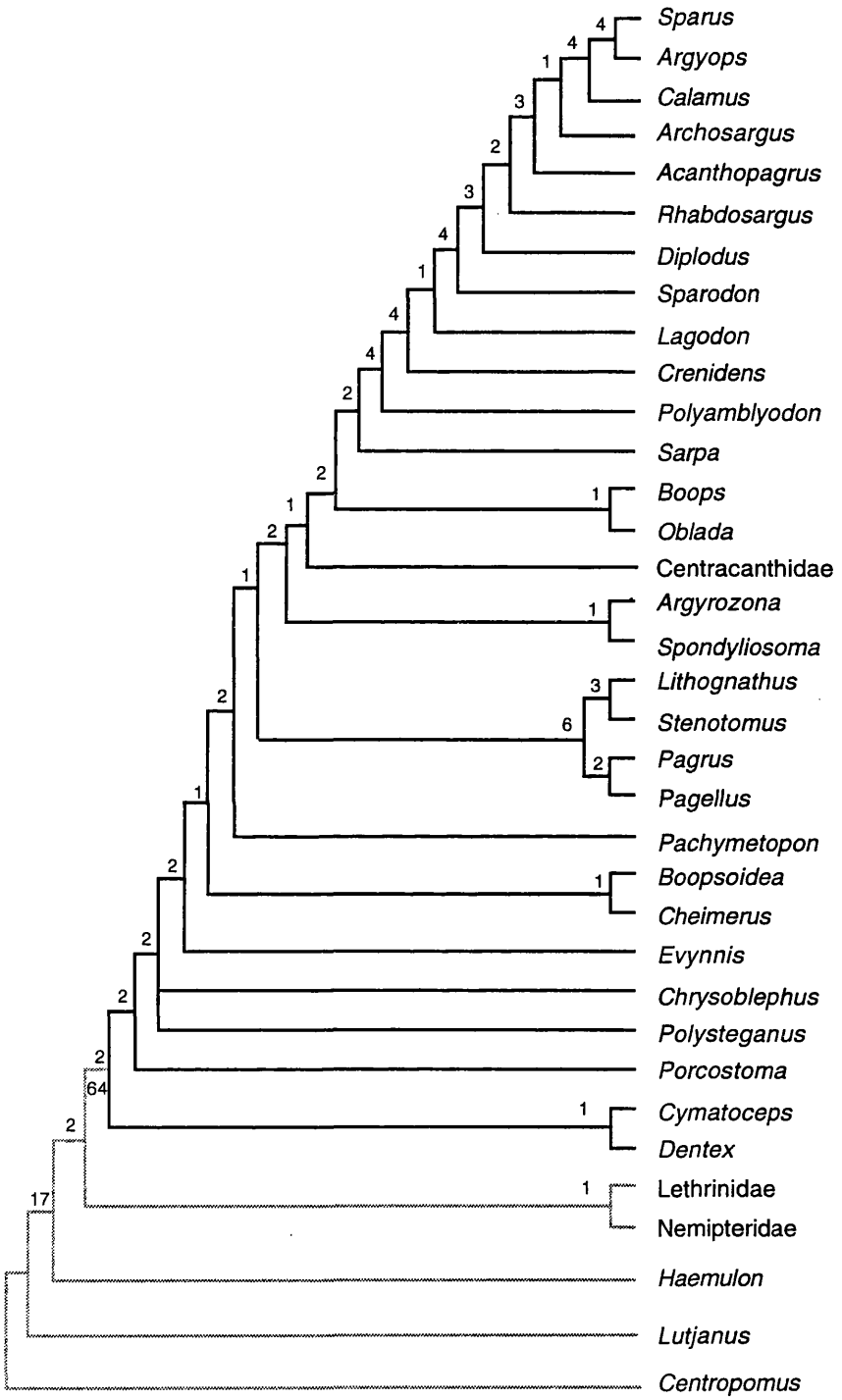

Figure 3.3 Strict component consensus of the 3 MPTs based on the character data in table 2.0. Values above branches indicate Bremer support values for all clades, while the Bootstrap value for the ingroup is given below the branch . Grey branches represent outgroup taxa.

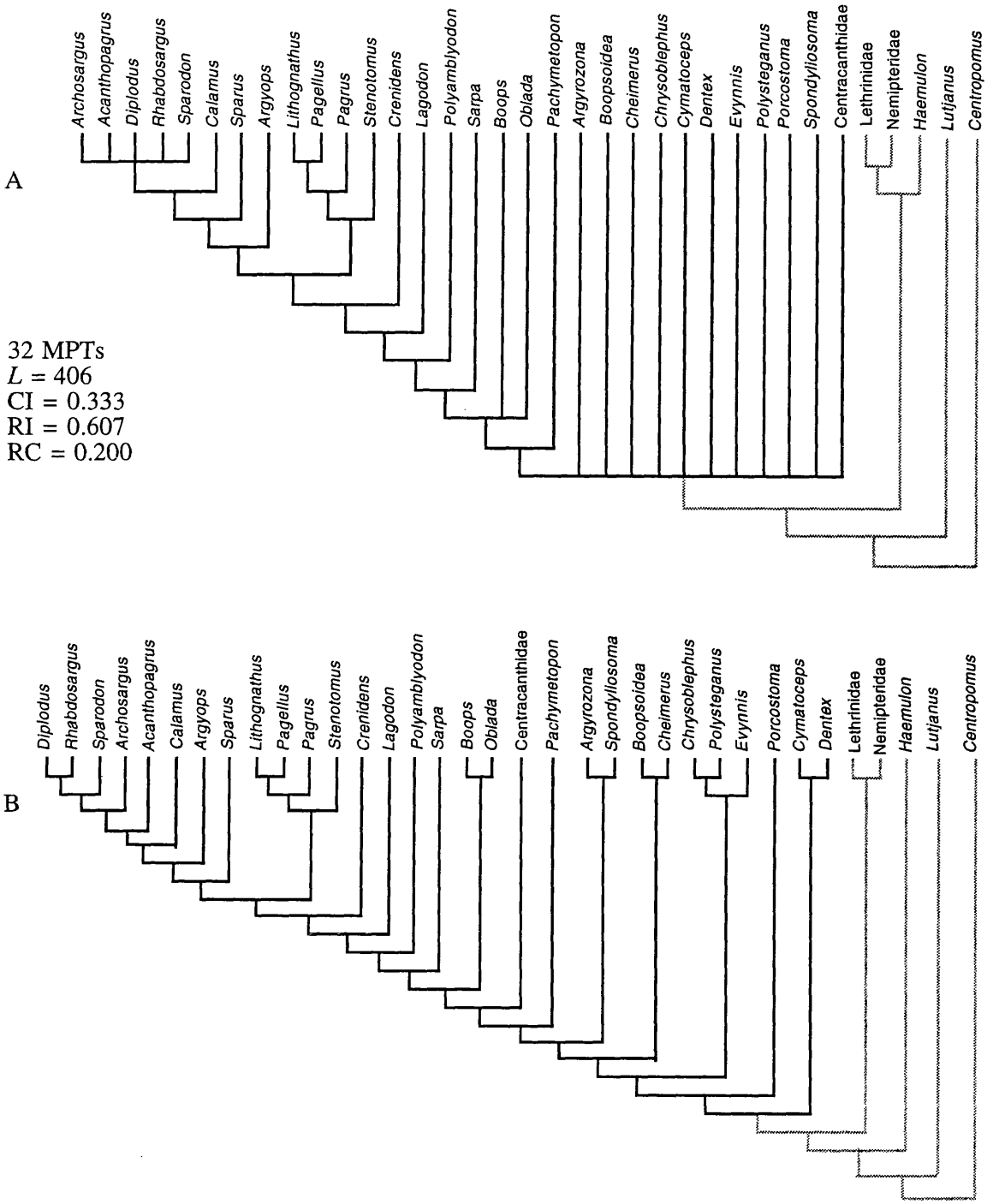

Figure 3.4.0 Analysis1 a) strict component consensus excluding characters using LQP $P > 0.05$ where the characters are equally weighted and b) MPT where characters are reweighted using rescaled consistency index. Grey branches represent outgroup taxa.

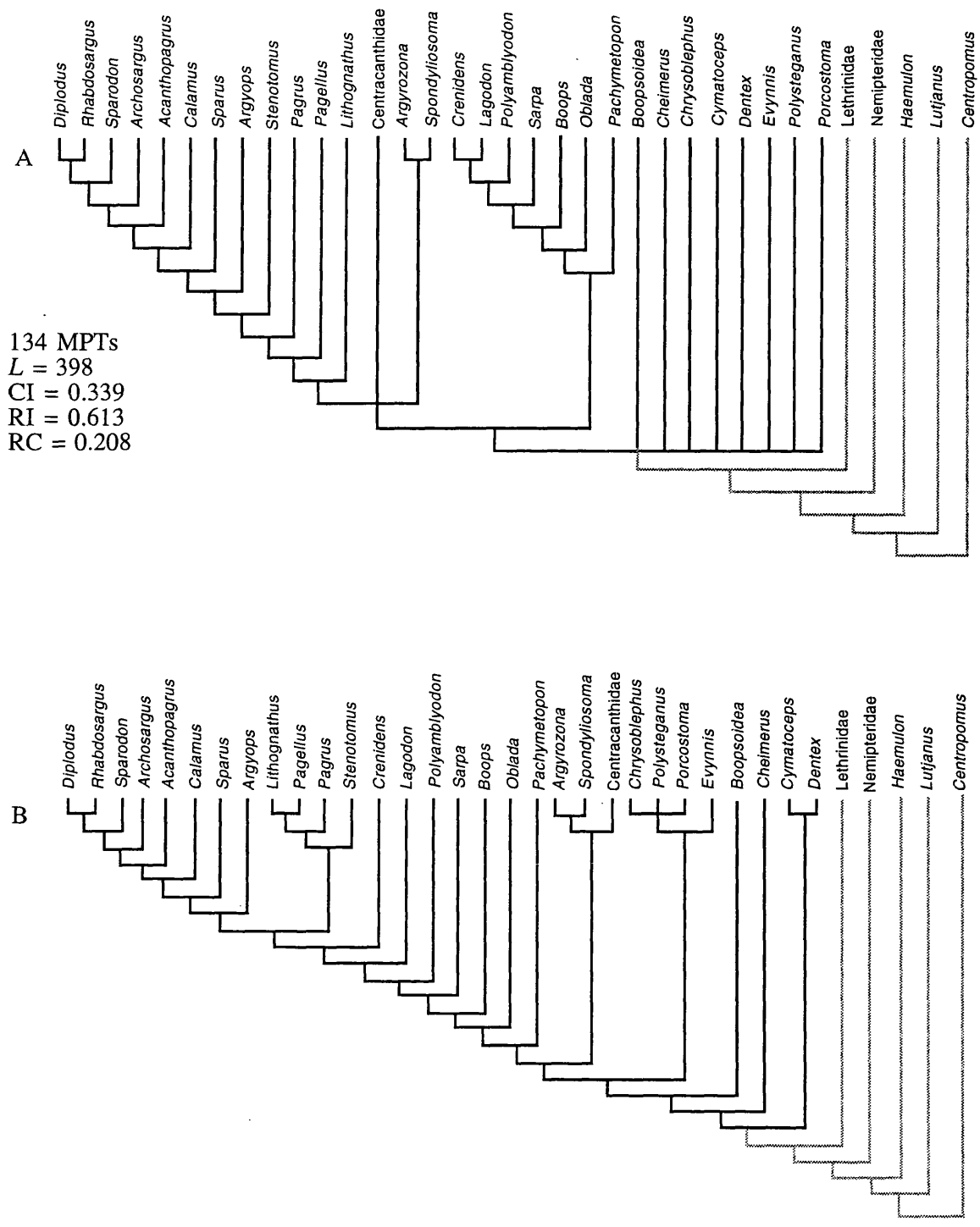

Figure 3.4.1 Analysis2. Strict component consensus trees using LQP where $P > 0.1$ a) characters equally weighted and b) characters reweighted using rescale consistency index found 2MPTs. Grey branches represent outgroup taxa.

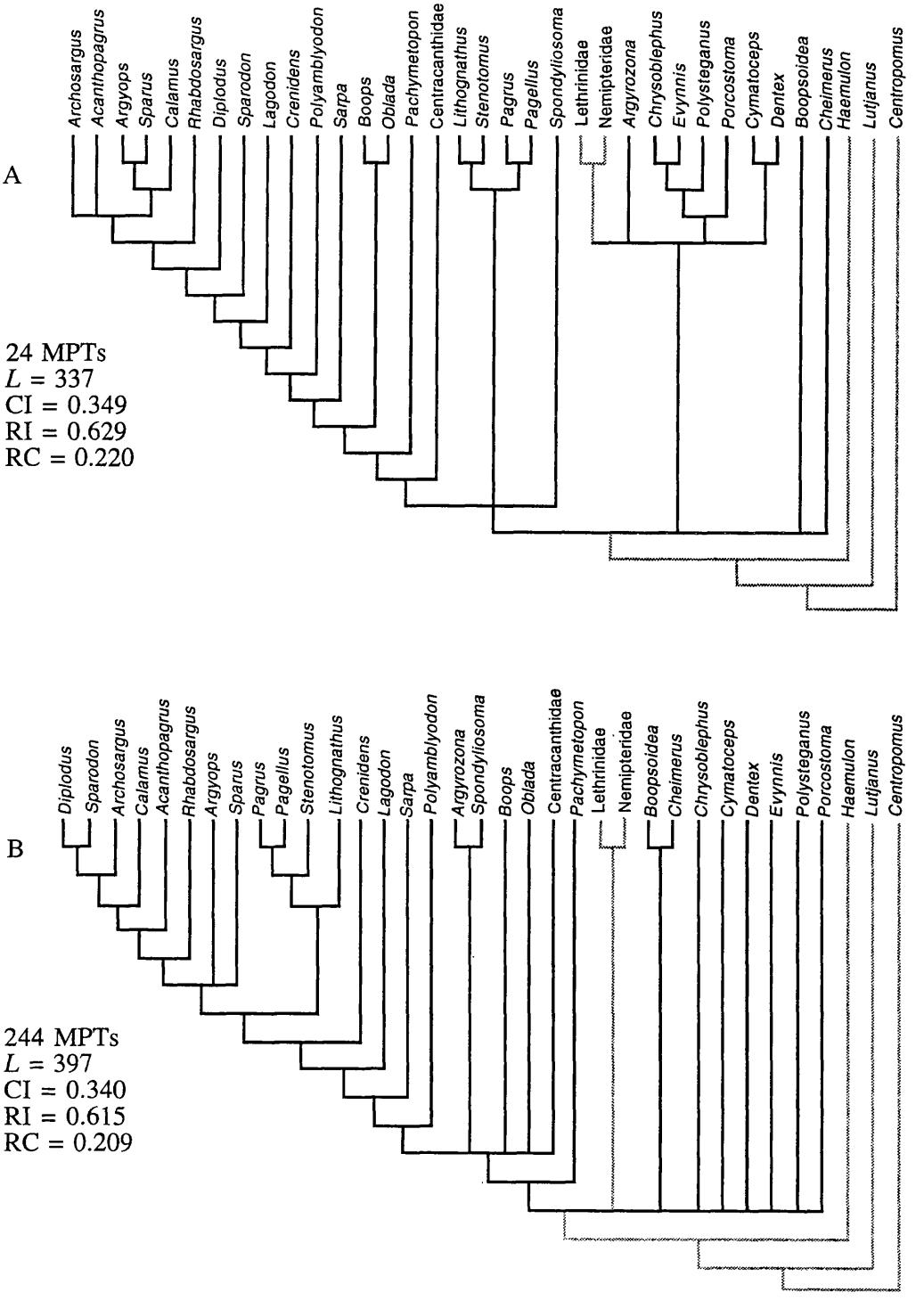

Figure 3.5 Strict component consensus trees of data partitions excluding a) post-cranial characters (C77-78) and b) braincase characters (1-25). Grey branches represent outgroup taxa.

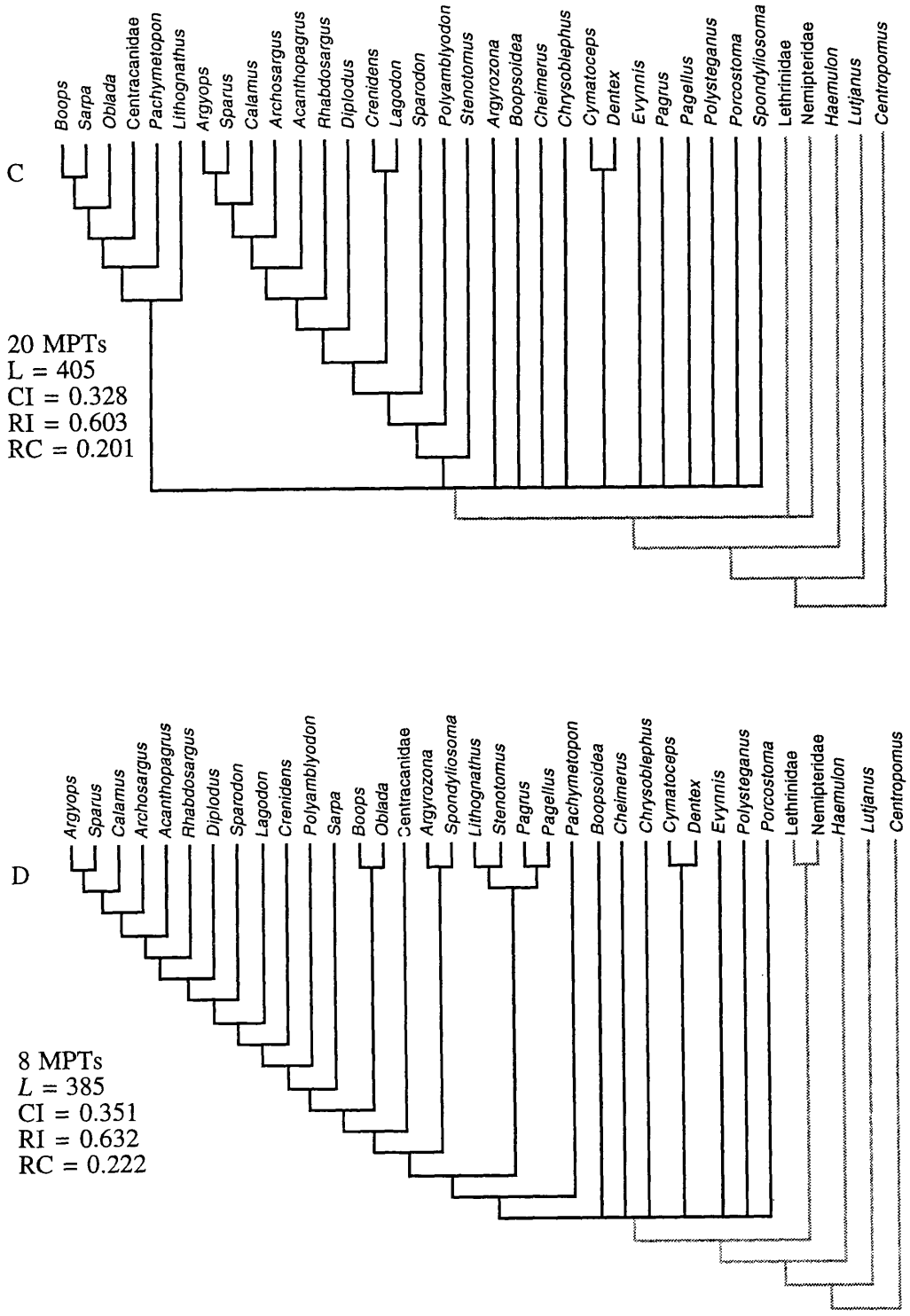

Figure 3.5 Strict component consensus trees of data partitions excluding c) jaw and dental characters (C26-49) and d) hyoid arch characters (C57-62). Grey branches represent outgroup taxa.

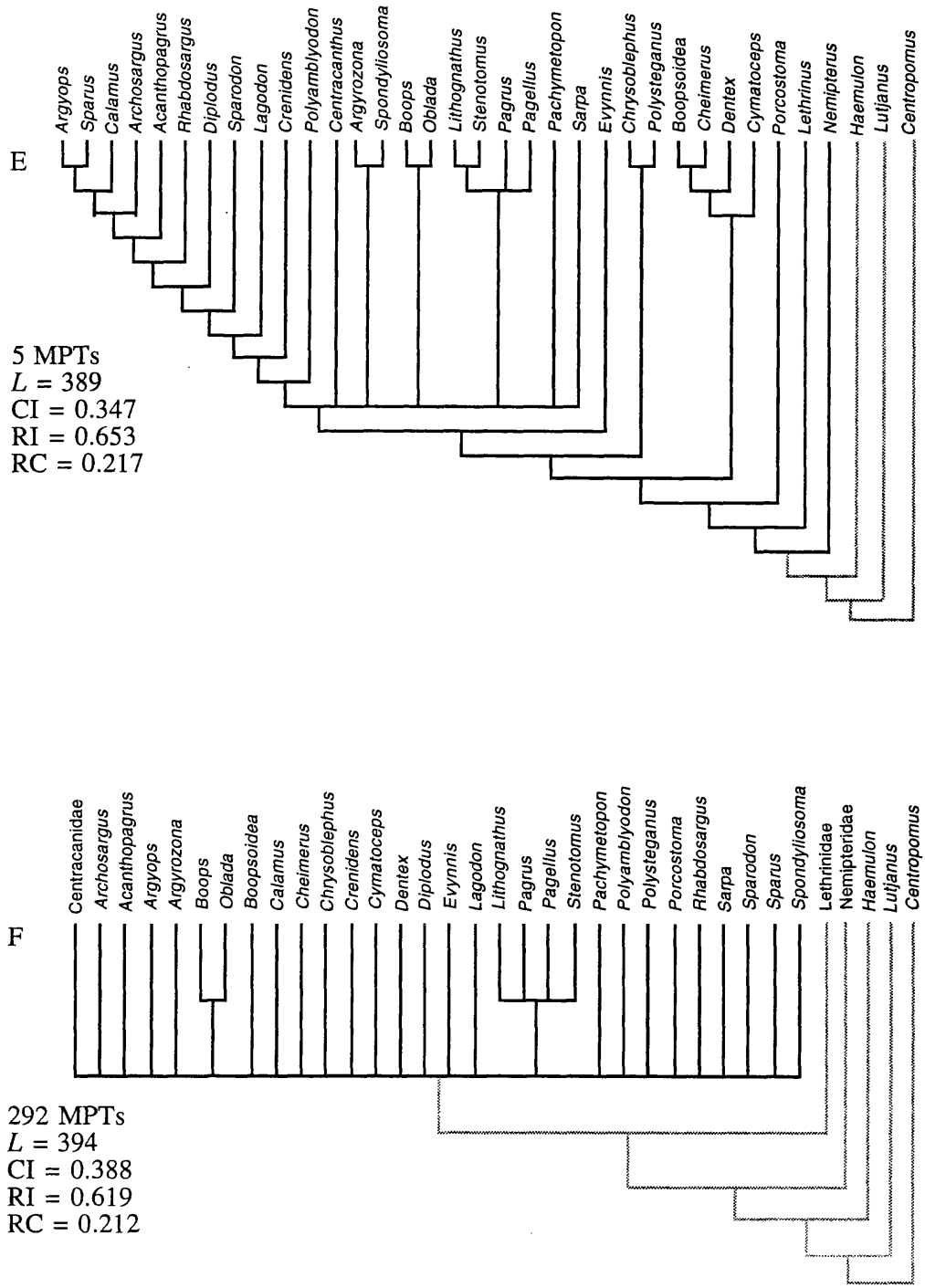

Figure 3.5 Strict component consensus trees of data partitions excluding e) gill arches (C63-76) and f)gill and hyoid arches (C57-76). Grey branches represent outgroup taxa.

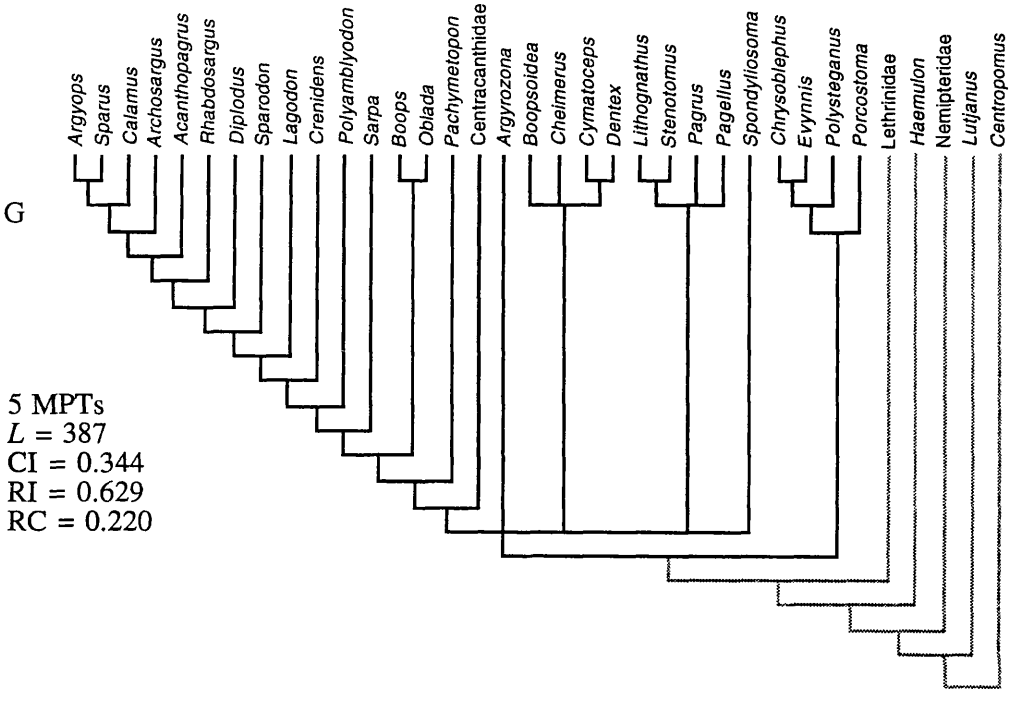

Figure 3.5 Strict component consensus of data partition excluding e) palatine arch characters (C50-55). Grey branches represent outgroup taxa.

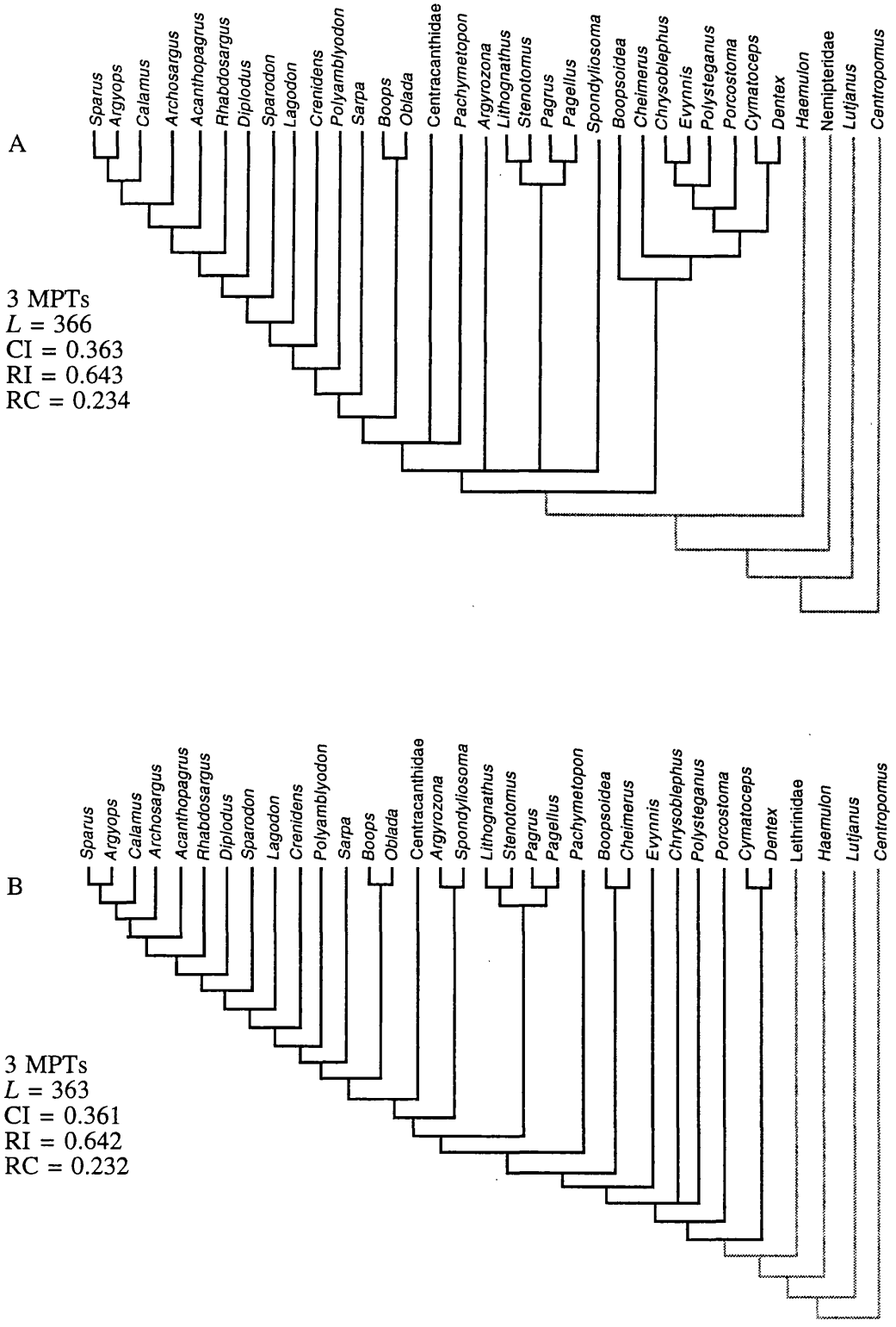

Figure 3.6 Strict component consensus trees after the exclusion of the outgroup taxa a) Lethrinidae and b) Nemipteridae. Grey branches indicate remaining outgroup taxa.

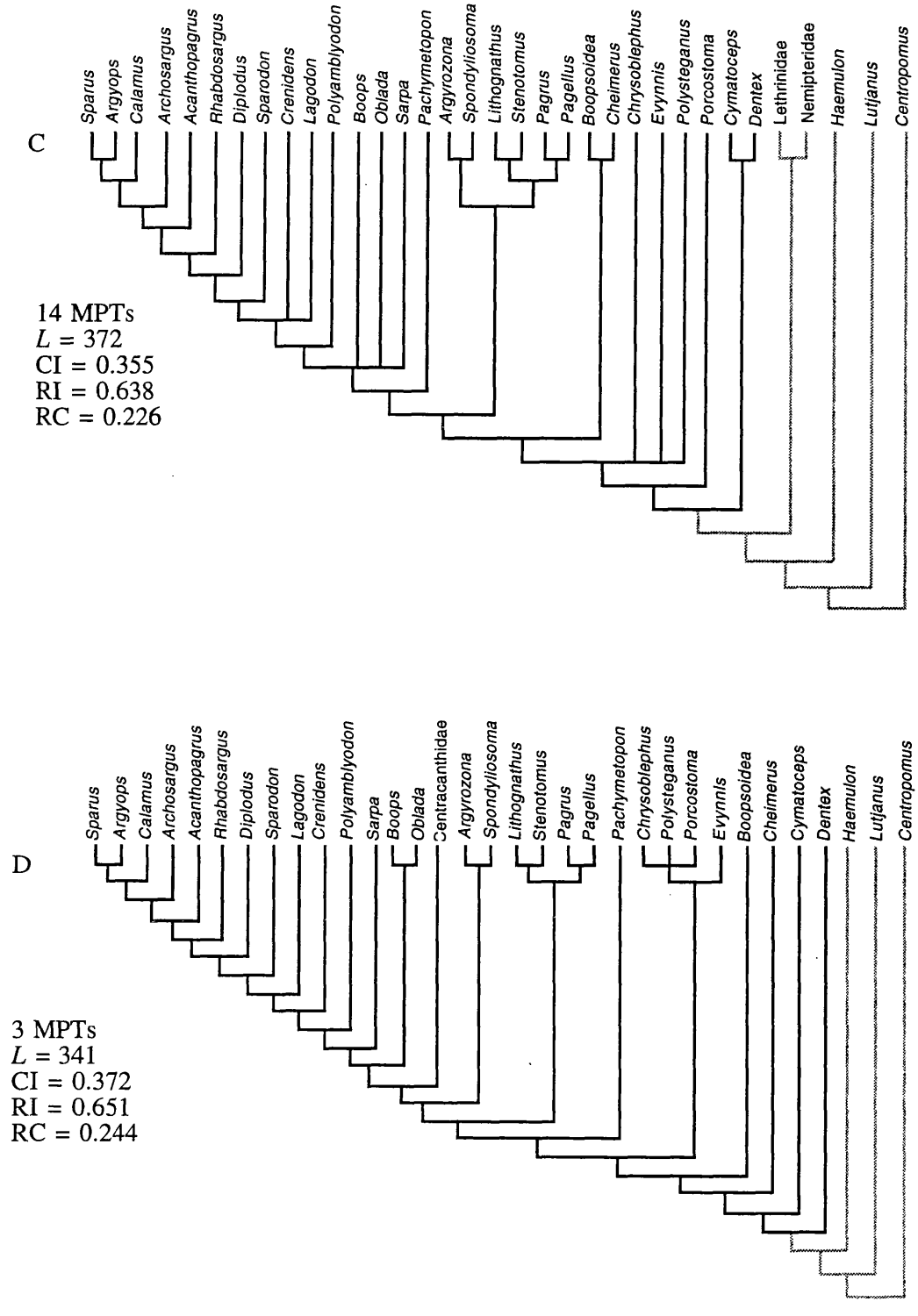

Figure 3.6 Strict component consensus trees after the exclusion of the outgroup taxon c) Centracanthidae and the taxa d) Lethrinidae and Nemipteridae. Grey branches indicate remaining outgroup taxa.

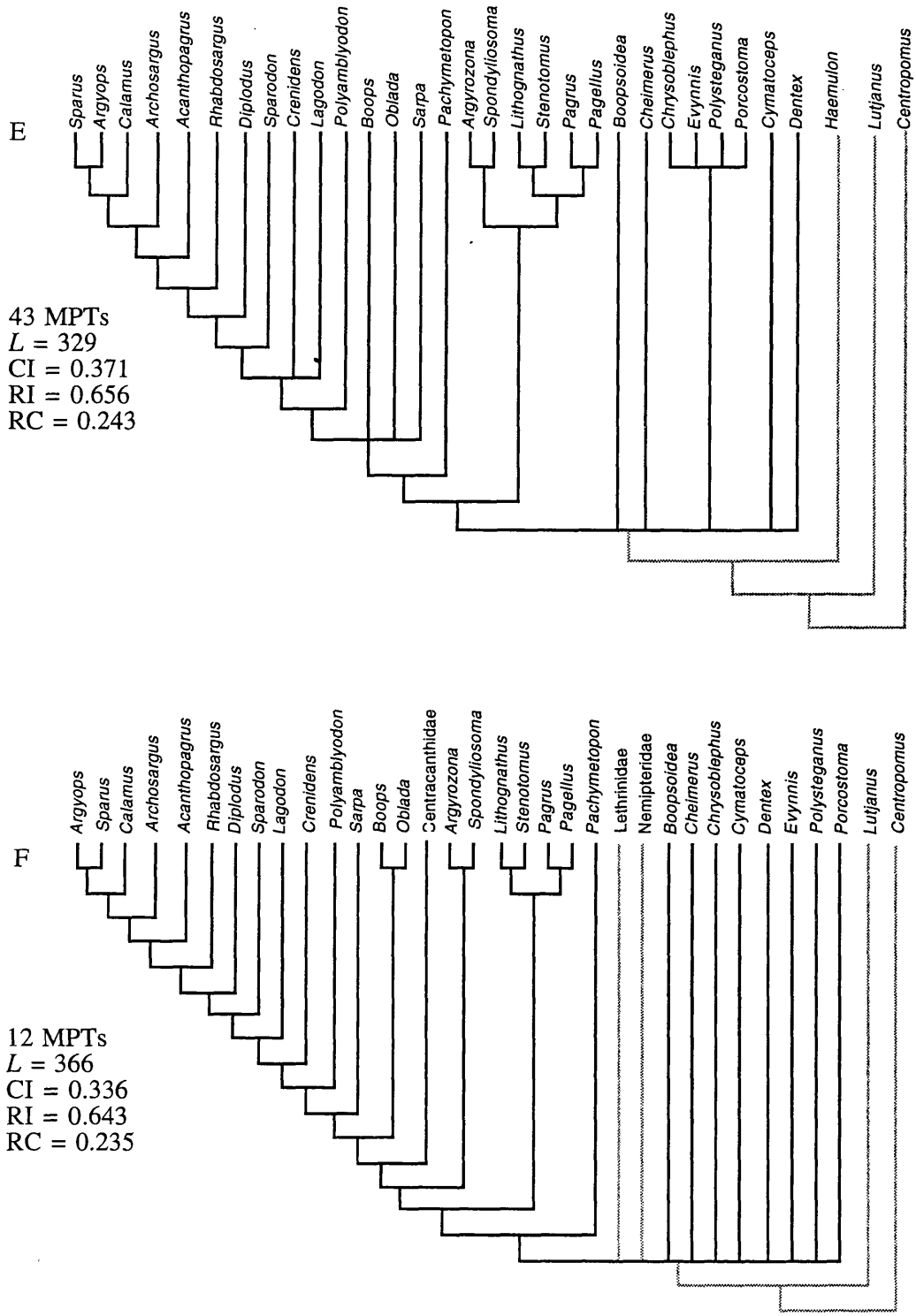

Figure 3.6 Strict component consensus after the exclusion of the outgroup taxa e) Centracanthidae, Lethridae and Nemipteridae and the taxon f) *Haemulon*. Grey branches indicate remaining outgroup taxa.

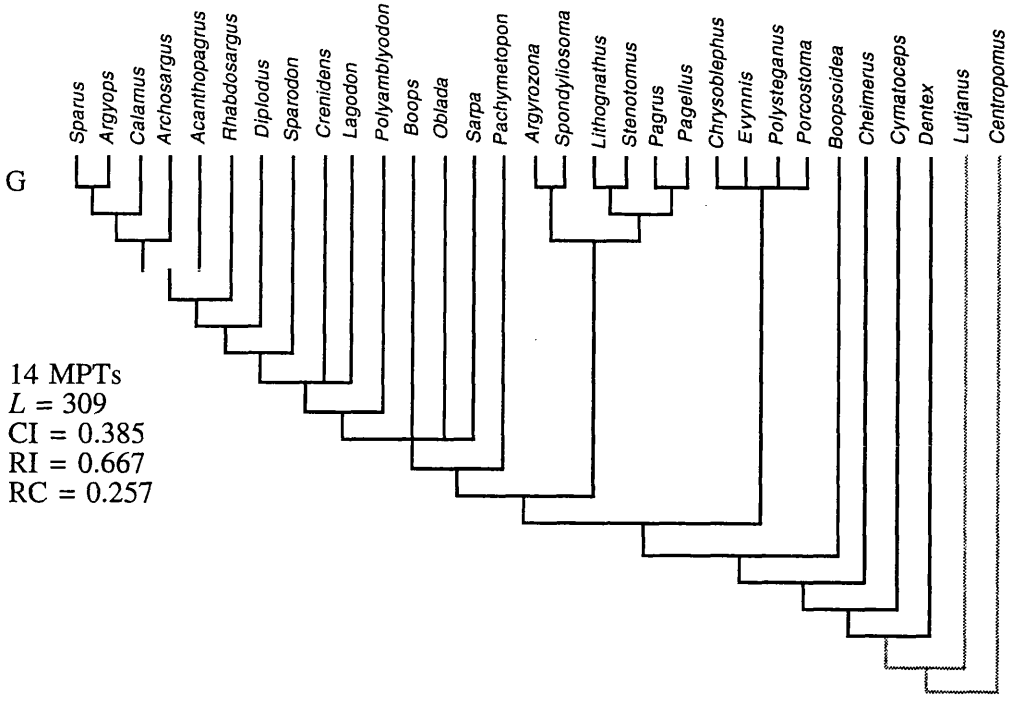

Figure 3.6 Strict component consensus after the exclusion of the outgroup taxa g) Centracanthidae, Lethrinidae, Nemipteridae and *Haemulon.* Grey branches indicate remaining outgroup taxa.

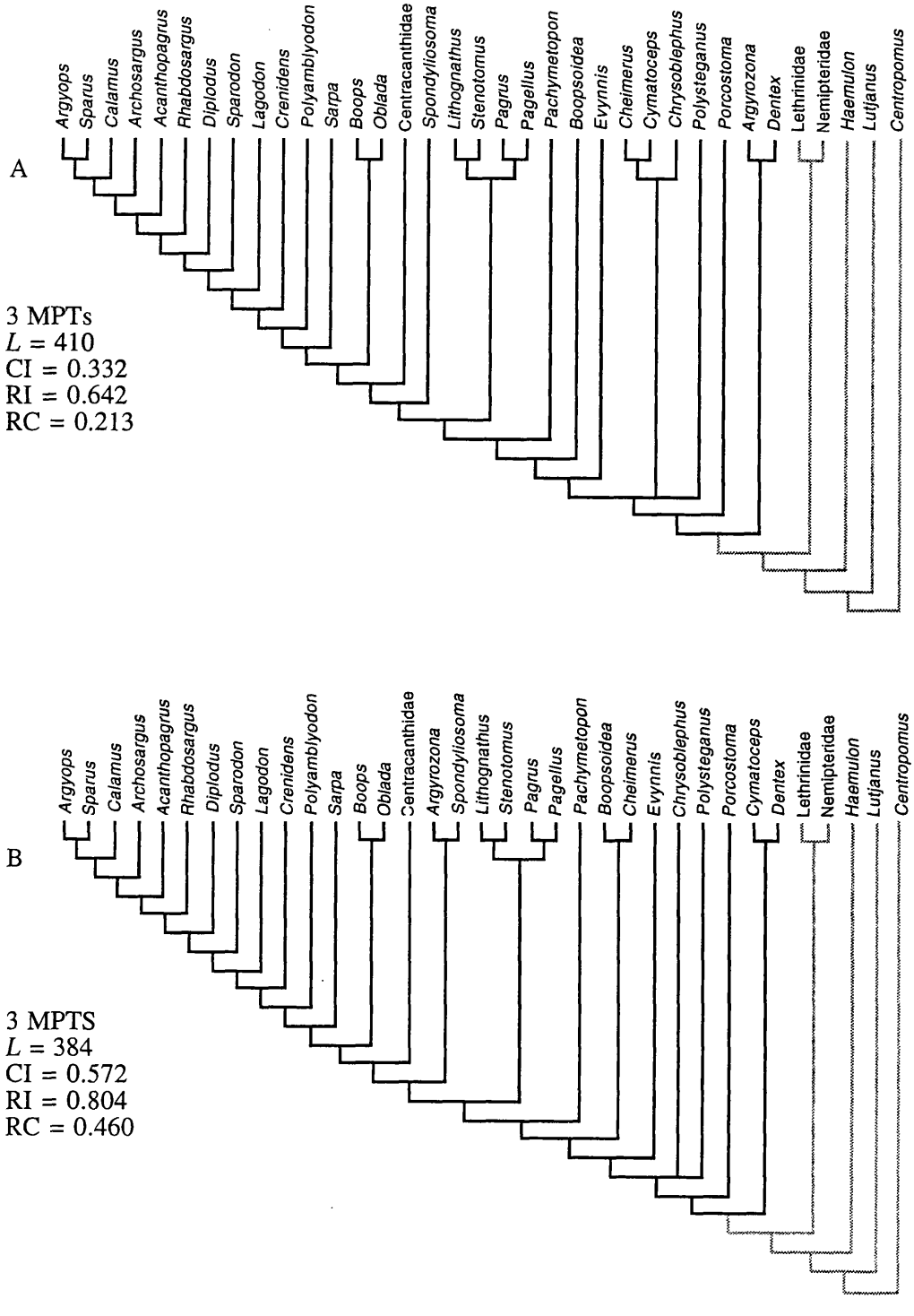

Figure 3.7a) Strict component consensus using ordered multistate characters, where characters are ordered by the method of intermediates (see character analysis Chapter 2); b) strict component consensus from the initial analysis where character are unordered.

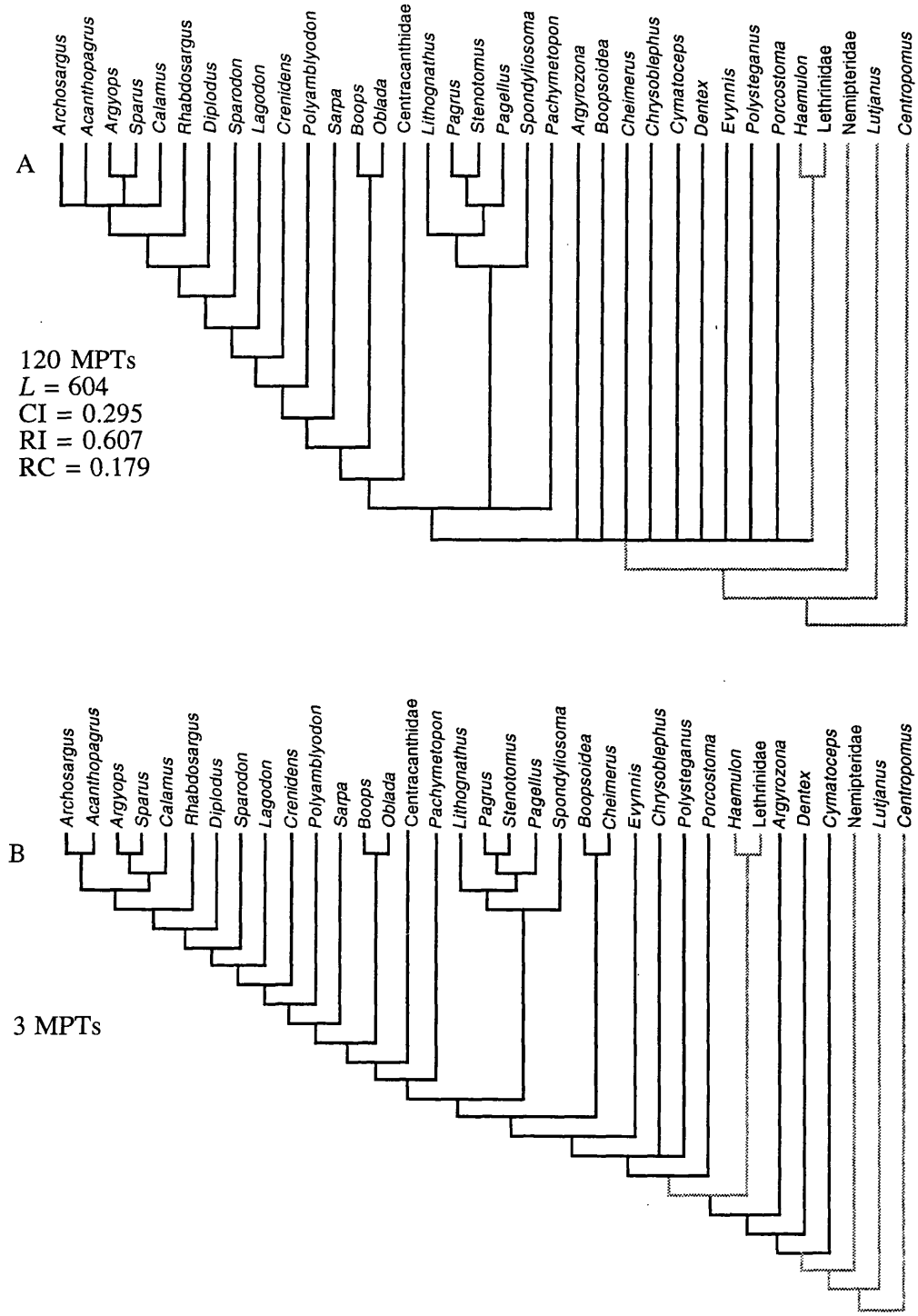

Figure 3.8 Non-additive binary coding (see Appendix; table 3.5) of the original data set a) strict component consensus using equally weighted characters b) strict component consensus after reweighting using rescale consistency index. Grey branches represent outgroup taxa.

TABLE 3.3 Numbers of unambiguous character state changes for tree 1 classified according to character types: B = braincase; J = jaws; D = dentition; I = infraorbitals; PA = palatine arch; HA = lower part of hyoid arch; BA = branchial arches; PG = pectoral and pelvic girdles; AS = axial skeleton and F = fins. A = ACCTRAN and D= DELTRAN optimisations.

Branch/ Node	CHARACTER TYPES									
	B	J	D	I	PA	HA	BA	PG	AS	F
0	-	1	-	-	3	2	1	1	-	1
1	1	1	-	1	-	-	-	1	-	-
2	1	1	-	-	-	-	2	-	-	-
3	1	2	-	-	-	-	-	-	-	1
4	-	1	-	-	1	1	2	-	-	-
5	-	-	-	-	-	-	2	-	-	-
6	-	1	-	-	-	1	-	-	-	1
7	1	1	-	-	1	-	-	-	-	-
8	1D/A	-	-	-	-	-	-	-	-	-
9	-	-	-	-	-	-	1	-	-	-
10	1	-	-	-	-	-	3	-	-	-
11	2	-	-	-	-	-	-	-	-	-
12	2	-	-	-	-	-	1	-	-	-
13	-	1	-	-	-	1	1	-	-	-
14	1	1	-	-	-	-	-	-	-	-
15	2	-	-	-	-	-	3	-	-	-
16	1	2	-	-	-	-	1	-	-	-
17	1	-	-	-	-	1	1	-	-	-
18	3	1	2	-	-	-	-	-	-	-
19	1	1	-	-	-	1	-	-	-	2
20	-	5	2	-	-	-	-	-	-	-
21	1	-	1	-	-	1	-	-	-	-
22	2	-	-	-	-	-	-	-	-	-
23	1	1	-	-	-	-	3	-	-	-
24	-	2	-	-	-	-	1	-	-	-
25	6	-	-	-	1	-	2	-	-	2
26	3	3	-	-	-	-	2	-	-	2
27	1	-	-	-	-	-	-	-	-	1
28	1	1	-	-	1	-	-	-	-	-
29	2	-	2	-	1	1	-	-	-	-
30	4	2	-	-	-	-	-	-	-	-
31	3	-	-	-	1	-	-	-	-	1
32	-	3	-	2	-	-	2	-	1	-
33	3	-	2	-	-	-	-	-	-	-
34	-	2	-	-	-	-	-	-	-	-
35	2	-	-	-	1	-	1	-	-	1
36	1	1	-	-	-	-	-	-	-	1
37	2	1	-	-	-	-	1	-	-	1
38	-	1	-	-	-	-	-	-	-	1
39	1	2	-	-	-	-	1	-	-	-
40	2	1	-	-	1	-	2	-	-	1
41	2	2	-	-	-	-	2	-	-	1
42	1	-	1	-	-	-	-	-	-	-
43	-	1	1	-	-	-	-	-	-	-
44	1	-	-	-	-	-	2	-	-	-
45	-	5	-	-	-	-	1	-	-	-
46	-	-	-	-	-	-	-	-	-	1
47	1	1	1	-	-	-	1	-	-	-
48	2	-	1	-	-	-	-	-	-	1
49	4	1	-	-	-	-	1	-	-	-

50	1	-	-	-	-	-	-	-	-	-
51	4	1	-	-	-	-	1	-	-	-
52	-	-	-	-	-	-	4	-	-	-
53	-	-	-	-	-	-	-	-	-	1
54	-	2	2	-	-	-	-	-	-	1
55	4		-	-	1	-	-	-	-	-
56	3	1	1	-	-	-	-	-	-	1
57	2	2	-	-	-	1	-	-	-	-
58	1	2	-	-	-	-	-	-	-	2
59	4	-	-	-	-	-	3	-	-	1

Table 3.6 Comparison of unordered and ordered analyses for characters whose lengths vary over trees. Trees 1-3 = ordered; trees 4-6 = unordered.

a) Using UNORDERED characters

Tree	1	2	3	4	5	6
Length	387	387	387	384	384	384

	Characters															
Tree	2	11	19	27	30	39	53	59	66	67	69	70	73	74	75	86
1	7	3	8	10	6	10	2	6	8	9	4	8	2	8	3	10
2	7	3	8	10	6	10	2	6	8	9	4	8	2	8	3	10
3	7	3	8	10	6	10	2	6	8	9	4	8	2	8	3	10
4	6	2	9	12	5	9	3	4	9	10	6	7	1	7	2	9
5	6	2	9	12	5	9	3	4	9	10	6	7	1	7	2	9
6	6	2	9	12	5	9	3	4	9	10	6	7	1	7	2	9
Min.	6	2	8	10	5	9	2	4	8	9	4	7	1	7	2	9
Max.	6	3	9	12	6	10	3	6	9	10	6	8	2	8	3	10

b) Using ORDERED characters

Tree	1	2	3	4	5	6
Length	410	410	410	411	411	411

	Characters																	
Tree	2	3	11	19	27	30	39	41	53	59	66	67	69	70	73	74	75	86
1	7	13	3	12	15	6	10	7	2	6	9	9	4	8	2	8	3	11
2	7	13	3	12	15	6	10	7	2	6	9	9	4	8	2	8	3	11
3	7	13	3	12	15	6	10	7	2	6	9	9	4	8	2	8	3	11
4	6	14	2	13	19	5	9	8	2	6	10	10	6	7	1	7	2	10
5	6	14	2	13	19	5	9	8	3	4	10	10	6	7	1	7	2	10
6	6	14	2	13	19	5	9	8	3	4	10	10	6	7	1	7	2	10
Min.	6	13	2	12	15	5	9	7	2	4	9	9	4	7	1	7	2	10
Max.	7	14	3	13	19	6	10	8	3	6	10	10	6	8	2	8	3	11

CHAPTER 4

PHYLOGENETIC PERSPECTIVES ON THE BIOGEOGRAPHY AND FEEDING STRATEGIES OF THE SPARIDAE

"Biogeography can be no better than the taxonomy it must use to describe distributions"

Colin Patterson 1981

Introduction

Cladistic biogeography is used here to reconstruct area distributions and centres of origin for the Sparidae. Other ecological aspects may also be assessed in the evolutionary framework based on examination of a cladogram using the principals associated with this methodology.

A phylogeny is an essential prerequisite to the formulation and testing of hypotheses of biogeography and evolutionary scenarios of a group. Using the preferred phylogenetic hypothesis as inferred in part 1 of Chapter 3 for Recent sparids, I apply three different methods of cladistic biogeography that are aimed at ancestral area reconstruction for a monophyletic Sparidae and in identifying the geographical area(s) that is likely to have been ancestral to the different clades of the internal taxa of the study group. The methods applied here include: 1) ancestral area analysis using irreversible parsimony (Bremer 1992, 1995), 2) ancestral area analysis using reversible parsimony (Ronquist 1994, 1995) and 3) dispersal-vicariance analysis or DIVA (Ronquist 1996, 1997).

In the second part of this chapter I aim to explore the different feeding strategies of sparids, with reference to the morphological characters outlined in Chapter 2. An evolutionary scenario of feeding strategies for the Sparidae is proposed, using the same principles as applied to taxon-area cladograms, with substitution of taxa by feeding modes. The proposition that feeding strategies have been fundamental to sparid evolution is also discussed.

Part 1 PHYLOGENETIC PERSPECTIVES ON BIOGEOGRAPHY

Background to cladistic biogeography

Cladistic biogeography is the understanding of relationships of areas through the discovery of biotic patterns, which become comparable and understandable when expressed as area cladograms (Humphries and Parenti 1999). The hypothesis that the Earth and its biotas have evolved together and share a common history is used for both coevolutionary (e.g. host-parasite relationships) and biogeographical inference by substituting taxa for areas or hosts.

The method proposed by Nelson and Platnick (1981) that Rosen (1978) put into practice combined Hennigian systematics with Croizat's (1958, 1964, 1982) vicariance approach, thereby applying cladistic methodology to biogeography from formulating cladograms of areas (Patterson 1981). A fundamental question that these authors addressed in their work was the mechanism of speciation involved as to why a taxon occupies a certain area. Allopatric speciation, (i.e. the evolution of one or more new species from an ancestral species as a result of the geographical separation or fragmentation of a breeding population) is thought to come about by two alternative mechanisms; vicariance or dispersal. Vicariance assumes that the taxon evolved in a particular area and predicts that the taxon and the barriers have the same age. Dispersal assumes that the taxa evolved elsewhere and dispersed into the area and predicts that the barrier predates the cladogenetic event.

Dispersal interpretations are not easy to test because they are proposed separately for each group of organisms. Many biogeographers (e.g. Koopman 1981) consider that each group has its own dispersal mechanism and therefore the individual histories of the groups are not comparable. Hypotheses of vicariant events, however, may be tested by other fossil or Recent taxonomic groups, that occur in the same area under investigation and that are assumed to have been affected by the same 'barriers' (Humphries and Parenti 1999).

The search for centres of origin and the patterns of area cladograms are seen as fundamental concepts in cladistic biogeography (Hennig 1966; Nelson and Platnick 1981; Patterson 1981; Bremer 1992; Rosen 1994; Humphries and Parenti 1999). Hennig (1966), introduced the progression rule which holds that to find the centre of origin for a monophyletic group, phylogenetically primitive members of that group will be found near to that centre. It is plausible that within the continuous range of species of a clade a transformation series of characters would run parallel with progression in space, such that the youngest members would be on the geographic periphery of a group (Humphries and Parenti 1999). Conversely, there is an alternative point of view, that argues that the more derived members of a group will be at the centre of origin because they are competitively superior, therefore 'forcing' more primitive members out.

While biogeography is usually concerned with general patterns of area relationships obtained by analysis of multiple taxon-area cladograms (de Jong 1998), an application of the

progression rule may be applied to a single cladogram using area optimizations, to infer centres of origin or dispersal. Contrary to Platnick and Nelson (1978), who refute individual taxonomic groups in historical biogeography as having conceptual difficulties; Enghoff (1993), maintains that cladistically founded biogeography should include area as well as taxon biogeographic inference on the basis that the search for distributional patterns requires both individual and general patterns (see also Liebherr 1989; Bremer 1992, 1995; Winterbottom and McLennan 1993; Enghoff 1995; Ronquist 1994, 1995, 1997; Ruta 1998 for recent applications of the progression rule).

As biogeography is dependent on systematics, it holds true that "*biogeography can be no better than the taxonomy it must use to describe distributions*" (Patterson 1981: 447). This is a meaningful reminder of the importance of *a priori* construction of the phylogenetic hypothesis when considering *a posteriori* questions regarding life history.

Delimitation of geographic regions

The distributions of inshore marine fish are represented by four major marine regions, which include, in order of decreasing biodiversity: i) Indo-Western Pacific ii) Western Atlantic iii) Eastern Pacific and iv) Eastern Atlantic (Helfman 1997). Although the Mediterranean is considered a depauparate part of the latter region, it is included here as a separate region, for geographical as well as ecological reasons. The Mediterranean is a relatively isolated area demarcated by the narrow Straights of Gibraltar, while many fish that occur in the Eastern Atlantic are not necessarily present in the Mediterranean, however, the two regions do have strong faunal links.

Sparids inhabit the inshore or shelf region (above 200m), which forms the largest ecological niche for marine fish. They have a broad distribution occurring in all the major marine regions listed above. The highest diversity of sparids occurs in the Indo-Western Pacific (approx. 41.0% of all sparid species); Eastern Central Atlantic (26.5%); Western Central Atlantic (15.4%); Mediterranean (11.1%) and the Eastern Pacific (6.0%).

Data of sparid distributions are taken from the following FAO species identification sheets: Western Indian Ocean (Fischer and Bianchi 1984); Western Central Atlantic (Fischer 1978); Eastern Central Atlantic (Fischer *et al.* 1981); Mediterranean and Black Sea (Fischer 1973); Eastern Indian Ocean and Western Central Pacific (Fischer and Whitehead 1974).

Geographic distributions

Sparids occupy a broad geographical distribution, yet ranges for individual species presents an interesting geographic picture. Using table 4.0 and the area cladogram (figure 4.0a) to evaluate distributions, 14 of the 30 genera are found to be "polymorphic" (i.e. they contain species which occur in more than one of the geographic regions). Five genera are present in three of the five regions, while the genus *Diplodus* occurs in all areas except the Indo-Pacific.

The high diversity of sparids found in the Indo-Pacific is consistent with this region being a high diversity region or focus for marine life (Rosen 1988), with the occurrence of 19 genera, represented by 48 species. In contrast to this region the Eastern Central Atlantic has a low diversity of many fish and invertebrate groups, containing only about 500 species of shore fish (Helfman *et al.* 1997). However, sparids are one of the few families to have radiated in this region, with the occurrence of 12 genera representing 31 species. Nine of these genera are also present in the Mediterranean.

The Caribbean is also considered a focus within the Atlantic Ocean. However, sparid diversity compared to the Indo-Pacific is lower with only six genera present, representing 18 species. However, while diversity is higher in the Indo-Pacific, endemicity is much greater in the Western Central Atlantic, with five out of the six genera endemic to this region, whereas 10 out of 19 genera of sparids are likewise endemic to the Indo-Pacific.

Many of the species restricted to the Western Indian Pacific are endemic to South African waters. Ten genera (three of which have not been included in this study, see table 4.0) are endemic to these waters, while more than two-thirds of species from a further five genera are also endemic. Most of the species present in the Western Indian Pacific include South Africa waters as part of their range.

Genera present in the Western Central Atlantic, with the exception of the genus *Diplodus*, are found to be restricted to this region. The most speciose genus, *Diplodus* contains 14 species in addition to a number of subspecies. It also has by far the widest distribution, occurring in all geographic areas, except the Indo-Pacific. Perhaps more interesting it is the only genus of sparid that occurs on both sides of the Atlantic, with two species representing the genus in the Western Central Atlantic (see table 4.0).

The species *Calamus taurinus* and *Archosargus pourtalesii* are the only known sparids from those genera restricted to the Western Central Atlantic that are endemic to the Galápagos Islands. The presence of these taxa whose ancestors are undoubtedly Caribbean, would have become separated from the ancestral population no later than the closure of the Isthmus of Panama, in the Middle Miocene, 3.5-3.1 Ma (Coates and Obando 1996). This relatively recent geological event supports the idea why further speciation of these taxa in this area has not yet occurred.

A further observation which can be made from table 4.0 is the paucity of taxa which occur in the Eastern Pacific, which is a consistent observation with the eastward trend of reduced diversity of fish species in general across the tropical Pacific (Choat 1991). Apart from the monospecific genus *Evynnis,* a relatively basal member of the Sparidae and endemic to this region, the other taxa present in this region are found to be more cladistically derived. These taxa, with the exception of *Sparus* also occur in the Western Indian Pacific. The genus *Sparus* is represented by four species, one of which is endemic to the Eastern Pacific, while the rest occur in the Eastern Central Atlantic and Mediterranean Sea However, the absence of this species from the

Indo-Pacific is interesting as the occurrence of this species in the two adjoining oceans implies that *Sparus major* would have had to have dispersed into this area to colonise either region (dependent on the ancestral area as to the direction of dispersal) and would imply that this species later become extinct from the Western Central Pacific.

The paucity of sparids from this region seems odd, considering that there are plenty of suitable habitat areas, such as reefs similar to those found in the Western Central Atlantic. An explanation of the low diversity may be attributed to the presence of other sparoid families in this region. Members of these families have similar ecological niches to those filled by sparids in the Western Central Atlantic, however, as they are not present in this region, sparids have instead exploited and diversified in this region.

Ancestral Areas

The phylogenetic hypothesis of Chapter 3 (Figure 3.0, tree 1) provides a basis for examining biogeographic patterns in the Sparidae. Taxon area cladograms for total species and for type species are given in (figure 4.0a and b respectively). By substituting the terminal taxa with geographic areas, a hypothesis of area relationships may be deduced. The use of taxon-area cladograms in cladistic biogeography is based on the assumption that the same quantitative methods applied to the cladistic construction of phylogenies may also be applied to biogeographic analyses (Humphries and Parenti 1999). Examination of these area relationships permits the evaluation of the biogeographic mechanisms; dispersal, vicariance and differential speciation/extinction events have had in determining current patterns of distribution.

Ancestral area analysis using irreversible parsimony

General

Bremer (1992, 1995), devised a phylogenetic approach, that aims to identify ancestral area(s) of a Recent monophyletic group, thus determining the region(s) occupied by the latest common ancestor. This approach follows two assumptions: 1) areas that are positionally more plesiomorphic (present on deep branches) in a cladogram of a particular group are more likely to be the ancestral area for that group than are the positionally more apomorphic areas and 2) areas represented on numerous branches of the cladogram are more likely to be parts of the ancestral area than are areas represented on a few branches (Bremer 1995). Ancestral area analysis utilizes forward and reverse Camin-Sokal parsimony (a transformation may deviate from its presumed ancestral state many times but not revert) to quantify the presence of areas on deep and numerous branches in cladograms. Actual area changes along the phylogenetic tree of the group are not dealt with in this method, as there are no assumptions regarding any underlying process. Recent applications of this method include: Ruta (1998) and Rodríguez-Robles and de Jesús-Escobar (1999).

The use of fossils for identifying ancestral areas is often justifiably criticized for assuming that the oldest member of a group is ancestral and therefore represents its site of origin, although fossil data can be important in biogeographic studies using appropriate cladistic techniques (Smith 1994). However, the phylogenetic hypotheses of Chapter 5 of the combined fossil and Recent data sets are not considered here as the fossils (with the exception of *Diplodus oranensis*) are basal and all come from the same locality. This would produce a biased result that the centre of origin was from central Tethys. This may be true, but more evidence is needed to ascertain this scenario.

Method

The null hypothesis of vicariance biogeography that the ancestral area is identical to the present area and is assumed as a starting point. Using an all-loss/no-gain model, the ancestral state for each terminal that is present is assumed to be the primitive condition, with the minimum number of losses (i.e. regional extinctions) that are implied from the cladogram structure (L) are calculated. The absence of a terminal area is regarded as the derived state, so that these areas have only been subsequently inhabited through immigration. The minimum number of these appearances described as gains implied by the cladogram structure (G) is subsequently calculated. The ratio between the number of gains and losses of the each assumed ancestral area gives a measure of the relative probability of that area being part of the ancestral range (Smith 1994).

Results

The ancestral area analysis suggests the vast region of the Western Indian Pacific as the most likely part of the original range of sparids (table 4.1a and b). The least likely areas when all species are considered include the Western Central Atlantic and the Eastern Indian Ocean and Western Central Pacific. When type species only are considered, the Mediterranean and Black Sea, plus the latter two regions are assumed the least likely ancestral areas.

When the distributions of all species are considered (figure 4.0a), fourteen of the thirty taxa considered here are polymorphic (i.e. they occur in more than one of the geographic areas), whereas the distributions of type species show that ten taxa are polymorphic (figure 4.0b).

Ancestral area analysis using reversible parsimony

General

Ronquist (1994) developed an alternative approach for reconstructing ancestral areas using reversible parsimony, thus allowing for reversible changes between states (i.e. areas). The results of this method conflict with those of Bremer's, which Ronquist considered flawed (1995), because it is unlikely that dispersal is irreversible. A criticism of Bremer's method (Ronquist 1994) is that the polarity of area state changes are not addressed and therefore it is not feasible to evaluate the probability that the ancestral geographic range of a clade is polymorphic.

Furthermore, constraining ancestral distributions to a single area may yield spurious results (Ronquist 1995).

Method

To calculate the ancestral area, this method uses the minimum number of steps; changes in areas (S) assuming the null hypothesis that the ancestral area is identical to the present area at the basal node of the cladogram. Using reversible parsimony to optimize area characters, the S values are calculated and subsequently inverted and rescaled to 1 by multiplying them by the smallest S value calculated for a region.

Results

When all species are considered (table 4.1a), the Eastern Indian Ocean and Western Central Pacific is identified as the ancestral area, whereas for type species (table 4.1b) the RP^b value reveals that several geographical areas are equally as likely to belong to the ancestral range of the ingroup. The Western Central Atlantic, Eastern Indian Ocean and Western Central Pacific and Mediterranean and Black Sea all have a RP^b value of 1. It is important to recognise that in using reversible parsimony only the minimum number of steps are calculated, hence regardless of the number of branches for which an area is plotted, the number of steps may be the same (Ruta 1998).

This method is often less decisive for determining the ancestral area distribution for large trees, as S values are dependent on the size of the cladogram. Therefore, RP^b values will be more similar for large cladograms with many steps than for small cladograms with few steps (Bremer 1995). However, Ronquist (1995) disputed that tree size is the factor effecting decisiveness, attributing it to homoplasy. Thus, the more homoplastic a distributional character, the less decisive the relative probability values will be. Large trees tend to generate more homoplasy, as measured by the consistency index than do smaller trees (Sanderson and Donoghue 1989).

Dispersal-vicariance analysis (DIVA)

General

Most methods used today are based on the assumption that there is a single branching pattern among areas of endemism caused by vicariance, which is common to different groups of organisms. Furthermore, these methods do not treat dispersal and extinction explicitly, thus the analyses often require a posteriori interpretation and/or a priori data manipulation (Ronquist 1997). Dispersal-vicariance analysis Ronquist (1996, 1997) is a quantitative biogeographic method for reconstructing ancestral distributions for a given phylogeny without any prior assumptions about the form of area relationships. The method is derived from charater optimizations, which like Fitch (unordered) optimizations minimizes dispersal and extinction, allowing for multiple and reticulate relationships among areas. However, unlike the latter method

vicariance rather than sympatric speciation is used (Ronquist 1997).

The reader is referred to Ronquist (1996, 1997) for a full account of the approach and procedures implemented in his method.

DIVA analysis

The program DIVA version 1.1 (Ronquist 1996) is used here. A fully resolved tree, with no more than 180 taxa and 15 areas are a prerequisite for running DIVA. For this analysis I chose to use tree 1 as the preferred phylogenetic hypothesis on those justifications outlined in chapter 3. MacClade version 3.0.1 (Maddison and Maddison) was used to create a distribution matrix, limited to the absence (0) or presence (1) of a whether a taxon occurs in a particular geographic area. Thirty taxa were incorporated in this analysis and all outgroup taxa (except *Centracanthus*) were deleted from this analysis. The preferred tree was also recreated using the tree file in the same NEXUS file.

This method is best used when terminal nodes are species, rather than higher taxa (e.g. genera or families etc.) such as in this study. Ronquist (1996) specifies that if the terminals in an analysis are higher taxa, then the distributions of the species belonging to that taxon cannot simply be added. As this study does not include lower level relationships this problem may be resolved by using the maxareas option in DIVA, thus restricting the number of unit areas that may have been occupied by any ancestral species. However, restricting the maximum number of areas using this option, in order to reduce the combination of areas suggested especially for clades such as ((*Pagrus Pagellus*)(*Lithognathus Stenotomus*)) did not greatly effect the outcome compared to the original analysis and therefore is not discussed further.

DIVA results

Two analyses were performed using different geographic distributions dependent on whether the total range of distributions for all species were considered (figure 4.1a), or the distribution for the type species only (figure 4.1b). The second analysis was conducted due to the problem of polymorphic taxa, such as the genus *Diplodus*, which contains species that occur in four of the five geographic distributions (table 4.0).

The optimal area distribution for all species requires 30 dispersal events, whereas when type species only are considered 19 dispersal events are required. Both analyses showed that the ancestral distribution of the group included the areas A, C and E (Western Indian Pacific, Eastern Central Atlantic and Mediterranean and Black Sea). However, a criticism of DIVA is that the ancestral distribution (i.e. root node state) is the least reliable node for the entire tree, with a tendency for the ancestral distribution to be large including most if not all areas occupied by the terminal taxa (Ronquist 1996). Two different methods may be applied to solve this problem. i) inclusion of outgroup taxa, thus making the basal node less basal and ii) constraining the maximum number of unit areas allowed in ancestral distributions using the maxareas option. On

inclusion of the outgroup using the taxa *Lethrinus* and *Nemipterus,* the ancestral area included A or ACE, whilst constraining the maximum number of areas to two found the ancestral areas A, AC or AE.

A single preferred ancestral area(s) is given for the basal nodes and those more crown-ward in both analyses. However, when the range of all species are considered, those nodes supporting the internal relationships and the clade ((*Pagellus Pagrus*) (*Steneotomus Lithognathus*)) plus the cladistically more derived taxa: *Spondyliosoma, Argyrozona, Centracanthus* and the clade (*Boops Oblada*) are supported by several different hypotheses (figure 4.1a). The DIVA analysis using the geographic range of type species only, provided less conflict for the clade and internal relationships of ((*Pagellus Pagrus*) (*Stenetomus Lithognathus*)). This is can be attributed to the reduction in polymorphic taxa causing conflicting area hypothesis if the geographic range of all species are taken into consideration (figure 4.1b).

Discussion

The pattern-based biogeographical analyses used here to elucidate the centre of origin for the Sparidae produce conflicting results. Using the irreversible parsimony method identified the Indo-Pacific as the ancestral area, whereas the reversible parsimony method identified both the Eastern Indian Ocean and the Western Central Atlantic as the preferred ancestral areas. The conflict is a consequence of the inferred character polarity, which is dependent on the rationale as to which biogeographic law is implemented. As the progression rule is followed here, then the ancestral area identified through Bremer's method, using irreversible parsimony is preferred to the area obtained using reversible parsimony. As such the Indo-Western Pacific (area A) is identified here as the ancestral area of this family.

In support of this result, the outcome from the event-based method DIVA, is similar to the result of Bremer's method, in identifying the Indo-Western Pacific as an ancestral area, but additionally optimizes the Eastern Atlantic as part of this ancestral range. Both the results from DIVA and the ancestral area analysis (AA) using irreversible parsimony contrast to those identified through using reversible parsimony, which optimizes both the Western Central Pacific or Eastern Indian Ocean as equally likely ancestral areas.

Sparids are the only member of the superfamily Sparoidei to occupy the Western Central Pacific region, of which only those taxa that are more cladistically derived are present in this area. As sister groups to the Sparidae, Centracanthidae, Lethrinidae and Nemipteridae have presumably had similar histories. Thus, if the hypothesis using reversible parsimony is accepted, then three of the four families would have to be assumed to have become extinct from this region, whereas the results from DIVA and the AA using irreversible parsimony favour the migration of sparid taxa into the area from the east. To test this hypothesis a study of all families, using a component based program would be necessary. As the ancestral area analysis using irreversible parsimony and DIVA identified similar areas, based on two different methodologies these results appear

more plausible.

While the fossil record of the Sparidae is inadequate, as will be discussed in Chapter 5, as regards to what may be deduced of their life history. The occurrence of the oldest known sparids appear to confirm the results of DIVA and AA using irreversible parsimony. The Eocene sparids are present from the Tethys Ocean by the early to middle Eocene. During late Mesozoic and early Cenozoic, Tethys was a major oceanic area which during its closure would have been linked to the Indo-Western Pacific and the Eastern Atlantic oceanic regions (see Osborne and Tarling 1996). However, until more is known of their fossil record these assumptions remain speculative.

Part 2 PHYLOGENETIC PERSPECTIVES ON FEEDING STRATEGIES

In Chapter 3 it was found that the cranium of sparids has an exceptionally high diversity of morphological characters when compared to other morphological data sets of fish groups. In particular the braincase, jaws, and gill arches are especially character rich anatomical units (see table 3.0). The morphological diversity in these areas, implies adaptations concerned with feeding, of which there are a number of different strategies employed within this family.

The wide range of feeding strategies associated with sparids therefore make them an interesting group to study in determining whether diet has played an important role in their evolution. To construct a hypothesis for the evolution of feeding strategies within the Sparidae, the same principals as applied in the construction of taxon-area cladograms are used here.

General

Sparids are able to exploit many different food sources, with some taxa feeding on a variety of prey items, while others are specialist feeders having restricted diets. Food types, observed from gut contents and field observations (Fischer 1973, 1978; Fischer and Whitehead 1974; Fischer *et al.* 1981; Fischer and Bianchi 1984) include the following categories: soft-bodied invertebrates (cephalopods, worms, isopods, amphiopods); hard-bodied invertebrates (molluscs e.g. mussels, echinoderms, crabs, brittlestars); and sea vegetation (algae, seaweed and seagrasses). Feeding involves two stages i) food acquisition i.e. handling and postcapture manipulation, especially fish that feed on hard-bodied invertebrates or prey with external defences such as spines; and ii) food processing. Therefore the morphology of these parts of the animal carrying out these functions is going to reflect the food type.

Animals which are able to exploit a variety of food sources are termed *generalized feeders.* Within this study, generalized feeders are carnivorous, including differing proportions of small fish and invertebrates in their diet. The invertebrate component of their diet include soft-bodied invertebrates and thin-shelled molluscs which may be dispatched even with relatively unspecialized mouth parts.

When a single food source predominates and requires particular morphological adaptations, the feeding strategy is term *specialized.* The food types of specialized feeders are often too demanding for a generalized feeder, which are not morphologically equipped to deal with them. There are two categories of specialized feeders within the Sparidae, those that feed on hard-bodied prey items and herbivores.

Specialized feeders in which hard-bodied prey items predominate, spend a greater amount of time in the prey manipulation, therefore expending a higher amount of energy at this stage of feeding than generalists. Shell breakage, through crushing with powerful durophagous dentitions requires a considerable amount of force, the spiny puffer *Diodon hystrix* for example, can crush shells of the Panamanian muricid *Vasula melones* that in compression test fail under loads of 5000N or more (Vermeij 1993).

Herbivory is relatively rare among fishes, due to the necessary mechanisms needed for digesting plant matter. However, herbivorous fish are the most widespread group of vertebrate herbivores (Choat 1991). Herbivory is more common among tropical marine fish found on coral reefs, but is less so in temperate waters. However, some temperate marine families including Sparidae, Kyphosidae, Aplodactylidae, Odacidae, Stichaeidae feed actively on plant matter (Horn 1989).

Taxon-feeding cladogram

Feeding strategies were catergorized to include the following groups: hard-bodied prey items, herbivory, invertebrates (soft-bodied and thin shelled prey) and piscivorous.

By substituting terminal taxa with feeding modes, a clear pattern emerges from the cladogram (figure 4.2). Four assemblages of taxa are identified on the basis of feeding strategies, with an overall transition from generalized to specialized feeding strategies. Of these assemblages the two clades: hbin or hbin + in+sv (specialist clade) and Gin are also identified. Within the specialist clade a clear division occurs between taxa that feed on hard-bodied prey items and those that are herbivorous. Within this clade the primitive condition is represented by herbivory, while the most cladistically derived taxa feed on hard-bodied invertebrates. The genus *Diplodus* represents a transitional taxon, as it exhibits both modes of feeding. A division between feeding types is also apparent within those taxa represented by generalists feeders, although this is a more arbitrary division than those clades identified for specialized feeding. Within the assemblage of generalized feeding, basal taxa are found to be dominantly piscivorous and secondarily feeding on invertebrates, while for more cladistically derived generalists forming the separate clade Gin the reverse seems to be true.

There are however, a few taxa which have a very different feeding strategy to the assemblage that they fall within. These include the taxon *Argyrozona* which is dominantly piscivorous, but occurs within the specialized feeding clade and *Pachymetopon* which is herbivorous, but is, however, grouped here with generalist feeders.

Morphology and diet

The evolution of feeding strategies is mirrored by the evolution of certain morphological complexes, used in food acquisition and processing, such as jaw bones and muscles, dentition, gill arches, and the digestive system. Less obvious modifications, although of equal importance, include eye placement, body shape, locomotion and pigmentation (Helfman 1997). From Chapters 2 and 3 it was found that the braincase, jaws and gill arches of sparids are particularly character rich, indicating modification to exploitation of different diets. The following sections outline the morphological features which characterize the feeding clades as defined from figure 4.2.

Generalist diet

The overall morphology for generalist feeders that have a predominately piscivorous diet includes the following. The braincase has an elongate ethmoid-vomerine region, with an ethmoid-vomerine dorsal crest, but no ascending process fossa. The occipital crest is greater in length than height and the otic-occipital region of the parasphenoid tends to be horizontal. The process for the m. adductor arcus palatini and pharyngeal apophysis are both relatively small in these taxa, whilst the parasphenoid carina is weakly developed.

The jaw construct of taxa that are generalist feeders exhibit a long lever arm jaw closing mechanisms facilitating a faster bite, but with less leverage at the tip. The upper jaws have an ascending process that is shorter than the alveolar process, weakly developed or absent maxillary crest of the premaxilla, knob-like dorsal maxillary crest, long maxillary arm and short palatine sulcus. The mandible has a short symphsial process, deep articular fossa, the descending process of the articular is the same length as the ventral margin of the dentary with the angular forming the caudoventral corner of this process. A single row of caniniform teeth are present along the occlusal margin of the jaws, with large, 'fangs' present anterolaterally.

Those taxa that include a larger proportion of invertebrates in their diet have an intermediate construction between the morphology of the piscivorous generalist and the specialist feeder. The dentitions of these fishes include conical and molariform teeth with caniniform teeth anteriorly. The elements of the gill arches are elongate, with 7-12 gill rakers, of moderate dimensions.

Diet of hard-bodied prey

The braincase of taxa which feed predominately on hard-bodied invertebrates have greatly reduced ethmoid-vomerine regions, with a foramen or fossa to house the ascending process of the premaxilla. These taxa tend to have wide preorbital flanges, which are most prominent in the genus *Calamus*, presumably for protecting the eyes against the spines of echinoderms - one of their favourite prey items. The dilatator fossa is more extensive in these taxa, piercing the rostral wall of the sphenotic so that the m. dilatatori operculi may attach to the ventral surface of the frontals. The occipital crest is approximately as long as it is high, while the otic-occipital region

of the parasphenoid is inclined dorsally. The process for the m. adductor arcus palatini, pharyngeal apophysis and parasphenoid carina are all well developed in these taxa.

The jaw morphology of these taxa are robust, and exhibit a short lever arm jaw closing mechanism, thus providing greater force, and is characterized by: an ascending process that is the same length or longer than the alveolar process, well developed maxillary crest of the premaxilla, maxilla with a well developed dorsal maxillary crest, long palatine sulcus, short maxillary arm; while the mandible has a long symphsial process, shallow articular fossa, and a descending process which extends beyond the ventral margin of the dentary, while the angular forming part of the caudal margin of the dentary. These fish are all strongly durophagous (i.e. the dentition is molarifom).

The lower part of the hyoid arch is robust and reduced in length compared to generalist feeders. The hypobranchials and epibranchials are also reduced, with additional uncinate processes present on the latter elements. The number of gill rakers is the same for that of the generalist, however, they are generally more squat in dimension.

Herbivory dominated diet

Herbivorous reef fishes may be recognized by a series of characteristic morphological features. In particular, the oral jaws are small and have a reduced gape for continuous feeding with numerous rapid bites, resulting in the reduction of the maxilla and dentary elements (Choat 1991). These similarities are also seen in herbivorous sparids.

The ethmoid-vomerine region of the braincase of herbivorous feeders is similar to the morphology described for those taxa that feed on hard-bodied invertebrates. However, morphological differences are observed in the otic-occipital region. The parasphenoid is strongly inclined, with angles as great as 45°, while the process for the m. adductor arcus palatini, pharyngeal apophysis and parasphenoid carina are weakly developed or absent in these taxa.

The jaw morphology is again similar to those described for hard-bodied invertebrate feeders, except that they are considerably more delicate. The dentitions are however different, as all these taxa exhibit a single row of crenulate incisiform teeth.

The most distinctive characteristic of the gill arches in these taxa are the gill rakers, which are long and slender and more numerous. Herbivores also tend to have longer guts than carnivores, due to the refractory nature of plant material (Helfman *et al.* 1997).

Habitat associations

While sparids exhibit very different modes of feeding, there appears to be little or no correlation with habitat associations. A similar study on the derived labroid family the Scaridae (Bellwood 1994), provided a clear pattern between feeding modes and habitat association. Sparids live in a variety of habitats, which include generalized sea floors such as sandy, muddy or gravely bottoms, vegetated bottoms such as sea grass beds and occur in coral and rocky reef

environments. The only clade that shows some correlation between feeding and habitat association is the clade represented by herbivory, as these taxa occur in seagrass beds and over rocky bottoms covered by seaweed. Furthermore, some genera have no preferred habitat association (e.g. species of *Calamus* may be found on coral, sandy, or muddy bottoms or in seagrass beds), while other genera frequent similar habitats (e.g. *Pagellus* occurs solely on mud and sandy bottoms).

Discussion

The morphological diversity found in structures related to feeding suggests that there has been a high rate of morphological evolution towards exploiting new feeding strategies within this family. The diversification of feeding strategies within the Sparidae, is probably the principal driving mechanism behind the speciation of this group, as they are by far the most successful family of the Sparoidei in terms of diversity. The term diversity usually reflects number of species. However, it also implies diversity in morphology, and diet as well. The Sparidae are also the most widely distributed family of this superfamily, occupying all of the major geographic regions, which may also be a consequence of their ability to fill a range of dietary niches.

The higher diversity of life found in the tropics results a more competitive environment than found in temperate habitats. Molluscs occurring in the tropics evolve far more elaborate shells for defence than temperate forms. Likewise, their predators tend to have shell breaking equipment that is more specialized than in temperate forms (Vermeij 1993). Herbivory is also more common in the tropics than in temperate waters (Helfman 1997). The Eastern Central Atlantic, with a high diversity of tropical species has a large number of species of herbivorous sparids (Choat 1991). However, specialized feeding within the Sparidae is not restricted to the tropics, with some members such as *Sparus* (hard-bodied invertebrate feeder) and *Sarpa* (herbivore) supported in sub-tropical to temperate habitats. Generalized feeders which are predominately piscivorous are absent from the tropics, although those which contain a higher proportion of invertebrates in their diet, such as *Pagrus* do occur in tropical waters.

Sparids from the earliest known modern reef-assemblages at Bolca (see Chapter 5) are assumed to be generalist feeders. This presents a different scenario to occurrence and feeding strategies found today, as sparids which exhibit generalist feeding strategies tend not to be found in association with reefs, preferring temperate water habitats.

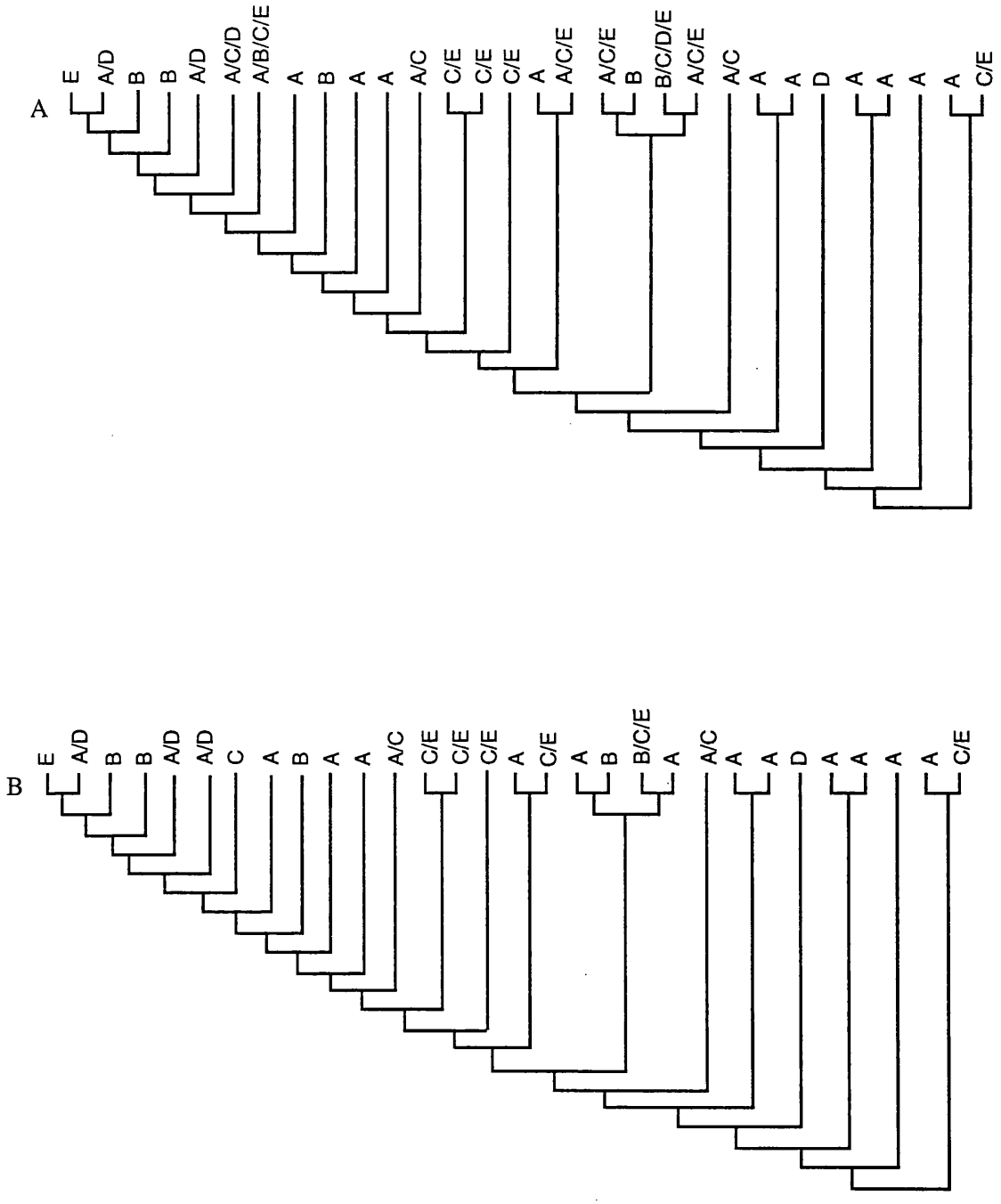

Figure 4.0 Area cladograms of the Sparidae a) distributions of all species b) distributions of type species. Tree 1(Chapter 3) is used here as the prefered phylogenetic hypothesis.

A= Western Indian Pacific; B= Western Central Atlantic; C= Eastern Central Atlantic; D= Eastern Indian Ocean & Western Central Pacific; E= Mediterranean and Black Sea

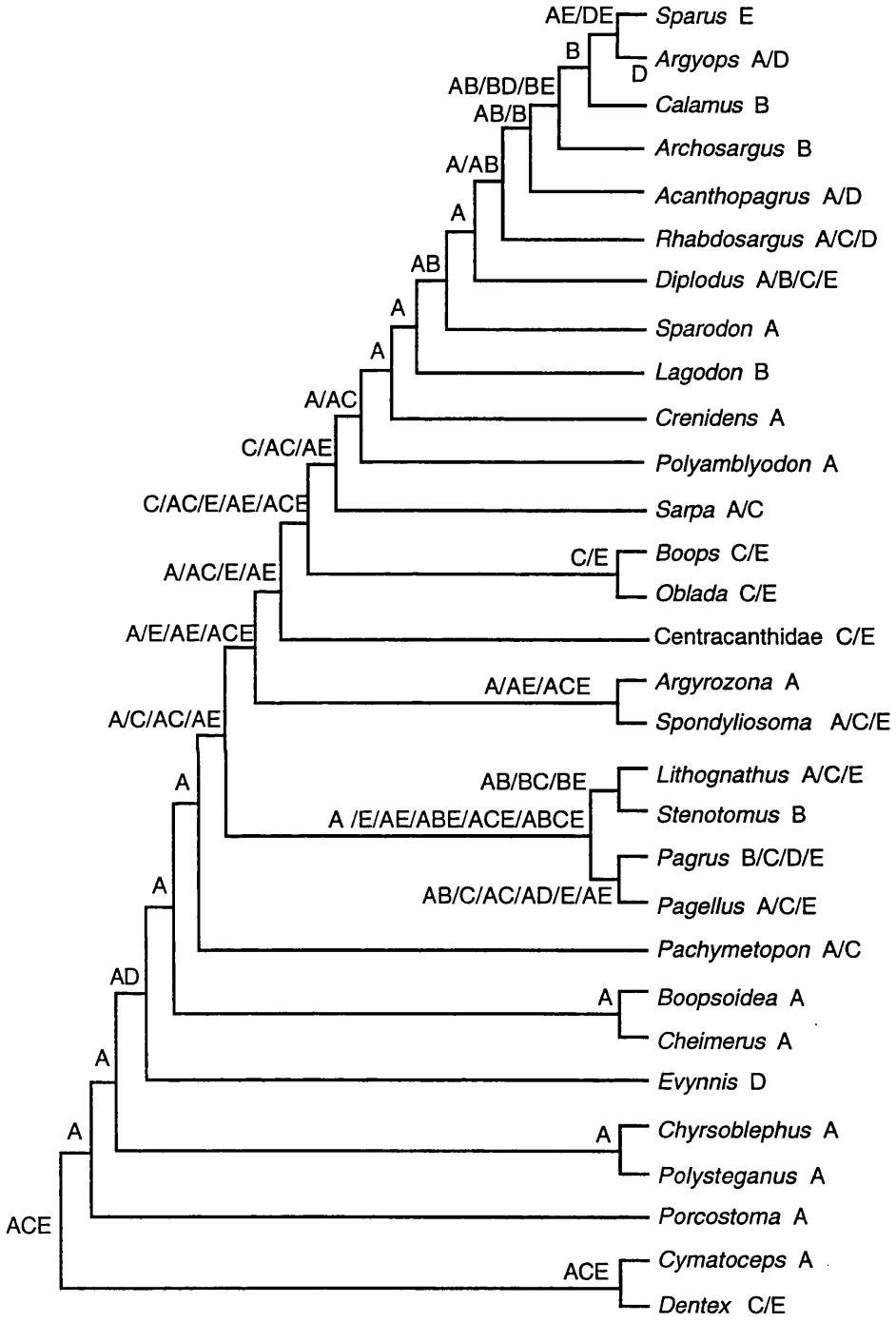

Figure 4.1a DIVA optimizations of area characters for tree 1(Chapter 3) using the distributions of all species examined.

A= Western Indian Pacific; B= Western Central Atlantic; C= Eastern Central Atlantic; D= Eastern Indian Ocean & Western Central Pacific; E= Mediterranean and Black Sea

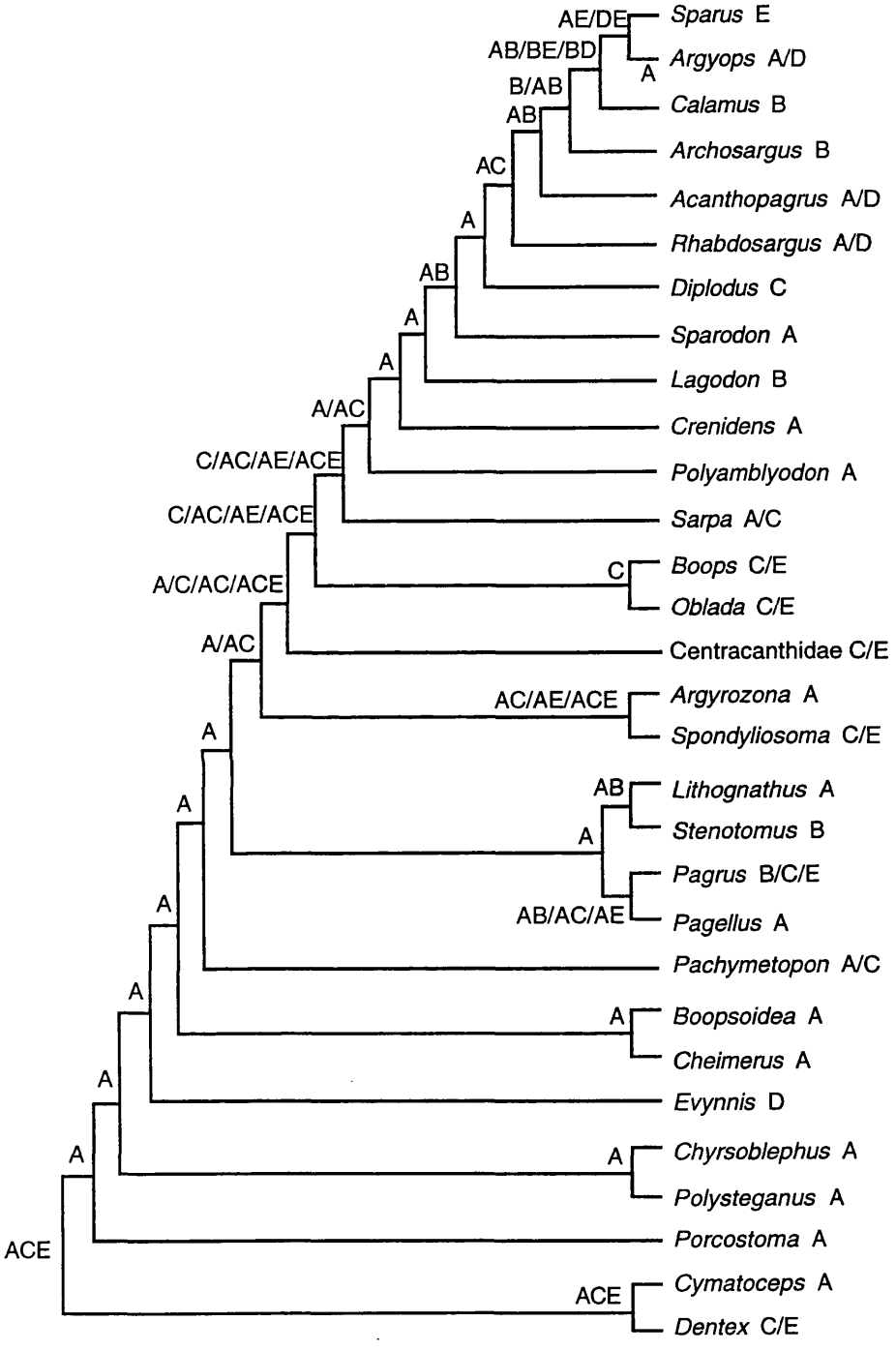

Figure 4.1b DIVA optimizations of area characters for tree 1 (Chapter 3) using the distributions for type species.

A= Western Indian Pacific; B= Western Central Atlantic; C= Eastern Central Atlantic; D= Eastern Indian Ocean & Western Central Pacific; E= Mediterranean and Black Sea

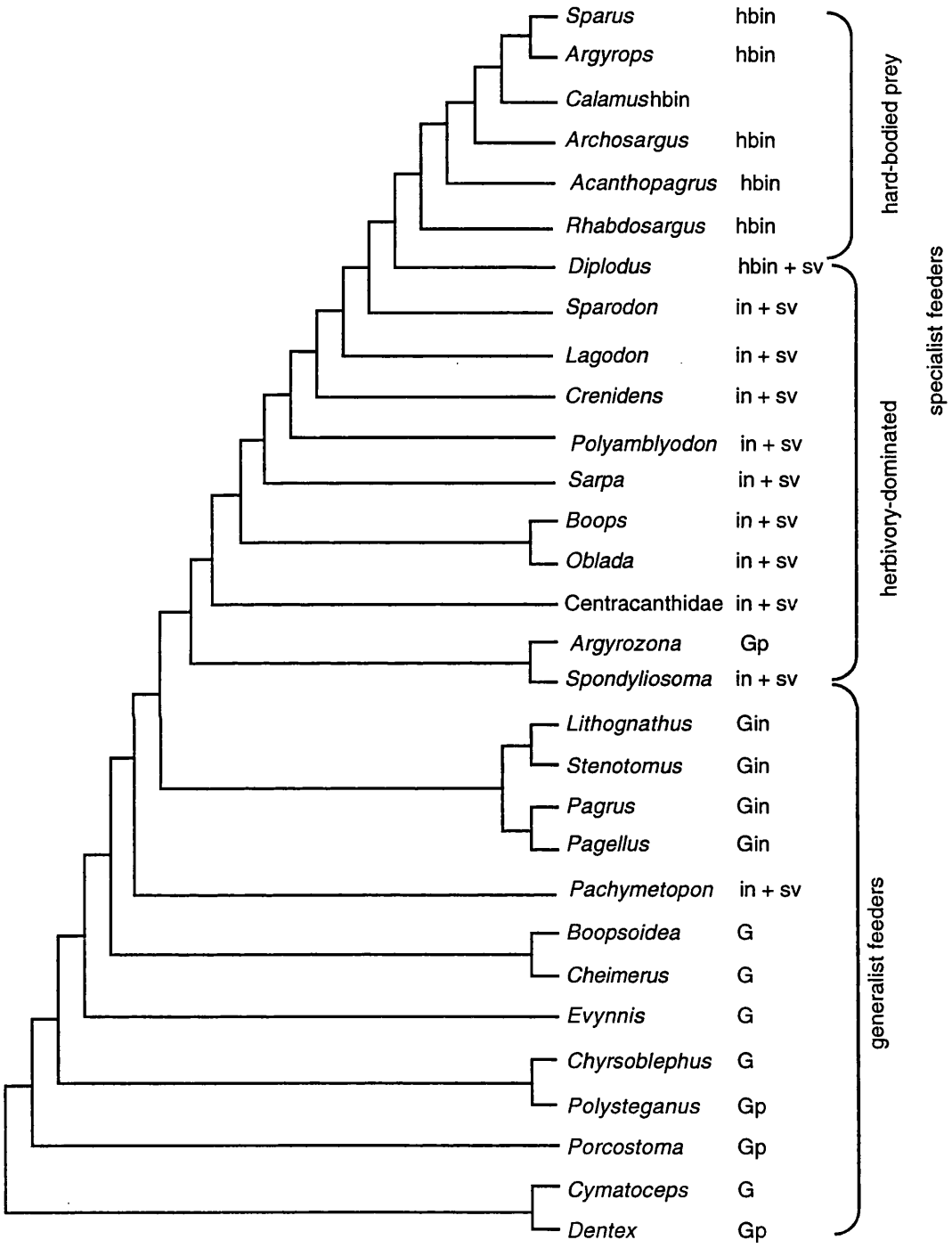

Figure 4.2 Cladogram of feeding strategies of sparids. Tree 1 from the inital parsimony analysis is used here as the prefered phylogenetic hypothesis. Key to feeding strategies: hbin = hard bodied invertebrates; in = invertebrates; sv = sea vegetation; p = piscivorous; G = generalist.

Table 4.0 Geographic distribution of sparid genera and species (Fischer and Whitehead 1974; Fischer 1978; Fischer *et al.* 1981; Fischer and Bionchi 1984). The total number of species (not including sub-species) of each genus are represented in parenthesis. For example the genus *Acanthopagrus* contains three species, all of which are found in the Indo-Western Pacific, and two of those in the Eastern Central Pacific. An asterisk indicates genera not included within the phylogenetic analysis of this study.

SPARIDAE	GEOGRAPHIC REGION				
Genus	Western Indian Pacific	Western Central Atlantic	Eastern Central Atlantic	Eastern Indian Ocean & Western Central Pacific	Mediterranean & Black Sea
Acanthopagrus (3)	3			2	
Archosargus (2)		2			
Argyops (2)	2			1	
Argyrozana (1)	1				
Boops (1)			1		1
Boopsoidea (1)	1				
Calamus (11)		11			
Cheimerus (3)	3				
Chrysoblephus (6)	6				
Crenidens (1)	1				
Cymatoceps (1)	1				
Dentex (8)			8		3
Diplodus (14)	3	2	8		1
Evynnis (2)				2	
*Gymnocrotaphus** (1)	1				

Lagodon (1)		1				
Lithognathus (3)	3		1		1	
Oblada (1)			1		1	
Pachymetopon (3)	2		1			
Pagrus (4)		1	2	1	4	
Pagellus (8)	1		4		3	
Petrus * (1)	1					
Polyamblyodon (2)	2					
Polysteganus (5)	5					
Porcostoma (1)	1					
*Pterogymnus** (1)	1					
Rhabdosargus (5)	5		1	1		
Sarpa (1)	1		1			
*Sparidentex** (1)	1					
Sparodon (1)	1					
Sparus (1)					1	
Spondyliosoma (2)	1		1		1	
Stenotomus (1)		1				
*Taius** (1)			1			
Viridentex (1)	1					

Table 4.1 Estimation of ancestral areas for the distribtuion of a) genera and b) type species through the application of irreversible and reversible parsimony.

A

	Irreversible parsimony				*Reversible parsimony*	
Area	*G*	*L*	*G/L*	*AA*	S^a	RP^b
A	16	9	1.7	1	9	0.67
B	4	18	0.27	0.16	7	0.86
C	11	16	0.69	0.41	10	0.6
D	5	17	0.23	0.14	6	1
E	8	19	0.42	0.25	10	0.6

B

	Irreversible parsimony				*Reversible parsimony*	
Area	*G*	*L*	*G/L*	*AA*	S^a	RP^b
A	15	12	1.25	1	14	0.43
B	5	19	0.26	0.21	6	1
C	9	17	0.53	0.43	11	0.55
D	4	18	0.22	0.18	6	1
E	5	19	0.26	0.21	6	1

Geographic areas

A = Western Indian Pacific; *B* = Western Central Atlantic; *C* = Eastern Central Atlantic; *D* = Eastern Indian Ocean & Western Central Pacific; *E* = Mediterranean & Black Sea

Irreversible

G = number of necessary gains under forward Camin-Sokal parsimony

L = number of necessary losses under reverse Camin-Sokal parsimony

AA = *G/L* quotients rescaled to a maximum value of 1 by dividing with the largest *G/L* value

Reversible

S^a = number of steps

RP^b = inversion of the S values, multipied by the smallest S value

CHAPTER 5

FOSSIL RECORD AND EVOLUTIONARY HISTORY OF THE SPARIDAE

> *"Clearly, extant taxa can offer a greater number and variety of characters than can extinct taxa. But this does not justify equating the mere amount of evidence with its relevance."*
>
> *Gauthier et al. (1988)*

Introduction

The fossil record of Sparidae provides an interesting opportunity to provide a temporal framework to construct an evolutionary scenario for the group. Previous work discussing classification of fossil sparids predates modern approaches of phylogenetic reconstruction and therefore initial descriptions and placement of genera have not been particularly rigorous. In this chapter I examine the fossil record of the better preserved sparids and investigate whether it can be used to increase our understanding of evolutionary patterns and processes. This chapter is consequently divided into two parts. Part 1 examines the fossil record of the Sparidae and provides a comprehensive morphological account of the earliest known and most complete fossil taxa from the middle Eocene, with reference to the Recent taxa described in Chapter 2. The comparative morphology of the fossils enables character states to be scored using the characters described in Chapter 2. In Part 2, I aim to assess the effects of combining both fossil and Recent data sets, to provide evidence of cladogenic rates, in addition to tracing morphological systems through time to determine the development of complex morphologies. As a result of both morphological and phylogenetic investigations, the systematic validity of some taxa is questionable and require new generic status.

Part 1 COMPARATIVE MORPHOLOGY AND THE FOSSIL RECORD

Previous work

With regards to osteological studies, fossil sparids have received more attention than their Recent counterparts. Much of the work is incorporated into the large monographs of Agassiz (1833-44) which includes all known sparids from the Eocene of Verona, Italy; fossil fishes from the Miocene of Algeria (Arambourg 1927), and fossil fish from the London Clay (Casier 1966). There is however, surprisingly little evidence from the literature supporting the placement of these taxa within Sparidae, while the placement of some taxa within Recent genera is indeed problematic.

Criteria used to identify fossil sparids

In order to investigate the fossil record of sparids, it is firstly important to ascertain whether the specimens do in fact belong to this family. The initial phylogenetic analysis in Chapter 3 (figure 3.2), found four unambiguous character state changes in support of a monophyletic Sparidae. As the data matrix 2.0 was primarily constructed using osteological characters, this information is directly relevant when defining fossil taxa. The characters represent four of the nine categories of character types delimited earlier in this work, which is useful when dealing with skeletons that are only partially preserved. However, of the four character types some will undoubtedly have a higher preservation potential than others. Considering that nearly all specimens examined, apart from *Sciaenurus*, were preserved two-dimensionally, the most useful and thus frequently observed character for defining family members is C48 (infraorbitals I & II are deeper than wide).

Overview of the fossil record

The fossil record of sparids is sparse compared to the speciose assemblage found today. This is undoubtedly due to the incompleteness of the fossil record, as articulated remains are known from only three formations: the London Clay Formation (Ypresian) of South East England; Monte Bolca Formation (Lutetian) of North East Italy and the Sahélien Formation (Messinian) of central Oman. The latter formation is separated from the former two formations by approximately 48Ma (see table 5.0). Four genera are confidently identified from the Eocene, in addition to a further five genera from the Miocene. The Eocene genera are monotypic, apart from *Sparnodus*, of which there are two species. The earliest records of sparids are from the Eocene of the London Clay and Monte Bolca deposits of Northern Italy. As the Bolca deposits are now thought to be Lutetian (Harland *et al.* 1990), they are therefore slightly younger than those of the London Clay, which are Ypresian; making *Sciaenurus* the oldest representative of the family.

The genera known from the Eocene have not been recorded in younger deposits, however, Arambourg (1927) describes eight genera of sparids from the Upper Miocene of Oman, which he

has assigned to Recent genera. The criteria by which many of these species are recognized are difficult to evaluate, and I consider that revision would be desirable. However, I was only able to examine the holotype of *Diplodus oranensis,* and did not have the opportunity to examine the other specimens first hand, but observations from photographs (Arambourg 1927; pl. 19-25) support that species of at least four of these genera; *Boops, Crenidens, Dentex* and *Pagrus* display some of the characteristics of the modern genera they have been assigned to. These features include jaw morphology and dentition, in addition to the overall shape of the braincase. There is little evidence to suggest that specimens assigned to the genus *Pagellus*(Arambourg 1927; pl. 20, fig. 19; pl. 22, figs. 2,3; pl. 25, fig. 2) are of sparid affinity, furthermore, isolated teeth assigned to *Sparus*, could equally be from *Pagrus.*

Articulated body fossils from the formations mentioned above are a fairly common component of the respective ichthyofaunas, however, I have no knowledge of articulated remains from other localities. Isolated teeth, particularly morphologies from durophagous sparids, are common vertebrate remains of some shallow marine Neogene deposits (Day 1999, Otero 1997). Information of both articulated and disarticulated remains are summarised in table 5.0.

SYSTEMATIC PALAEONTOLOGY

Division TELEOSTEI sensu Nelson, 1969
Order PERCIFORMES Bleeker, 1859
Suborder PERCOIDEI Bleeker, 1859
Superfamily SPAROIDEA Johnson, 1980
Family SPARIDAE Bonaparte, 1852

The Bolca sparids

Background

Monte Bolca fishes represent the earliest defined coral reef fish assemblage (Blot 1980; Sorbini 1983; Bellwood 1996). The diversity of fishes found in this assemblage contains representatives of almost all Recent coral reef and reef-associated families. Furthermore, for most families the diversity of species is matched by numerical abundance. While the dominance of perciform fishes in the Bolca assemblage is consistent with modern reef environments, a link to the Mesozoic era persists with one of the latest records of the extinct order Pycnodontiformes. However, it would appear that by the early Tertiary the final transition from non-perciform to perciform-dominated faunas has taken place (Bellwood 1996). For these reasons the Bolca assemblage provides an unique insight into the evolution of coral reef and reef-associated fishes.

Geology of the Bolca deposits

The Monte Bolca deposits are marine limestones, the age of which is generally treated as topmost Ypresian (e.g. Blot 1980), following the discovery of nannoplankton, placing the beds in the zone of *Discoaster sublodoensis* (NP 14), which covers a time period of between 49.5 - 47.2 Ma (Neal 1996). However, more recently Harland *et al.* (1990) place NP 14 as lowermost Lutetian, which is accepted by Patterson (1993). The Bolca deposits are thought to have been located in what was the centre of the Tethys sea (Bellwood 1996). Tethys was largely a continuous marine region connecting the Atlantic to the Indian Ocean until the final closure in the Miocene, and would have certainly contained cosmopolitan biotas (Rosen and Smith 1988).

Preservation

The site at Bolca is regarded as a fossil-Lagerstätte, due to the abundance, diversity and exceptional preservation of the primarily perciform-dominated benthic fish assemblage (Bellwood 1996). However, while even pigmentation may be preserved in some specimens, a common feature of the Bolca material is that much of the anatomy of the braincase remains relatively unknown (C. Sorbini, J.Tyler; pers. comm. 1998). The paucity of well documented braincases is because they are largely flattened during their preservation, but may also be attributed to the method of collection Most fossils are extracted by splitting the encasing rock. Thus, while the overall skeleton remains relatively intact, complex 3-dimensional structures such as the braincase are destroyed. However, BMNH 44867 used in this study has been set in resin and subsequently acid prepared, after the method described by Tooms and Rixon (1959) and while not complete, yields far more information than specimens which have not been prepared in this way.

Genus *SPARNODUS* Agassiz 1839

The extinct genus *Sparnodus* is known from two species; *Sparnodus microstomus* (Agassiz) and *Sparnodus vulgaris* (de Blainville) of which the latter is by far the most numerous. As a consequence of this, there is a greater possibility for a more informative assessment of the anatomy of S*parnodus vulgaris*. From the specimens I was able to examine I consider the affinity of *S. microstomus* to be somewhat problematic, an assumption that is based on the distinct differences in jaw morphology between these two taxa. The morphology of the upper jaws in particular differ more than would be expected for species-level diagnosis. Recent species are defined using external features such as fin ray counts or colour (see Chapter 1). However, apart from overall shape, morphological variation is discrete and does not provide adequate differences for species-level relationships to be resolved using phylogenetic analysis. I am therefore cautious to reassign *S. microstomus* to a new genus on the basis of observations from a few incompletely preserved specimens.

A third species originally recognized as *Sparnodus elongatus* is here synonomised with *Sparnodus vulgaris*. This name was originally intended for a third species found at the Bolca, however, it has now been placed in a new genus.

Diagnosis: Due to the uncertain affinity of ?*Sparnodus microstomus*, the diagnosis is the same as for the type species (see below).

Type species: *Sparnodus vulgaris* Agassiz, 1839

SPARNODUS VULGARIS de Blainville, 1818

(plates 5.0 - 5.3)

1796 *Sparus macrophthalmus* Volta: 247, pl. 60.

1796 *Cyprinus* Volta: *ibid.* pl. 73.

1796 *Sparus dentex* Volta: *ibid.* 62, pl. 13, fig. 1.

1796 *Sparus sargus* Volta: *ibid.* 76, pl 17, fig. 1.

1796 *Sparus erythrinus* Volta: *ibid.* 249, pl. 60, fig. 3.

1818 *Sparus vulgaris* de Blainville: vol. 27, 349.

1835 *Sparnodus macrophthamus* Agassiz: 300 (name only).

1835 *Sparnodus ovalis* Agassiz: *ibid.* 300 (name only).

1835 *Sparnodus altivelis* Agassiz: *ibid.* 300 (name only).

1835 *Sparnodus micracanthus* Agassiz: *ibid.* 164, pl. 28, fig. 2.

1836 *Sparnodus elongatus* Agassiz: *ibid.* 165, pl. 28, fig. 1

1839 *Serranus ventralis* Agassiz: vol. iv. 104, pl. 23b

1839 *Sparnodus macrophthamus* Agassiz: vol. 4, 158, pl. 28, fig. 3.

1839 *Sparnodus ovalis* Agassiz: *ibid.* 161, pl. 29, fig. 2.

1839 *Sparnodus altivelis* Agassiz: *ibid.* 162, pl. 29, fig. 3.

1839 *Sparnodus micracanthus* Agassiz: *ibid.* 164, pl. 28, fig. 2.

1886 *Sparnodus lethriniformis* Szajnocha: vol. 12, 106, pl. 1, fig. 1.

1876 *Sparnodus ovalis* Bassani: vol. 3, 177.

1876 *Sparnodus micracanthus* Bassani: *ibid.* 177.

1901 *Sparnodus macrophthamus* Woodward: vol. 4, 525.

1911 *Sparnodus vulgaris* (Blainville); Eastman: vol. 4 no.7 part 1, 377. fig. 2

1980 *Sparnodus vulgaris* Blot:

1983 *Sparnodus vulgaris* Sorbini: pl. 12, 13, 19, 48.

Holotype: MNHN 10796/10797 (part and counterpart), skeleton is preserved in limestone matrix.

Age: Lutetian , Lower Middle Eocene.

Type locality: Monte Bolca, Verona, Italy.

Diagnosis: A sparid fish, distinguished from other fossil taxa by a robust jaw morphology, containing large, conical teeth. The dorsal margin of the ethmoid is depressed directly anterior to the ethmoid-frontal suture, and is presumably the fossa for the ascending process of the premaxilla. Relatively deep-bodied form with a length to width ratio of 3:1. The supraneural formula appears to be 0/0+0/2+1/1, and the anterodorsal processes of the supraneurals overlap. The hypurals 1-2 and 3-4 are separate and the caudal fin is of low aspect ratio. Formula of the dorsal fin XII/9, anal fin III/9.

Additional material examined: MNHN 10804/10803, 10805, 10789/10790; BMNH 44867; Bol. I.G 24547, II P.136.

DESCRIPTION

CRANIUM

The Braincase

The braincase is triangular in lateral view (Figure 5.3), the most prominent feature being the large occipital crest, which covers over half of the total length of the braincase. The ethmoid region or snout forms approximately a third of the total length of the braincase. The vomer is edentulous and has a posterior shaft that terminates level to the anterior margin of the frontals. The vomer and ethmoid form a dorsal medial crest, while the posterior surface of the ethmoid contains a shallow fossa for the ascending process of the premaxilla (Figures 5.1 and 5.2; *f.as.p.pm*). The lateral ethmoids are expanded posteriorly forming a preorbital flange, the dorsal margin of which contains a large triangular-shaped fossa, as in all sparoids. A laterally inclined facet of the lateral ethmoids provides the articulation surface for the maxillary process of the palatine.

The ventral margin of the parasphenoid is concave, and forms a narrow carina. On the otico-occipital region of the parasphenoid a process for the m. adductor arcus palatini is present ventrally, which in BMNH 44867 is stalk-like (see Plate 5.2b; *ap*), whilst in Bol. P143 the process is smaller, resembling the process described for *Dentex dentex* (see Chapter 2). Directly posterior to the process m.adductor arcus palatini, a weakly developed pharyngeal apophysis is observed in Bol. P265. The parasphenoid in this region is dorsally inclined at 20° (measured from BMNH 44867).

The frontals are protuberant anteriorly, and are inclined anterodorsally at 30°. They form the anterior third of the frontal crest, in addition to the lateral and medial walls and floor of the post-temporal fossa. A number of pores perforate the dorsolateral surface of the frontals which are opening for branches of the laterosensory canal. Anteriorly, there appears to be a shallow sulcus on BMNH 44867. This structure is probably connected to one of the pores of the laterosensory

canal, as observed on an extant neurocranium of *Lithognathus mormyrus* BMNH 1855.9.19.

The supraoccipital separates the parietals throughout their length. It forms a large dorsal occipital crest, the length of which is greater than the height. The anterior margin of the crest is level with the anterior third of the orbit, and therefore covers well over half of the total length of the braincase. A dorsally convex ridge occurs posteriorly, which presumably helps to strengthen such a large area of relatively unsupported bone. The spina occipitalis extends ventrally between the epioccipital and exoccipitals to the dorsal margin of the foramen magnum.

The epioccipital forms the posterodorsal region of the skull as usual. In Bol P143 a lateral projection is partially visible and may be interpreted as the fossa for the articulation of the dorsal process of the post-temporal (Figure 2.0; *fptd*), but provides no further information as the posterior margin of this bone is unclear. The epioccipital forms the posterior part of the medial wall of the post-temporal fossa, in addition to forming the posterior third of the frontal crest.

The parietal is a small bone that forms the central third of the frontal crest and lateral wall of the post-temporal fossa.

The pterotic forms the posterior part of the floor and medial wall of the post-temporal fossa, the posterior third of the pterotic crest and posterior parts of the dilatator fossa and hyomandibular facets. The post-temporal fossa is a large deep conical feature, extending a third of the total length of the skull and is completely unroofed. The laterosensory canal enters the pterotic through a large pore at the posterior extremity of the crest and subsequently punctuates the crest along its length with smaller pores. The posterior margin of the pterotic crest forms a depression for the ventral process of the post-temporal.

The sphenotic forms the posterolateral wall of the orbit, the anterior hyomandibular facet, the anterior part of the dilatator fossa and the central third of the medial wall of the post-temporal fossa. The dilatator fossa is a large triangular cavity, covering both the sphenotic and the pterotic, extending anteriorly over the posterior third of the orbit and would appear to penetrate the frontals. In Bol. P143 it appears that the dilatator fossa pierces the anterior wall of the sphenotic, as in some of the Recent taxa, although this is not clear on other specimens.

The pars jugularis of the trigemino-facialis chamber is only partially preserved, as such the lateral commissure, which in Recent sparoid fish, contains a third opening is missing.

There are two hyomandibular facets, positioned directly below the dilatator fossa. The facets both appear to be of a similar size, however, they are interpreted from the internal moulds of the original facets and therefore the actual dimensions may not be entirely accurate.

Other features preserved as internal moulds include a circular fossa in the basioccipital, which is the attachment site for Baudelot's ligament and a single foramen in the exoccipital. This foramen may have contained both the n. vagi (X) and n. glossopharngei (IX), however, I would hesitate to suggest this, as the bone anterior to this foramen is poorly preserved and therefore it may be likely that a separate foramen for the n. glossopharngei existed.

Unfortunately it is hard to distinguish many sutures on the braincase, the most obvious ones

are those in the post-temporal fossa, while those of the occiput are obscured due to preservation.

The infraorbital region

The infraorbital series comprises six bones, which are seen most clearly in Bol. P143. Infraorbitals I and II are much larger than the succeeding bones, the second of these is preserved entirely, and is deeper than wide. From the position of this bone in relation to the jaws it can be seen that, in life, the ventral margin would have covered the maxilla. On the medial margin of the third bone a well developed subobercular shelf extends posteromedially. The remaining infraorbitals are rod-like and appear to decrease in length from front to rear.

Jaws

The premaxilla is characterized by having an alveolar process which is longer than the ascending process. In Bol. P143 the alveolar process is thin and tapering, the dorsal margin is convex, however, no prominent maxillary process is present. The articulation between the premaxilla and the maxilla (Figure 5.2b) appears to be the specialized articulation that is found to be a synapomorphy of Recent sparids (see Chapter 3; *description of characters*). The coalescence of the articular process with the ascending process is a feature observed in the Sparidae, as well as the sparoid family Lethrinidae.

The maxilla has a straight dorsal margin with a low anterodorsal crest, represented as a knob-like process. This configuration describes a primitive percomorph maxilla (Rosen and Patterson 1990). In addition, the palatine sulcus is short and does not extend as far as the anterior margin of the ascending process of the premaxilla. A small process is present on the anterolateral margin of the sulcus. The maxilla has a ventroposterior expansion extending well behind the premaxilla.

The dentary is reasonably short, as the symphysal process extends to approximately a quarter of the total length of the ventral margin. On the lateroventral surface the mandibular canal of the laterosensory system is represent by a single a row of pores. The coronoid process is narrow and is inclined at a low angle and the lateral margin of the articular fossa is concave.

The articular is only partially preserved, however, the facet for the quadrate is entirely formed by the articular, while the angular forms the posteroventral corner of the articular. The descending process is level with the ventral margin of the dentary.

Dentition

The jaws contain a single row of conical teeth, as the morphology is too blunt for them to be considered as caniniform when compared to those found in *Dentex*. In the premaxilla the two anterior-most teeth are larger than the rest of the jaw, while in the dentary there is a gradual decrease in size posteriorly.

The hyo-palatine bones

The palatine bones are well preserved in Bol. P136 and BMNH 44867. The hyomandibular is double-headed, and when articulated with the skull would lie at shallow angle inclined anteriorly. There is the usual ridge on the lateral face of the hyomandibular against which the preopercle lies. The opercle is a large triangular sheet of bone that becomes thicker towards the anterior margin.

The symplectic lies in a sulcus on the medial face of the quadrate, while beyond the dorsal margin of the quadrate it becomes expanded (Plate 5.2b).

The quadrate is triangular, with a large double condyle which articulates with the articular. The ventral margin of the quadrate overlaps the anterior limb of the preopercle. This margin is much longer than the dorsal, extending posterodorsally beyond the convex posterior margin.

The ectopterygoid is bent through 50° and is sutured to the anterior edge of the quadrate. The bone tapers ventrally, however, the ventral margin does not extend as far as the condyle. The posterior margin of the dorsal part of the bone lies against the endopterygoid, while the anteriorly it is sutured to the palatine.

The metapterygoid is a large triangular sheet, the anterior margin of which lies against the endopterygoid, whilst a fontanelle separates part of the anterior margin of the metapterygoid and endopterygoid from posterior margin of the quadrate, as observed in Recent taxa. The posterior margin would lie against the hyomandibular, although this is not preserved.

The endopterygoid is a small triangular sheet, the anterior margin lies against the ectopterygoid, while the posterior margin meets the metapterygoid.

The palatine is large and robust. The maxillary process of the palatine is long, extending beyond the end of the vomer, and is deflected medially. This process articulates with a facet on the lateral ethmoids. A short process extending posteriorly from this facet (Figure 5.2b) is the same as that described for *Dentex* (Figure 2.5). The anterior margin of the palatine is convex, while the posteroventral margin is sutured to the ectopterygoid.

Opercular bones

The preopercle is bent through about 40°. The ventral limb is shorter than the dorsal limb and lies medial to the posteroventral margin of the quadrate. The dorsal limb is narrower and lies against a ridge on the lateral face of the hyomandibular. Fine ridges occur perpendicular to the posterior margin of the angle. The opercle is large and thick and articulates via a condyle on the anterodorsal margin with the hyomandibular. The interopercle lies medial to the preopercle, while the subopercle is overlain by the opercle dorsally and by the interopercle anteriorly.

Lower part of the hyoid arch

In no specimens examined so far are the branchial arches preserved well enough for them to be reconstructed. However, crushed remains of the hyoid arch and branchiostegals are

preserved in most specimens, although there is little useful information to recover.

The hyoid arch preserved in Bol. P143 is short, the anterior part of the ceratohyal and hypohyals (although the latter bones are not clearly preserved) are expanded. There are six acinaciform branchiostegal rays. The first four are large and attach to the ceratohyal, while the two posterior rays are distinctly smaller. The placement of the fifth ray is unclear, as it either attaches to the interspace between the ceratohyal and the epihyal or to the epihyal. The posterior most ray attaches directly to the epihyal. The basihyal is also preserved in this specimen and is narrow and toothless.

POST-CRANIAL SKELETON

Vertebral column

There are 10 + 14 vertebrae, including the urostyle, which agrees with the observations of Agassiz (1835: 155). The centra of the first two vertebrae are compressed and have lower neural spines than the other vertebrae. Due to the preservation it is impossible to tell which vertebrae the intermusculatures attach to.

Pectoral girdle and fin

The pectoral girdle is only partially preserved. However, little structural variation is detected compared with the morphology of Recent sparids, with only minor variability in the shape of the bones, which in sparoids, is at least as great within each group as among them (Johnson 1980). The posttemporal has a long dorsal process which articulates with the posterior fossa of the epioccipital, while the shorter ventral process articulates with the pterotic.

The supracleithrum is the usual elongate oval with a thickened anterior margin, lying lateral to the cleithrum. The cleithrum is inclined anteriorly at about 80°, the ventral part is especially long and would appear to be double the length of the dorsal part. The anterior process of the corocoid is slender and attaches to the cleithrum.

The posterior margin of the scapula and corocoid are preserved, therefore allowing the positions of the radials to deduced. There are four pectoral radials, the three uppermost articulating with the scapula, while the lowermost radial articulates against the interspace between the scapula and corocoid. In addition, the long, slender ventral postcleithrum is present in this specimen. The pectoral fin contains 14 rays.

The pelvic girdle and fin

The posterior margin of the pelvic girdle lies on a vertical level with the second vertebrae, the angle at which the girdle intersects the pectoral girdle is 65°. The fin is large, extending to a point level with the last abdominal vertebrae.

Dorsal and anal fins

The dorsal fin contains X, 9 rays. Two supernumery spines are supported by the first radial. There are three supraneurals, the formula of which appears to be 0/0+0/2+1/1. The anterodorsal process of the supraneurals overlie the preceding supraneurals, but the process of the first supraneural does not overhang the occipital crest.

The anal fin comprises the usual 3 fin spines, as with the dorsal fin there are two supernumeraries associated with the first radial. The first radial is considerably larger than the others, extending to the haemal arch of the last abdominal. It is also buttressed anteriorly, presumably a result of being associated with two fin spines.

Caudal skeleton and fin

The caudal skeleton is complete, and differs very little from that described for *Dentex* (Chapter 2) to which the I refer the reader. It is worth noting that the hypurals are separate and the hypurapophysis extends to the medial margin of hypural 2. The caudal fin contains 9:8 principal rays. The fin is large and has a shallow forked outline. There appear to be six to seven? procurrent rays above and below the respective principal rays.

?*SPARNODUS MICROSTOMUS* (Agassiz,) 1835

(Plate 5.4)

1796 *Sparus brama* Volta: clxxxvii, pl xlv, fig. 3 (error, a Recent species)

1818 *Sparus brana=Sparus vulgaris* Blainville: vol. 27, 350

1835 *Serranus microstomus* Agassiz: 300 (name only)

1835 *Serranus occipitalis* Agassiz: *ibid.* 102, pl. 23

1835 *Dentex breviceps* Agassiz: *ibid.* 300 (name only)

1839 *Serranus microstomus* Agassiz: vol. 4, 100, pl. 23a

1839 *Dentex breviceps* Agassiz: ibid. 149, pl. 27, figs. 3, 4

1901 *Sparnodus microstomus* Woodward: 527

Holotype: MNHN 10729/10730, (part and counterpart), entire skeleton partially preserved in limestone matrix.

Age: Lutetian , Lower Middle Eocene.

Type locality and horizon: Monte Bolca, Verona, Italy.

Diagnosis: A sparid fish, that is deep bodied, with a standard length to depth ratio of 2:1 giving it an overall oval shape. The frontals are inclined at 50° from the horizontal. Description of the jaws are based on specimen Bol. T.886 which include the following observations: A low sub-terminal maxillary crest is present. The ascending process of the premaxilla is more than half of the length

of the alveolar. Articular process is fused to the ascending process of the premaxilla. Dentition consists of small caniniform teeth along the occlusal margin of the jaw, while anterolaterally larger recurved caniniform teeth are present. Formula of the dorsal fin XII/9, anal fin III/9.
Additional material examined: Bol. T.886.

Validity of Sparnodus elongatus

On the basis of the holotype MHN 10803/10804 (Plate 5.5) the morphology of *Sparnodus elongatus* is not dissimilar enough to that described for *Sparnodus vulgaris* to warrant a separate species as named by Agassiz (1839). Morphological features of the braincase, oral jaws and preopercle, in addition to fin ray counts provide no validity for the distinction of *S. elongatus*. However, some specimens labelled as *S. elongatus* are very clearly different from either *S. vulgaris* or *S. elongatus* and are here assigned to a new genus *Ellaserrata.*

Genus *ELLASERRATUS* gen. nov.

Diagnosis: As for the type and only known species.
Etymology: From *Ella* (Latin) for small, while the suffix *-serratus* (Latin) means serrated. Named as such due to the small serrations along the posterior margin of the preopercle, which are unique to this genus.

Type species: *Ellaserrata monksi*

ELLASERRATA MONKSI, gen. et sp. nov.
(Plate 5.6)

Etymology: After the palaeontologist Dr Neale Monks.

1796 *Perca radula* Volta: 134, pl. 31, fig. 1
1796 *Sparus chromis* Volta: *ibid.* 138, pl. 32, fig. 1
1796 *Sparus salpa* Volta: *ibid.* 130, pl 56, fig. 1
1911 *Sparnodus elongatus* Eastman: vol. 4, no. 7, 378, pl. 91, fig. 3 and pl. 98

Holotype: BMNH P1938/3900 (part and counterpart), skeleton is preserved in limestone matrix.
Age: Lutetian , Lower Middle Eocene.
Type locality and horizon: Monte Bolca, Verona, Italy.
Diagnosis: A sparid fish, distinguished by a serrated preopercle. Elongate body with a length:

depth ratio of approximately 4:1 in adult specimens. Widely spaced supraneurals. Ethmoid-vomerine dorsal crest present. Dorsal maxillary crest is sub-terminal. Dentition consists of caniniform teeth, which are fang-like anteriorly. Hypurals 1-2 and 3-4 appear fused. Formula for the dorsal and anal fins are: X/10 and III/9.

Additional material examined: BMNH P6855, P3901, P1900.

DESCRIPTION

CRANIUM

Braincase

The ethmoid-vomerine region of the braincase appears to be fairly elongate, forming a third of the total length of the braincase, while the posterior margin of the vomer is level with the anterior margin of the frontals. The dorsal margin of the ethmoid-vomerine forms a prominent crest, as described for the Recent genus *Dentex*, and there appears to be no obvious fossa for the ascending process of the premaxilla as observed in *S. vulgaris*. A triangular fossa is present along the dorsal margin of the preorbital flange as found in all members of the Sparoidea.

The frontals are inclined at an angle of 22°, which is approximately 10° lower than those recorded for *S. vulgaris*. They also appear to be smooth. While the occipital crest is greater in length than height it is, however, smaller overall than that of *S. vulgaris* as it only extends forward to the posterior margin of the orbit. The dilatator fossa extends anteriorly to a point level with the anterior margin of the occipital crest.

The parasphenoid deepens posteriorly for the attachment of the m. adductor palatini, while the process for the m. adductor palatini and pharyngeal apophysis of the basicranium are weakly developed. The ventral margin of the parasphenoid carina is concave. The otico-occipital region of the parasphenoid is only slightly inclined from the horizontal, thus the occipital condyles are orientated posteroventrally. The posteroventral part of the braincase is well preserved in BMNH P6855, a large foramen for the vagus nerve is present piercing the exoccipital, although it is difficult to see whether a separate foramen exists for the glossopharngeal nerve. Additionally, the foramen n. spino-occipitalis is present in the lateral margin of the occipital condyle, and a large fossa for the attachment of Baudelot's ligament is present as usual on the ventrolateral face of the basioccipital.

Infraorbitals

While the infraorbitals are only partially preserved, importantly infraorbitals I and II are present (Plate 5.6c) The first two infraorbitals are both large, with vertical ribbing, the ventral margin extending to the maxilla. The two bones are deeper than wide.

Jaws

Upper jaw

The jaws are less robust than in *S. vulgaris*. The ascending process of the premaxilla is just over half the length of the alveolar process. The premaxilla has a dorsal maxillary crest which is sub-terminal, although the crest is not well developed as in some genera of Recent sparids. The maxilla is, however straight, with a knob-like dorsal crest. Posteriorly, the maxilla is expanded. The articular process of the premaxilla does appear to be separate from the ascending process.

Mandible

The dentary is long, with a short symphysal process. The ventral process of the symphysis is however prominent. The lateral margin of the articular fossa is v-shaped, and deep; the articular and the angular forming a third of the total length of the mandible. The descending process of the articular does not extend further than the ventral margin of the dentary, the angular forming the posteroventral corner of the mandible.

Dentition

A single row of caniniform teeth are present along the occlusal surface of the jaws, in addition to larger recurved caniniform teeth situated anterolaterally. Villiform teeth are also present along the medial margins of the jaws.

The hyo-palatine bones

The palatine arch is not particularly well preserved, and therefore provides little information. It is worth noting that the ventral margin of the quadrate forms a confluent ridge with the preopercle as usual, but the ridge is not as prominent as in some genera, flattening posteriorly.

Opercular series

The opercular series is similar to that described for *Dentex*, however, small serrations occur along the posteroventral margin of the preopercle, which are visible to the naked eye (Plate 5.6c). The preopercle is bent through 60°.

Lower part of the hyoid arch

This structure is not preserved, apart from the branchiostegal rays, which number six, and as usual are acinaciform in shape.

POST-CRANIAL SKELETON

Pectoral and pelvic girdle and fins

Only partially preserved in specimens examined, however, there is nothing unusual about the morphology which is preserved.

Vertebral column

There are 10 + 14 vertebrae (including the urostyle).

Dorsal and anal fins

There are three supraneurals, which are widely spaced so that the anterior processes do not overlap. This construction is similar to the Recent genus *Boops* for example. The neural spines of the first vertebrae are not preserved well enough to deduce a formula. The fin spines for both fins are poorly preserved, as such it is hard to be accurate about a formula. However, it would appear that there are X/10 in the dorsal fin, and III/9 for the anal fin. The first radial of the anal fin is buttressed anteriorly, but is not as robust as that of *S. vulgaris*.

Caudal fin

Morphological features worth mentioning include the apparent fusion of hypural Plates 1-2, and 3-4 and the moderately high aspect ratio of the fin. The number of principal rays seems to be consistent with that of the family with a formula of 9:8.

Genus *ABROMASTA*, gen. nov.

Diagnosis: As for the type and only known species.
Etymology: From *Abro* (Greek) for delicate, while the suffix *-masta* (Greek) means mouth or jaws.

Type species: *Pagellus microdon* Agassiz, 1835

ABROMASTA MICRODON (AGASSIZ, 1835)
(Plate 5.7)

1835 *Pagellus microdon* Agassiz: 300 (name only).
1839 *Pagellus microdon* Agassiz: vol. 4, 152, pl. 27, fig. 1.

Holotype: MNHN 10784/10785 (part and counterpart), skeleton is preserved in limestone matrix.
Age : Lutetian , Lower Middle Eocene.
Type locality and horizon: Monte Bolca, Verona, Italy.
Diagnosis: A sparid fish, distinguished by the strongly convex shape of the anterodorsal margin of the frontals, short ethmoid-vomerine region and delicate upper jaw. The frontals are also cancellose in texture, and the occipital crest is equal in height and length. The dorsal crest of the maxilla is knob-like. The dentition consists of villiform teeth which cover the occlusal surface of

the premaxilla and dentary. The hypurals are fused and the tail is of high aspect ratio.
Additional material examined: Bol. II 0.121, II 0.123, II 0.124, II 0.125, II 0.126, II 0.127, II 0.128, T83, T84; BMNH P62113

DESCRIPTION

CRANIUM

Braincase

The braincase is only partially known. However, some useful characters are present. The ethmoid-vomerine region is greatly reduced and the posterior margin of the vomer is level with the anterior margin of the frontals and orbit. A depression is present along the posterior margin of the ethmoid which houses the ascending process of the premaxilla. The posterior wall of the fossa for the ascending process of the premaxilla is steeply concave. A triangular fossa is present on the preorbital flange of the lateral ethmoids. The dorsal margin of the frontals prior to the anterior margin of the occipital crest are strongly convex. This region of the frontals are also strongly textured with a cancellose structure, in addition to the anterior base of the occipital crest.

The occipital crest is as usual a prominent feature of the neurocranium. The crest is approximately the same height as the length, thus giving the braincase a depth which is nearly equal to the total length. A near vertical occipital ridge is present posteriorly. The outline of the body above the crest and supraneurals is further enlarged, presumably in life as a fleshy protuberance which is particularly apparent from MHN 10784 (Plate 5.7). The ventral margin of the otico-occipital part of the braincase is steeply inclined at about 40°. The parasphenoid is narrow anteriorly, widening posteriorly as a site of attachment for the m. adductor palatini. A process for this muscle does appear to be present as the parasphenoid extends slightly ventrally below the posterior margin of the orbit, however, the otico-occipital part of the braincase is covered in most specimens by the palatine arch.

Nasals

The nasals are broken or disarticulated in most specimens, however, in BMNH P62113 the posterior part is preserved as the usual tubular bone. If the length of the nasal is extrapolated to the anterior margin of the vomer then the total length would have been short.

Jaws

The jaw is considerably less robust than for the other Eocene sparids described here. The bones of the upper jaw in particular are slender and not substantially thickened as in *Sparnodus vulgaris* for example. As a result of this the upper and lower jaw are disarticulated and only partially preserved in all specimens examined.

Upper jaw

The ascending process of the premaxilla is shorter than the alveolar process, The alveolar process is very slender, tapering posteroventrally. The articular process appears to be fused to the ascending process, although this is hard to see clearly.

The maxilla is also slender, and can be described from the medial view preserved in BMNH P62113. A dorsal crest is present anteriorly, while the palatine sulcus appears to extend quite far anteriorly and may possibly extend as far as the anterior margin of the premaxilla, although this is needs to be checked in additional specimens. The posterior ramus of the maxilla is bent through approximately 40° and is posteriorly enlarged.

Mandible

The mandible is elongate. It is deep posteriorly, tapering significantly anteriorly to a narrow symphysis. The articular fossa is also deep, with a v-shaped lateral margin that extends half way into the dentary. The descending process of the articular appears to extend below the ventral margin of the dentary, however, the angular forms the posteroventral corner of the mandible.

Dentition

The dentition is formed from villiform teeth, which are barely visible without the aid of a microscope.

Palatine arch

The palatine arch is deep rather than broad. The ventral process of the palatine and the ectopterygoid form a long, slender structure, extending diagonally from the anterior margin of the arch. The maxillary process of the palatine is short and straight, as observed in the Recent genus *Diplodus* for example.

The ventral margin of the quadrate extends over the ventral limb of the preopercle, and forms a confluent ridge, which flattens posteriorly.

The metapterygoid is the usual large concave bone, however, the rest of the palatine arch is only partially preserved and provides little other useful information.

Opercular bones

The preopercle is bent through about 70°, the length of the ventral limb is less than one third of the total length of the dorsal limb. It is difficult to see whether there are tiny serrations along the posteroventral margin, nevertheless the margin is not serrated to the degree observed in *Ellaserrata monksi.*

The width of the opercle is just over half that of the total length. The posterior margin is symmetrically concave.

Lower part of the hyoid arch

The only part of the arch which is preserved are the branchiostegal rays which total six. The

rays are acinaciform.

POST-CRANIAL SKELETON

Pectoral and pelvic girdle and fins

The girdles and fins are only partially preserved, however, they do not appear to differ notably from those of the genus *Dentex.*

Vertebral column

The total number of vertebrae is 10 + 14 including the urostyle. The first two vertebrae are compressed, with significantly shorter neural spines.

Dorsal and anal fins

The supraneural formula is 0/0/0+2/1+1; was observed in more than one specimen and therefore I can be certain of its validity. The fin comprises XII, 11 and the membrane is continuous.

The anal fin comprises of III, 9 fin rays. The radial of the first anal fin is buttressed anteriorly, the radial extending to a point level with the distal tip of the last haemal arch.

Caudal fin

The posterior fin skeleton is similar to that described for *Dentex*, except that the hypural plates 1-2 and 3-4 appear to be fused. The gap between hypurals 2 and 3 is deep extending to the urostyle. The principal caudal ray count is 9:8. The caudal fin is deeply forked and hence has quite a high aspect ratio.

Genus *SCIAENURUS* Agassiz, 1845

Diagnosis: As for the type and only known species

Type species: *Sciaenurus bowerbanki* Agassiz, 1845

SCIAENURUS BOWERBANKI Agassiz, 1845

(Plates 5.8 - 5.12)

1845 *Sciaenurus bowerbanki* Agassiz: 295-301, pl. 40.

1845 *Sciaenurus crassior* Agassiz: 307 (name only).

1854 ?*Sciaenurus brevior* Owen: 171.

1901 *Sparnodus bowerbanki* (Agassiz) Woodward: 527.

1966 *Scianurus bowerbanki* (Agassiz) Casier: 198-211. pl. 26, 27.

Holotype: BMNH P3975, dorsal surface of braincase, palatine arch, left maxilla, lower part of the hyoid arch partially preserved, opercular series, pelvic girdle, partially preserved pectoral girdle, initial vertebrae and ribs.

Age: Lower Eocene, Ypresian

Locality and horizon: London Clay, London Basin Sheppey (Kent), UK.

Diagnosis: A sparid fish, distinguished by a steeply inclined ethmoid-vomerine region and posterior ethmoid platform. Lever arm of maxilla is straight and elongate, with knob-like dorsal crest. Dorsal margin of the alveolar process of the premaxilla is also straight. The dentition consists of a single row of caniniform teeth along the occlusal margin, while a tooth field of villiform teeth occurs medially. The infraorbitals are heavily ornamented.

Additional material examined: BMNH P39441, P44314, P44324, P44499, P39442, P25707, P44506, P34824, P44501, P26820, P44503.

Geology of the London Clay

The Isle of Sheppey (Kent) is famous for the exceptional preservation of vertebrate remains, including: fish, reptiles, birds, land mammals as well as yielding extensive macrofloras.

The London Clay was deposited during the Early Eocene, Ypresian (King 1981) at a time of high sea-level stand (Huggett and Gale 1998). During this time SE England was covered by a shallow shelf sea, the shores of the London Clay sea supported a flora of subtropical aspect (Collinson 1983), while seawater temperatures obtained from $\partial\ ^{18}O$ analysis of mollusc carbonate are in the high 20°s (Buchardt 1978).

The exact placement of the vertebrate material from Sheppey is uncertain, as much of the material has not been collected insitu. However, some specimens have been collected from nodule layers 5-10m above the base of the exposed section in Division D, P6 B (King 1981: 52, fig. 15) and it is reasonable to suppose that most museum specimens are from similar horizons. Division D comprises a dominantly homogenous clay/silt lithology, with silt and sand partings at some levels in addition to beds of sandy silt (King 1981).

DESCRIPTION

CRANIUM

The Braincase

The snout, orbital region and anterior cavity all form approximately a third of the total length of the braincase (Plate 5.10b and c). These dimensions are similar to the braincases found in basal sparid genera (see Figure 2.0).

The ethmoid-vomerine region forms a steep mid-dorsal crest, inclined at about 60° with respect to the parasphenoid. Posteriorly, the ethmoid crest reverts to a shallower angle of 30°, forming a platform, the dorsal surface of which is slightly concave. Apart from this structure,

there is no obvious fossa present as found in a number of Recent sparid genera, which the ascending process of the premaxilla may slide in and out of. However, the steepness of the crest suggests that an adequate cavity is present to house the ascending process of the premaxilla. There also appears to be an anterodorsal facet on the crest of the vomer, a result of the articulation of the articular process of the premaxilla, when the jaws open.

The vomer is edentulous, the ventral surface is inclined at a shallow angle posteriorly. The posteroventral margin of the vomer is level with the posterior margin of the lateral ethmoids and the anterior margin of the frontals, indicating that the snout region in this fish is short.

The ethmoid is the usual long, narrow bone, separating the lateral ethmoids. The lateral ethmoids form a preorbital flange posteriorly, which extend laterally to a point that is greater than the width of the braincase at the contact of the dorsal limb of the posttemporal, but less than the width of the braincase at the contact of the ventral limb of the posttemporal. A triangular fossa occupies the dorsal surface of the preorbital flange. The orbitonasal canal exits just anterior to the preorbital flange, as a anteriorly orientated foramen. The canal becomes expanded posteriorly to form the anterior myodome.

The frontals are inclined at about 20° and are separated anteromedially, forming a concave margin, similar to that found in *Diplodus* sp. (pers. obs.). The frontal sagittal crest and occipital crest meet anteromedially forming a ridge of bone. Furthermore, the dorsal surface of the frontals prior to the occipital crest are finely textured, which is particularly apparent in BMNH P39441 and P443324, while posteriorly they are smooth. Supraorbital pores of the laterosensory system are also present anterior to the occipital crest. Posteriorly, the frontals form the anterior floor and walls of the posttemporal fossa.

Occipital region

The supraoccipital forms the usual large medial occipital crest, which is greater in length than height. The crest is broken in all specimens examined apart from BMNH P39441, where it is still embedded in matrix. Nevertheless, it is possible to deduce that the crest extends anteriorly, so that the anterior margin is level to a point that is a third of the width of the orbit, while posteriorly the crest overhangs the margin of the foramen magnum. The spina occipitalis extends ventrally, between the epioccipital and exoccipitals.

The posttemporal fossae are large open conical cavities, extending anteriorly to a point level with the anterior insertion of the occipital crest and cover much of the otico-occipital part of the skull roof.

The parietals form the central third of the frontal crest and part of the medial wall and floor of the posttemporal fossa.

The exoccipitals form much of the occipital area of the cranium. Dorsal to the foramen magnum the exoccipitals are separated medially by the spina occipitalis. The dorsal margin of the foramen magnum is strongly emarginated, so that the height is greater than the length, which differs from Recent sparids as the dimensions of the foramen magnum are more or less equal. The

exoccipital condyles are orientated posteroventrally, and are weakly separated from each other medially. On the lateral surface of the condyles, just ventral to the suture between the epioccipital and the exoccipital is the spinal occipital foramen. The vagus foramen lies anterodorsal to the occipital condyle. The opening for the vagus foramen is large in comparison to the glossopharyngeal foramen which lies close to the suture between the exoccipital and prootic.

The basioccipital forms the occipital condyle posteriorly. The fossa for the attachment of Baudelot's ligament is present on the lateral face of the basioccipital as a small pit. The ventral surface of this bone is poorly preserved and therefore I am unable to tell whether the posterior myodome is open.

In occipital aspect the braincase is narrow, differing from Recent sparids examined, as it is deeper than wide. The occipital fossa covers both the epioccipital and exoccipital, forming an extensive depression, which deepens ventrally. When compared with Recent taxa this fossa is observed only as a shallow cavity in *Dentex,* is barely visible in *Lithognathus* and is appears to be absent from *Diplodus.*

Otic region

The epioccipital forms the posterodorsal corner of the braincase, the ventral suture extends to a point level with the dorsal margin of the anterior hyomandibular facet, while just over a third of the medial wall of the posttemporal fossa and frontal sagittal crest are formed by this bone. A large dorsolaterally orientated fossa for the dorsal process of the post-temporal forms the posterior margin of the crest.

The pterotic forms the most significant proportion of the posttemporal fossa, as the posterior floor and posterolateral wall, in addition to forming the posterior third of the pterotic sagittal crest. The crest is punctuated along its length by pores of the laterosensory canal, however, the posterior limit of the crest is incompletely known. The pterotic also forms the posterior half of the dilatator fossa, and ventrally the suture between the pterotic and the intercalar bisect the posterior facet for the hyomandibular.

The intercalar is a small bone that faces ventrally, however the posterolateral margin extends posteroventrally as a flattened process, the dorsal surface of which forms a shallow depression, for the attachment site for the m. levator operculi, rather than for the reception of the ventral process of the posttemporal. A slightly larger fossa formed from the pterotic is situated directly dorsal from the process and articulates with the ventral process of the posttemporal is observed in the Recent taxa *Diplodus* and *Calamus* for example.

The sphenotic forms the anterior part of the dilatator fossa, the ventral margin of which, is sutured to the prootic and bisects the anterior facet of the hyomandibular. The dimensions of the hyomandibular facets differ little from those described for *Dentex.*

The dilatator fossa extends over the posterior third of the orbit. So far as can be seen the m. dilatatori operculi would have been totally enclosed anteriorly by the sphenotic.

The prootics are complex bones forming the trigemino-facialis chamber along their

anterolateral margins. The external part of this chamber; the pars jugalaris, is well preserved on the right side of the braincase BMNH P44503. The pars jugalaris is short, as is usual in perciform fishes. Furthermore, there appear to be three openings in the pars jugalaris. However, while the anterior and posterior openings are obvious, the central opening for the hyomandibular trunk of the facial nerve (VII), is poorly preserved. Observations of Recent sparids support these findings as this opening is considerably smaller than the anterior and posterior openings. Along the contact between the prootic and the parasphenoid is a large posteriorly facing foramen for the internal carotid artery. The prootics also forms the ventral half of the anterior facet of the hyomandibular.

The otico-occipital part of the braincase is well preserved in BMNH 44503, from which a number of key characteristics can be observed. On the ventral margin of the parasphenoid is the process for the attachment of the m. adductor palatini, which is not particularly well developed (Plate 5.11a). In addition, the parasphenoid forms a ventral carina which deepens posteriorly, the lateral margins are textured and also provide an attachment site for the m. adductor palatini. The pharyngeal apophysis of the basicranium is developed directly posterior to the process m. adductor palatini. It is weakly developed in this taxon (Plate 5.11b), and is comparable in size and shape to the apophysis described the modern genera *Dentex*. Nevertheless, the v-shaped facet for the articulation with pharyngobranchial 3 of the upper pharyngeal jaw is clearly present.

Nasals

The nasals are either missing or broken anteriorly in all specimens examined. However, it is possible from some specimens to observe that the posterior margin is attached only to frontals, as described in the Recent genus *Dentex*. The postromedial surface of the nasals would probably have been supported by the ethmoid crest, which forms a well developed platform posteriorly (Figure 5.10a)

The infraorbital region

The infraorbital region is incompletely known. However, infraorbitals I and II are present, contrary to Casier's (1966) description in which he considered these to be a single bone, labelled as the lacrymal. The first two infraorbitals are deeper than wide, a feature which is unique to sparids. The ventral margins extend to the a point level with the ventral margin of the maxilla, while the first infraorbital attaches to the ventral margin of the preorbital flange. The lateral surface of these bones are ornamented with vertical pleats, while they are thickened dorsally.

Jaws

The ascending process of the premaxilla is broken. However, it is possible to deduce that the process would probably have been shorter than the alveolar process, because no fossa for the reception of the ascending process of the premaxilla is present on the ethmoid. The alveolar process is slender, and has a straight dorsal margin. The maxilla also has a straight dorsal margin,

while posteroventrally the maxilla is expanded and extends well beyond the alveolar process. The shallow dorsolateral crest of the maxilla is represented by a knob-like process, which is separated from the articular condyle by a shallow palatine sulcus.

The mandible is long and deep posteriorly. The symphysal process is short, forming approximately a quarter of the total length of the dentary. A single row of pores on the lateroventral surface of the dentary mark the path of the mandibular sensory canal. The articular fossa has v-shaped margins. The descending process of the articular is broad, but extends only to the ventral margin of the dentary. The angular therefore forms the posteroventral corner of the mandible, while the facet for the quadrate is formed as usual by the articular.

The dentition of the upper and lower jaws are similar. It is more usual for the teeth to be missing in most of the specimens examined. However, caniniform teeth are present in some specimens, as a single row along the lateral occlusal margin, while the medial margin is covered by villiform teeth. From the size of the alveoli it would appear that the caniniform teeth are particularly large anteriorly, decreasing in size posteriorly.

The hyo-palatine bones

The hyomandibular is inclined at a shallow angle anteriorly. The head is divided into two condyles. The anterior condyle forms a lateral ridge connecting with the ventral process of the hyomandibular. A large flange of bone forms anterior to the condyles, which just touches the metapterygoid. The mandibular branch of the facial nerve exits from a foramen and continues along a sulcus down the ventral process of the bone. On the posterodorsal margin of the hyomandibular is the short opercular process.

The quadrate forms a confluent ridge with the preopercle, which appears to be continuous along the entire ventral margin, although the ridge is not as prominent as in the Recent genus *Sparus* for example. The ventral margin of the quadrate also overlaps the preopercle. The symplectic lies in a sulcus on the medial face of the quadrate, and is expanded both posterodorsally and posteroventrally, so that it overlaps the metapterygoid and preopercle.

The ectopterygoid and endopterygoid are only partially preserved. In BMNH P3975 the ectopterygoid is bent through approximately 50°, the ventral part of the ectopterygoid is sutured to the anterior margin of the quadrate, extending ventrally to the condyle. The metapterygoid is the usual large sheet of concave bone, separated from the quadrate by a fontanelle.

The palatine is not preserved in many of the specimens examined, however, the maxillary process of the palatine is observed to be fairly long and is deflected medially.

The opercular bones

The opercle articulates with the hyomandibular via a facet along the anterodorsal margin. The anterior margin fits into a sulcus running along the length of the vertical process of the hyomandibular.

The preopercle is bent through 56°, the ventral limb as usual is shorter than the dorsal limb. The lateral surface of the flange is ornamented by parallel ridges which are perpendicular to the posterior margin. In addition, it is observed that the posterior margin is not smooth (Plate 5.9a) as in the Recent genus *Calamus* for example, but neither does not have obvious serrations as described for the taxon *Ellaserrata monksi.*

An interopercle and subopercle are present, however there is nothing unusual about these bones which warrants further comment.

Lower part of the hyoid arch

The ventral hypohyal is present as the usual square-shaped bone. A sulcus for the hyoid artery crosses the lateral face, close to the dorsal margin of both the ceratohyal and epihyal. The dorsal margin of the ceratohyal is distinctly bifurcated with a well developed dorsal process articulating with the dorsal hypohyal. The posterior margin of the ceratohyal is also greatly expanded, while the dorsal margin of this bone is deeply concave (Plate 5.10c). The ventral margin of the urohyal forms a keel, although provides no more useful information.

In most specimens the branchiostegal rays are preserved in situ, so that the rays overlap each other making it impossible to determine the number of rays and their position. However, in BMNH P44501, five rays are preserved, one of which is an impression, and a probable sixth ray was present due to a large gap between the anterior margin of the ceratohyal and the first preserved ray. The head of the penultimate ray is preserved in close proximity to the interspace between the ceratohyal and the epihyal. The posterior most ray is attached to the epihyal, while the other rays attached to the ceratohyal. The rays are acinaciform in shape (McAllister 1968) and all appear to be a similar size.

The only bone of the branchial arches identifiable in BMNH P44324, is the basihyal, which is edentulous, like that of Recent sparids.

POST-CRANIAL SKELETON

Pectoral girdle and fin

The posterior flange of the posttemporal has a smooth margin. The dorsal process is long and narrow, while the ventral process is shorter as is usual.

The long tubular dorsal process of the extrascapular is preserved in BMNH P3975, extending anteromedially over the supraoccipital.

The supracleithrum contacts the lateral surface of the cleithrum, which is bent through approximately 32°. The scapula and coracoid are preserved in BMNH P34824, the foramen n. pterygialis is formed mainly from the scapula, however, the anterior margin is formed by the cleithrum. The coracoid appears to be a thick as the scapula along its posterior margin, having a long anterior process, in addition to a small projection along its posterior margin. The pectoral fin is preserved in a few specimens, but not the radials.

The dorsal and ventral postcleithrum are not as narrow as those described for *Dentex*, forming wide flanges ventrally.

Pelvic girdle and fin

The posterior margin of the girdle lies directly beneath the posterior margin of the braincase. The anterior subpelvic process is well developed, while the postpelvic process appear to be absent.

General remarks

Size

For living fishes, body shape is more commonly used for descriptions, rather than diagnoses (McCune 1987), however, shape is useful when considering fossils, as often morphological characters maybe scarce. While, morphometric shape or landmark analyses are beyond the scope of this thesis, simple parameters such as length versus depth provides information to assess whether a species is deep-bodied or not. The deepest point is at a maximum when measured along a vertical trajectory from a point level with the occipital crest. The length to depth ratio of body size for *Abromasta* is 2:1 whereas for similar sized individuals of *Sparnodus vulgaris* it is 3:1, while for *Ellaserrata monksi* the ratio is approximately 4:1. However, *Sparnodus vulgaris* gains similar dimensions to those of *Abromasta* as it matures. For the largest individual measured of *Sparnodus vulgaris* (Bol. T 1012), the deepest point is half of the total length, implying that the increase in body depth appears to be consistent with age for this species. These observations are in agreement with those of Recent deep bodied forms.

Locomotion

The posterior fin of *Sparnodus* has a relatively low aspect ratio, whist the aspect ratio for *Pagellus* is much higher. In addition, the width of the posterior peduncle in *Abromasta* is narrower than in *Sparnodus*. At the species level the peduncle of *Sparnodus vulgaris* is narrower anteroposteriorly than in *Ellaserrata monksi*, while it is slightly greater than in *Sparnodus microstomus*. *Abromasta* also appears to have fused hypural plates, whereas in *Sparnodus* they appear to be separate or semi-fused. The tail and more rigid skeleton of *Abromasta* therefore suggests a morphology better adapted to faster, sustained swimming.

The generalized type of swimming of *Sparnodus* equates to that of Labriform (Helfman *et al.* 1997), where the pectorals fins are largely employed for slow swimming, while the tail is used for bursts of faster activity. Many fish that inhabit complex environments such as coral reefs or vegetation beds develop laterally compressed, short bodies that facilitate pivoting for low-speed manoeuvrability, although clearly this is not always the case (e.g. gobies). Both *Abromasta* and *Sparnodus* are nearer to being locomotion generalists than locomotion specialists, however, the morphologies suggest that *Abromasta* has more potential for faster swimming than *Sparnodus*.

Diet

On the basis of cranial morphology, in particular jaw morphology and dentition, it is possible to deduce the feeding strategies of Eocene sparids. The skulls of *Ellaserrata* and *Sciaenurus* both have elongate ethmoid-vomerine regions of the generalized type described for *Dentex*. The jaw construction consists of an upper jaw with an alveolar process longer than the ascending process, long maxilla with knob-like condyle, while the mandible is elongate and has a short symphysis. The dentition consists of a row of sharp caniniform teeth, with a medial tooth field of villiform teeth. Modern sparids with similar morphologies such as the genus *Dentex* are predominately piscivorous, although may feed secondarily on soft-bodied invertebrates (see Chapter 4).

Sparnodus differs by having a slightly reduced ethmoid-vomerine region, in addition to a depression in the ethmoid which are features associated with more derived taxa. The jaw has both primitive and slightly more derived features. The maxilla still has a long lever arm. However, the condyle has a weakly developed dorsal crest and the ascending process of the premaxilla is much closer in length to the alveolar process, while the mandible is more reduced than in *Ellaserrata* and *Sciaenurus*. The jaws described for *Sparnodus* have an overall powerful construction, which is similar to that observed in the Recent genus *Pagellus,* which has a varied diet including fish, and invertebrates, such as molluscs, worms and crustaceans (see Chapter 4).

The jaws of *Abromasta* have a long lever arm closing mechanism which facilities a faster bite, but less leverage at the tip. The villiform dentition is similar to that found in centropomids which have a largely piscovorous diet.

Diversity

Sparids are reef-associated fish, rather than exclusively associated with this environment as are scarids for example. However, the diversity of sparid genera at this particular site, does not differ substantially to the number of genera found in similar reefal environments today. Six genera are present in the Caribbean, whereas three genera occur in the Red Sea. The presence of sparids in the Bolca assemblage is contrary to Bellwood's (1997) claim that 'there are no families represented in Bolca that occur in the Caribbean'. However, while generic numbers seem plausible, species diversity is much lower than that found on present day reef environments. The Bolca sparids may also be monospecific, although it is hard to identify fossil species using the same criteria applied to Recent species, such as colour pattern, scale distribution, gill raker and fin-ray counts.

In fossil taxa, fin-ray counts provide the only means to assess variation if the sample group is large enough. *Sparnodus vularis* is a relatively abundant fossil, and therefore fin-ray counts may be taken for a large number of individuals. The counts in the dorsal and anal fin do show some variation, however, the variation does not provide enough evidence to split this genera into further species.

The diversity of sparids found at the Oman site (Late Miocene) also appears to be

consistent with the Recent genera found in the Mediterranean.

Part 2 INFLUENCE OF FOSSILS ON RECENT CLASSIFICATION

In the second part of this chapter, phylogenetic analysis is used to resolve the evolutionary relationships of the Eocene and Miocene sparids described in part 1. Furthermore, I examine the effects of incorporating the fossil data within the Recent data set discussed in the first part of Chapter 3. The combined analysis allows further elucidation of the interrelationships of the Sparisae, and the evolutionary history of the group may then also be examined from a temporal perspective.

Fossils in phylogeny

The incorporation of fossils within a phylogenetic framework, is important if evolutionary relationships of character changes are to be discovered (Forey 1992; Nixon and Wheeler 1992; Smith 1994). Criticism of including fossils into phylogenetic analyses was maintained primarily because of the incompleteness of fossils, which usually add many question marks to data sets. Patterson (1977) and Nelson (1978), argued that fossils could only be interpreted in the light of Recent representatives, while others (e.g. Wiley 1981; Patterson 1981, Schoch 1986, Nelson 1989) provided evidence that ancestors could not be recognized through morphological criteria. Furthermore, evidence of ancestry or character polarity from stratigraphic successions was based on an *ad-hoc* assumptions (Smith 1994). However, with a reappraisal of the use of fossils in phylogeny, it has been shown that fossils can sometimes overturn existing theories of relationships between Recent organisms (e.g. Gauthier *et al.* 1988), although this is not always the case (Doyle and Donoghue 1987). While fossils are organisms which are anatomically incomplete, they provide additional information on character combinations and contribute to a total evidence approach. Thus, a more complete sampling of skeletal characters is gained from combined data sets, which allows further statements of homology in these charcters to be deduced. In addition, branches within a Recent-only classification that are poorly supported may, with the inclusion of fossil data provide an alternative phylogenetic hypothesis by reassessing statements of homology.

Phylogenetic analysis

Fossils included into a Recent data set should be treated as terminal taxa and coded with reference to the Recent taxa (Forey 1992). Thus, the matrices were processed using the same methods as those implemented in Chapter 3, further to which the fossil taxa were coded using the same multistate characters as for the Recent data set (table 2.0). However, with the inclusion of fossil taxa into the Recent matrix, this then presents the problem of missing data.

Missing values

More recently, the problem of missing values in phylogenetic inference has been recognized as a severe hindrance to the accuracy of phylogenies (e.g. Platnick *et al.* 1991; Nixon and Wheeler 1992; Novacek 1992; Wilkinson 1995; Wiens 1998). Missing values in data sets are the result of a number of different causes, but are particularly common in those which contain fossils, due primarily to poor preservation. The inclusion of missing values, may readily destabilize certain relationships thereby dramatically increasing numbers of multiple most parsimonious trees (MPTS), with loss of resolution in the consensus trees. However, MPTs may often be the result of a particular unstable taxon/taxa, the removal of which can lead to a dramatic reduction in number of trees. Safe Taxonomic Reduction (STR) of Wilkinson (1995) and Reduced Cladistic Consensus (RCC) of Wilkinson (1994) are two methods of resolving problems of multiple trees using *a prior* and *a posterior* approaches respectively.

STR aims to eliminate 'rogue' taxa, i.e. taxa that have no effect upon relationships inferred for other taxa and may also increase numbers of MPTs (see Wilkinson and Benton 1995; Wilkinson and Benton 1996). The results show that there is no equivalence in the fossil data sets, as all taxa have a unique set of character states. This is also true for the combined matrix. However, as the character states changes are similar for the Recent and fossil representatives of the taxon *Diplodus*, STR therefore suggests the deletion of one of these taxa.

Table 5.2 *Dispersion of missing entries across characters for the following data sets (ds)*

	Number of characters		
Missing entries	*Eocene ds*	*Fossil ds*	*Combined ds*
none	45	42	39
1	3	6	9
2	-	-	1
3	5	2	1
4	12	5	4
5	24	10	7
6	-	24	12
7	-	-	15
9	-	-	1

From the original 89 morphological characters complied for the Recent data set (table 2.0), 65 of these characters were applicable to the most completely known fossil taxon *Sciaenurus bowerbanki*, while only 45 characters are scored for the taxon *?Sparnodus microstomus* (table 5.1). When these taxa are compared with the Recent data set, *Sciaenurus bowerbanki* is 70.8% informative, while *?Sparnodus microstomus* is 54.0% informative. The Eocene data set has a total

of 34.8% missing values, while the inclusion of the Miocene taxon *Diplodus oranensis*, increases the total proportion of missing values by 1.5%. The inclusion of the fossil taxa to the original data set of Recent sparids, causes a significant increase in number of missing values as would be expected from 0.86% to 6.88%. Table 5.2 is the combined output from each STR analysis of the Eocene; fossil (includes Eocene and Miocene taxa) and combined (fossil and Recent taxa) data sets (Wilkinson 1995) and illustrates the number of missing entries for each character. As would be expected there are fewer missing entries for each character for the combined data set, as most of the Recent taxa do not have any missing entries. The fossil data set, while only including one additional taxon has a greater dispersion of missing entries across the characters than the Eocene data set.

Those areas of the skeleton that are character abundant in the Recent taxa, such as the braincase, jaws and gill arches, are, with the exception of the latter, relatively well preserved in the fossil taxa. The absence of data from the gill and hyoid arch leaves a void of morphological information, however, a partition homogeneity test of this character grouping performed using the Recent data set in Chapter 3 found that the null hypothesis of congruence can be rejected as the measure of incongruence is significantly larger than if the data is no more incongruent than random A PTP tests suggests that the data is not random, so that the conflicting signal may reasonably be attributed to homoplasy. While the data for this group of characters, may help to improve character hypotheses, the missing data for these characters does not further increase the homoplasy for this data set.

Fossil data set of Eocene taxa

An analysis of the Eocene taxa provided a hypothesis that is both fully resolved and well supported (Figure 5.0a). The single MPT has a length of 54 steps: CI = 0.926; RI = 0.667; RC = 0.593. From the total number of character state changes, only six have a ci value of <1 and the value for the characters: C1, C27, C43, C47, C50, C82 is not lower than 0.500.

Table 5.3 *Statistics from PCPTP output*

incompatibility count for original data = 43
PCPTP = 0.001
mean = 71.148±5.684
normal deviate = 4.953
95% cut-off = 62
incompatibility excess ratios
IER_1 = 0.396
IER_2 = 0.267

The tree shape is symmetrical, with the clade (*Ellaserrata Sciaenurus*), forming the sister group to (*?S. microstomus* (*S. vulgaris Abromasta microdon*)).

The parsimony and pairwise incompatibilty PTPs are 0.01 and 0.001 respectively, which is the minimum possible for the number of random permutations, therefore allowing for the rejection of the null hypothesis that the data is acting randomly with respect to hierarchial structure.

Fossil data set of Eocene and Miocene taxa

With the inclusion of the Miocene taxa *Diplodus oranensis*, 3 MPTs with a length of 70 steps were found. CI = 0.871; RI = 0.667; RC = 0.581 (Figure 5.0). In tree 1, as in the previous analysis of Eocene taxa (*Ellaserrata Sciaenurus*) forms the basal clade, which is the sister group to (*Abromasta* (*S. vulgaris* (*?S. microstomus Diplodus*))). Tree 3 is similar to tree 1, except for the position of the taxon *Abromasta*, which in this hypothesis forms a sister grouping with *Diplodus*. Tree 2 is dissimilar to trees 1 and 3 in terms of tree shape, as the taxa form a pectinate series. After reweighting a single tree was found with the same topology as tree 2.

The increase in number of MPTs with the inclusion of the genus *Diplodus oranensis* is a consequence of including a single taxon with a combination of characters introducing homoplasy. These derived character states are noted in the matrix but for the purpose of this analysis are uninformative. However, these autamorphic characters are included because they have relevance for the fossil and Recent analysis. As the characters in this analysis are unordered, most multistate characters with three or more states are therefore redundant, with the automorphies adding only to tree length.

Table 5.4 *Statistics from PCPTP output*

incompatibility count for original data = 31
PCPTP = 0.027
mean = 41.375±4.443
normal deviate = 2.335
95% cut-off = 33
incompatibility excess ratios
IER_1 = 0.251
IER_2 = 0.048

The PCPTP for this data set is 0.027, which is not the minimum possible for the number of random permutations. This does not therefore allow for the rejection of the null hypothesis, which is a consequence of the high number of automorphies in this data set. The lower IER_1 and IER_2 values of this data set compared to the Eocene data set,also suggest relatively higher levels of

incompatibility/incongruence and thus a lower quality of data .

Combined data set of Recent and fossil sparids

(Note † refers to fossil taxa when described in the conjunction with Recent taxa)

The initial heuristic search of the combined data set of Recent and fossil data found 112 most parsimonious trees of a length of 415 steps. CI = 0.330; RI = 0.636; RC = 0.210. A strict component consensus (Figure 5.1a) of these trees, reveals that the base of the tree has collapsed, leaving no resolution apart from the following terminal clades: (*Dentex* †*Ellaserrata*), ((*Lithognathus Stenotomus*) (*Pagrus Pagellus*)) and (†*Abromasta*, †?*S. microstomus* and †*S. vulgaris*), whilst the relationships of the cladistically 'higher' sparids are the same as those of the Recent hypothesis (Figure 5.1b). The inclusion of †*Diplodus oranensis* forms a clade with the Recent taxon *Diplodus vulgaris* confirming its affintiy to this genus.

A posterori weighting using rescale consistency indicies offers a solution for reducing the number of MPTs (Smith 1994), because of the high RI value After reweighting a total of 15 trees were found with a length of 416 steps: CI = 0.329; RI = 0.634; RC = 0.209. The strict component consensus of these trees is shown in Figure 5.2a.

Table 5.5 *Statistics from PCPTP output*

incompatibility count for original data = 2168
PCPTP = 0.001
mean = 2728.394±31.035
normal deviate = 18.057
95% cut-off = 2679
incompatibility excess ratios
IER_1 = 0.205
IER_2 = 0.187

The relationships of the fossil taxa in the reweighted consensus are similar to those found for the single MPT found for the Eocene sparids (Figure 5.3a). The inclusion of †*Diplodus oranensis* has little effect upon topology, as the automorphies present for this taxon in the fossil data set, are now synapomorphies with one or other of the more derived clades of Recent sparids within this data set. Further, the PCPTP is now 0.001, allowing for the rejection of the null hypothesis, which indicates that the data contains significant cladistic structure (see table 5.6).

However, a salient difference between the higher sparids of the Recent and the combined (fossil and Recent) MPTs after reweighting is the position of the Recent taxon *Pachymetopon.* In the combined trees *Pachymetopon* forms a sister grouping to the clade (*Boops Oblada*) and cladistically higher taxa, whereas it is more basal in the Recent MPTs forming a sister group

relationship with the clade ((*Pagellus Pagrus*)(*Stenotomus Lithognathus*)) and cladistically higher taxa. The shift in position of this taxon is interesting. However, before asserting whether the inclusion of the fossil taxa may indeed overturn the Recent hypothesis, it is important to reanalyize the data as this result maybe an artefact of reweighting.

The position of Pachymetopon

The shift of position of *Pachymetopon* with the inclusion of fossil data after reweighting is interesting as there are few cases of fossils overturning Recent hypothesis (Doyle and Donoghue 1987; Gauthier *et al.* 1988).

MacClade was used to assess the effect on tree length from placing *Pachymetopon* to its 'Recent' position. This simple procedure found the same tree length of 416 steps, as for the MPTs of the combined tree. This hypothesis was not found in the original search, amounting to an unsuspected failure of the heuristic methods employed. A reanalysis of the data using a backbone constraint tree formulated in PAUP, retained all taxa more cladistically derived than *Pachymetopon* when in its Recent position (Figure 5.2b) which maintained *Pachymetopon* outside of this clade. This analysis found fewer trees (82 MPTs), with a shorter length of 415 steps. All 85 trees placed *Pachymetopon* in the same position as the Recent hypothesis. However, three trees (T22,T42 and T55) did not match the topologies of any of the 15 MPTs obtained after reweighting the fossil and Recent analysis (Figure 5.2a).

These analyses show that reweighting affects the phylogenetic position of *Pachymetopon,* as the inclusion of the fossil taxa changes the weighting contingent on taxa selection. However, the fossil taxa, apart from effecting number of MPTs and resolution, do not influence the relationships of the Recent taxa.

The base of the tree shows greater structure, with the taxa (*Cymatoceps* (†*Sciaenurus* (*Dentex* †*Ellaserrata*))), forming a partially resolved clade (termed here as clade A; see Figure 5.2b), and united by by the single unambiguous character C30 (dorsal maxillary crest is knob-like). In addition, (†*S. microstomus* (†*S. vulgaris* †*Abromasta*)) now form a completely resolved clade (termed B; see Figure 5.2b) which are united by three unambigious character state changes including: C15 (exoccipital facets are orientated posteriorly), C42 (villiform teeth present on the medial edge of the occlusal margin) and C86 (hypurals are unfused). However, the relationship between clade B and the taxon *Porcostoma* is unresolved.

The polytomies at the base of the tree may further be resolved by assessing character distribution. Of the 15 trees found from the reweighted analysis, those which did not group *Polysteganus* and *Chyrsoblephus* as a clade (see section on unresolved taxa , Chapter 3) were excluded, leaving five trees T4, T7, T9, T10 and T12 (Figure 5.3). To resolve the placement of the taxa *Porcostoma* further trees maybe excluded. Under the optimizations DELTRAN and ACCTRAN T10 and T12 have no unambigious character state changes supporting either the clade

(*Porcostoma* (*Abromasta* (*S. vulgaris* ?*S. micrastomus*))) or *Porcostoma* as the sister group to the clade (*Abromasta* (*S. vulgaris* ?*S. micrastomus*)) respectively. However, T4, T7 and T9 are supported by two unambigous character state changes C18 (single foramen for n. vagus + n. glossopharyngeal) and C39 (descending process of the articular extends below the ventral margin but not beyond the ventral process), placing *Porcostoma* as the sister group to more cladistically derived taxa.

There is no preferred hypothesis for the relationships within the clade (*Cymatoceps* †*Sciaenurus* (*Dentex* †*Ellaserrata*)) as there are no unambigious characters supporting relationships between *Cymatoceps* and †*Sciaenurus*. In T4 two characters (C74 and C75) under the DELTRAN optimization support this relationship, however both characters are associated with the branchial arches, which are not preserved and are therefore represented as missing data in †*Sciaenurus*. In T7 a single charcter C3 under ACCTRAN supports this association, which is scored for both taxa.. In T9 these taxa are also supported by C39 again under the ACCTRAN optimization. The clade (*Dentex* †*Ellaserrata*) is supported by a single character (83) under both optimizations in all MPTs. However, it is important to remember that using distribution of character state changes is a somewhat arbitary approach as the character optimizations maybe an artefact of tree structure.

A reduced cladistic consensus (RCC) is implemented if by the removal of a taxon, the tree can say more about relationships than by its presence. Thus, if a taxon is found to have a number of different positions in a particular clade in the MPTs for example, the consensus will show a clade with little or no resolution. However, subsequent pruning of the unstable taxon will help to partially resolve or fully resolve relationships.

The constraint tree (Figure 5.2b) is also the only member of the RCC profile, implying that there is no additional cladistic information shared by the MPTs that is not in the consensus tree. While three unresolved areas in the consensus tree remain, there are no other n-taxon statements (i.e. taxa that are more closely related to each other than they are to some other taxa) that do not include those taxa. Thus, while the relationships within clade A are not fully resolved, no cladistic information is lost by the inclusion of *Cymatoceps*, as this taxon does not group with either *Dentex* or *Ellaserrata*, which form a clade in each of the MPTs. Likewise, the 'rogue' taxon *Porcostoma* while seemingly causing the most conflict does not reduce the amount of cladistic information by its inclusion.

Discussion

The incorporation of fossil taxa into the Recent data set provides a basis for calculating minimum ages of cladogeneic events, furthermore it provides a time scale of character acquistion and transformation, and the evolution of character complexes.

The inclusion of fossil data into the Recent data set does not have a significant effect on tree structure, implying that no novel characters are present in these taxa. The placement of

Pachymetopon in a more crownward position, was rejected after reanalysis of the data found a shorter tree with *Pachymetopon* reverting to the position found in the 'Recent' analysis.

The monophly of the family is retained and is supported by the same four unambigious character state changes as described in part 1 of Chapter 3. The Bremer support values for the 'higher' sparid clade is relatively good, while basal relationships are weakly supported, as found in the Recent analysis.

The assertion that fossil taxa are not detrimental, regarding the relationships of the Recent taxa, is valid as none of the existing relationships described for the Recent hypothesis have been overturned. Furthermore, the inclusion of fossil taxa, increases the number of better supported character state changes supporting the monophyly of the Sparidae.

The morphology of the basal most fossil sparids *Sciaenurus* and *Ellaserrata* is analogous with that of the generalized sparid *Dentex*, with which they form a clade. However, the morphologies of the taxa forming the clade (*S. microstomus*, (*S. vulgaris Abromasta microdon*) have certain features, particularly those of the braincase and jaws that form both cladistically primitive and derived character states i.e. in the taxon *Sparnodus vulgaris*, the presence of a maxillary dorsal crest on the premaxilla is associated with a lever arm of the maxilla that is straight and has a knob-like dorsal crest, while the ascending process of the premaxilla is shorter than the alveolar process, yet a fossa for the ascending process is observed in the ethmoid region.

The inclusion of fossil data causes the base of the tree to collapse, however this may be evaluated through reweighting, assessment of character state distribution and from the RCC profile. With the inclusion of fossil taxa, there is a decrease in the CI from 0.572 to 0.330, which implys that there has been a slight increase in homoplastic characters with the inclusion of fossil data. However, the IER values (see table 3.2 and 5.6) are not significantly different, thus the data for the combined hypothesis does not contain higher levels of incompatibility/ incongruence than the Recent hypothesis which would otherwise suggest this data to be of a lower quality. The assessment of character acquistion shows that the ci for characters even at those nodes supported by the same character state changes are slightly lower in the combined trees than the Recent trees.

The minimum age of origin for the Sparidae can be confidentally placed at approximately 55Ma., as the combination of possible relationships for clade A (Figure 5.2b) do not effect the minimum age of origin for the Sparidae. Furthermore, the clade including both fossil and Recent species of *Diplodus* place the minimum age for this clade between 7.1-5.3 Ma, which implies that cladistically more derived taxa radiated within this time period. However, there are a number of genera of the same age which are not included in this analysis (see overview of the fossil record), the most basal of these is assigned to *Pagrus*. Thus, the minimum age of origin would include a far greater diversity than suggested from the hypothesis present here. If true, then the diversity of 'higher' sparids found today has occured within the last 7.1-5.3 Ma.

Table 5.0 Summary of selected fossil sparid material

Taxa	Age	Formation	Locality	Remarks on preservation
Sparidae	Pliocene	Red Crag	Felixstowe, Suffolk, U.K	Left dentary containing molariform teeth. Partially preserved.
?Diplodus	Pliocene	Bone Valley Foramtion	Garginier Mine, Polk Co. Florida, U.S.A	Roof of braincase partially preserved; mainly frontals and supraoccipital. Steep angle of frontals, textured dorsal surface, unfused rostromedially forming posterior margin of the fossa/foramen for the ascending process of the premaxilla
Sparidae	Miocene		Grand Canary	Isolated molariform teeth
Sparidae	Miocene, Langhian	Faluns de Touraine	France	Isolated molariform and anterior caniniform/conical teeth, plus alveolar process (with teeth) from a durophagous genus
Diplodus oranensis	Miocene, Messinian	Sahélien	Oman	Articulated skeleton, preserved two-dimensionally
Dentex sp.	Miocene, Messinian	Sahélien	Oman	Cranium preserved, preserved two-dimensionally
Pagrus pagrus	Miocene, Messinian	Sahélien	Oman	Articulated skeleton, preserved two-dimensionally
Crenidens crenidens	Miocene, Messinian	Sahélien	Oman	Articulated skeleton, preserved two-dimensionally
Pagellus leptosomus	Miocene, Messinian	Sahélien	Oman	Post-cranial skeleton preserved.
Boops boops	Miocene, Messinian	Sahélien	Oman	Articulated skeleton, preserved two-dimensionally.
Sparidae	Lower Miocene	Formation de Dam	Saudi Arabia	Isolated molariform and rostral caniniform/conical tooth morphologies
?Diplodus	Oligocene		Skouriatissa, Cyprus	Incisiform teeth
Sparidae	Lower Oligocene	Formation d'Ashawq	Thaytiniti and Taqah, Oman	Isolated molariform and anterior caniniform/conical tooth morphologies
Sparnodus vulagris	Eocene, Lutetian	Monte Bolca	Verona, Italy	Articulated skeleton, preserved two-dimensionally. By far the most abundant sparid from the Bolca deposits
?Sparnodus microstomus	Eocene, Lutetian	Monte Bolca	Verona, Italy	Articulated skeleton, preserved two-dimensionally
Ellaserrata monksi	Eocene, Lutetian	Monte Bolca	Verona, Italy	Articulated skeleton, preserved two-dimensionally
Abromasta microdon	Eocene, Lutetain	Monte Bolca	Verona, Italy	Articulated skeleton, preserved two-dimensionally
Sciaenurus bowerbanki	Eocene, Ypresian,	London Clay Formation	Sheppey, Kent, U.K	Preserved in nodules, usually just cranium, occasionally girdle as well. Preservation is three-dimensional. Common Sheppey fossil

Table 5.1 Fossil data matrix

CHARACTERS

TAXA	1	2	3	4	5	6	7	8	9	10	11	12	13	14	15	16	17	18
Lutjanus	0	0	0	0	0	0	0	0	0	0	0	0	0	0	0	0	0	0
Abromasta microdon	2	1	1	1	1	?	1	0	?	1	0	0	1	?	1	?	?	?
Sciaenurus bowerbanki	1	0	0	1	0	1	1	0	?	0	0	0	0	0	0	1	1	0
Sparnodus vulgaris	1	1	1	1	0	?	1	0	?	0	0	0	0	?	1	?	?	0
Ellaserrata monksi	1	0	0	1	0	?	1	0	?	0	0	0	0	?	0	?	?	?
?Sparnodus microstomus	2	1	1	1	?	?	1	0	?	0	0	0	0	?	1	?	?	?
Diplodus oranensis	2	1	3	1	1	?	1	?	?	1	0	0	2	?	1	?	?	?

TAXA	19	20	21	22	23	24	25	26	27	28	29	30	31	32	33	34	35	36
Lutjanus	0	0	0	0	0	0	0	0	0	0	0	0	0	0	0	0	0	0
Abromasta microdon	?	?	0	1	1	1	?	0	3	1	2	0	0	?	0	2	0	0
Sciaenurus bowerbanki	0	1	0	1	1	1	0	0	3	1	2	0	0	?	0	1	0	0
Sparnodus vulgaris	2	?	0	1	1	1	?	0	3	1	2	1	0	?	0	1	0	0
Ellaserrata monksi	?	?	0	1	1	1	?	0	2	1	2	0	0	?	0	1	0	0
?Sparnodus microstomus	?	?	0	1	1	1	?	0	2	1	2	1	0	?	0	1	0	0
Diplodus oranensis	2	?	0	1	1	1	?	2	2	1	2	2	1	?	?	2	2	?

TAXA	37	38	39	40	41	42	43	44	45	46	47	48	49	50	51	52	53
Lutjanus	0	0	0	0	0	0	0	0	0	0	0	0	0	0	0	0	0
Abromasta microdon	?	0	0	0	2	0	0	0	0	0	0	?	?	1	?	?	0
Sciaenurus bowerbanki	0	0	0	0	2	1	1	0	0	0	1	2	?	0	?	0	0
Sparnodus vulgaris	?	2	0	0	2	3	0	1	0	0	1	2	0	0	0	1	0
Ellaserrata monksi	?	0	0	0	2	1	1	0	0	0	1	2	?	0	?	?	0
?Sparnodus microstomus	?	2	0	0	2	3	1	0	0	0	1	2	?	1	?	?	0
Diplodus oranensis	?	2	2	1	2	3	0	0	1	1	2	2	?	1	1	1	1

CHARACTERS cont

TAXA	54	55	56	57	58	59	60	61	62	63	64	65	66	67	68	69	70	71
Lutjanus	0	0	0	0	0	0	0	0	0	0	0	0	0	0	0	0	0	0
Abromasta microdon	1	1	2	?	?	?	?	1	?	?	?	?	?	?	?	?	?	?
Sciaenurus bowerbanki	1	1	2	1	2	?	?	1	1	?	?	?	?	?	?	?	?	?
Sparnodus vulgaris	1	1	2	?	?	?	?	1	1	?	?	?	?	?	?	?	?	?
Ellaserrata monksi	1	1	1	?	?	?	?	1	?	?	?	?	?	?	?	?	?	?
?Sparnodus microstomus	1	1	2	?	?	?	?	1	?	?	?	?	?	?	?	?	?	?
Diplodus oranensis	1	1	2	?	?	?	?	1	?	?	?	?	?	?	?	?	?	?

TAXA	72	73	74	75	76	77	78	79	80	81	82	83	84	85	86	87	88	89
Lutjanus	0	0	0	0	0	0	0	0	0	0	0	0	0	0	0	0	0	0
Abromasta microdon	?	?	?	?	?	1	?	?	?	0	1	0	0	?	2	?	?	?
Sciaenurus bowerbanki	?	?	?	?	?	1	?	1	?	?	1	0	0	?	?	?	?	?
Sparnodus vulgaris	?	?	?	?	?	1	?	?	?	0	1	0	0	?	1	?	?	?
Ellaserrata monksi	?	?	?	?	?	1	?	?	?	?	0	0	0	?	2	?	?	?
?Sparnodus microstomus	?	?	?	?	?	1	?	?	?	?	1	0	0	?	1	?	?	?
Diplodus oranensis	?	?	?	?	?	1	?	1	?	?	1	0	0	?	1	?	?	?

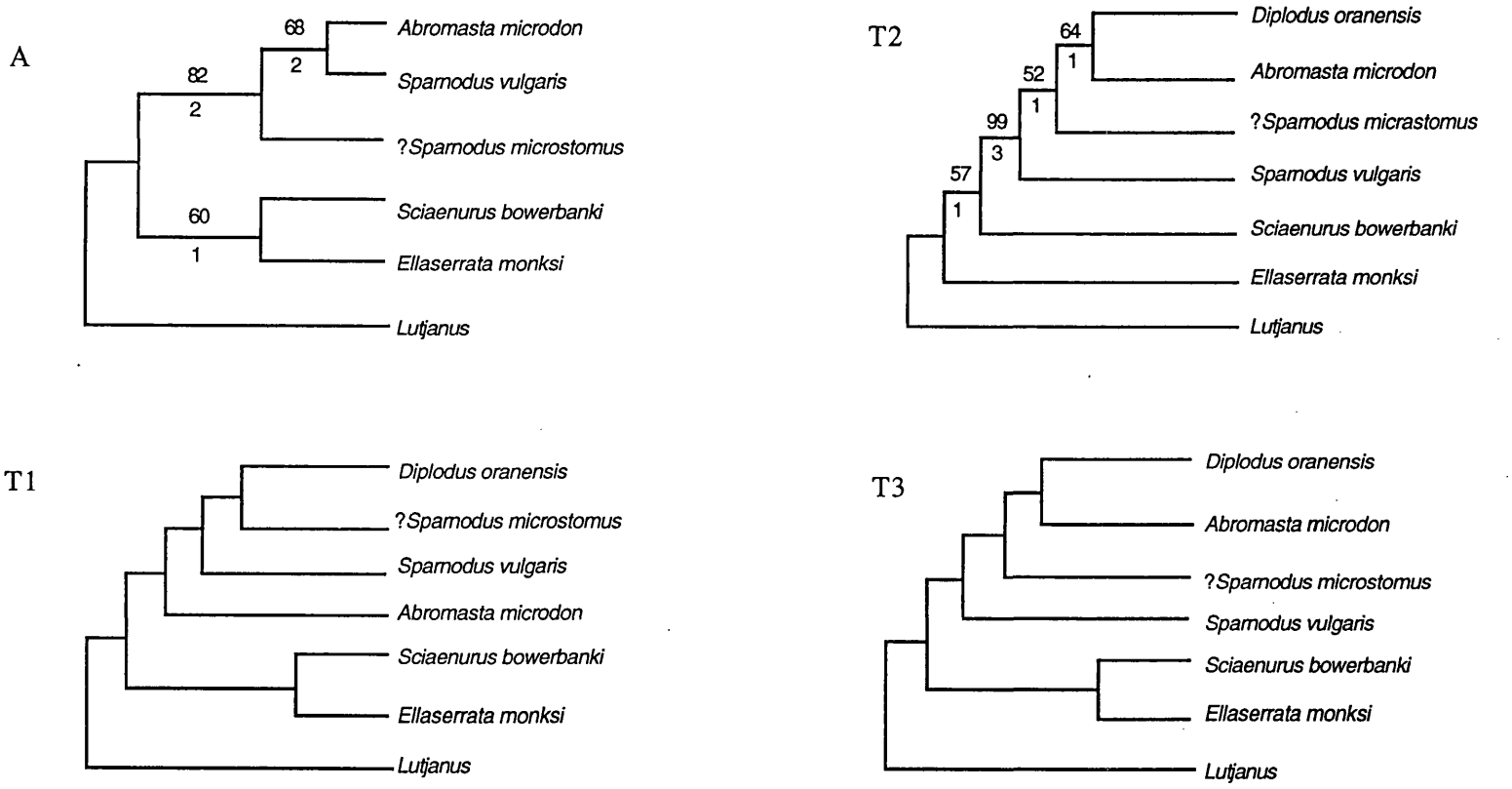

Figure 5.0 MPTs of fossil sparids based on character data from table 5.1 a) Single MPT found for the Eocene taxa; b) 3MPTs found for all fossil taxa The toplogy of T2 is the same for the single MPT found after the characters were reweighted using rescale consistency index. Bootstrap percentages and decay index values are shown above and below the branches respectively

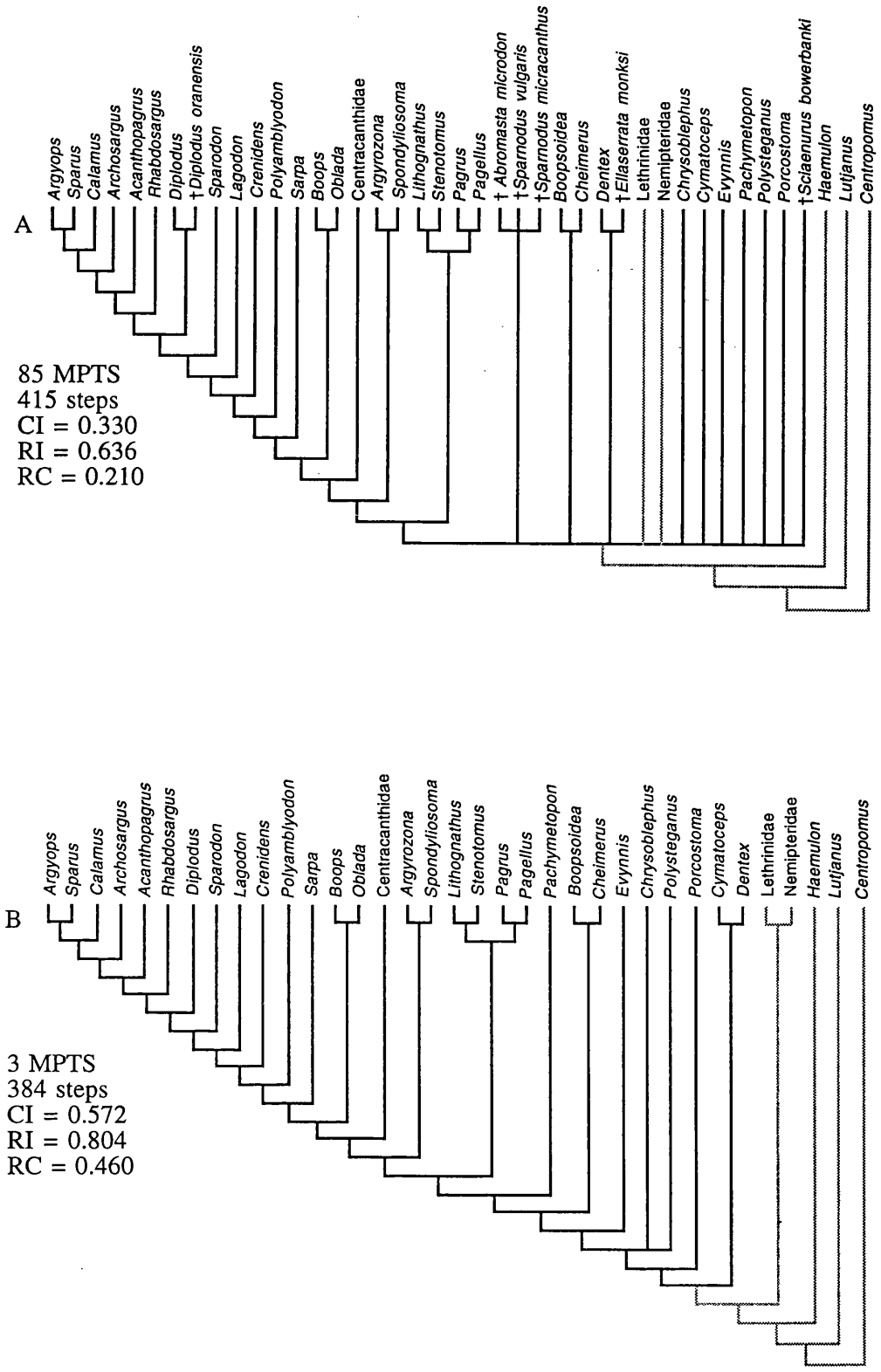

Figure 5.1a) Strict component consensus of the 112 MPTs for the fossil and Recent analysis produces the same topology as the 85 MPTs found after reanalysis of the data using a constraint tree, the statistics of which are shown here b) the Recent hypothesis is included for comparison. Grey branches represent outgroup taxa.

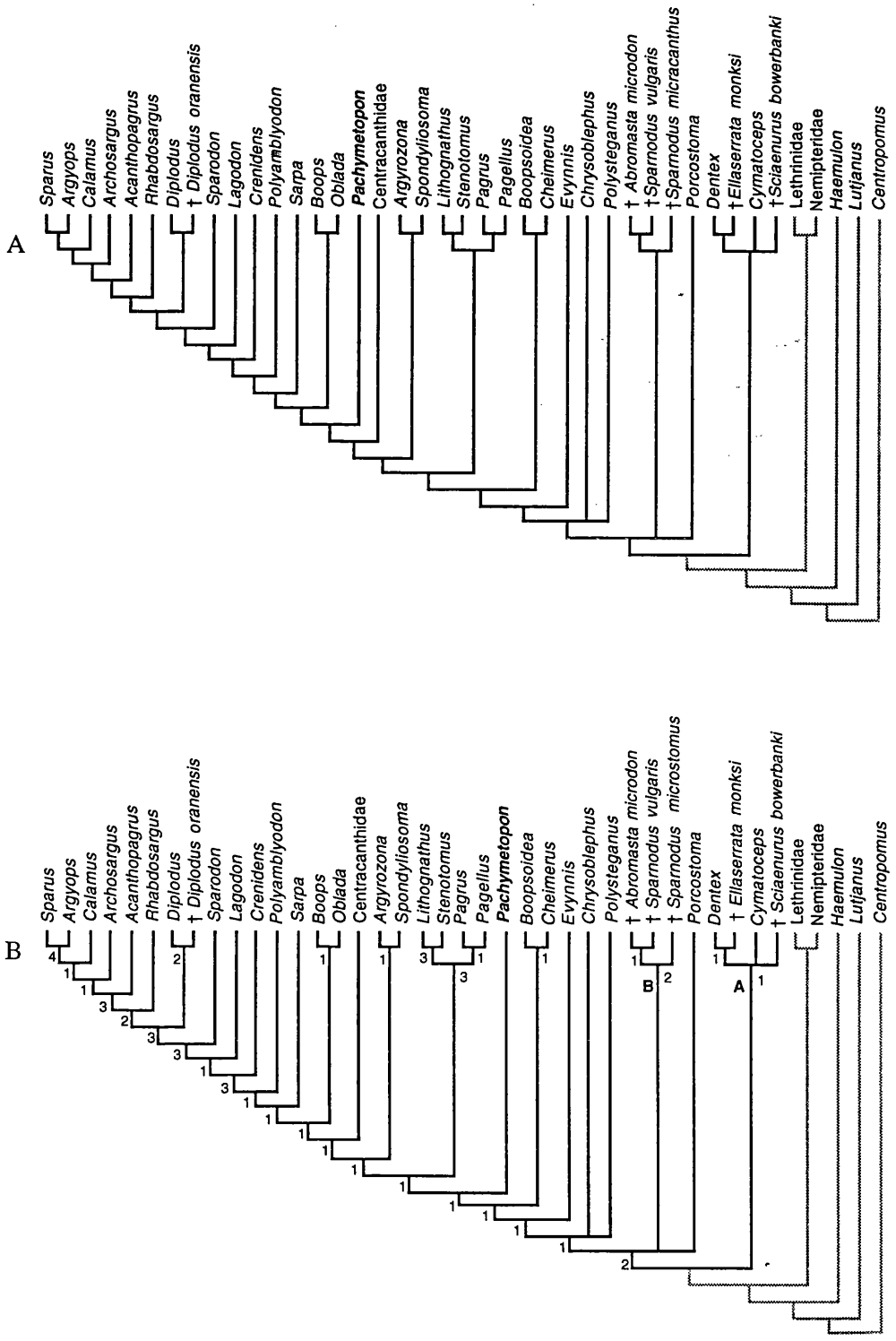

Figure 5.2 The effect of fossil data on the Recent hypothesis a) strict component consensus tree of the reweighted analysis, places *Pachymetopon* in a more cladistically derived position; b) utilization of a constraint tree forcing *Pachymetopon* outside the clade *Pagellus* - *Sparus* found a shorter tree which placed *Pachymetopon* into its 'Recent' position (see figure 5.1b). Values next to branches indicate Bremer support. The symbol † indicates fossil taxa. Grey branches indicate outgroup taxa.

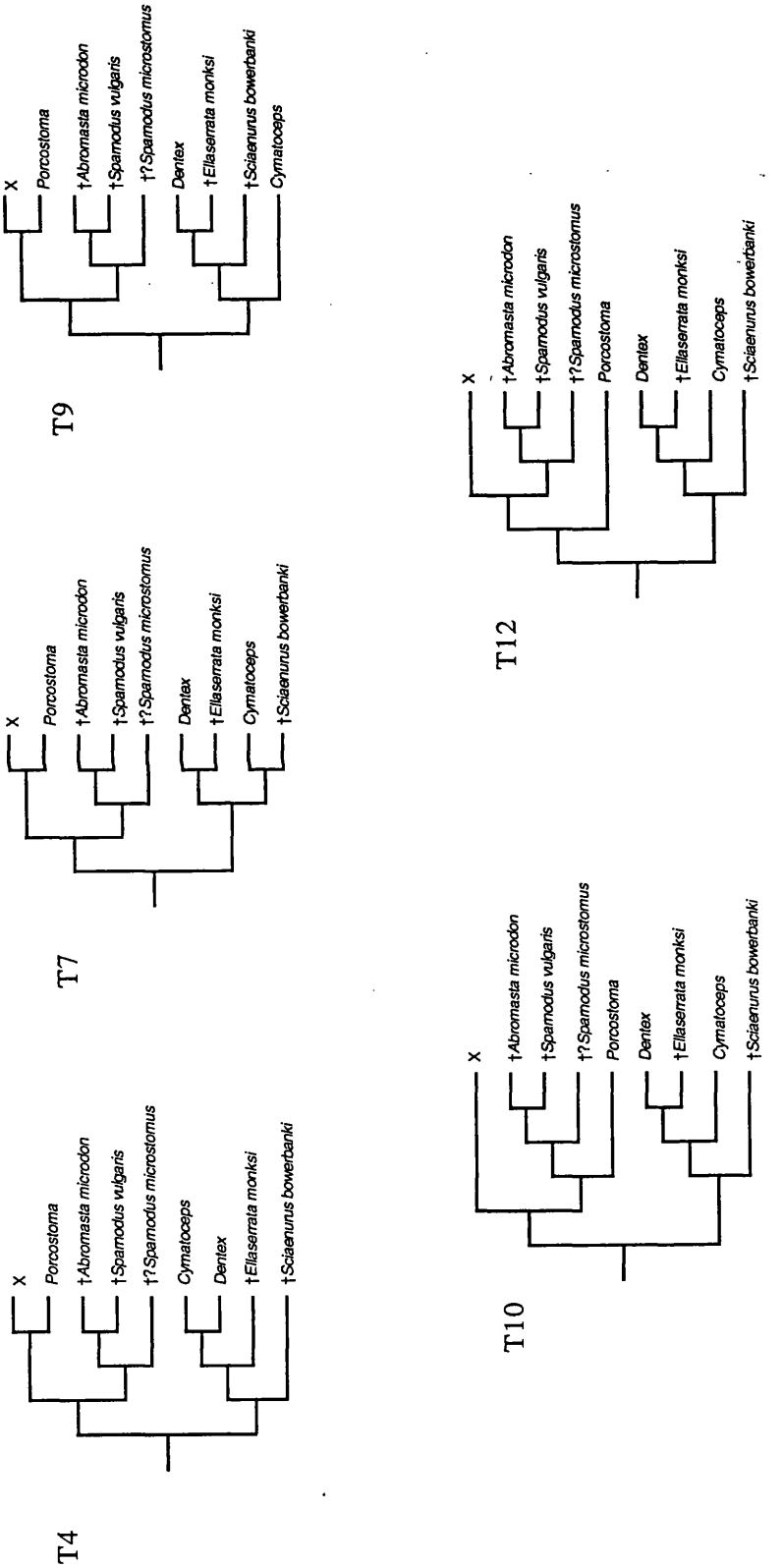

Figure 5.3 Areas of conflict at the base of five of the 15 MPTs after reweighting. These trees were initially selected as they have the same structure as the preferred Recent hypothesis for the more cladistically derived taxa *Chyrsoblephus* and *Polysteganus*. Branch X represents all 'higher' taxa.

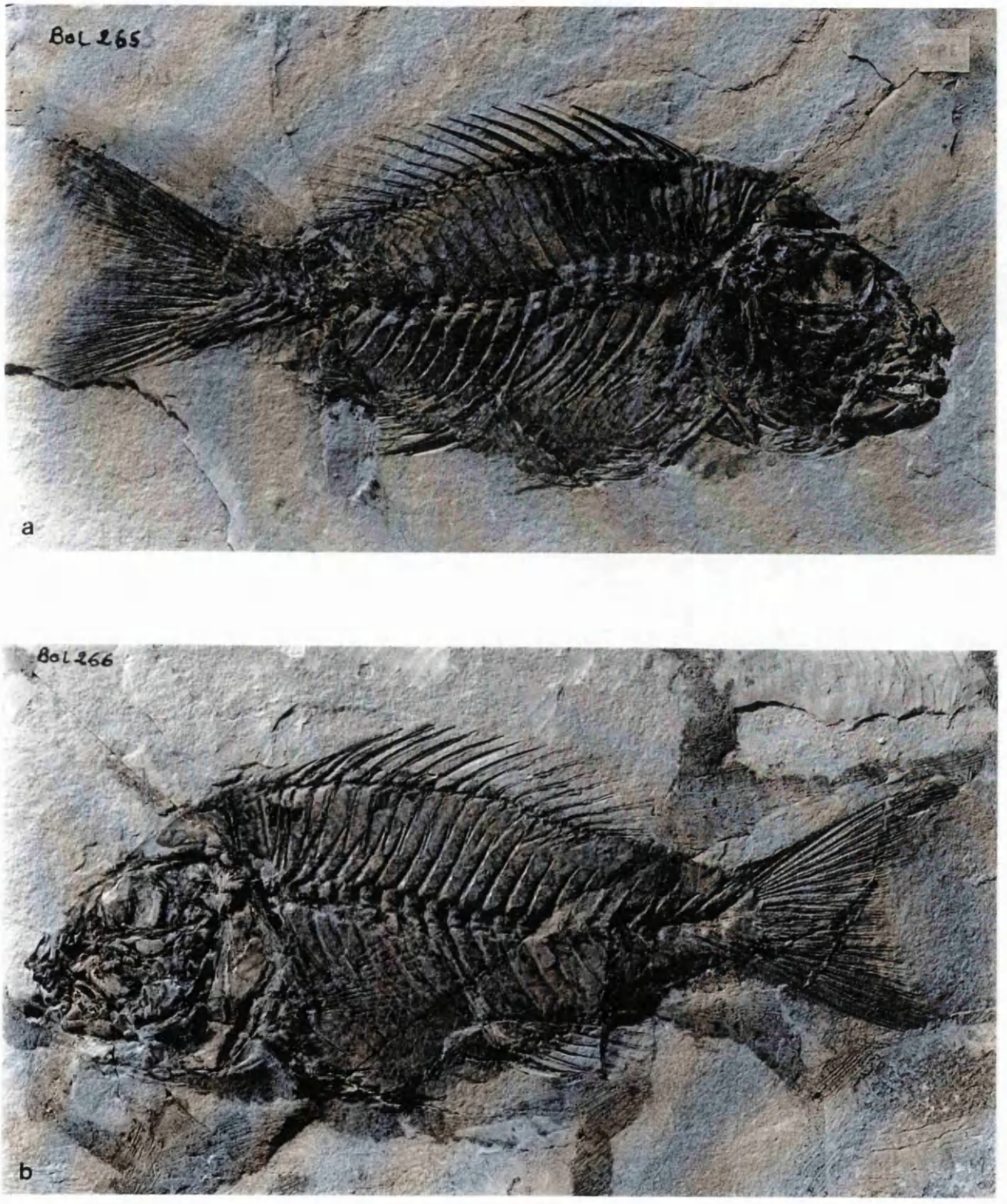

PLATE 5.0 The type of *Sparnodus vulgaris*, Eocene, Monte Bolca, Italy

a. Lateral view of MNHN 10796 / Bol 265 (part)

b. Lateral view of MNHN 10797 / Bol 266 (counterpart)

Scale bar = 10 mm

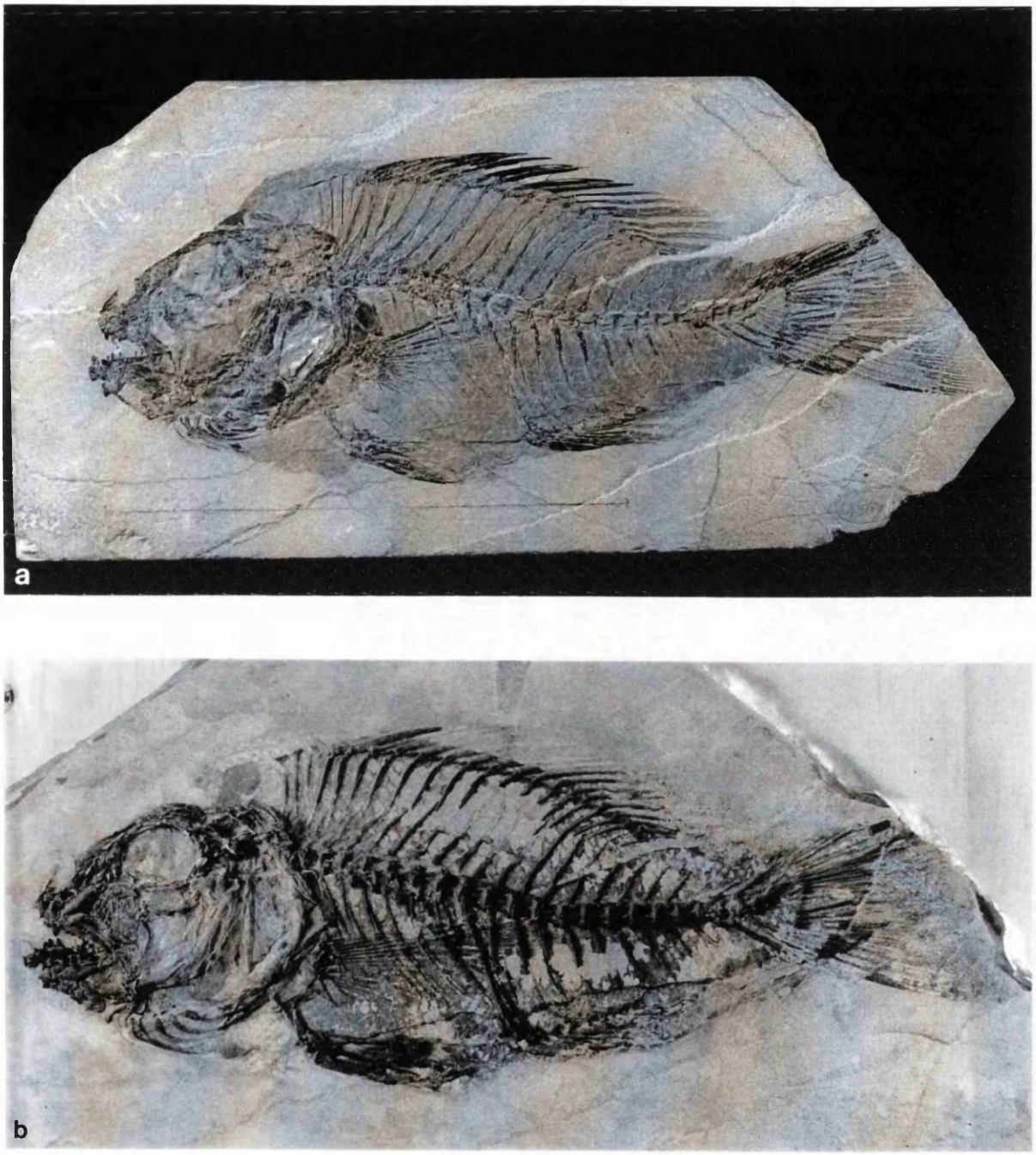

PLATE 5.1 ***Sparnodus vulgaris*, Eocene, Monte Bolca, Italy**

This specimen represents the most informative fossil of this species. The higher degree of morphological detail preserved in this specimen, is due to the method of preparation. Acid preparation dissolves the rock matrix leaving the fossil in relief, a technique utilized effectively by Patterson (1964). From this specimen it is possible to see features, particularly those from the braincase (see figure 5.2b) that are not preserved in other specimens.

a. Lateral view of BMNH 44867 (part)

b. Lateral view of BMNH 44867 (counterpart) which has been acid prepared

Scale bar = 10 mm

PLATE 5.2 ***Sparnodus vulgaris*****, Eocene, Monte Bolca, Italy**

a. Lateral view of the cranium of BMNH 44867

b. *Camera lucida* drawing of the cranium of BMNH 44867 (see Chapter 1 for abbreviations of anatomical terminology)

Scale bar = 10 mm

A

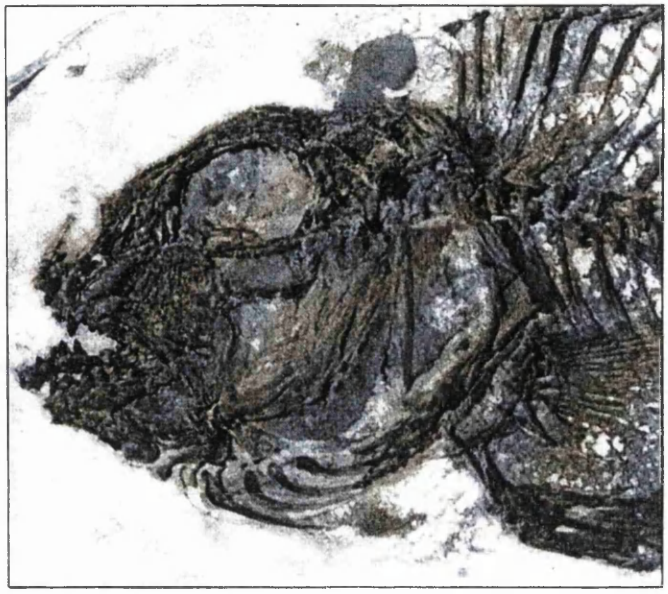

B

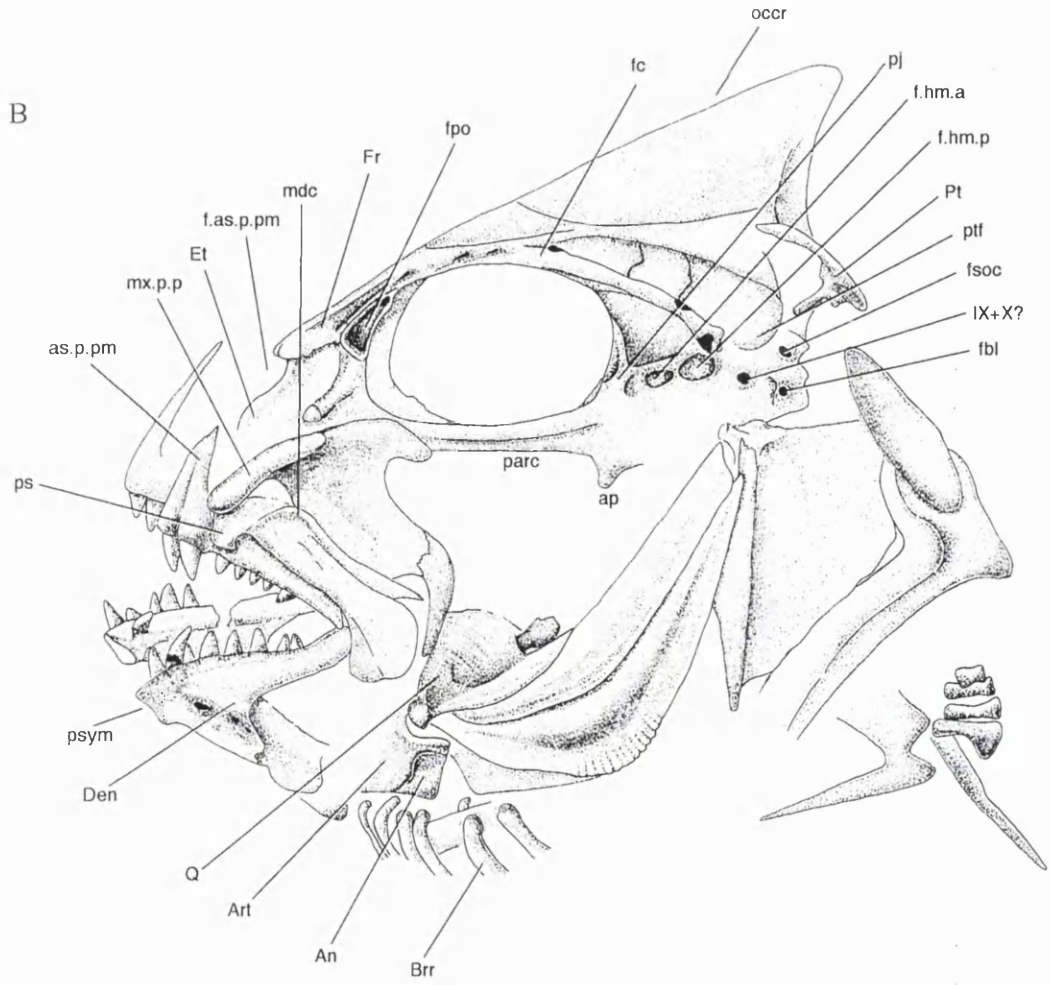
occr
fc
pj
f.hm.a
f.hm.p
fpo
Fr
mdc
Pt
f.as.p.pm
ptf
Et
fsoc
mx.p.p
IX+X?
as.p.pm
fbl
parc
ps
ap
psym
Den
Q
Art
An
Brr

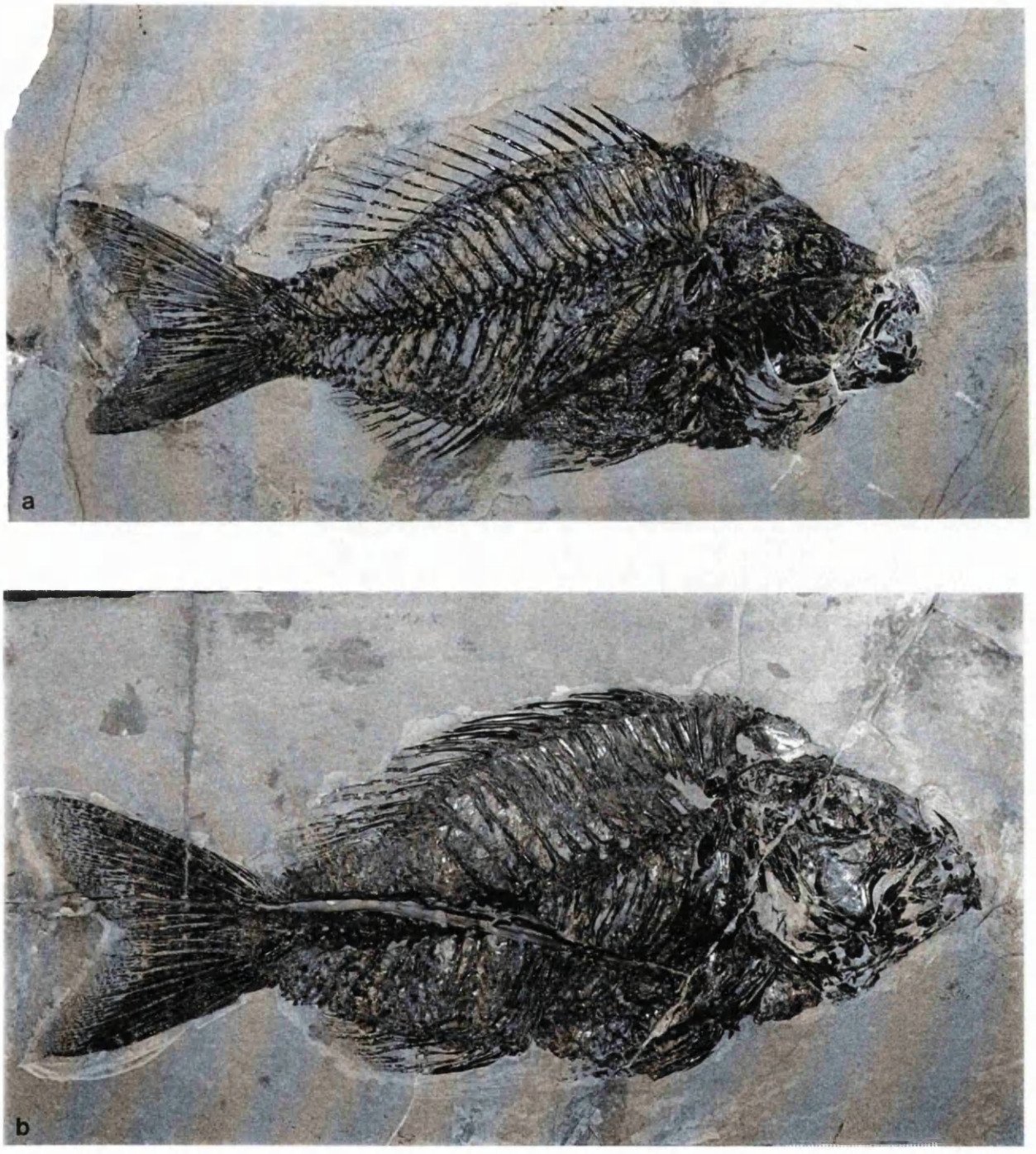

PLATE 5.3 ***Sparnodus vulgaris,*** **Eocene, Monte Bolca, Italy**

Jaw and cheek morphology, in particular the upper jaw in specimen a and palatine arch in specimen b provide useful character information

a. Lateral view of Bol I.G 24547

b. Lateral view of Bol II P. 136

Scale bar = 10 mm

PLATE 5.4 ?*Sparnodus microstomus*, Eocene, Monte Bolca, Italy

a. Lateral view of the type (part) MNHN 10730 / Bol. 260

b. Lateral view of the type (counterpart) MNHN 10729 / Bol. 254

c. Lateral view of Bol. T.886 in which both upper and lower jaws are preserved. The jaws differ in morphology to those of *S. vulgaris* (see figure 5.0), making the affinity of this taxon questionable

Scale bar = 10 mm


a

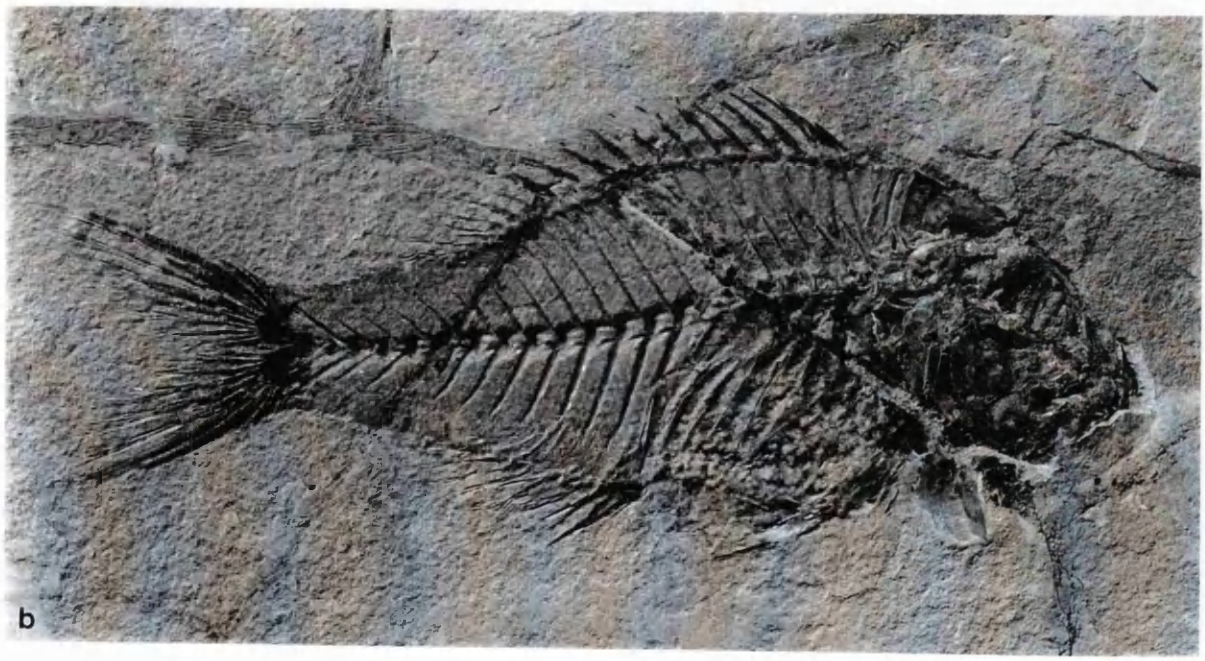
b


c

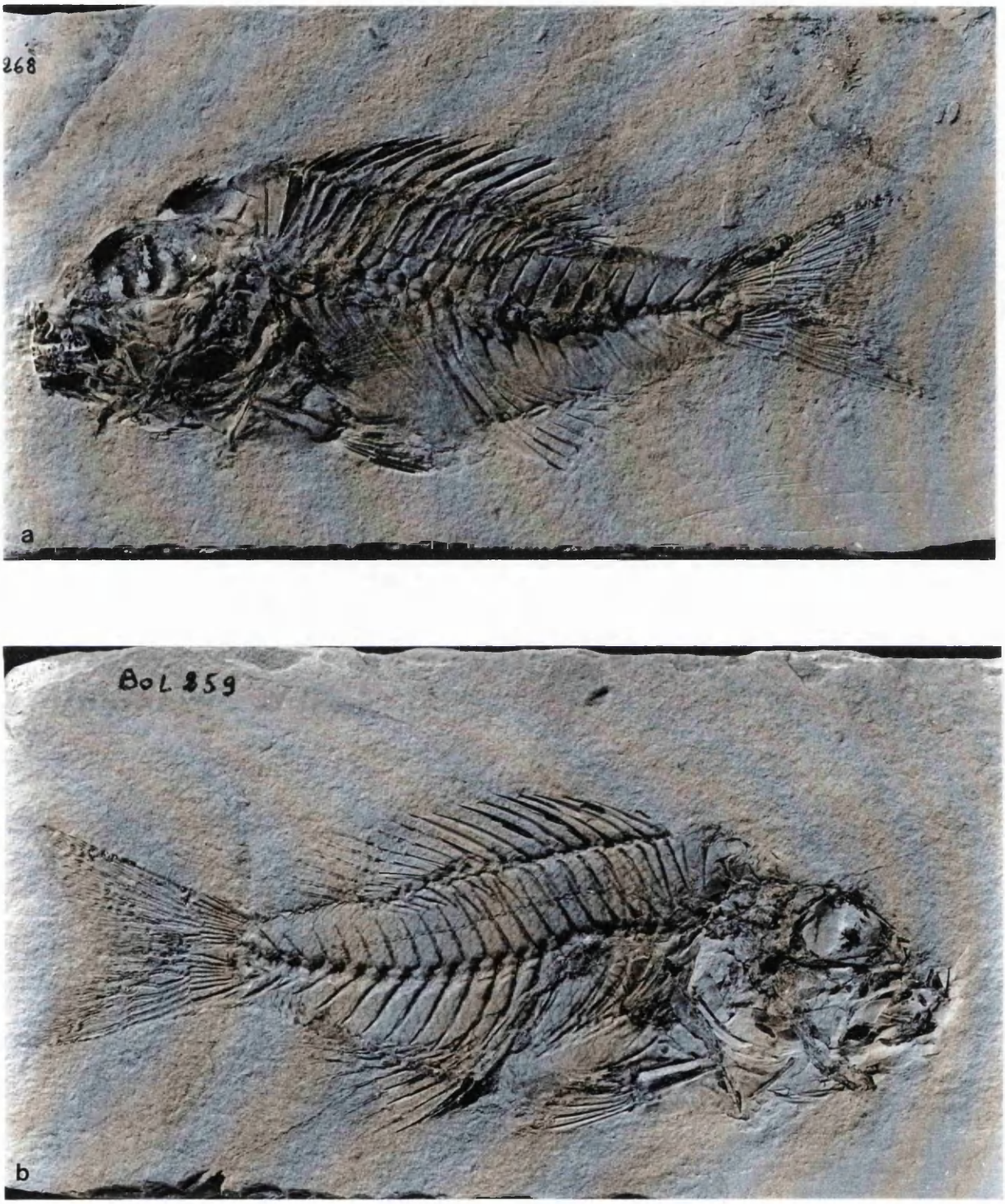

Plate 5.5 ***Sparnodus elongatus,*** **Eocence, Monte Bolca, Italy**

a. Lateral view of the holotype of '*Sparnodus elongatus*' MNHN 10804 / Bol. 268 figured by Agassiz (1836: pl. 28, fig. 1), which is here synonimzed with *S. vulgaris*

b. Lateral view of the counterpart of '*Sparnodus elongatus*' MNHN 10803 / Bol. 259

Scale bar = 10 mm

PLATE 5.6 ***Ellaserrata monksi*****, Eocene, Monte Bolca, Italy**

a Lateral view of the holotype BMNH P1938

b Lateral view of the counterpart BMNH P3900

c Lateral view of the cranium, detailing the serrated caudal margin of the preoperculum

Scale bar = 10 mm


a

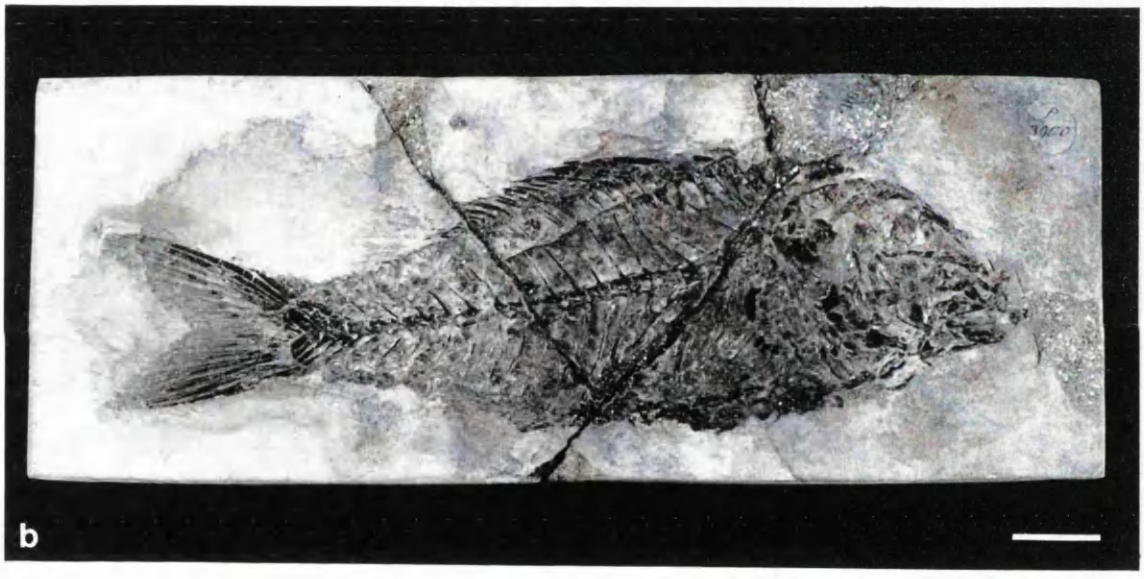
b


c

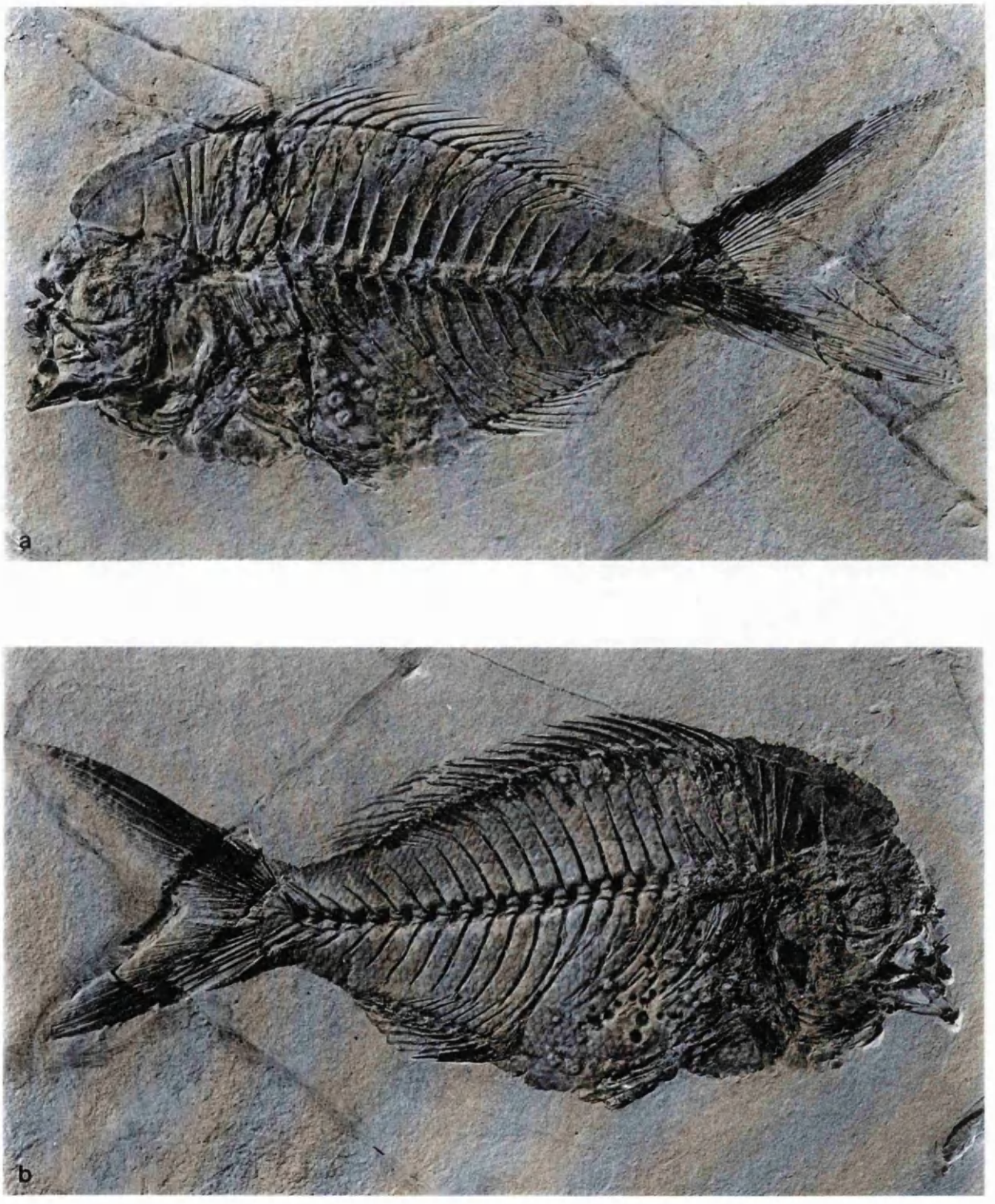

PLATE 5.7 ***Abromasta microdon,*** **Eocene, Monte Bolca, Italy**

a Lateral view of the holotype MNHN 10785 / Bol. 47

b Lateral view of the counterpart of MNHN 10784 / Bol. 46

Scale bar = 10 mm

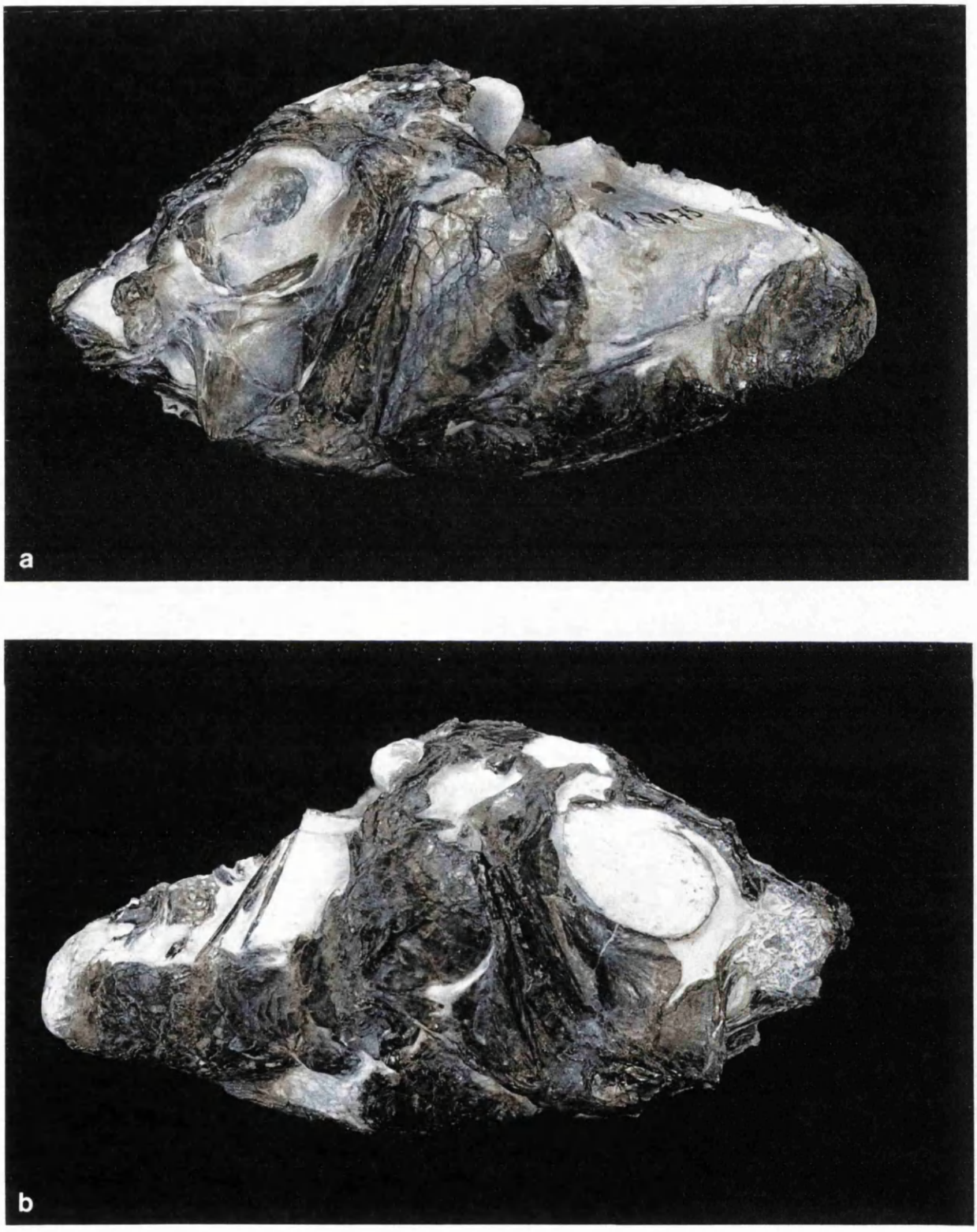

PLATE 5.8 Holotype of *Sciaenurus bowerbanki*, BMNH P3975, Eocene, London Clay, UK

a. Left lateral view of the cranium and initial abdominal vertebrae

b. Right lateral view

Scale bar = 10 mm

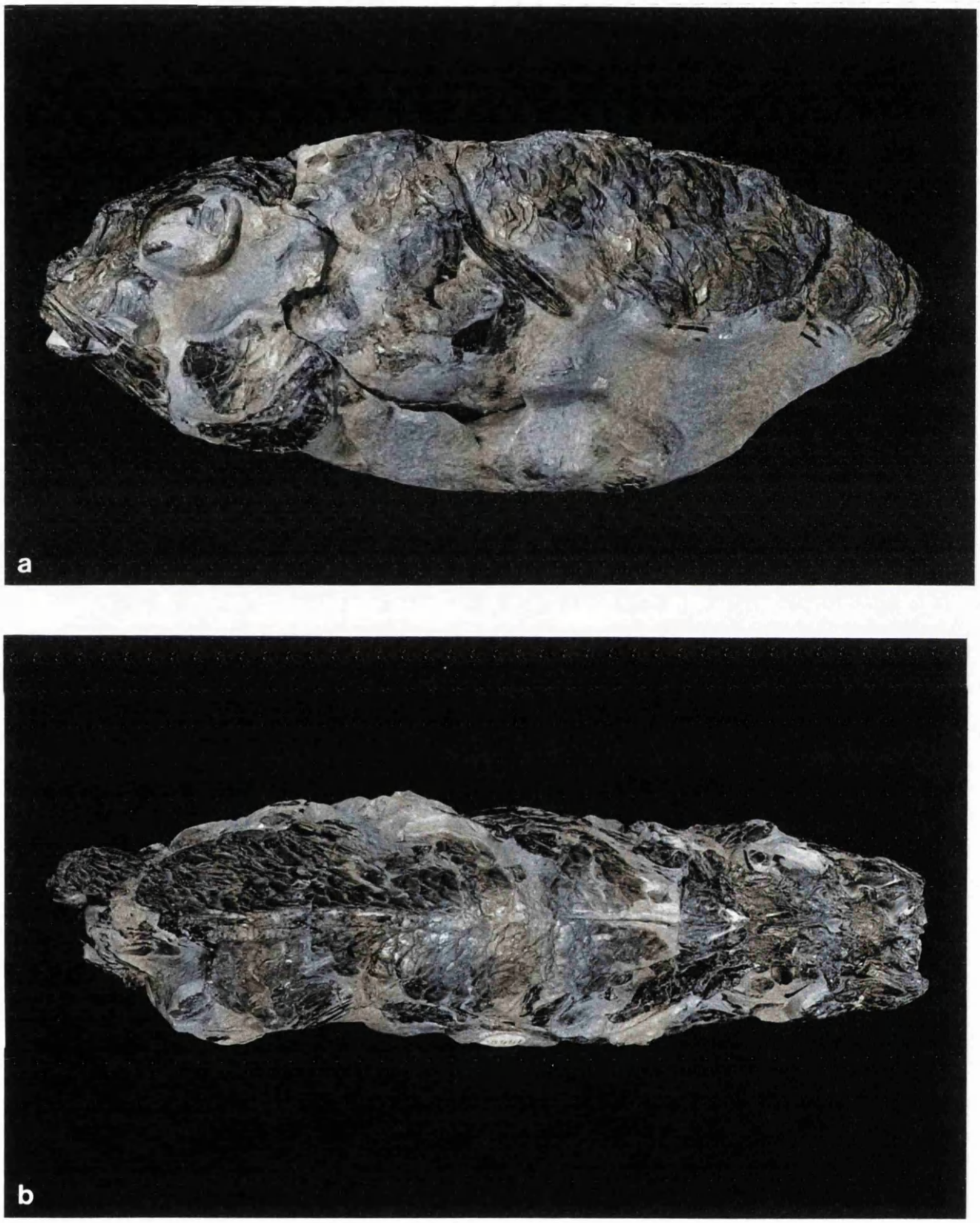

PLATE 5.9 ***Sciaenurus bowerbanki*, BMNH P39441, Eocene, London Clay, UK**

a. Left lateral view with enlarged first and second infraorbitals, in addition to articulated lower and upper jaws

b. Dorsal view of the most complete body fossil of this genus

Scale bar = 10 mm

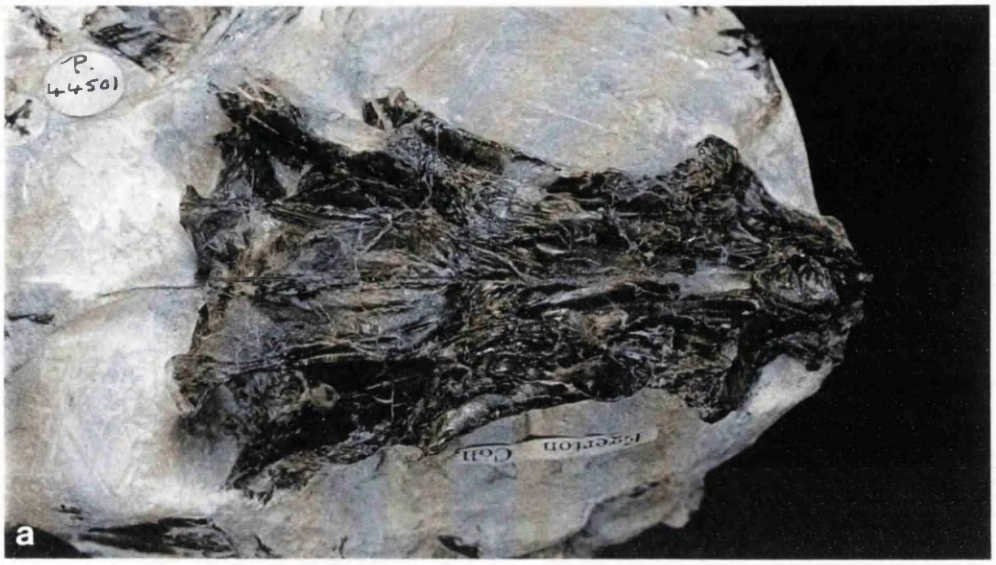

PLATE 5.10 Braincase of *Sciaenurus bowerbanki*, BMNH P44503, Eocene, London Clay, UK

a. Dorsal view of braincase

b. Rostral view of braincase

c. Lateral view of part of the lower hyoid arch

Scale bar = 10mm

PLATE 5.11 Braincase of *Sciaenurus bowerbanki*, BMNH P44503, Eocene, London Clay, UK

a *Camera lucida* drawing of the otic-occipital part of the braincase

b *Camera lucida* drawing of the occipital view of the braincase

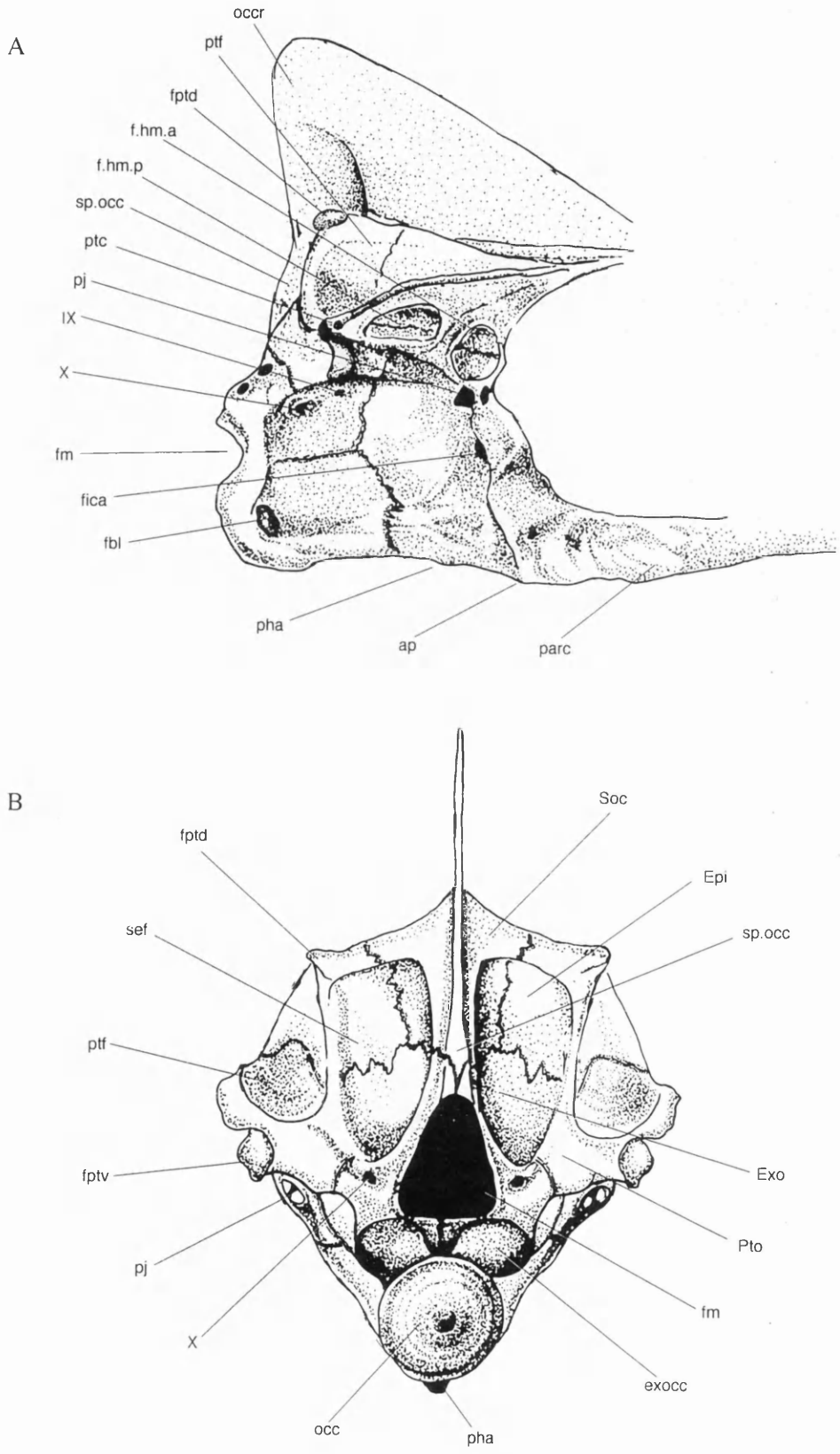
A
occr
ptf
fptd
f.hm.a
f.hm.p
sp.occ
ptc
pj
IX
X
fm
fica
fbl
pha
ap
parc
B
Soc
fptd
Epi
sef
sp.occ
ptf
fptv
Exo
Pto
pj
fm
X
exocc
occ
pha

CHAPTER 6

SUMMARY

"To form a clear idea of anything is an undeniable argument for its possibility..."

Hume (1739: 136)

Introduction

Previous work on the Sparidae has largely been confined to alpha-taxonomic studies involving examination of external features, colouration etc., with limited detailed morphological work or phylogenetic interpretations. The main aim of this thesis has therefore been to produce a phylogenetic hypothesis of the interrelationships of the Sparidae, based on a comprehensive survey of the comparative morphology of this group with respect to related families. Separate analysis, using different methodologies reveal useful insights into agreement or incongruence between data sets. The fossil record provides an historical perspective. Furthermore, phylogenetic hypotheses can be used to determine phylogenetic perspectives into aspects of their ecology and life history. This chapter summarises the conclusions from each of the previous chapters and discusses possibilities for future research.

The Sparidae are described comprehensively for the first time, the examination of the was necessary for the formulation of a data matrix to be used for phylogenetic inference. Previous descriptions (see Chapter 1), provided some character information, but they were generally limited with regards to a comprehensive account of sparid morphology, which is a prerequisite for elucidating the interrelationships of the group. Much variation observed within the Sparidae as a source for characters had been largely overlooked. The comparative morphology was therefore examined to 1) assess the monophyly of the family; 2) ascertain the monophyly of the genera and 3) to determine the phylogenetic relationships at the generic level.

The morphology of sparids displays considerable variation between genera, although few morphological differences were observed at the species level. The morphology reveals an interesting array of constructs, that may be broadly characterized into those with a generalized or specialized morphology. By this term I imply an overall similar appearance to that of lower

percoids and those with clearly more specialized functional adaptations.

A survey of the comparative morphology, from using the character groupings or systems outlined in Chapter 3 showed that the highest morphological variation is from the cranium; in particular the braincase, jaws and gill arches were most character rich. Comparision of this data set to other similar morphological analyses on teleosts (table 3.1), provided a basis for determining character diversity in the cranium versus postcranial skeleton, although some observational bias must be accounted for. Sparids were found to have considerably higher morphological variability in the cranium, which is an observation consistent with the labroid family Scaridae. The comparison between these two groups is something that I will return to later in this Chapter.

Parsimony analysis performed using unordered multistate characters produced a hypothesis that is both fully resolved with the exception of a basal node, and supports the Sparidae as a natural group. The monophyly is supported by four unambiguous characters of which three are synapomorphies of the group: presence of three or more openings in the pars jugularis; a specialized premaxilla/maxillary articulation and reduced or absent post-pelvic processes. Bootstrap support for the Sparidae is relatively good, although when judged by its Bremer support the group is rather weakly supported. The data, however, passes matrix randomisation tests, which represent a minimum requirement if the data is used to infer phylogeny (Wilkinson 1999). Further confidence of the phylogenetic hypothesis may be ascertained from the diversity of characters types supporting this clade. As discussed in Chapter 3, partitioning characters into different systems may be somewhat artificial, but the differences between the morphological systems provides greater support for the phylogenetic hypothesis than if they belong to a single anatomical system.

Assessment of data quality and manipulation of the original data matrix, through a priori and a posteriori approaches enabled the subsequent analyses to be compared with the original parsimony run in order to determine levels of incompatibility and incongruence. Support for more cladistically derived clades is better than for those more basal. This holds true when a) characters were excluded as judged by their Le Quesne probabilities; b) data partitions excluding groups of 'related' characters and c) exclusion or inclusion of different members of the outgroup are applied to the data. From these analyses the relationships of 'higher' sparids remain relatively unaffected, while there is, however, little or no resolution at the base of the tree. The low support of basal clades and their susceptibility to the influence from further analyses suggests that the data supporting these clades has a weak phylogenetic signal.

The ordered analysis found a similar result to the unordered analysis, with the relationships of the 'higher' sparids remaining unchanged. However, this analysis found a significant shift in the position of the taxon *Argyrozona*, so that it forms a clade with *Dentex* as the most basal members of the family. The new position of this taxon is interesting as its morphology suggests an animal adapted to a more generalized mode of life, with which its basal position would agree.

This observation has implications in the light of the evolutionary hypothesis concerning feeding strategies, which I will discuss later.

A preliminary binary analysis was performed using non-additive binary coding, the results of which showed incongruence with those hypotheses where the data was coded as multistate. The increase of characters for this analysis found a greater number of most parsimonious trees, while the tree statistics indicate higher levels of homoplasy when compared to the unordered and ordered multistate analyses. However, these results required further analysis before they can be thoroughly interpreted.

The conflict observed in the data presented here is characterized by high levels of homoplasy, which is common feature of percoid phylogenetics (Johnson 1993). However, the value of the ci expected suggests that there is no more homoplasy than would be expected for any data set of this size (Sanderson and Donoghue 1989). The lack of synapomorphies supporting nodes are a consequence of the homoplasy present in many characters. This is confirmed from testing character quality using Le Quesne probability, which rejected nearly half of all characters when $P = >0.05$. Testing data quality maybe considered an experiment in order to relate further information regarding the informativeness of certain characters, or character complexes.

The position of *Centracanthus* as a member of the Sparidae is supported in all analyses, the placement of which is virtually identical. This observation also appears to be consistent with Recent molecular work (Orrell 1999). The implications of these findings therefore suggest that the Sparoidei is composed of the three families; Lethrinidae, Nemipteridae and Sparidae rather than four as Johnson (1980) proposed. However, the fourth, Centracanthidae is now, according to my analysis embedded within the Sparidae.

The phylogenetic hypothesis of sparid genera provides a basis for examining biogeographic as well as ecological patterns of the family. Sparids have an interesting biogeographic pattern, with a broad global distribution. They are most speciose in the Indo-Pacific, however they have radiated in the Eastern Central Atlantic, an area considered to have low diversity, and are the only family of the Sparoidea to be found in the Western Central Atlantic. Pattern and event-based biogeographical analyses following the progression rule identify the Indo-Western Pacific and the Eastern Central Atlantic as possible ancestral areas for the Sparidae. The occurrence of the oldest known sparid fossils from Tethys, which was linked to both of these oceans during its closure suggests that these areas are likely centres of origin.

The distribution of characters as previously mentioned provides an interesting pattern that indicates a high degree of morphological diversity in the braincase, jaws and gill arches. These character systems are directly related to feeding and therefore suggest that there has been a high rate of morphological evolution towards exploiting new feeding strategies. Four assemblades of taxa, two of which are reasonably well supported clades, based on feeding strategies are recognized becoming increasingly specialized: i) generalized piscivore, secondarily feeding on invertebrates; ii) generalized invertebrate and piscivore feeder; iii) herbivore and iv) hard-bodied

invertebrate feeder. One ambiguity in this hypothesis is the taxon *Argyrozona*, which from its jaw morphology, suggests a dominantly piscivorous diet, groups with taxa which are herbivorous. However, in the ordered analysis, this taxon is found to be basal, forming a clade with *Dentex*, which is also largely piscovorous.

The evolution of feeding strategies has thus been mirrored by the evolution of certain morphological complexes. This would appear to be a similar scenario for the Scaridae, which have also evolved several different modes of feeding (Bellwood 1996). However, unlike, many specialized feeders of hard-bodied invertebrates, the specialized feeding adaptations found in some sparids are not necessarily restricted to the tropics. Furthermore, herbivory is rare in percoid fish, yet a related group of sparids clearly feed on plant matter as a dominant part of their diet. The broad range of feeding strategies that are found within this family, suggests that the exploitation of different food types has been the key innovation towards the success of this family, both in terms of diversity (i.e. number of species) and their distribution.

Fossil specimens from the Eocene provide insights into early sparid morphology, as they contain a melange of cladistically primitive and derived features. Yet the fossil record of sparids is inadequate, in terms of answering questions regarding rates of morphological evolution, due to the absence of intermediate fossils. However, from their inclusion with the Recent taxa in phylogenetic analysis, a minimum age of origin for the group maybe postulated at 55Ma. Clearly, further fossils are needed in order to postulate rates of evolution, disparity and minimum ages of origin for the proposed feeding clades.

The major points of this thesis include:

- Sparids are a morphologically diverse group, with strong morphological adaptations observed in the braincase, jaws and gill arches.
- Sparidae is a monophyletic group.
- An internal phylogeny of sparids is proposed.
- The taxon *Centracanthus* is included as a member of the Sparidae due to its placement within the 'higher' sparids.
- The data contains significant amounts of homoplasy, causing increased conflict towards the base of the tree.
- The phylogeny of 'higher' sparids are better supported when judged by Bootstrap and Bremer support, whilst basal sparids are poorly supported.
- The likely ancestral area for the Sparidae is the Indo-Pacific.
- Four types of feeding strategy are recognized, becoming increasingly specialized in more cladistically derived taxa.
- Feeding strategies are considered the key innovation regarding the evolutionary success of the group.
- Fossil taxa from the Eocene contain a melange of cladistically primitive and advanced

characters.

- The fossil record provides a minimum age of origin for the group at 55Ma.

Further work and concluding remarks

One of the main implications of this study is that the diagnosis of the monophyly of the Sparidae will further aid studies of higher order relationships. It is only from defining lower order relationships such as at the family level that questions concerning the validity of higher order relationships may be successfully tackled. With particular relevance to this study is the large diversity of fishes that collectively form the assemblage Percoidei, the monophyly of which has yet to be ascertained.

However, the phylogeny presented here is based largely on osteological data and is by no means the complete picture. As with any phylogenetic study, the current picture is incomplete, and therefore requires further work in order to elucidate areas of conflict. Clearly, a more comprehensive knowledge of their morphology using additional information, such as myology and neuroanatomical data would provide a more informative analysis, as would comparison with molecular data. While there is still debate in phylogenetic inference as to whether data sets should be combined of analysed separately (see Chapter 3), these additional sources of data would greatly benefit knowledge of phylogeny. In addition, developmental series of individual species for obtaining ontogenetic information, although not utilised in this study due to time constraints, are important for testing the homology of osteological characters. Johnson (1993) emphasized the significance of ontogenic criterion, as this may help to reduce levels of homoplasy in data sets. Homoplasy is an apparent problem in percoid fishes and indeed throughout the other groups in the Percomorpha, and is particularly acute when investigating higher order relationships. If morphology is to be used to elucidate the complex history of these groups then ontogeny may indeed be an important consideration. At the very least it will help determine character polarity.

Furthermore, while there is still a great wealth of information to be obtained from non-traditional morphological characters (i.e. non-osteological) for use in phylogenetic inference, the evident homoplasy of many morphological characters poses several problems to the systematist. In the light of the conflict associated with these data sets, which is particularly acute when answering questions regarding high order relationships, it is perhaps to molecules that we should turn in order to help elucidate the relationships concerning these fishes. It is astounding that as yet that there has been no overall or partial phylogeny proposed for a group as large as the Percoidei which is one of the largest and diverse suborders of vertebrates.

REFERENCES

Agassiz, L. 1833-1844. *Recherches sur les poisson fossiles.* 1420pp., 396 pls.

Ahlstrom, E. H., J. L. Butler, and B. Y. Sumida. 1976. Pelagic stromateoid fishes (Pisces, Perciformes) of the eastern Pacific: kinds, distributions, and early life histories and observations on five of these from the northwest Atlantic. *Bulletin of Marine Science* **26:** 285-402.

Akazaki, M. 1962. *Studies on spariform fishes–anatomy, phylogeny, ecology and taxonomy.* Osaka Japan. 8° Kosugi co. Ltd., 368pp.

Allegrucci, G., A. Caccone, and V. Sbordoni. 1998. Cytochrome b sequence divergence in the European sea bass (*Dicentrarchus labrax*) and phylogenetic relationships among some Perciformes species. *Journal of Zoology, Systematic, Evolution Research* **37:** 149-156.

Allis, E. P. 1897. The cranial muscles and cranial and first spinal nerves in *Amia calva. Journal of Morphology* **12:** 487-808, pls 20-38.

Allis, E. P. 1898. The homologies of the occipital and the first spinal nerves of *Amia* and telosts. *Zoological Bulletin* **2:** 83-97.

Allis, E. P. 1903. Skull, cranial and first spinal muscles and nerves of *Scomber scomber. Journal of Morphology 18:* 45-328, 10 pls.

Allis, E. P. 1909. The cranial anatomy of mail-cheeked fishes. *Zoological, Stuttgart* **22:** 1-219, 8 pls.

Allis, E. P. 1919. The myodome amd trigemion-facialis chamber of fishes and the corresponding cavities in higher vertebrates. *Journal of Morphology* **32:** 207-322, 4 pls.

Alroy, J. 1994. Four permutation tests for the presence of phylogenetic structure. *Systematic Biology* **43:** 430-437.

Arambourg, C. 1927. Les poissons fossiles d'Oran. *Matériaux pour la carte géologique de l'Algérie* **6:** 1-298pp 45pls.

Archie, J. W. 1989. A randomisation test for phylogenetic information in systematic data. *Sysytematic Zoology* **38:** 329-252.

Baldwin, C. C., and G. D. Johnson. 1993. Phylogeny of the Epinephelinae (Teleostei: Serranidae). *Bulletin of Marine Science* **52:** 240-283.

Balwin, C. C., and G. D. Johnson. 1996. Interrelationships of Aulopiformes, p. 355-404. In: *Interrelationships of fishes,* M. L. Stiassny, R. L. Parenti and G. D. Johnson (eds.). Academic Press.

Barrett, M., M. J. Donoghue, and E. Sober. 1991. Against consensus. *Systematic Zoology* **40:** 486-493.

Barriel, V., and P. Tassy. 1998. Rooting with multiple outgroups: consenus versus parsimony. *Cladistics* **14:** 193-200.

Basagila, F. 1991. Interspecific gene differences and phylogeny of the Sparidae family (Perciformes, Teleostei), estimated from electrophoretic data on enzymatic tissue-expression. *Comparative Biochemistry Physiology* **99B:** 495-508.

Basagila, F. 1992. Comparative examination of soluble red muscle proteins of fifteen Sparidae species. *Journal of Fish Biology.* **40:** 557-566.

Bauchot, M. L., Hureau, J. C. 1986. Sparidae. In: *Fishes of the Northern-Eastern Atlantic and the Mediterranean, vol 2.* P. J. P. Whitehead, M. L. Bauchot, J. C. Hureau, J. Nielsen and E. Tortonese (eds.). United Nations Educational Scientific and Cultural Organization, Paris.

Bauchot, M. L., Hureau, J. C., and Miquel, J. C. 1981. Sparidae, Eastern Central Atlantic (Fishing areas 34, 47). In: *FAO species identification sheets for fishery purposes 4,* W. Fischer, G. Bianchi and W. B. Scott (eds.). Canada Funds in Trust Ottawa, Department of Fisheries and Oceans, Canada.

Baumel, J. J. 1993. *Handbook of Avian Anatomy: Nomina Anatomica Avium.* Nattall Ornithological Society, Cambridge, Massachusetts.

Bellwood, D. R. 1994. A phylogenetic study of the parrotfish family Scaridae (Pisces: Labroidei) with a revision of genera. *Records of the Australian Museum.* supplement **20:** 1-86.

Bellwood, D. R. 1996. The Eocene fishes of Monte Bolca: the earliest coral reef fish assemblage. *Coral Reefs* **15:** 11-19.

Bellwood, D. R. 1997. Reef fish biogeography: habitat associations, fossils and phylogenies. *Proceedings of the 8th International Coral Reef Symposium* 379-384.

Belon, P. 1555. *L'histoire de la nature des oyseaux.* Guillaume Cavellat, Paris.

Bianchi, G. 1984. Study on the morphology of five Mediterranean and Atlantic sparid fishes with a reinstatement of the genus Pagrus Cuvier, 1917. *Cybium* **8:** 31-56.

Blot, J. 1980. La fauna ichthyologique des gisements due Monte Bolca (Province de Vérone, Italie). Catalogue systématique présentant l'état actuel des recherches concernant cette faune. *Bulletin du Muséum National d'Histoire,* Paris **4:** 339-396.

Bock, W. J. 1963. Evolution and phylogeny in morphologically uniform groups. *American Naturalist* **97:** 265-285.

Bock, W. J. 1977. Foundations and methods of evolutionary classification, p. 851-895. In: *Major patterns in vertebrate evolution,* M. K. Hecht, P. C. Goody and B. M. Hecht (eds.). Plenum Press, New York,

Bonde, N. 1977. Cladistic classification as applied to vertebrates, p. 741-804. In: *Major patterns in vertebrate evolution,* M. K. Hecht, P. C. Goody and B. M. Hecht (eds.). Plenum Press, New York,

Bookstein, F. L. 1994. Can biometrical shape be a homologous character?, p. 197-227. In: *Homology: the hierarchial basis of comparative biology,* B. K. Hall (eds.). Academic Press, London.

Brady, R. H. 1983. Parsimony, hierarchy and biological implications, p. 49-59. In: *Proceedings of the Second Meeting of the Willi Hennig Society. Advances in Cladistics 2,* N. Platnick and V. Funk (eds.). Columbia University Press, New York,

Bremer, K. 1988. The limits of amino acid sequence data in angiosperm phylogenetic reconstruction. *Evolution* **42:** 795-803.

Bremer, K. 1992. Ancestral areas: A cladistic reinterpretation of the centre of origin concept. *Systematic Biology* **41:** 436-445.

Bremer, K. 1994. Branch support and tree stability. *Cladistics* **10:** 295-304.

Bremer, K. 1995. Ancestral areas: optimization and probability. *Systematic Biology* **44:** 255-259.

Brower, A. V. Z., and V. Schawaroch. 1996. Three steps of homology assessment. *Cladistics* **12:** 265-272.

Bryant, H. N. 1989. An evaluation of cladistic and character analyses as hypothetico-deductive procedures, and the consequences for character weighting. *Systematic Zoology* **38:** 214-227.

Buchardt, B. 1978. Oxygen isotope palaeotemperatures from the Tertiary period in the North Sea area. *Nature* **275:** 121-123.

Carpenter, J. M. 1992. Random cladistics. *Cladistics* **8:** 147-53.

Carpenter, K. E., and T. M. Orrell. 1999. Osteological and molecular evidence refuting the monophyly of traditional subfamilies of the Sparidae (Percoidea: Perciformes) *Seventy-Ninth Annual Meeting of the American Society of Ichthyologists and Herpetologists.* [Abstract]

Casier, E. 1966. *Faune ichthyologique du London Clay.* British Museum (Natural History), 496pp 68pls.

Chappill, J. A. 1989. Quantitive characters in phylogenetic analysis. *Cladistics* **5:** 217-234.

Choat, J. H. 1991. The biology of herbivorous fishes on coral reefs, p. 120-155. In: *The ecology of fishes on coral reefs,* P. F. Sale (eds.). Academic Press,

Clark, G. A. J. 1993. Termini situm et directionem partium corporis indicantes, p. 1-6. In: *Handbook of Avian Anatomy: Nomina Anatomica Avium,* J. J. Baumel (eds.). Nuttall Ornithological Society, Cambridge, Massachusetts.

Coates, A. G., and O. F. M. 1996. The geological evolution of the Central American Isthmus, p. 21-104. In: *Evolution and environment in tropical America,* J. B. C. Jackson, A. F. Budd and A. G. Coates (eds.). University of Chicago Press.

Collinson, M. E. 1983. *Fossil plants of the London Clay.* The Palaeontological Association, London, 121pp.

Cracraft, J. 1978. Science, philosphy, and systematics. *Systematic Zoology* **27:** 213-216.

Croizat, L. 1958. *Panbiogeogeography.* Published by the author, Caracas.

Croizat, L. 1964. *Space, time form: the biological synthesis.* Published by the author, Caracas.

Croizat, L. 1982. Vicariance, vicariism, panbiogeography, 'vicariance biogeography', etc. a clarification. *Systematic Zoology* **31:** 291-304.

Cuvier, G. 1817. *Le régne animal distribué d'après son organisation, pour servir de base à l'histoire naturelle des animaux et d'introduction à l'anatomie comparée.* Nouvelle édition, Paris, **1:** 272

Darwin, C. 1859. *On the origin of species by means of natural selection, or the preservation of favoured races in the struggle for life.* John Murray, London.

Day, J. J. 1999. A new species of labrid fish (Teleostei: Perciformes) from the Early Miocene of Northern Cape Province, South Africa. *Tertiary Research* **19:** 85-89.

de Blainville, 1818. H. D. Poissons fossile Nouveau Dictionnaire d'Histoire Naturelle **27:** 349.

de Jong, H. 1998. In search of historical biogeographic patterns in the western Mediterranean terrestrial fauna. *Biological Journal of the Linnean Society* **65:** 99-164.

de Pinna, M. C. C. 1991. Concepts and tests of homology in the cladistic paradigm. *Cladistics* **7:** 367-394.

de Pinna, M. C. C. 1996. Comparative biology and systematics: some controversies in retrospective. *Journal of Comparative Biology* **1:** 3-16.

Donoghue, M., and M. Sanderson. 1992. The suitability of molecular and morphological evidence in reconstructing plant phylogeny, p. 340-368. In: *Molecular systematics of plants,* P. Soltis, D. Soltis and J. Doyle (eds.). Chapman and Hall, New York,

Doyle, J. A., and M. J. Donoghue. 1987. The importance of fossils in elucidating seed plant phylogeny and macroevolution. *Reviews in Palaeobotany and Palynology* **50:** 63-95.

Eldredge, N., and J. Cracraft. 1980. *Phylogenetic patterns and evolutionary process.* Columbia University Press, New York,

Enghoff, H. 1993. Phylogenetic biogeography of a Holarctic group: the julidan millipedes. Cladistic subordinateness as an indicator of dispersal. *Journal of Biogeography* **20:** 252-536.

Eriksson, T., and N. Wikström. 1995. *Autodecay.* Version 3.0. Apple Macintosh computer programme.

Eschymeyer, W. N., Ed. 1998. *Catalogue of fishes,* Californian Academy of Sciences.

Faith, D. P., and P. S. Cranston. 1991. Could a cladogram this short have arisen by chance alone?: on permutation tests for cladistic structure. *Cladistics* **7:** 1-28.

Farris, J. S. 1983. The logical basis of phylogenetic analysis, p. 7-36. In: *Advances in Cladistics,* N. I. Platnick and V. A. Funk (eds.). Columbia University Press, New York,

Farris, J. S. 1988. *Hennig86.* Version 1.5 manual; software and MSDOS program.

Farris, J. S. 1989. The retention index and rescaled consistency index. *Cladistics* **5:** 417-19.

Farris, J. S., M. Källersjö, A. G. Kluge, and C. Bult. 1995. Testing significance of incongruence. *Cladistics* **10:** 315-319.

Farris, J. S., A. G. Kluge, and M. J. Eckhardt. 1970. A numerical approach to phylogenetic systematics. *Systematic Zoology* **19:** 172-89.

Felsenstein, J. 1982. Numerical methods for inferring evolutionary trees. *Quarterly Review of Biology* **57:** 379-404.

Felsenstein, J. 1988. Phylogenies and quantitative characters. *Annual Review of Ecology and Systematics* **19:** 445-71.

Fischer, W. 1973. Mediterranean and Black Sea (Fishing area 37). *FAO species identification sheets for fishery purposes.* Food and Agriculture Organization of the United Nations, Rome, 1.

Fischer, W. 1978. Western Central Atlantic (Fishing area 31). *FAO species identification sheets for fishery purposes.* Food and Agriculture Organization of the United Nations, Rome, 5.

Fischer, W., G. Bianchi, and W. B. Scott. 1981. Eastern Central Atlantic (Fishing areas 34, 47). *FAO species identification sheets for fishery purposes.* Canada Funds in Trust Ottawa, Department of Fisheries and Oceans, Canada, 4.

Fischer, W., and G. Bionchi. 1984. Western Indian Ocean (Fishing area 51). *FAO species identification sheets for fishery purposes.* Food and Agriculture Organization of the United Nations, Rome, 4.

Fischer, W., and P. J. P. Whitehead. 1974. Eastern Indian Ocean (Fishing area 57). *FAO species identification sheets for fishery purposes.* Food and Agriculture Organization of the United Nations, Rome, 3.

Forey, P. L. 1992. Fossils and cladistics, p. 124-136. In: *Cladistics: a practical course in systematics*, 10. P. L. Forey, C. J. Humphries, I. L. Kitching, R. W. Scotland, D. J. Siebert and D. M. Williams (eds.). Oxford University Press.

Forey, P. L., C. J. Humphries, I. L. Kitching, R. W. Scotland, D. J. Siebert, and D. M. Williams. 1992. *Cladistics: a practical course in systematics.* Oxford University Press. Oxford University Press, Systematics Association Publication no. 11:pp191.

Forey, P. L., and I. J. Kitching. in press. Exeriments in coding mulistate characters, In: *Homology and systematics,* R. W. Scotland and T. W. Pennington (eds.). Taylor and Francis.

Frey, E. 1988. Anatomie des Köperstammes von *Alligator mississippiensis* Daudin. *Stuttgarter Beiträge zur Natrkunde* **424:** 106.

Fujita, K. 1990. *The caudal skeleton of teleostean fishes.* Tokai University Press, Tokyo. 897pp.

Gaffney, E. S. 1979. An introduction to the logic of phylogeny reconstruction, p. 79-111. In: *Phylogenetic analysis and paleontology,* J. Cracraft and N. Eldredge (eds.). Columbia University Press, New York.

Garland, T., and S. C. Adolphi. 1994. Why not to do two species comparative studies: limitations on inferring adaptation. *Physiological Zoology* **67:** 797-828.

Garrido-Ramos, M. A., M. Jamilena, R. Lozano, S. Cárdenas, C. Ruiz Rejón, and M. Ruiz Rejón. 1995. Phylogenetic relationships of the Sparidae family (Pisces, Perciformes) inferred from satellite-DNA. *Hereditas* **122:** 1-6.

Gauthier, J., A. G. Kluge, and T. Rowe. 1988. Amniote phylogeny and the importance of fossils. *Cladistics* **4:** 105-209.

Gill, A. C., and R. D. Mooi. 1993. Monophyly of the Grammatidae and of the Notograptidae, with evidence for their phylogenetic positions among perciforms. *Bulletin of Marine Science* **52:** 327-350.

Godkin, C. M., and R. Winterbottom. 1985. Phylogeny of the family Congrogadidae (Pisces: Perciformes) and its placement as a subfamily of the Pseudochromidae. *Bulletin of Marine Science* **36:** 633-671.

Goodrich, E. S. 1930. *Studies on the structure and development of vertebrates.* Macmillan, London. 837pp., 754 figs.

Gosline, W. A. 1961. The perciform caudal skeleton. *Copeia* **1961:** 265-270.

Gosline, W. A. 1966. The limits of the fish family Serranidae, with notes on other lower percoids. *Proceedings of the California Academy Sciences* **33:** 91-111.

Greenwood, P. H. 1976. A review of the family Centropomidae (Pisces, Perciformes). *Bulletin of the British Museum (Natural History) Zoology* **29:** 81.

Greenwood, P. H. 1986. The *pars jugularis* and the intrarelationships of cichlid fishes (Labroidei, Teleostei). *Journal of Natural History* **20:** 949-974.

Greenwood, P. H., D. E. Rosen, S. H. Weitzman, and E. Myers. 1966. Phyletic studies of teleostean fishes with a provisional classification of living forms. *Bulletin of the American Museum of Natural History.* **131:** 339-456.

Günther, A. C. L. G. 1859-70. *Catalogue of fishes in the British Museum.* British Museum, London. 1-8.

Harland, W. B., R. L. Armstrong, A. V. Cox, L. E. Craig, A. G. Smith, and D. G. Smith. 1990. *A geologic time scale.* Cambridge University Press, Cambridge. 263pp.

Hauser, D. L., and W. Presch. 1991. The effect of ordered characters on phylogenetic reconstruction. *Cladistics* **7:** 243-265.

Hawkins, J. A., C. E. Hughes, and R. W. Scotland. 1997. Primary homology assessment, characters and character states. *Cladistics* **13:** 275-283.

Heemstra, P. C. and J. E. Randall. 1977. A revision of the Emmelichthyidae (Pisces: Perciformes). *Australian Journal of Marine and Freshwater Research* **28:** 361-96.

Helfman, G. S., B. B. Collette, and D. E. Facey. 1997. *The diversity of fishes.* Blackwell Science, 528pp.

Hennig, W. 1950. *Grundzüge einer theorie der phylogenetischen systematik.* Deutsche Zentralverlag, Berlin.

Hennig, W. 1966. *Phylogenetic systematics.* University of Illinois Press, Urbana, Illinois.

Herrick, C. J. 1899. A contribution upon the cranial nerves of the cod fish. The *Journal of Comparative Neurlogy* **10:** 265-322, pls 21-22.

Herrick, C. J. 1899. The cranial and first spinal nerves of *Menidia*; A contribution upon the nerve components of bony fish. *Journal of Comparative Neurology* **9:** 153-455, pls 14-20.

Hilderbrand, M. 1995. *Analysis of vertebrate structure.* Wiley, New York. 657pp.

Horn, M. H. 1989. Biology of marine herbivorous fishes. *Oceanography and Marine Biology Annual Review* **27:** 167-272.

Huelsenbeck, J. P., J. J. Bull, and C. W. Cunningham. 1996. Combining data in phylogenetic analysis. *TREE* **11:** 152-158.

Huggett, J. M., and A. S. Gale. 1998. Petrography and diagenesis of the Thames Group at Whitecliff Bay, Isle of Wight, U.K. *Proceedings of the Geologists Association* **109:** 99-113.

Humann, P., *Reef fish identification: Florida, Caribbean and Bahamas,* N. Deloach (ed.). New World Publications, Inc. Florida. 396pp

Hume, D. 1739. *Treatise of Human Nature: Book I — The Inference from the Impression to Idea.* Fontana/Collins. 383pp

Humphries, C. J., and L. R. Parenti. 1999. *Cladistic biogeography.* Oxford biogeography series no. 12. Oxford University Press. 187pp.

Janvier, P. 1984. Cladistics: theory, purpose and evolutionary implications, p. 39-75. In: *Evolutionary theory paths into the future,* J. W. Pollard (eds.). Wiley Interscience, New York.

Jardine, N. 1969. The observational and theoretical components of homology: a study on the morphology of the dermal skull-roofs of rhidpidistian fishes. *Biological Journal of the Linnean Society* **1:** 327-361.

Johnson, G. D. 1975. The procurrent spur: an unpublished perciform caudual character and its phylogenetic implications. *Occasional papers of the California Academy of Sciences* **121:** 1-23.

Johnson, G. D. 1980. The limits and relationships of the Lutjanidae and associated families. *Bulletin of the Scripps Institution of Oceanography of the University of California* **24:** 1-114.

Johnson, G. D. 1983. *Niphon spinosus*: a primitive epinepheline serranid, with comments on the monophyly and intrarelationships of the Serranidae. *Copeia* **1983:** 777-787.

Johnson, G. D. 1984. Percoidei: development and relationships, p. 760 (464-499). In: *Ontogeny and Systematics of Fishes,* Special Publication Number 1. American Society of Ichthyologists and Herpetologists, La Jolla, California.

Johnson, G. D. 1986. Scombroid phylogeny: an alternative hypothesis. *Bulletin of Marine Science* **39:** 1-41.

Johnson, G. D. 1993. Percomorph phylogeny: progress and problems. *Bulletin of Marine Science* **52:** 1-28.

Johnson, G. D., and R. A. Fritzsche. 1989. *Grasus nigra*, an Omnivorous Girellid, with a comparative osteology and comments on relationships of the Girellidae (Pisces: Perciformes). *Proceedings of the Academy of Natural Sciences of Philadelphia* **141:** 1-27.

Johnson, G. D., and C. Patterson. 1993. Percomorph phylogeny: a survey of acanthomorphs and a new proposal. *Bulletin of Marine Science* **52:** 554-626.

Jordan, D. S., and B. Fesler. 1893. A review of the sparoid fishes of America and Europe. *Report of U.S. Commercial Fisheries* **1889-91:** 421-544, 55pls.

Jollie, M. 1985. A primer of bones for the understanding of the actinoptergian head and pectoral girdle. *Canadian Journal of Zoology* **64:** 365-379.

Kardong, K. V. 1995. *Vertebrates.* Wm. C. Brown Publishers, 777pp.

King, C. 1981. The stratigraphy of the London Clay and associated deposits. *Tertiary Research Special Paper* **6:** 158.

Kitching, I. J., P. L. Forey, C. J. Humphries, and D. M. Williams. 1998. *Cladistics: the theory and practice of parsimony analysis.* Oxford University Press, Systematics Association Publication no. 11: 228.

Klassen, G. J., R. D. Mooi, and A. Locke. 1991. Consistency indicies and random data. *Systematic Zoology* **40:** 446-457.

Kluge, A. G. 1998. Total evidence or taxonomic congruence: cladistics or consensus classification. *Cladistics* **14:** 151-158.

Koopman, K. F. 1981. (Discussion of) Taxon pulses, vicariance and dispersal, p. 184-7. In: *Vicariance biogeography: a critique,* G. Nelson and D. E. Rosen (eds.). Columbia University Press, New York.

Lauder, G. V., and K. F. Liem. 1983. The evolution and actinopterygian fishes. *Bulletin of the Museum of Comparitive Zoology* **150:** 95-197.

Le Quesne, W. J. 1969. A method of selection of characters in numerical taxonomy. *Systematic Zoology* **18:** 201-205.

Liebherr, J. 1989. General patterns in West Indian insects, and graphical biogeographic analysis of some circum-Caribbean Platynus beetles (Carabidae). *Systematic Zoology* **37:** 385-409.

Lipscomb, D. L. 1992. Parsimony, homology and the analysis of mulistate characters. *Cladistics* **8:** 45-65.

Mabee, P. M. 1988. Supraneural and predorsal bones in fishes: development and homologies. *Copeia* **1988:** 827-838.

Maddison, W. P. 1993. Missing data versus missing characters in phylogenetic analysis. *Systematic Biology* **42:** 576-581.

Maddison, W. P., and D. R. Maddison. 1992. *MacCLADE: Analysis of Phylogeny and Character Evolution.* Version 3.0.1. Sinauer Associates, Sunderland, Massachusetts,

Matsubara, K. 1943. Studies on the scorpaenid fishes of Japan (I and II). *Transactions of the Sigenkagaku Kenkyusyo (Tokyo)* 1-486.

Mayr, E. 1974. Cladistic analysis or cladistic classification? *Zoologische Systematik Evolutionsforschung* **12:** 94-128.

McAllister, D. E. 1968. Evolution of branchiostegals and association of the opercular, gular, and hyoid bones and the classification of teleostome fishes, living and fossil. *Bulletin of the Natural Museum Canada* **221:** 1-239.

McCune, A. R. 1987. Towards the phylogeny of a fossil species flock: semionotid fishes from a lake deposit in the early Jurassic Towaco Formation, Newark Basin. *Peabody Museum Bulletin* **43:** 1-108.

Meacham, C. A. 1994. Phylogenetic relationships at the basal radiation of angiosperms: further study by probability of character compatibility. *Systematic Botany* **19:** 506-522.

Meier, R. 1994. On the inappropriateness of presence/absence recoding for non-additive multistate characters in computerized cladistic analyses. *Zoologischer Anzeiger* **232:** 201-212.

Mickevich, M. F., and S. J. Weller. 1990. Evolutionary character analysis: tracing character change on a cladogram. *Cladistics* **6:** 137-70.

Monod, T. 1967. Le complexe urophore des téléosteans: Typologie et evolution (note préliminaire). *Colloques Internationaux Centre National de la Recherche Scientifique* **163:** 111-131.

Monod, T. 1968. Le complexe urophore des poissons téléostéans. *Mémoires de l'Institut Fondamental d' Afrique Noire* **81:** 1-705.

Müller, J. 1844. Über den Bau und die Grezen der Ganoiden und über das natuliche system der Fische. *Sitzsungsberichte der Deutschen Akademie der Wissenschaften zu Berlin* **1844:** 416-422.

Müller, J. 1845. Über den Bau und die Grenzen der Ganoiden und über naturliche system der Fische. *Archiv fuer Naturgeschichte* **11:** 91-141.

Müller, J. 1846. Über den Bau und die Grenzen der Ganoiden und über das naturliche system der Fische. *Physikalische Mathematische Abhandlungen der Königlichen Akademie der Wissenschaften zu Berlin* **1846:** 117-216 [English translation by J. W. Griffith, 1846, *Scientific Mememoirs* **4:** 499-588].

Munro, I. S. R. 1949. Revision of Australian silver breams *Mylio* and *Rhabdosargus*. *Memoirs of the Queensland Museum*, **12**(4).

Neal, J. E. 1996. A summary of Paleogene sequence stratigraphy on northwest Europe and the North Sea, p. 15-42. In: *Correlation of Early Paleogene in Northwest Europe,* Special publication 101. R. W. O. B. Knox, R. M. Corfield and R. E. Dunay (eds.). The Geological Society.

Nelson, G. J. 1969. Gill arches and the phylogeny of fishes with notes on the classification of vertebrates. *Bulletin of the American Museum of Natural History* **141:** 475-552.

Nelson, G. J. 1989. Species and taxa: systematics and evolution, p. 60-81. In: *Speciation and its consequences,* D. Otto and J. A. Endler (eds.). Sinauer Associates, Sunderland, Massachusetts.

Nelson, G. J. 1978. Ontogeny, phylogeny, palaeontology and the biogenetic law. *Systematic Zoology* **27:** 324-345.

Nelson, G. J., and N. I. Platnick. 1981. *Systematics and biogeography: cladistics and vicariance.* Columbia University Press, New York.

Nelson, J. S. 1994. *Fishes of the World.* Wiley, New York. 600pp.

Nixon, K., C, and Q. D. Wheeler. 1992. Extinction and the origin of species, p. 1-253. In: *Extinction and phylogeny,* M. J. Novacek and Q. D. Wheeler (eds.). Columbia University Press, New York.

Nixon, K. C., and J. M. Carpenter. 1993. On outgroups. *Cladistics* **9:** 413-426.

Novacek, M. J. 1992. Fossils as critical data for phylogeny, p. 46-88. In: *Extinction and phylogeny,* M. J. Novacek and Q. D. Wheeler (eds.). Columbia University Press,

Orrell, T. M. 1999. Parsimony analysis of molecular data refutes the monophyly of traditional subfamilies (Percoidea: Perciformes) *Seventy-Ninth Annual Meeting of the American Society of Ichthyologists and Herpetologists.* [Abstract]

Osbourne, R., and D. Tarling. 1996. *The historical atlas of the Earth.* Henry Holt, New York.

Otero, O. 1997. *Paléoichthyofaune de l'Oligo-Miocène de la Plaque Arabique, approches phylogénétique, paléoenvironnementale et paléobiogéographique.* Ph.D. Thesis, l'Universite Claude Bernard, Lyon 1.

Owen, R. 1843. Lectures on the comparative anatomy and physiology of invertebrate animals. Royal College of Surgeons, London. Longman, Brown, Green and Longmans, London.

Panchen, A. L. 1992. *Classification, evolution and the nature of biology.* Cambridge University Press, Cambridge and New York. 403pp.

Panchen, A. L. 1994. Richard Owen and the concept of homology, p. 21-62. In: *Homology: the hierarchial basis of comparative biology,* B. K. Hall (eds.). Academic Press.

Patterson, C. 1964. A review of Mesozoic Acanthopterygian fishes, with special reference to those of the English Chalk. *Philosophical Transactions of the Royal Society* **247:** 213-483.

Patterson, C. 1968. The caudal skeleton in Meszoic acanthopterygian fishes. *Bulletin of the British Museum of Natural History, Geology* **17:** 47-102.

Patterson, C. 1975. The braincase of pholidophorid and leptolepid fishes, with a review of the actinopterygian braincase. *Philosophical Transactions of the Royal Society of London* **269:** 275-579.

Patterson, C. 1977. The contributions of paleontology to teleostean phylogeny, p. 579-643. In: *Major pattern of vertebrate evolution,* M. K. Hecht, P. C. Goody and M. K. Hecht (eds.). Plenum, New York.

Patterson, C. 1978. Verifiability in systematics. *Systematic Zoology* **27:** 218-222.

Patterson, C. 1981. Significance of fossils in determining evolutionary relationships. *Annual Review of Ecology and Systematics* **12:** 195-223.

Patterson, C. 1982. Morphological characters and homology. *Systematic Association Special Volume.* **21.** K. A. Joysey and A. E. Friday. Academic Press, London and New York.

Patterson, C. 1988. Homology in classical and molecular biology. *Molecular Biology and Evolution* **5:** 603-625.

Patterson, C. 1992. Supernumerary median fin-rays in teleostean fishes. Zoological *Journal of the Linnean Society 106:* 147-161.

Patterson, C. 1993a. An overview of the early fossil record of acanthomorphs. *Bulletin of Marine Science* **52:** 29-59.

Patterson, C. 1993b. Vertebrates, Osteichthyes: Teleostei, p. 621-657. In: *The Fossil Record 2,* M. J. Benton (eds.). Chapman and Hall.

Patterson, C. 1998. Comments on basal teleosts and teleostean phylogeny, by Gloria Arratia. *Copeia* 4: 1107-1113.

Patterson, C., and G. D. Johnson. 1995. The intermuscular bones and ligaments of teleostean fishes. *Smithsonian Contributions to Zoology* **559:** 1-85.

Pimentel, R. A., and R. Riggins. 1987. The nature of cladistic data. *Cladistics* **3:** 201-9.

Pirsig, R. M. (1974). *Zen and the Art of Motorcycle Maintenance.* Vintage.

Platnick, N. I. 1979. Gaps and prediction in classification. *Systematic Zoology* **27:** 472-474.

Platnick, N. I., and H. D. Cameron. 1977. Cladistic methods in textual, linguistic and phylogenetic analysis. *Systematic Zoology* **26:** 380-385.

Platnick, N. I., C. E. Griswold, and J. A. Coddington. 1991. On missing entries in cladistic analysis. *Cladistics* **7:** 337-343.

Pleijel, F. 1995. On character coding for phylogeny reconstruction. *Cladistics* **11:** 309-315.

Popper, K. 1962. *The open society and its enemies vol.2 Hegel and Marx.* Routledge and Kegan Paul, London.

Popper, K. R. 1992. *Realism and the aim of science.* Routledge, London.

Potthoff, T. 1983. Clearing and staining techniques, p. 760 (35-37). In: *Ontogeny and Systematics of fishes, Special Publication Number 1.* American Society of Ichthyologists and Herpetologists, La Jolla, California.

Rae, T. 1995. Continous characters and fossil taxa in phylogenetic reconstruction. *American Journal of Physical Anthropology* Supplement **20:** 176-177.

Rae, T. C. 1998. The logical basis for the use of continuous characters in phylogenetic systematics. *Cladistics* **14:** 221-228.

Randall, J. E. 1983. A review of the fishes of the subgenus *Goniistius* genus *Cheilodactylus*, with a descripition of a new species from Easter Island and Rapa. *Occasional Papers of the Bishop Museum* **25:** 1-24.

Regan, C. T. 1913. The classification of Percoid fishes. *Annals and Magazine of Natural History* **8:** 111-145.

Rieppel, O. C. 1992. Homology and logical fallacy. *Journal of Evolutionary Biology* **5:** 701-715.

Rieppel, O. C. 1988. *Fundamentals of comparative biology.* Birkhäuser Verlag, Basel. 1-202.

Roberts, C. 1993. The comparative morphology of spined scales and their phylogenetic significance in the Teleostei. *Bulletin of Marine Science* **52:** 60-113.

Rodrígues-Robles, J. A., and J. M. de Jesús-Escobar. 1999. Molecular systematics of New World lampropeltinine snakes (Colubridae): implications for biogeography and evolution of food habits. *Biological Journal of the Linnean Society* **68:** 355-385.

Rognes, K. 1973. Head skeleton and jaw mechanism in labrinae (Teleostei: Labridae) from Norwegian waters. *Arbok for Universetel I bergen. Matematisk - naturvitenskaplig* serie **1971:** 149pp, 21 pls.

Rojo, A. L. 1991. Dictionary of evolutionary fish osteology. CRC Press, Inc., Florida, U.S.A.

Ronquist, F. 1994. Ancestral areas and parsimony. *Systematic Biology* **43:** 267-274.

Ronquist, F. 1995. Ancestral areas. *Systematic Biology* **44:** 572-575.

Ronquist, F. 1996. DIVA version 1.1. Uppsala University, Uppsala, Sweden.

Ronquist, F. 1997. Dispersal-Vicariance Analysis: A new approach to the quantification of historical biogeography. *Systematic Biology* **46:** 195-203.

Rosen, B. R. 1988. Progress, problems and patterns in the biogeography of reef corals and other tropical marine organisms. *Helgolaender Wissenschaftliche Meeresuntersuchungen* **42:** 269-301.

Rosen, B. R. 1994. Neobiogeography *versus* palaeobiogeography, p. 291-303. In: Studies on Ecology and Palaeoecology of Benthic Communities, *Bollettino della Società Paleontologica Italiana* special volume 2. R. Matteucci, Carboni, M. G. and Pignatti, J. S. (eds.). Mucchi, Modena.

Rosen, B. R., and A. B. Smith. 1988. Tectonics from fossils? Analysis of reef-coral and sea urchin distributions from the late Cretaceous to Recent, using a new method., p. 317 (275-306). In: *Gondwana and Tethys, Special Publication Number 37.* M. G. Audrey-Charles and A. Hallam (eds.). Published for the Geological Society by Oxford University Press, Oxford.

Rosen, D. E. 1973. Interrelationships of higher euteleostean fishes., p. 397-514. In: *Interrelationships of Fishes,* P. H. Greenwood, R. S. Miles and C. Patterson (eds.). Zoological Journal of the Linnean Society, London.

Rosen, D. E. 1978. Vicariant patterns and historical explanation in biogeography. *Systematic Zoology* **27:** 159-88.

Rosen, D. E., and C. Patterson. 1990. On Müller's and Cuvier's concepts of pharyngognath and Labyrinth fishes, with an Atlas of Percomorph dorsal gill arches. *American Museum Novitates* **2983:** 1-57.

Russell, E. S. 1916. *Form and function: a contribution to the history of animal morphology.* John Murray, London.

Ruta, M. 1998. *The interrelationships of the anomalocystitid mitrates.* Ph.D. Thesis, University of London.

Ruta, M. 1999. A cladistic analysis of the anomalocystitid mitrates. *Zoological Journal of the Linnean Society* **127:** 345-421.

Sanderson, M. J., and M. J. Donoghue. 1989. Patterns of variation in levels of homoplasy. *Evolution* **43:** 1781-1795.

Schaeffer, B., and D. E. Rosen. 1961. Major adaptive levels in the evolution of the actinopterygian feeding mechanism. *American zoologist* **1:** 187-204.

Schoch, R. M. 1986. *Phylogeny reconstruction in palaeontology.* Van Nostrand Reinhold, New York.

Scotland, R. W., and D. L. Williams. 1993. Multistate characters and cladograms: when are two stamens more similar to three stamens than four? A reply to Lipscomb. *Cladistics* **9:** 343-350.

Siebert, D. J. 1992. Tree statistics; trees and 'confidence'; alternatives to parsimony; character weighting; character conflict and its resolution, p. 72-88. In: *Cladistics: a practical course in systematics,* P. L. Forey, C. J. Humphries, I. J. Kitching, R. W. Scotland, D. J. Siebert and D. M. Williams (eds.). Oxford University Press, Oxford.

Smith, A. S. 1994. *Systematics and the fossil record.* Blackwell Scientific Publications, Oxford. 223pp.

Smith, C. L., and R. M. Bailey. 1962. The subocular shelf of fishes. *Journal of Morphology* **110:** 1-17.

Smith, J. L. B. 1938. Sparidae and Denticidae. *Transactions of the Royal Society of South Africa,* **26:** 255.

Smith, J. L. B., and Smith M. M 1986. Family No. 183: Sparidae, p. 580-594. In: *Smith's sea fishes,* M. M. Smith and P. C. Heemstra (eds). Macmillian, South Africa, Johannesburg.

Smith-Vaniz, W. F., and G. D. Johnson. 1988. Redescription of *Gracila albomarginata* (Fowler and Bean) and *Cephalopholis polleni* (Bleeker) with comments on the generic limits of selected Indo-Pacific groupers (Pisces: Serranidae: Epinephelinae). *Proceedings of the Academy of Natural Sciences of Philadelphia* **140:** 1-23.

Sorbini, L. 1983. *La collezione Baja di pescie piante fossili de Bolca.* Museo Civico di Storia Naturale, Verona.

Springer, V. G., and W. C. Freihofer. 1976. Study of the monotypic fish family Pholidichthyidae (Perciformes). *Smithsonian Contributions Zoology* **216:** 43.

Stiassny, M. L. J. 1981. The phyletic status of the family Cichlidae (Pisces: Perciformes): a comparative anatomical investigation. *Netherlands Journal of Zoology* **31:** 275-314.

Stiassny, M. L. J. 1986. The limits and relationships of the acanthomorph teleosts. *Journal of Zoology* **1:** 411-460.

Stiassny, M. L. J. 1990. Notes on the anatomy and the relationships of the bedotiid fishes of Madagascar, with taxonomic revision of the genus *Rheocles* (Atherinomorpha: Bedotiidae). *American Museum Novitates* **2979:** 1-33.

Stiassny, M. L. J., and J. A. Moore. 1992. A review of the pelvic girdle of acanthomorph fishes, with comments on hypotheses of acanthomorph intrarelationships. *Zoological Journal of the Linnean Society* **104:** 209-242.

Swiderski, D. L., M. L. Zelditch, and W. L. Fink. 1998. Why morphometrics is not special: coding quantitative data for phylogenetic analysis. *Systematic Biology* **47:** 508-519.

Swofford, D. L. 1993. *PAUP: Phylogenetic Analysis Using Parsimony.* Version 3.1.1. Computer program distributed by the Illinois Natural History Survey, Champaign, Illinois.

Swofford, D. L. 1998. *PAUP* Phylogenetic Analysis Using Parsimony (*and other methods).* Version 4.0 Sinauer Associates, Sunderland, Massachusetts.

Swofford, D. L., and W. P. Maddison. 1987. Reconstructing ancestral character states under Wagner parsimony. *Mathematical Biosciences* **87:** 199-229.

Szalay, F. S. 1977. Phylogenetic relationships and a classification of the eutherian Mammalia, p. 315-374. In: *Major patterns in vertebrate evolution,* M. K. Hecht, P. C. Goody and M. K. Hecht (eds.). Plenum Press, New York.

Taylor, W. T., and G. C. Van Dyke. 1985. Revised procedures for staining and clearing small fishes and other vertebrates for bone cartilage study. *Cybium* **9:** 107-119.

Thiele, K. 1993. The Holy Grail of the perfect character: the cladistic treatment of morphometric data. *Cladistics* **9:** 275-304.

Tominaga, Sakamoto and Matsuura. 1996. Posterior extension of the swimbladder in percoid fishes, with a literature survey of other teleosts. *Bulletin of the University Museum, University of Tokyo*: **36:** 1-73.

Tominaga, Y. 1965. The internal morphology and systematic position of *Leptobrama mulleri*, formerly included in the family Pempheridae. *Japanese Journal of Ichthyology* **15:** 43-95.

Tomiyama, I. 1931. Comparative studies on the opisthotic bone of Sparidae. *Journal of the Faculty of Science, Tokyo University, Tokyo* **4:** 2(4): 309-317.

Toombs, H. A., and A. E. Nixon. 1959. The use of acids in the preparation of vertebrate fossils. *Curator 2*: 304-312

Van Neer, W. 1987. A study on the variability of the skeleton of *Lates niloticus* (Linnaeus, 1758) in view of the validity of *Lates maliensis* Gayet, 1983. *Cybium* **11:** 411-425.

Van Velzen, J., N. Bouton, and R. Zandee. 1998. A procedure to extract phylogenetic information from morphometric data. *Netherlands Journal of Zoology* **48:** 305-322.

Vari, R. P. 1978. Terapon perches (Percoidei, Teraponidae). A cladistic analysis and taxonomic revision. *Bulletin of the American Museum of Natural History* **159:** 177-340.

Vermeij, G. J. 1993. *A natural history of shells.* Princeton University Press, pp207.

Wagner, G. P. 1994. Homology and the mechanisms of development, p. 273-299. In: *Homology: the hierarchial basis of comparative biology,* B. K. Hall (eds.). Academic press,

Wake, M. H. 1993. Non-traditioal characters in the assessment of caecilian phylogenetic relationships. *Herpetological Monographs* **7:** 42-55.

Wake, M. H. 1994. The use of unconventional morphological characters in the analysis of systematic patterns and evolutionary processes, p. 173-200. In: *Interpreting the Hierarchy of Nature,* L. Grande and O. C. Rieppel (eds.). Academic Press, San Diego,

Weitzman, S. H. 1962. The osteology of *Brycon meeki*: a generalized characid fish, with an osteologiacl defintion of the family. *Stanford Ichthyological Bulletin* **8:** 3-77.

Westneat, M. W. 1993. Phylogenetic relationships of the tribe Cheilinini (Labridae: perciformes). *Bulletin of the Marine Science* **52:** 351-394.

Wiens, J. J. 1998. Does adding characters with missing data increase or decrease phylogenetic accuracy. *Systematic Biology* **47:** 625-640.

Wiley, E. O. 1975. Karl R. Popper, systematics, and classificaion: a reply to Walter Bock and other evolutionary taxonomists. *Systematic Zoology* **24:** 233-243.

Wiley, E. O. 1976. Phylogeny and biogeography of fossil and recent gars. *Miscellaneous publications of the Museum of Natural History, University of Kansas* **64:** 1-111.

Wiley, E. O. 1981. *Phylogenetics: the theory and practice of phylogenetic systematics.* Wiley Interscience, New York.

Wilkinson, M. 1992. Ordered versus unordered characters. *Cladistics* **8:** 375-385.

Wilkinson, M. 1995a. A comparison of two methods of character construction. *Cladistics* **11:** 297-308.

Wilkinson, M. 1995b. Coping with missing entries in phylogenetic inference using parsimony. *Systematic Biology* **44:** 501-514.

Wilkinson, M. 1995c. *TAXEQ$_2$ software and documentation.* School of Biological Sciences, University of Bristol,

Wilkinson, M. 1995d. *PICA$_{95}$ software and documentation.* School of Biological Sciences, University of Bristol,

Wilkinson, M. 1997. Characters, congruence and quality: a study of neuroanatomical and tradional data in caecilian phylogeny. *Biological Review* **72:** 423-470.

Wilkinson, M., and M. J. Benton. 1995. Missing data and rhynchosaur phylogeny. *Historical Biology* **10:** 137-150.

Wilkinson, M., and M. J. Benton. 1996. Sphenodontid phylogeny and the problems of multiple trees. *Philosophical Transactions of the Royal Society, London, Series B* **351:** 1-16.

Wilkinson, M., and R. A. Nussbaum. 1997. Comparative morphology and evolution of the lungless caecilian *Atretochoana eiselti* (Taylor) (Amphibia: Gymnophiona: Typhlonectidae). *Biological Journal of the Linnean Society* **62:** 39-109.

Wilkinson, M., and R. A. Nussbaum. 1999. Evolutionary relationships of the lungless caecilian Atretochoana eiselti (Amphibia: Gymnophiona: Typhlonectidae). *Zoological Journal of the Linnaean Society* **126:** 191-223.

Winterbottom, R. 1974. A descriptive synonomy of the striated muscles of the teleostei. *Proceedings of the Academy of natural Sciences of Philadelphia* **125:** 225-317.

Winterbottom, R., and D. A. McLennan. 1993. Cladogram versatility: evolution and biogeography of acanthuroid fishes. *Evolution* **47:** 1557-71.

Witmer, L. M. 1997. The evolution of the antorbital cavity of archosaurs: A study in soft-tissue reconstruction in the fossil record with an analysis of the function of pneumaticity. *Journal of Vertebrate Palaeontology Memoir 3* **17** (supplement to number 1): 1-73.

Yabe, M. 1985. Comparative osteology and myology of the superfamily Cottoidea (Pisces: Scorpaeniformes) and its phylogenetic classification. *Memoirs of the Faculty of Fisheries, Hokkaido University* **32:** 1-130.

Zelditch, M. L., W. L. Fink, and D. L. Swiderski. 1995. Morphometrics, homology and phylogenetics: quantified characters as synapomorphies. *Systematic Biology* **44:** 179-189.

SPECIMEN LIST

The type of preservation of each specimen was recorded as follows: alc = alcohol specimen, cs cleared and stained, dis = dissected alcohol specimen, rad = radiograph, sk = dried skeleton.

PERCOIDEI

Centropomidae

Centropomus unidecimalis BMNH 1883.12.16 (sk)

Centropomus pedimacula BMNH 1894.12.10 (sk)

Lutjanidae

Lutjanus aya BMNH 1899.2.9 (sk)

Lutjanus griseus UF 92012 x2 (cs)

Lutjanus macolor BMNH 1958.4.21 (sk)

Haemulidae

Haemulon plumieri AMNH 93254 (sk); AMNH 56786 SL210 (sk); AMNH 56916 SL200 (sk); AMNH 093254 SL 182 (sk); UF 10912 (cs)

Haemulon chromis BMNH 44.5.14.58 SL145 (sk)

SPAROIDEA

Centracanthus

Centracanthus cirrus BMNH 1895. 5. 28 (sk)

Spicara smaris USNM 290493 (cs); BMNH 1963.5.14 (rad)

Lethrinidae

Gnathodentex aurolineatus USNM 290485 (cs)

Gymnocranius griseus USNM 290494 (cs); BMNH 1986.9.29 (rad)

Lethrinus miniatus AMNH 099522 SL320 (sk); AMNH 214032 SL265 (sk)

Lethrinus nebulosus AMNH 099144 SL260 (sk); AMNH 099139 SL240 (sk)

Lethrinus rhodopterus USNM 290483 (cs)

Nemipteridae

Nemipterus celebrus AMNH 098982 (sk)

Nemipterus furcosus AMNH 098887 (sk)

Nemipterus hexod AMNH 098700 (sk)

Scolopsis bilineateus USNM 290482 (cs)

Sparidae

Acanthopagrus australis AMNH 98471 SL200 (sk)

Acanthopagrus butcheri AMNH 095778 SL260 (sk); AMNH 095773 SL250 (sk)

Acanthopagrus latus AMNH 099180 SL200 (sk); AMNH 099179 SL200 (sk); BMNH 1974.2.22 (cs); BMNH 1987.2.12 (rad)

Archosargus probatocephalus AMNH 94499 (sk); AMNH 94491 (sk); AMNH 79551 SL130 (sk); AMNH 56258 SL380 (sk); USNM 184241 x2 (cs)

Archosargus rhomboides AMNH 89527 SL200 (sk); AMNH 56976 SL184 (sk); AMNH 56900 SL176 (sk), AMNH 56809 SL159 (sk); USNM 342987 (cs)

Argyops bleekeri BMNH 1986.11.28 (rad)

Argyops spinifer AMNH 98386 SL215 (sk); AMNH 98387 SL310 (sk); AMNH 98388 (sk);

Argyops sp. BMNH 1946.5.10 (cs); BMNH 1979.3.23 (rad)

Argyrozona argyrozona J.L.B 28.1.1992 37367 (sk).

Boops boops AMNH 210627 SL188 (sk); AMNH 210598 SL242 (sk); BMNH 1982.5.10 (cs); BMNH 1895.5.28 (sk); BMNH 1964.8.6 (rad)

Boopsoidea inornata BMNH 1997.9.18 [former RUSI 37782] (cs); BMNH 1899.6.9 (rad)

Calamus arctifrons AMNH 88550 SL209 (sk); FMNH 7012 x2 (cs); BMNH 1884.7.7 (rad)

Calamus bajonado AMNH 093375 SL470 (sk); AMNH 35484 (sk); AMNH 088738 (sk); FMNH4907 x2 (cs); BMNH 1951.12.5 (rad)

Calamus calamus AMNH 35430 (sk); BMNH 1905.3.19 (sk).

Calamus campechanos AMNH 94509 (sk); AMNH 94510 (sk); AMNH 94508 (sk); AMNH 94507 (sk).

Calamus leucosteus AMNH 94607 SL220 (sk); AMNH 56263 SL285 (sk).

Calamus nodosus AMNH 56628 SL230 (sk).

Calamus penna BMNH 1985.7.16 (cs).

Calamus pennatula AMNH 56883 SL115.50 (sk).

Calamus proridens AMNH 56965 SL207 (sk); AMNH 56996 SL202 (sk); AMNH 88891 (sk).

Cheimerius nufar BMNH 1997.9.18 [RUSI 54042] (cs)

Chrysoblephus puniceps BMNH 1997.9.18 [RUSI 2707] (cs)
Chrysoblephus cristiceps BMNH 1997.9.18 [RUSI 2763] (cs)

Cymatoceps nasutus BMNH 1997.9.18 [RUSI 49904] (cs)

Crenidens crenidens BMNH 1951.1.16 (cs); BMNH 1898.6.29 (sk); BMNH 1984.2.13 (rad)

Dentex dentex BMNH 1945.6.22 (sk); BMNH 1910.4.19 (sk); BMNH 1967.2.1 160-164 (2cs + 2alc); BMNH 1988.2.3 (rad)
Dentex canariensis AMNH 88592 SL228 (sk)
Dentex macrophthalmus BMNH 1955.2.23 (cs); BMNH 1971.7.21 (rad)

Diplodus annularis BMNH 1997.9.18 [RUSI 36449]; BMNH 1983.10.11 (rad)
Diplodus bellotti BMNH 1975.5.4 (cs)
Diplodus cervinus AMNH 093383 SL395 (sk); BMNH 1997.9.18 [RUSI 38157] (cs); BMNH 1983.10.11 (cs); *Diplodus cervinus hottentotus* BMNH 1958.7.9 (rad)
Diplodus helenæ BMNH 1975.5.4 (rad)
Diplodus holbrookei AMNH 088782 SL260 (sk); AMNH 56325 SL200 (sk), AMNH 088785 (sk), AMNH 56956 SL124 (sk); BMNH 1933.10.12 (rad)
Diplodus noct BMNH 1951.1.16 (rad)
Diplodus rondeletii BMNH 1890.6.29 (sk); BMNH 1935.5.11 (cs)
Diplodus sargus BMNH 1953.11.1 (cs); *Diplodus sargus capensis* BMNH 1997.9.18 [RUSI 37791]
Diplodus vulgaris AMNH 210980 SL155 (sk); BMNH 1975.5.4 (rad)
Diplodus puntayyo AMNH 88896 SL330 (sk)

Evynnis cardinalis FMNH 57497 (cs)

Lagodon rhomboides BMNH 1948.8.6 (cs); AMNH 89317 SL142 (sk); AMNH 88507 SL314 (sk); AMNH 88624 (sk); AMNH 57567 (sk); UF 5184 (cs)

Lithognathus mormyrus BMNH 1855.9.19 (sk); BMNH 1982.5.10 (cs); BMNH 1997.9.18 [RUSI 8375] (cs); BMNH 1983.10.11 (rad)

Oblada melanurum BMNH 1898.1.26 (sk); BMNH 1859.9.19 (sk); BMNH 1978.7.20 (cs); BMNH 1898.1.26 (sk); BMNH 1862.6.20 (rad); BMNH 1898.1.26 (rad)

Pachymetopon aeneum 1997.9.18 [RUSI 44060] (cs)
Pachymetopon blochii 1997.9.18 [RUSI 38734] (cs)

Pagellus acarne BMNH 1983.10.11 (rad)

Pagellus affinis BMNH 1887.11.11 (sk); BMNH 1898.9.10 (rad)

Pagellus bellotii AMNH 088881 SL320 (sk); *Pagellus bellotiinatalensis* BMNH 1997.9.18 [RUSI 2813]

Pagellus erythrinus BMNH 1982.5.10 (cs); BMNH 1997.9.18 (cs); BMNH 1935.3.5 (rad)

Pagrus pagrus AMNH 56321 SL230 (sk); AMNH 210544 SL155 (sk); AMNH 218180 (sk); BMNH 1997.9.18 [RUSI 51516] (cs); BMNH 1890.1.3 (rad)

Polyamblydon germanum BMNH 1997.9.18 [RUSI 153544] (cs)

Polysteganus coeruleopunctatus BMNH 1997.9.18 [14134] (cs)

Polysteganus undulosus BMNH 1997.9.18 [RUSI 11708] (cs)

Porcostoma dentata BMNH 1997.9.18 [RUSI 43685] (cs)

Rhabdosargus haffa BMNH 1987.5.11 (rad)

Rhabdosargus sarba BMNH 1890.9.23 (sk); AMNH 217906 SL170 (sk); BMNH 1997.9.18 [RUSI 8638]; BMNH 1890.9.23 (sk)

Rhabdosargus globiceps BMNH 1997.9.18 [RUSI 13600] (cs)

Sarpa salpa BMNH 1997.9.18 [RUSI 11708] (cs); BMNH 1960.6.04 (cs); BMNH 1859.5.4 (sk); BMNH 1872.12.13 (rad)

Sparodon durbanensis BMNH 1997.9.18 [RUSI 34466] (cs)

Sparus auratus AMNH 093436 (sk); AMNH 093436 (sk); AMNH 88591 SL233 (sk); AMNH 88590 SL222 (sk); USNM 347127 (cs); BMNH 1938.11.1 (rad)

Sparus auriga AMNH 88593 SL273 (sk); BMNH 1936.4.14 (rad)

Sparus caeruleostrictus BMNH 1858.8.3 (sk); BMNH 1982.5.10 (cs); BMNH 1932.5.12 (rad); BMNH 1930.8.26 (rad).

Sparus pagrus AMNH 210945 SL255 (sk); AMNH 210958 SL275 (sk); AMNH 210944 SL207 (sk)

Spondyliosoma cantharus AMNH 211059 SL178 (sk); AMNH 210591 SL108 (sk); BMNH 1953.11.1 (cs); BMNH 1959.10.28 (rad); BMNH 1983.10.11 (rad)

Stenotomus caprinus AMNH 56604 SL190 (sk); AMNH 57973 SL 175 (sk); USNM 155372 (cs)

Stenotmus chrysops USNM 118315 (cs); BMNH 1997.9.18 [RUSI 10444] (cs)

List of apomorphies for the three equally parsimonous trees for both ACCTRAN and DELTRAN optimisations. Nodes correspond to those labelled on figure 3.1. Characters are represented in bold and are followed by their consistency index and by the relative character-state change. For those nodes which differ between trees, apomorphies are listed following the nodes outlined in figure 3.2.

Character-state optimization: Accelerated transformation (ACCTRAN)

Node 0 -> Node 1: 20: 1.000, 0 => 1; **28**: 1.000, 0 => 1; **48**: 0.667, 1 -> 2; **71**: 0.250, 2 -> 0; **79**: 1.000 0 => 1; **87**: 0.111, 1 -> 0. **Node 1 -> Node 5**: **2**: 0.167, 0 => 1; **67**: 0.200, 2 => 1; **73**: 1.000, 0 => 1. **Node 5 -> Node 7**: **25**: 0.200, 0 => 1; **26**: 1 0.250, 0 => 1; **27**: 0.250, 3 -> 1; 53, 0.333, 0 => 1. **Node 7 -> 11**: **2**: 0167, 1 => 0; **3**: 0.273, 1 => 2; **9**: 0.222, 1 => 2. **Node 11 -> Node 13**: **14**: 0.125, 1 -> 0; **39**: 0.222, 1 => 0; **59**: 0.250, 0 => 1; **67**: 0.200, 1 => 0; **70**: 0.143, 0 -> 1. **Node 13 -> Node 17**: **19**: 0.222, 0 => 2; **57**: 0.667, 1 => 2; **66**: 0.333, 1 => 2. **Node 17 -> Node 19**: **25**: 0.200, 1 => 0; **27**: 0.250, 1 -> 2; **58**: 0.333, 1 => 2; **86**: 0.222, 0 => 1; **87**: 0.111, 0 => 1. **Node 19 -> Node 27**: 3: 0.273, 2 => 0; **82**: 0.167, 1 => 0. **Node 27 -> Node 31**: **1**: 0.400, 1 => 2; **6**: 0.286, 1 => 0; **24**: 0.333, 1 => 0; **38**: 0.286, 0 -> 1; **51**: 0.250, 0 => 1; **63**: 0.500, 1 -> 0; **86**: 0.222, 1 => 2.. **Node 31 ->** *Centracanthus*: **26**: 0.250, 1 => 3; **29**: 0.750, 2 => 3; **38**: 0.286, 1 -> 2; **48**: 0.667, 2 => 1; **49**: 0.667, 0 => 1; **70**: 0.143, 1 => 0; **71**: 0.250, 0 => 1; **80**: 0.667, 1 => 2. **Node 31 -> Node 35**: **5**: 1.000, 0 => 1; **15**: 0.200, 0 => 1; **25**: 0.200, 0 => 1; **42**: 0.500, 1 => 3; **43**: 0.167, 1 -> 0; **46**: 0.400, 0 => 2; **58**: 0.333, 2 -> 1. **Node 35 -> Node 37**: **19**: 0.222, 2 => 1; **35**: 0.400, 0 => 1; **39**: 0.222, 0 => 1; **63**: 0.500, 0 -> 1; **76**: 0.167, 0 => 1. **Node 37 -> Node 39**: **2**: 0.167, 0 => 1; **3**: 0.273, 0 -> 1; **6**: 0.286, 0 => 1; **47**: 0.500, 1 => 2; **58**: 0.333, 1 -> 2; **67**: 0.200, 0 -> 1; **71**: 0.250, 0 => 1; **82**: 0.167, 0 => 1; **86**: 0.222, 2 -> 0. **Node 39 -> Node 41**: **3**: 0.273, 1 -> 2; **24**: 0.333, 0 => 1; **31**: 0.250, 0 => 1; **34**: 0.500, 1 => 2; **66**: 0.333 2 => 3; **67**: 0.200 1 -> 2; **87**: 0.111, 1 => 0. **Node 41 -> Node 43**: **19**: 0.222, 1 => 2; **26**: 0.250, 1 => 2; **32**: 0.333, 1 -> 2. **Node 43 -> Node 42**: **30**: 0.400, 1 => 2; **35**: 0.400, 1 => 2; **36**: 0.500, 0 => 1; **38**: 0.286, 1 -> 2; **39**: 0.222, 1 => 2; **40**: 0.500, 0 => 1; **50**: 0.200, 0 => 1; **69**: 0.167, 0 => 1. **Node 45 -> Node 47**: **3**: 0.273, 2 -> 3; **13**: 0.500, 0 => 2; **14**: 0.125, 0 -> 1; **32**: 0.333, 2 -> 1; **33**: 0.500, 0 -> 1; **37**: 0.500, 0 => 1; **45**: 0.250, 0 => 1; **46**: 0.400, 2 -> 0; **72**: 0.286, 1 => 2. **Node 47 -> Node 49**: **23**: 1.000, 1 => 2; **24**: 0.333, 1 => 2; **38**: 0.286, 2 -> 1; **43**: 0.167, 0 => 1; **44**: 0.333, 0 => 1; **51**: 0.250, 1 => 0. **Node 49 -> Node 51**: **3**: 0.273, 3 -> 2; **8**: 0.400, 0 => 1; **12**: 0.500, 0 => 1; **13**: 0.500, 2 => 1; **14**: 0.125, 1 -> 0; **22**: 0.500, 1 => 2; **26**: 0.250, 2 => 1; **33**: 0.500, 1 -> 0; **68**: 0.500, 0 => 1. **Node 51 -> Node 53**: **16**: 0.167, 0 -> 1; **87**: 0.111, 0 => 1. **Node 53 ->** *Archosargus*: **38**: 0.286, 1 => 2; **39**: 0.222, 2 => 1; **43**: 0.167, 1 => 0; **46**: 0.400, 0 => 1; **86**: 0.222, 0 => 1. **Node 53 -> Node 55**: **1**: 0.400, 2 => 1; **8**: 0.400, 1 => 2; **15**: 0.200, 1 => 0; **21**: 1.000, 0 => 1; **32**: 0.333, 1 -> 2. **Node 55 -> Node 57**: **12**: 0.500, 1 => 0; **16**: 0.167, 1 -> 0; **19**: 0.222, 2 => 0; **31**: 0.250, 1 => 0; **35**: 0.400, 2 => 1; **36**: 0.500, 1 => 0; **50**: 0.200, 1 => 0. **Node 57 ->** *Argyops*: **11**: 0.500, 0 => 1; **27**: 0.250, 2 => 1; **39**: 0.222, 2 => 1; **83**: 0.500, 0 => 1; **87**: 0.111, 1 => 0. **Node 57 ->** *Sparus*: **8**: 0.400, 2 => 0; **10**: 0.200, 0 => 1; **14**: 0.125, 0 => 1; **24**: 0.333, 2 => 1; **32**: 0.333, 2 -> 1; **72**: 0.286, 2 => 1; **74**: 0.286, 1 => 0; **76**: 0.167, 1 => 0; **86**: 0.222, 0 => 2. **Node 55 ->** *Calamus*: **6**: 0.286, 1 => 2; **9**: 0.222, 2 => 0; **13**: 0.500, 1 => 2; **26**: 0.250, 1 => 2; **42**: 0.500, 3 => 2; **84**: 0.500, 0 => 1. **Node 51 ->** *Acanthopagrus*: **70**: 0.143, 1 => 0; **72**: 0.286, 2 => 1; **74**: 0.286, 1 => 0; **76**: 0.167, 1 => 0. **Node 49 ->** *Rhabdosargus*: **9**: 0.222, 2 => 1. **Node 47 ->** *Diplodus*: **6**: 0.286, 1 => 2; **10**: 0.200, 0 => 1; **46**: 0.400, 0 -> 1; **86**: 0.222, 0 => 1. **Node 45 ->** *Sparodon*: **87**: 0.111, 0 => 1. **Node 43 ->** *Lagodon*: **16**: 0.167, 0 => 1; **67**: 0.200, 2 -> 1; **76**: 0.167, 1 => 0. **Node 41 ->** *Crenidens*: **1**: 0.400, 2 => 1; **45**: 0.250, 0 => 1. **Node 39 ->** *Polyamblyodon*: **9**: 0.222, 2 => 1; **15**: 0.200, 1 => 0; **27**: 0.250, 2 => 1; **50**: 0.200, 0 => 1; **69**: 0.167, 0 => 1; **72**: 0.286, 1 => 2; **86**: 0.222 0 -> 1. **Node 37-> *Sarpa***; **38**: 0.286, 1 -> 2; **81**: 0.500, 1 => 0. **Node 35 -> Node 34**: **27**: 0.250, 2 => 3; **41**: 0.286, 2 => 1. **Node 34 ->** *Boops*: **9**: 0.222, 2 => 1; **26**: 0.250, 1 => 0; **81**: 0.500, 1 => 0. **Node 34 ->** *Oblada*: **10**: 0.200, 0 => 1; **14**: 0.125, 0 => 1; **43**: 0.167, 0 -> 1; **51**: 0.250, 1 => 0; **74**: 0.286, 1 => 0; **87**: 0.111, 1 => 0. **Node 27 -> Node 28**: **11**: 0.500, 0 => 1; **41**: 0.286, 2 => 1; **53**: 0.333, 1 => 0; **74**: 0.286, 1 -> 0. **Node 28->** *Argyrozona*: **8**: 0.400, 0 => 1; **9**: 0.222, 2 => 1; **16**: 0.167, 0 => 1; **19**: 0.222, 2 => 1; **26**: 0.250, 1 => 0; **27**: 0.250, 2 => 3. **Node 28 ->** *Spondyliosoma*: **2**: 0.167, 0 => 1; **15**: 0.200, 0 => 1; **42**: 0.500, 1 => 0; **47**: 0.500, 1 => 0; **52**: 0.333, 1 => 0; **59**: 0.250, 1 => 0. **Node 19 -> Node 20**: **30**: 0.400, 1 => 2; **34**: 0.500, 1 => 2; **37**: 0.500, 0 => 1; **39**: 0.222, 0 => 1; **40**: 0.500, 0 => 1; **42**: 0.500, 1 => 2; **45**: 0.250, 0 -> 1; **47**: 0.500, 1 => 2. **Node 20 -> Node 24**: **26**: 0.250, 1 => 2; **31**: 0.250, 0 => 1; **76**: 0.167, 0 => 1. **Node 24 ->** *Lithognathus*: **3**: 0.273, 2 =>

0; **16**: 0.167, 0 => 1; **18**: 0.167, 1 => 0; **1**: 0.333, 1 => 2; **38**: 0.286, 0 => 1; **39**: 0.222, 1 => 2; **71**: 0.250, 0 => 1; **72**: 0.286, 1 => 2; **82**: 0.167, 1 => 0; **86**: 0.222, 1 => 0. **Node 24-> *Stenotomus***: **2**: 0.167, 0 => 1; **8**: 0.400, 0 => 1; **14**: 0.125, 0 => 1; **19**: 0.222, 2 => 1; **22**: 0.500, 1 => 2; **25**: 0.200, 0 => 1; **50**: 0.200, 0 => 1; **66**: 0.333, 2 => 3; **67**: 0.200, 0 => 1; **83**: 0.500, 0 => 1; **84**: 0.500, 0 => 1. **Node 20 -> Node 21**: **19**: 0.222, 2 => 0; **44**: 0.333, 0 => 1; **59**: 0.250, 1 => 0. **Node 21-> *Pagrus***; **16**: 0.167, 0 => 1; **35**: 0.400, 0 => 1; **66**: 0.333, 2 => 3; **67**: 0.200, 0 => 1; **71**: 0.250, 0 => 1. **Node 21 -> *Pagellus***: **14**: 0.125, 0 => 1; **18**: 0.167, 1 => 0; **45**: 0.250, 1 -> 0. **Node 17 -> *Pachymetopon***: **1**: 0.400, 1 => 2; **2**: 0.167, 0 => 1; **24**: 0.333, 1 => 0; **26**: 0.250, 1 => 2; **43**: 0.167, 1 => 0; **46**: 0.400, 0 => 2; 70: 0.143, 1 -> 0. **Node 13 -> Node 14:18**: 0.167, 1 => 0; **27**: 0.250, 1 -> 0; **30**: 0.400, 1 => 0. **Node 14 -> *Boopsoidea***: **15**: 0.200, 0 => 1; **26**: 0.250, 1 => 0; **27**: 0.250, 0 -> 3; **41**: 0.286, 2 => 1; **71**: 0.250, 0 => 1. **Node 14 -> *Cheimerus***: **3**: 0.273, 2 => 0; **25**: 0.200, 1 => 0; **66**: 0.333, 1 => 0; **67**: 0.200, 0 => 2; **69**: 0.167, 0 => 1. **Node 11 -> *Evynnis***: **10**: 0.200, 0 => 1; **71**: 0.250, 0 => 1. **Node 7 -> *Polysteganus***: **70**: 0.143, 0 => 1; **Node 5**: **-> *Porcostoma***: **35**: 0.400, 0 => 1; **60**: 0.333, 1 => 0; **87**: 0.111, 0 -> 1. **Node 1 -> Node 2**: **3**: 0.273, 1 -> 0; **18**: 0.167, 1 => 0; **30**: 0.400, 1 => 0; **74**: 0.286, 1 => 0; **75**: 0.500, 1 => 0. **Node 2 -> *Cymatoceps***: **27**: 0.250, 3 => 0; **53**: 0.333, 0 => 1; **58**: 0.333, 1 => 0; **66**: 0.333, 1 => 0; **69**: 0.167, 0 => 1. **Node 2 -> *Dentex***: **9**: 0.222, 0 => 1; **39**: 0.222, 1 => 0; **41**: 0.286, 2 => 1; **82**: 0.167, 1 => 0.

Tree 1: Node A -> B: **27**: 0.250, 1 -> 2. **Node A -> *Polysteganus***: **70**: 0.143 0 => 1. **Node B -> *Chrysoblephus***: **14**: 0.125, 0 => 1; **18**: 0.167, 1 => 0; **66**: 0.333, 1 => 2; **67**: 0.200, 1 => 2, **69**: 0.167 0 => 1

Tree 2: Node A -> Node B: 14: 0.125, 0 -> 1. **Node A -> *Polysteganus***: **70**: 0.143, 0 => 1. **Node B -> *Chrysoblephus***: **18**: 0.167, 1 => 0; **27**: 0.250 1 --> 2; **66** 0.333, 1 => 2: **67** 0.200 1 => 2: **69**: 0.167 0 => 1

Tree 3: Node A -> Node B: 70: 0.143, 0 -> 1. **Node A -> *Chrysoblephus***: **14**: 0.125, 0 => 1; **18**: 0.167, 1 => 0; **27**: 0.250, 1 -> 2; **66**: 0.333, 1 => 2; **67**: 0.200, 1 -> 2; **69**: 0.167 0 => 1. **Node B -> *Polysteganus***: **70**: 0.143, 0 => 1.

Character-state optimization: Delayed transformation (DELTRAN)

Node 0 -> Node 1: **6**: 0.286, 0 -> 1; **9**: 0.222, 0 -> 1; **17**: 0.500, 0 -> 1; **20**: 1.000, 0 => 1; **28**: 1.000, 0 => 1; **41**: 0.286, 0 -> 2; **48**: 0.667 0 -> 2; **79**: 1.000, 0 => 1; **80**: 0.667, 0 -> 1. **Node 1-> Node 5**: **2**: 0.167, 0 => 1; **3**: 0.273, 0 -> 1; **67**: 0.200, 2 => 1; **73**: 1.000, 0 => 1. **Node 5 -> Node 7**: **25**: 0.200, 0 => 1; **26**: 0.250, 0 => 1; **53**: 0.333, 0 => 1. **Node 7 -> Node 11**: **2**: **1**: 0.167, 1 => 0; **3**: 0.273, 1 => 2; **9**: 0.222 1 => 2. **Node 11-> Node 13**: **39**; 0.222 1 => 0; **59**: 0.250, 0 => 1; **67**: 0.200, 1 => 0. **Node 13 -> Node 17**: **19**: 0.222 0 => 2; **57**: 0.667, 1 => 2; **66**: 0.333, 1 => 2. **Node 17 -> Node 19**: **25**: 0.200 1 => 0; **27**: 0.250, 3 -> 2; **58**: 0.333, 1 => 2; 70: 0.143, 0 -> 1 **86**: 0.222, 0 => 1; **87**: 0.111, 0 => 1. **Node 19 -> Node 27**: 3: 0.273, 2 => 0; **82**: 0.167, 1 => 0. **Node 27 -> Node 31**: 1: 0.400, 1 => 2; **6**: 0.286, 1 => 0; **24**: 0.333, 1 => 0; **51**: 0.250 0 => 1; **86**: 0.222 1 => 2. **Node 32 -> *Centracanthus***: **26**: 0.250, 1 => 3; **29**: 0.750, 2 => 3; **38**: 0.286, 0 -> 2; **48**: 0.667 2 => 1; **49**: 0.667 0 => 1; **63**: 0.500, 1 -> 0; **70**: 0.143, 1 => 0; **71**: 0.250 0 => 1; **80**: 0.667, 1 => 2. **Node 31-> Node 37**: 5: 1.000, 0 => 1; **15**: 0.200 0 => 1; **25**: 0.200, 0 => 1; **38**: 0.286, 0 -> 1; **42:** 0.500, 1 => 3; **46**: 0.400, 0 => 2. **Node 33 -> Node 37**: **19**: 0.222, 2 => 1; **35**: 0.400, 0 => 1; **39:** 0.222, 0 => 1; **43**: 0.167, 1 -> 0; **76**: 0.167, 0 => 1. **Node 37 -> Node 39**: **2**: 0.167, 0 => 1; **6**: 0.286, 0 => 1; **47**: 0.500, 1 => 2; **71**: 0.250, 0 => 1; **82**: 0.167, 0 => 1. **Node 39-> Node 41**: **3**: 0.273, 0 -> 2; **24**: 0.333, 0 => 1; **31**: 0.250, 0 => 1; **34**: 0.500, 1 => 2; **66**: 0.333, 2 => 3; **67**: 0.200, 0 -> 2; **86**: 0.222, 2 -> 0; **87**: 0.111 1 => 0. **Node 41 -> Node 43**: **19**: 0.222 1 => 2; **26**: 0.250 1 => 2. **Node 43 -> Node 45**: **30**: 0.400, 1 => 2; **35**: 0.400, 1 => 2; **36**: 0.500, 0 => 1; **39**: 0.222, 1 => 2; **40**; 0.500, 0 => 1; **50**: 0.200, 0 => 1; **69**: 0.167, 0 => 1. **Node 45-> Node 47**: **13**: 0.500, 0 => 2; **37**: 0.500, 0 => 1; **45**: 0.250, 0 => 1; **72**: 0.286, 1 => 2. **Node 47 -> Node 49**: **23**: 1.000, 1 => 2; **24**: 0.333, 1 => 2; **43**: 0.167, 0 => 1; **44**: 0.333, 0 => 1; **46**: 0.400, 2 -> 0; **51**: 0.250, 1 => 0. **Node 49 -> Node 51**: **8**: 0.400, 0 => 1; **12**: 0.500, 0 => 1; **13**: 0.500, 2 => 1; **22**: 0.500, 1 => 2; **26**: 0.250, 2 => 1; **68**: 0.500, 0 => 1. **Node 51 -> Node 53**: **87**: 0.111 0 => 1. **Node 53 -> *Archosargus***: **16**: 0.167, 0 -> 1; **38**: 0.286, 1 => 2; **39**: 0.222, 2 => 1; **43**: 0.167, 1=> 0; **46**: 0.400 0 => 1; **86**: 0.222 0 => 1. **Node 53 -> Node 55**: **1**: 0.400, 2 => 1; **8**: 0.400, 1 => 2; **15:** 0.200, 1 => 0; **21**: 1.000 0 => 1. **Node 55 -> Node 57**: **12**: 0.500 1 => 0; **19**:.222 2 => 0; 0.250 1 => 0; **35**: 0.400, 2 => 1; **36**: 0.500, 1 => 0; **50**: 0.200, 1 => 0. **Node 57 -> *Argyops***: 11: 0.500, 0 => 1; **27**: 0.250; **39**: 0.222, 2 => 1; **83**: 0.500, 0 => 1; **87**: 0.111, 1 => 0. Node 57-> *Sparus*: **8**:

0..400), 2 => 0; **10**: 0.200, 0 => 1; **14**: 0.125, 0 => 1; **24**: 0.333, 2 => 1; **72**: 0.286, 2 => 1; **74**: 0..286), 1 => 0; **76**: 0.167, 1 => 0; **86**: 0.222, 0 => 2. **Node 55 ->** *Calamus*: **6**: 0.286 1 => 2; **9**: 0..222), 2 => 0; **13**: 0.500, 1 => 2; **16**: 0.167, 0 -> 1; **26**: 0.250, 1 => 2; **32**: 0.333, 1 -> 2; **42**: 0.500 3 => 22; **84**: 0.500, 0 => 1. **Node 51 ->** *Acanthopagrus*: 70: 0.143, 1 => 0; 72: 0.286, 2 => 1; **74**: 0..286) 1 => 0; **76**: 0.167, 1 => 0. **Node 49 ->** *Rhabdosargus*: **3**: 0.273, 2 -> 3; **9**: 0.222, 2 => 1; **14**:. 0).125, 0 -> 1; **33**: 0.500 0 -> 1. **Node 47 ->** *Diplodus*: **3**: 0.273, 2 -> 3; **6**: 0.286, 1 => 2; **10**: 0..200), 0 => 1; **14**: 0.125, 0 -> 1; **33**: 0.500 0 -> 1; **38**: 0.286, 1 -> 2; **46**: 0.400, 2 -> 1; **86**: 0.222, 0 => 1. **Node 45 ->** *Sparodon*: 32: 0.333, 1 -> 2; **38**: 0.286 1 -> 2; **87**: 0.111 0 => 1. **Node 43 ->** *Lagoddon*: **16**: 0.167, 0 => 1; **32**: 0.333, 1 -> 2; **67**: 0.200, 2 -> 1; 76: 0.167 1 => 0. **Node 41 ->** *Crenidens*: 1: 0.400, 2 => 1; **45**: 0.250, 0 => 1. Node 39 -> *Polyamblyodon*: 3: 0.273, 0 -> 1; **9**: 0..222,, 2 => 1; **15**: 0.200, 1 => 0; **27**: 0.250, 2 => 1; 50: 0.200, 0 => 1; 67: 0.200 0 -> 1; **69**: 0.167, 0 => 11; **72**: 0.286, 1 => 2; **86**: 0.222, 2 -> 1. **Node 37->** *Sarpa*: 38: 0.286, 1 -> 2; **58**: 0.333, 2 -> 1; **81**:: 0).500, 1 => 0. **Node 33 -> Node 34**: 27: 0.250, 2 => 3; **41**: 0.286, 2 => 1; **58**: 0.333, 2 -> 1; **63**: 0.5500, 1 -> 0. **Node 34->** *Boops*: **9**: 0.222, 2 => 1; **26**: 0.250, 1 => 0; 43: 0.167, 1 -> 0; 81: 0..500,, 1 => 0. **Node 34 ->** *Oblada*: 10: 0.200, 0 => 1; **14**: 0.125, 0 => 1; 51: 0.250, 1 => 0; **74**: 0..286,, 1 => 0; **87**: 0.111, 1 => 0. **Node 27 -> Node 28**: 11: 0.500, 0 => 1; **41**: 0.286 2 => 1; 53.veNN.rid. q 0.333 1 => 0. **Node** 50 -> ArgyrozoNa 8.lat.eth pr 0.400, 0 => 1; **9**: 0.222, 2 => 1; **16**: 0.1167, 0 => 1; **19**: 0.222, 2 => 1; **26**: 0.250 1 => 0; 27: 0.250, 2 => 3. **Node 28 ->** *Spondyliosoma*: **2**: 0.167, 0 => 1; **15**: 0.200, 0 => 1; **42**: 0.500, 1 => 0; **47**: 0.500, 1 => 0; **52**: 0..333,, 1 => 0; **59**: 0.250, 1 => 0; **74**: 0.286, 1 -> 0. **Node 19 -> Node 20**: **30**: 0.400, 1 => 2; 34: 0..500,, 1 => 2; **37**: 0.500, 0 => 1; **39**: 0.222, 0 => 1; **40**: 0.500 0 => 1; **42**: 0.500, 1 => 2; **47**: 0..500,, 1 => 2. **Node 20 -> Node 24**: **26**: 0.250, 1 => 2; **31**: 0.250 0 => 1; **45**: 0.250, 0 -> 1; **76**: 0.167,, 0 => 1. **Node 24 ->** *Lithognathus*: **3:** 0.273, 2 => 0; **16**: 0.167, 0 => 1; **18**: 0.167, 1 => 0; **32**: 0.3333, 1 => 2; **38**: 0.286 0 => 1; **39**: 0.222, 1 => 2; **71**: 0.250, 0 => 1; **72**: 0.286, 1 => 2; **82**: 0.167,, 1 => 0; **86**: 0.222, 1 => 0. **Node 24 ->** *Stenotomus*: 2: 0.167, 0 => 1; **8**: 0.400, 0 => 1; **14**: 0.125,, 0 => 1; **19**: 0.222, 2 => 1; **22**: 0.500, 1 => 2; **25**: 0.200 0 => 1; **50**: 0.200 0 => 1; **66**: 0.333, 2 => 33; 67: 0.200, 0 => 1; **83**: 0.500, 0 => 1; **84**: 0.500, 0 => 1. **Node 20-> Node 21**: **19**: 0.222, 2 => 0; 44: 0.333, 0 => 1; **59**: 0.250, 1 => 0. **Node 21 ->** *Pagrus*: **16**: 1 0.167, 0 => 1; **35**: 0.400, 0 => 1; 45: 0.250 0 -> 1; **66**: 0.333, 2 => 3; **67**: 0.200, 0 => 1; **71**: 0.250 0 => 1. **Node 21->** *Pagellus*: **14**: 0.125, 0 => 1; **18**: 0.167, 1 => 0. **Node 17 ->** *Pachymetopon*: 1: 0.400, 1 => 2; **2**: 0.167,, 0 => 1; **24**: 0.333,1 => 0; **26**: 0.250, 1 => 2; **27**: 0.250, 3 -> 1; **43**: 0.167, 1 => 0; **46**: 0.400, 0 => 22. **Node 13 -> Node 14**: **18**: 0.167, 1 => 0; **30**: 0.400 1, => 0; **70**: 0.143, 0 -> 1. **Node 14 ->** *Boopscoidea*: 15: 0.200, 0 => 1; **26**: 0.250 1 => 0; **41**: 0.286, 2 => 1; **71**: 0.250, 0 > 1. **Node 14 ->** *Cheimaerus*: **3**: 0.273, 2 => 0; **25**: 0.200, 1 => 0; **27**: 0.250, 3 -> 0: **66**: 0.333, 1 => 0; **67**: 0.200, 0 => 2; **69**: 0.167, 0 => 1. **Node 11** -> *Evynnis*: **10**: 0.200, 0 => 1; **14**: 0.125, 0 -> 1; **27**: 0.250, 3 -> 1; **71**: (0.250, 0 => 1. **Node** 60 -> *Chrysoblephus*: **14**: 0.125, 0 -> 1; **18**: 1 => 0; **27**: 0.250, 3 -> 2; **66**: 0.3333, 1 => 2; **67**: 0.200, 1 => 2; **Node** 61 -> *Polysteganus*: **70**: 0.143 0 => 1. **Node 5 ->** *Porcosstoma*: **35**: 0.400, 0 => 1; **60**: 0.333, 1 => 0; **87**: 0.111, 0 -> 1. **Node 1 -> Node 2: 18**: 0.167 1 => 0); **30**: 0.400,1 => 0; **74**: 0.286, 1 => 0; **75**: 0.500, 1 => 0. **Node 2 ->** *Cymatoceps*: **27**: 0.250 3 => 0); **53**: 0.333, 0 => 1; **58**: 0.333, 1 => 0; **66**: 0.333, 1 => 0; **69**: 0.167, 0 => 1. **Node 2 ->** *Dentex* : **19**: 0.222, 0 => 1; **39**: 0.222 1 => 0; **41**: 0.286 2 => 1; **82**: 0.167 1 => 0.

Tree 11: **Node A -> B**: **2**: 0.167, 0 --> 1. **Node B** -> *Chrysoblephus*: **14**: 0.125, 0 => 1; **18**: 0.167, 1 => 0); **27**: 0.250, 1 -> 2; **66**: 0.333, 1 => 2; **67**: 0.200, 1 -> 2; **69**: 0.167 0 => 1. **Node B ->** *Polysteeganus*: **70**: 0.143, 0 => 1.

Tree 22: **Node A ->** *Polysteganus*: **70**: 0.143, 0 => 1. **Node B ->** *Chrysoblephus*: **14**: 0.125, 0 -> 1; **18**: 0.1167, 1 => 0; **27**: 0.250 1 --> 2; **66** 0.333, 1 => 2: **67** 0.200 1 => 2: **69**: 0.167 0 => 1

Tree 33: **Node A -> Node B**: **67**: 0.200, 2 -> 1. **Node A** -> *Chrysoblephus*: **14**: 0.125, 0 => 1; **18**: 0.1167, 1 => 0; **27**: 0.250, 3 --> 2; **66**: 0.333, 1 => 2; **69**: 0.167 0 => 1. **Node B ->** *Polysteganus*: **70**: 0.1143, 0 -> 1.

Table 3.3 of the incompatibly output from DNALQP.

Le Quesne Probability

* = $P > 0.05$; ** = $P > 0.1$

C	Incompatibilities Obs	Expected	Le Quesne Probability	Minimum Probability/Obs	
1 :	53	77.31	0.001	0.001	58
2 :	55	77.53	0.001	0.001	59
3 :	70	81.63	0.032	0.002	62
4 :	4	31.13	0.002	0.002	4
5 :	51	76.99	0.001	0.001	55
6 :	76	73.18	0.537**	0.002	53
7 :	Equivalent to Character 4				
8 :	50	63.54	0.106**	0.001	36
9 :	81	78.59	0.560**	0.003	59
10 :	61	60.42	0.565**	0.001	33
11 :	45	46.37	0.520**	0.001	15
12 :	23	46.96	0.012	0.001	13
13 :	62	69.92	0.267**	0.002	46
14 :	56	69.80	0.091*	0.002	44
15 :	60	75.54	0.028	0.001	55
16 :	52	64.99	0.104**	0.001	37
17 :	39	55.03	0.071*	0.003	29
18 :	61	71.57	0.165**	0.001	49
19 :	72	81.14	0.055*	0.002	64
20 :	41	60.55	0.020	0.001	35
21 :	27	46.79	0.039	0.001	17
22 :	58	72.02	0.070*	0.001	48
23 :	38	69.35	0.001	0.001	40
24 :	72	77.28	0.232**	0.001	54
25 :	53	77.85	0.002	0.001	52
26 :	77	81.94	0.117**	0.001	64
27 :	77	81.48	0.133**	0.003	63
28 :	Equivalent to Character 20				
29 :	28	33.61	0.355**	0.003	6
30 :	69	80.85	0.033	0.001	59
31 :	68	74.82	0.213**	0.001	55
32 :	49	67.19	0.024	0.001	45
33 :	13	33.50	0.027	0.001	8
34 :	50	79.05	0.001	0.001	59
35 :	59	78.72	0.001	0.001	60
36 :	34	64.92	0.001	0.002	43
37 :	46	74.89	0.001	0.001	53
38 :	61	79.79	0.001	0.006	62
39 :	69	81.17	0.026	0.002	64
40 :	45	75.66	0.001	0.001	57
41 :	66	74.35	0.186**	0.001	50
42 :	80	81.83	0.231**	0.001	65
43 :	78	73.42	0.623**	0.001	50
44 :	62	71.70	0.177**	0.001	50
45 :	49	74.98	0.001	0.001	52
46 :	54	73.46	0.003	0.001	51
47 :	70	79.20	0.086*	0.001	61
48 :	50	63.95	0.067*	0.001	33
49 :	31	33.40	0.495**	0.002	6
50 :	65	71.81	0.265**	0.001	51

51 : 62	72.14	0.166**	0.001	48
52 : 46	55.13	0.221**	0.001	25
53 : 47	72.50	0.002	0.001	45
54 : 32	47.08	0.083*	0.001	15
55 :	Equivalent to Character 54*			
56 : 32	48.23	0.075*	0.001	16
57 : 51	74.66	0.001	0.002	54
58 : 65	79.68	0.017	0.001	59
59 : 61	77.22	0.012	0.002	59
60 : 48	55.15	0.270**	0.001	25
61 :	Equivalent to Character 54*			
62 : 31	47.36	0.069*	0.001	16
63 : 64	63.91	0.549**	0.001	37
64 : 29	34.62	0.387**	0.004	6
65 : 6	34.01	0.002	0.002	6
66 : 72	82.55	0.015	0.002	66
67 : 67	81.29	0.011	0.001	63
68 : 67	68.07	0.467**	0.001	44
69 : 67	77.40	0.082	0.001	58
70 : 69	75.10	0.213**	0.001	53
71 : 68	79.71	0.035	0.001	60
72 : 64	74.41	0.126**	0.001	52
73 : 43	67.93	0.002	0.001	40
74 : 70	70.55	0.484**	0.006	51
75 : 36	55.96	0.021	0.001	22
76 : 68	76.07	0.143**	0.001	58
77 :	Equivalent to Character 54*			
78 :	Uninformative Character			
79 : 39	54.79	0.050	0.002	25
80 : 42	55.34	0.096*	0.001	23
81 : 47	55.88	0.235 **	0.002	23
82 : 66	74.18	0.167**	0.001	52
83 : 28	33.76	0.347**	0.002	6
84 : 27	33.49	0.350**	0.001	6
85 : 6	33.56	0.003	0.003	6
86 : 75	79.39	0.219**	0.001	62
87 : 78	78.40	0.406*	0.001	60
88 :	Uninformative Character			
89 : 32	47.60	0.082*	0.001	19

Table 3.6 Binary data matrix

TAXA	CHARACTER
	1111111111222222222233333333334444444444555555555566666666667777777778888888888999999999000000000111111111222222222233333333334444444445555555556666666667777777788 1234567890123456789012345678901234567890123456789012345678901234567890123456789012345678901234567890123456789012345678901234567890123456789012345678901234567890123456789012345678901
Centropomus	1000000000100000000000010000000000000000000001000010100010010000000100100001001000010010000000100010000010000010000100000010000100000010000100100100001001000100
Lutjanus	1000000000100000000000010000000000000000000001000010100001010000000100100001001000010010100000101000010000001000010000000100001000010000010010000100100???100
Haemulon	0100011001000110001010001000000100000110101100001010000000010101111000101000001001000001000110000001010010000100010000111010100001001110000101100011100100?100010100001100100???100
Centracanthus	0010000010100100010100010000011101101101100000000100101110001001100010100000111000100010100000100100100111110011001011110101000110100100000101101001101000110010100000100011??????
Lethrinus	0100011001001010001101000010000110000010111011000001100000001010011000011000010001000100010110000010010100001011001111001101001111001110000011010010001001010001001010010001
Nemipterus	0100000010100100000000010000001101001101101100100001010000100100110001010000100010010000101000000100100011100110011000000010010011111001100100000101001011100010000100010010101010010
Archosargus	0011101011010111010100101001111101101101101101101000001011000100111100001001110100011100100001111000100110111100110010111010010011001110101011001111001010100100010010101010010
Acanthopagrus	0011101011010111010100101001011101101011011011010000010110001001111000010011101000111001000111000010010011011110011001011101001001100110010110101010100101010010100010000100010
Argyops	0101101011010110110101001000011000111011011011010100010011000100101010001010010110110001001000111000010010010111100110010111101001001100111010101100111100101010010100110000100010
Argyrozona	0100000010010111011001010000111110101101101100100000000100010100110001010000100100001000101000000100010010010110011?????111010?????????????????????????????1001010100100001001010100010
Boops	0010000011100100011000010010111010110111000011000000001000101001100010100000101000010100000010101000100101111100110011011101010001101010010001100110100110100101010100000010001101001 0
Boopsoidea	0100101010010100001010000100?1000010110110110110000000010001100011000101000010010000100010100000100010010011110010011101110100100??3010001011010011010010100101000100001000010
Calamus	0101101011001110100000100100111101111011011011001000101100010011101000100111010000111100000111000001001001101111001100101111010010011001100111010101100111100101010010100101000100010
Cheimerus	0100000010010100010100010000010000101101101100010001010100011000100010100010000100100010000101000001000100100111100100111011101001000010001110011010010100101001010001010000100010
Chrysoblephus	0101111001001010001100001001001000010110110110101000001011000101001100010100001000100100001010000001000100100111100100111001010010001010100100101001010001010000100010
Crenidens	0101101011010100010100010001011110101101101101010000101100010101110000101000010010010010000010100100100101111100100111001010010001010100100101001010001010000100010
Cymatoceps	0100000010010100011000010000010000101101101100100001010101000110001100010100001000100100001010000001000100100111100100130001010010001000101001100100010100101000100010
Dentex	0100000010010100011000010000010110101101101100100010000100011000110001010000100100001000100010000010001001001011001110010000010011000100100101001000010100001000010
Diplodus	0011100111001100010110000111011101101101101101010001010110001011110100100111001001110001000111000100100111111100110010111010010011001100011010101100111100101010010100010010000100010
Evynnis	0100101010010100001011001001001100101101101101101010001001100010100100010001000100100010000010100100100111100100111001100010110100101001010010100010100001000010
Lagodon	0011101011010100010100010001111101101101101101010001010110001010101000101000010010010010000001010010010111100100101111010010011001001001010110100110100101010010100010100001000010
Lithognathus	0100000010010100010100010000110101101101101100001000101100010011101001100010100011100000110100000100100111001100101111010010011010100010101011001111001010100100001001010100010
Oblada	0010000011100100010110010011011011011011000001010010000100010100110001010000101000010100010010101000100100111100110011011101010001101010010001100110101010100101010010000010001001001 0
Pachymetopon	0011????1001010001010001000001110110110110000100100100110001010011000101000010010001000010000101010001001001111001100110111010010011010010000100110100110100101010010100010100001000010
Pagrus	0100101010010100010100010000111000101101101100010000101100010011010000110010010010000011110000010010011111001100101011010010011010010000100110100110100101010010100010100001000010
Pagellus	0100101010010100010100010010010000101101101100010000101100010011010000110001100010110000011100000010010010011110011001010110100100110100100010011010011010010101001010001001010100010
Polyamblyodon	0011110010101000110000100001111010110110000101000100110001010011000100100001000010100100100000010100100100111111001100101111010010110101011001111001010100100010010101001010 0
Polysteganus	0101110010010100011000010000011000101101101101010?????10001010011000101000010001000100010100000100010010011110010011100101001100001001100110100110100101010010100010100001000010
Porcostoma	0101110010010100011000010000011000101101101100100010001010011000100100010001000100100010100000100010010011010010011100001000100110100110100101010010100010100101001010 0
Rhabdosargus	0011100111010100011000000111011011011010101101100010101100010011110100100111010011101000111000010010010111100100101111010010011001100011010101100111100101010010100010111000100010
Sarpa	0010000011100100010100010001011110101101101100001010000101000101100010100100100000010100100100000010101000100101111100110010111010010011010010000100110100111100101010100000010011010010
Sparodon	0011101010101000101000100010111011011011010100100010101000100111010001001100010011100100000010100100100111111001100101111010010011001100011010111010011110010101001010001010010100100
Sparus	0101110101010100011100010100110001101101110101000010100010010100001010001100100100111000001001001001111001100101111010010011001100011010101100111100101010010100010001101001 0
Spondyliosoma	0101000010010100010101010001011101101101101100010000101100010100110001010000100100001001001000000100010010000011001100101011010010011010010001100110101010010100100000010010100100
Stenotomus	0101101010010111010100010010011110101011101101001000101100010011110000102?01100010110000011010000010010011011110011001011110100100110010010011001101001111001010100101110100101010010